

مجــلة ديالـــى الطبيــة

Print ISSN 2219-9764 Online ISSN 2617-8982



Diyala Journal of Medicine

> Vol 29 Issue 1 October 2025



www.djm.uodiyala.edu.iq

editor@djm.uodiyala.edu.iq

مجلة دورية محكمة صادرة عن كلية الطب - جامعة ديالي



DJM

Divala Journal of Medicine

Published by College of Medicine - University of Diyala - Diyala - Iraq. Editorial Board

Editor in Chief

Assistant Professor Dr. Anfal Shakir Motib

PhD in Molecular Microbiology - Department of Microbiology - College of Medicine - University of Diyala anfal shaker@yahoo.com

Editor Manager

Lecturer Dr. Saad Ahmed Ali Jadoo Al-ezzi

PhD in Community Medicine - College of Medicine - University of Diyala

saadalezzi@uodiyala.edu.iq

Editorial Board

Professor Dr. Ismail Ibrahim Latif

PhD in Clinical Immunity-College of Medicine - University of Diyala

ismail 6725@vahoo.com

Professor Dr. Ghanim Mustafa Al-Sheikh

PhD in Human Neurosciences - Imperial College London –UK

 ${\bf alsheikhg@gmail.com}$

Professor Dr. Karim Alwan Mohamed

PhD in Pathology and Forensic Medicine - Head of Pathology Unit -

Faculty of Medicine- SEGi University -Malaysia

jashamy@yahoo.com

Professor Dr. Talib Jawad Kadhum

PhD in Anatomy- College of Medicine - University of Diyala

talibjwd@yahoo.com

Professor Dr. Saad Muhmood Hussain Arraki

Board in Surgery - Newcastle University Medicine- Malaysia

Drsaad1961@gmail.com

Professor Dr. Jalil Ibrahim Alezzi

FICMS, DCH in Medicine pediatrics-College of Medicine - University of

Diyala

adil_alhusseiny@yahoo.com

Professor Dr. Amer Dawood Majeed

PhD in Medical Physics - College of Medicine -University of Diyala

amer_dmk@yahoo.com

Professor Dr. Zuhair Maroof Hussain

PhD in Biochemistry - College of Medicine - University of Diyala

zuhair@medicine.uodiyala.edu.iq

Professor Dr. Mehdi Shamkhi Gebir

Board in Pediatrics - College of Medicine - University of Diyala

meh_sh2000@yahoo.com

Professor Dr. Ahmed Mohamed Badheeb

Jordanian Board of Medical Oncology - Head of Medical Oncology

department at King Khalid Hospital - Najran-Saudi Arabia

abadheeb@moh.gov.sa

Professor Dr. Salwa Sh. Abdul-Wahid

PhD in Community Medicine - College of Medicine - University of

Diyala

s_sh_abdulwahid@yahoo.co.uk

Professor Dr. Salih Mahdi Salman

PhD in Organic Chemistry - College of Medicine - University of Diyala

salih@medicine.uodiyala.edu.iq

Professor Dr.Kamile Marakoglu

PhD in Family Medicine - College of Medicine - University of Selcuk-

Konya-Turkey

Professor Dr. Aydin beyatli

PhD in Ophtalmolojist Medicine- Ankara University- Turkey

avdinbevatli@hotmail.com

Professor Dr. Marwan Salih Al-Nimer

PhD in Pharmacology and Therapeutics- College of Medicine - University

of Diyala

marwanalnimer@yahoo.com

Professor Dr. Ali Mohammed BatarfiBoard in Surgery- College of Medicine and Health, Sciences Roadstead-

Hadhramout- Yemen

ambatarfi@yahoo.com

Assistant Professor Dr.Muqdad Fuad Abdulkareem

Board in Surgery - College of Medicine-University of Diyala

muqdadfuad@yahoo.com

Assistant Professor Dr.Fayez Alghofaili

PhD in Medical Microbiology - College of Applied scinces - University of

Majmaah-Saudi Arabia

F.alghofaily@mu.edu.sa

Assistant Professor Dr.Melike Emiroglu

PhD in Child Health and Diseases-College of Medicine - University of

Selcuk-Konya-Turkey mkeser17@gmail.com

Dr. Omer Layth Qassid

FRCPath(UK) IFCAP(USA)- University of Leicester-Consultant

Histopathologist-The university hospitals of Leicester – United Kingdom

Omer.qassid@uhl-tr.nhs.uk

Assistant Professor Dr. Mustafa Gheni Taher

PhD in Dentist- Oral and Maxillofacial Pathology- College of Medicine-

University of Diyala

gheny@uodiyala.edu.iq

Professor Dr. Nadhim Ghazal Noaman

Head of Community Medicine Department - College of Medcine - University of Diyala

drnadhimg@yahoo.com

DJM Design Ahmed Jabbar Mohammed ahmed.jabbar@uodiyala.edu.jq

Correspondence: DJM Office/ College of Medicine/ University of Diyala / PO Box (2) Baquba office/ Baquba/ Diyala/ Iraq. E-mail: djm.diyala@yahoo.com, editor@djm.uodiyala.edu.iq

Instruction to Authors

Papers are accepted on the understanding that the subject matter has not and will not be submitted simultaneously to another journal. The following notes are expected to be considered carefully in writing manuscripts:-

- 1- The manuscript including figures and tables should be submitted on line to http://djm.uodiyala.edu.iq/index.php/djm/about/submissions Or as an attachment to djmeditor@djm.uodiyala.edu.iq.
- 2- Manuscripts must be accompanied by a covering letter signed by all authors that the paper has not been published and will not be submitted to another journal if accepted in the Iraqi Medical Journal.
- 3- The title page should include:

Title of the paper is in Arabic and English

Correct first name, middle name and family name of all authors in Arabic and English as well as a maximum of two highest academic degrees for each author.

Name (s) and address (es) of the institution (s) where the work was carried out.

The name and address of the author responsible for correspondence together with telephone number, fax number and e-mail address (if any).

- 4- Abstract for original articles should contain a structured abstract of not more than 200 words in Arabic and English. Abstract heading include: background, objectives, Methods, Results, and conclusions. Abstracts in Arabic and English of review articles and case reports should be unstructured and of not more than 150 words.
- 5- Three to ten keywords should be provided on the same page as the abstract in English and Arabic. As far as possible, the keywords should be selected from the national library of medicine, medical subject headings.
- 6- The main text of the original article should be divided into section, each section should be started on a new page after the title page:

- Introduction: is should state clearly the purpose and rationale of the study.
- Methods: should include selection of subjects, identification of the methods,
 apparatus and chemicals used and include statistical analysis.
- Results: They presented in a logical sequence preferably with tables and illustrations emphasizing in the text only the important observation.
- Discussion: it emphasizes new findings of the study, implications and reference to other relevant studies.
- Acknowledgement: it is only to persons who have made substantive contribution to the study.
- References: should be in the Vancouver style. They should appear in the text by numbers in the order. List all authors when six or less; when seven or more, list only first six and add et al. journal titles should be abbreviated in accordance with Index Medicus. Examples of correct reference forms are given as follows:

Al-Salihi AR, Hasson EH, Al-Azzawi HT. A short review of snakes in Iraq with special reference to venomous snake bite and their treatment. Iraqi Med J 1987; 36:57-60.

Book chapter: Pen AS. Immunological features of myasthenia gravis. In: Aguayo AJ, karapti G, editors. Topics in nerves and muscle research. 31^{st} ed. Amsterdam: Experta Medica; 1975. p. 123-32.

7- Illustration: Photographs unmounted on glossy paper should be provided with magnification scale if appropriate. Lettering should be in either letraset or stencil of comparable size. Illustration should be marked on the back with the figure number, title of the paper and name (s) of the author (s) with soft pencil. All photographs, graphs and diagrams should be referred to as figures and should be numbered consecutively in the text. The legends to illustration should be typed on a separate sheet. Tables should be numbered consecutively in the text in and each typed on a separate sheet. Vertical lines normally will not be printed.

- 8- Measurements are preferably expressed in SI (standard international) units.
- 9- Authors are advised to follow the Webster's collegiate dictionary in spelling.
- 10- Articles and abstracts which written in Arabic should follow the unified medical dictionary (council of Arab ministers of health/WHO/Arab medical union/ALESCO, 3rd edition)
- 11- Use only SI standard abbreviations in the title and abstract. The full term for which the abbreviations stand should precede its first use the text.
- 12- After the manuscripts has been accepted for publication, authors are required to supply the final version of the manuscript on CD IBM compatible disc in MS word 1997-2003 and more.
- 13- Page proof will be sent to the corresponding author for proof correction. Major alterations from the text cannot be accepted.
- 14- Through sending the manuscripts, authors from outside Iraq are requested to send upon acceptance of the paper, a publishing charge of 150 ID is required. For authors from Iraq, the total charge is 120\$ on sending the article.

DJM

<u>Diyala Journal of Medicine</u>

No.	Paper Title	Page
1	Serum Neudesin Levels in Gestational Diabetes Mellitus: A Potential Biomarker for Disease Prediction Alaa Jumae Esmail, Areej Sh. Hameed, Ekhlas Khalid Hameed	1-10
2	Association Between Uremic Pruritus and Differential Leukocyte Counts Among Hemodialysis Patients in Ibn Sina Dialysis Center Hiba M. Al-Darraji, Ismail Ibrahim Latif, Fatimah khazaal khamees Al-majmaie, Nabeel Khalid Al Wandi	11-20
3	The Efficacy and Safety of Using a Stone Cone During Ureteroscopic Pneumatic Lithotripsy Waleed Kh. Mohammed, Issam S. AL-Azzawi, Yousif S. Khalaf, Athanasios Papatsoris	21-30
4	Pentraxin-3 Level Assessment Among Ischemic Stroke Patients with Polycystic Ovarian Syndrome Mufeed Akram Taha, Sahar A. Taha, Esraa Abdulkareem Mohammed	31-41
5	Interplay Between Biometric Profiles, Biomarkers, Body Fat, and Bone Health: A Statistical and Machine Learning Approach Jawad Kadhum Abass, Wisam A. Hussein, Ahmed Naseer Kaftan	42-58
6	Classification and Prediction of Human Blood Cells Using Artificial Intelligence and Advanced Image Processing Techniques Ahmad S. Lateef, Ahmed J. M. Al-Zuhairi, Mohammed Y. Kamil	59-73
7	Interleukin-20 Gene Polymorphism and Serum Levels of Interleukin-20 and Interleukin-23 in Rheumatoid Arthritis Iman Najat Ali, Najat Jabbar Ahmed Berwary	74-88
8	Prevalence of Oral Aphthous Stomatitis and Recurrent Herpes Labialis Among Dental Students Hayder Mahdi Idan, Ghasaq Abdullah Mahmood, Ibtehal Qhtan Othman	89-98
9	Investigation of Methylglyoxal, soluble Receptor for Advanced Glycation End-products, and Malondialdehyde in Type 2 Diabetes Mellitus with and Without Cardiovascular Risk Factors Weaam F. Hussien, Estabraq A. R. Al-Wasiti, Mahood. Sh. Khudair, Hayder A. AL-Aubaidy	99-110
10	Changes in the Levels of Methionine Adenosyltransferase, Methionine Sulfoxide Reductase A, and Thioredoxin are Associated with Oxidative Stress in Patients with Hyperthyroidism Marwa A. Al-Badrany, Luay A. Al-Helaly	111-124

Serum Neudesin Levels in Gestational Diabetes Mellitus: A Potential Biomarker for Disease Prediction

Alaa Jumae Esmail (1), Areej Sh. Hameed (1), Ekhlas Khalid Hameed (1)

Abstract

Background: A common metabolic disorder during pregnancy is gestational diabetes mellitus (GDM). It is linked to insulin resistance and impaired glucose tolerance. The role of neudesin, a regulatory peptide hormone involved in glucose metabolism, as a potential biomarker for GDM remains unclear.

Objectives: To assess Neudesin's predictive value for GDM and evaluate its correlation with insulin resistance indices and glycemic indicators.

Patients and Methods: This case-control study was conducted in Baghdad, Iraq, from January to July 2025 at the Department of Chemistry, College of Science for Women, University of Baghdad, in collaboration with the Department of Obstetrics and Gynecology at Al-Yarmouk Teaching Hospital. Eighty healthy controls and 120 women with GDM were included. Serum Neudesin, fasting blood glucose (FBG), insulin, HOMA-IR, HbA1c, TyG index, and TyG-BMI index were evaluated.

Results: Women with GDM had significantly higher serum Neudesin levels compared to controls $(2.372 \pm 0.36 \text{ ng/mL} \text{ vs. } 0.919 \pm 0.156 \text{ ng/mL}, \text{p}<0.001)$. Neudesin levels were positively correlated with BMI, FBG, HbA1c, insulin, HOMA-IR, and TyG indices (p<0.001). Logistic regression identified neudesin as an independent predictor for GDM. ROC analysis showed high diagnostic accuracy (AUC = 0.986), with a cut-off value of 1 1185 ng/ml, which yielded 100% sensitivity and 86.7% specificity.

Conclusion: Circulating neudesin concentrations are markedly higher in individuals with GDM and show a strong correlation with the degree of insulin resistance and poor glycemic control. Neudesin may serve as a promising diagnostic biomarker and potential target for early identification and management of GDM.

Keywords: Gestational diabetes mellitus, Neudesin, Insulin resistance, Biomarker.

Introduction

GDM is defined as any degree of glucose intolerance with onset or first recognition during pregnancy, typically diagnosed between 24 and 28 weeks of gestation". The diagnostic criteria for GDM have evolved over decades, reflecting advancements in glucose testing methods and a deeper understanding of associated risks (1). Globally, GDM affects more than 16.5% of pregnancies; this figure is predicted to increase as the obesity pandemic increases. An increased risk of type 2 diabetes, maternal cardiovascular disease, macrosomia, and delivery complications is associated with GDM, having a higher chance of obesity, type 2 diabetes, and cardiovascular disease (2, 3).

OPEN ACCESS

Correspondence: Ekhlas Khalid Hameed Email: ikhlaskhalid@yahoo.com
Copyright: ©Authors, 2025, College of Medicine, University of Diyala. This is an open access article under the CC BY 4.0 license (http://creativecommons.org/licenses/by/4.0/)
Website:

https://djm.uodiyala.edu.iq/index.php/djm

Received: 09 July 2025 Accepted: 08 September 2025 Published: 25 October 2025

¹ Department of Chemistry, College of Science for Women, University of Baghdad, Baghdad, Iraq.

² Al-Kindy College of Medicine, University of Baghdad, Baghdad, Iraq.

further investigations. Currently, there are a few contradictory studies about the levels of neudesin in body fluids.

This study aimed to investigate whether neudesin contributes to GDM and to examine its association with insulin resistance, as well as key metabolic and anthropometric factors.

Pancreatic β -cell failure, accompanied by chronic insulin resistance, leads to glucose intolerance and subsequent hyperglycemia. Obesity, excess weight, advanced maternal age, and a family history of diabetes are all recognized risk factors for GDM (4, 5).

Given that GDM is characterized by insulin resistance and cell dysfunction, the primary focus should be on deepening our understanding of the underlying mechanisms driving these processes. By understanding how these pathways function, we can develop targeted strategies to improve pancreatic function (3-5).

neuron-derived Neudesin, also known as neurotrophic factor, is a protein broadly expressed in the brain, adipose tissue, heart, kidneys, and lungs (6). Its cytochrome b5-like heme/steroid binding domain is essential for initiating intracellular signaling cascades. In neurons, neudesin activates the phosphatidylinositol-3 kinase and mitogenactivated protein kinase pathways through Gi/Go proteins (7). Additionally, it promotes cell differentiation and proliferation by increasing cyclic AMP levels and activating the protein kinase A pathway, among others. Beyond its neurotrophic effects, neudesin supports the development and differentiation of brain precursor cells (8).

Mice lacking the neudesin gene exhibit increased energy expenditure, enhanced lipolysis in white adipose tissue, and heat production in brown adipose tissue. These findings suggest that neudesin may act as a negative regulator of energy consumption. Neudesin elevates cyclic AMP levels and promotes cell differentiation and proliferation through the protein kinase A pathway and other signaling cascades. In addition to its neurotropic activity, neudesin supports the growth and differentiation of neural precursor cells (9,10). However, current literature (10) presents conflicting evidence regarding neudesin levels in body fluids, indicating the need for

Patients and Methods

Study design: This case-control study was conducted in Baghdad, Iraq, from January to July 2025 at the Department of Chemistry, College of Science for Women, University of Baghdad, in collaboration with the Department of Obstetrics and Gynecology at Al-Yarmouk Teaching Hospital. Two hundred pregnant women between the ages of 20 and 40 participated in the study: 80 healthy pregnant women (control group), and 120 pregnant women with GDM as the case group. Participants were matched for age and gestational age to minimize confounding effects.

Inclusion criteria were pregnant women diagnosed with GDM according to standard criteria (OGTT-based diagnosis). In contrast, women with preexisting diabetes, thyroid diseases, chronic metabolic diseases, multiple pregnancies, and any disease or on medication that affects serum neudesin level were excluded from the study to ensure homogeneity.

Data collection and laboratory analysis: Every participant had five milliliters of venous blood extracted and split into two tubes. A polymer with thixotropic qualities was present in the gel separator tube, to which two milliliters of blood were transported. The serum was separated after centrifugation at 3000 rpm for five minutes. Using the Siemens Healthineers Atellica Solution analyzer, Biochemical parameters like fasting blood glucose, total cholesterol, triglycerides, high-density lipoprotein cholesterol, and blood urea were measured. Furthermore, enzyme-linked immunosorbent assay kits (Finetest) were used to evaluate the serum concentrations of neudesin and insulin.

Blood for Glycated hemoglobin (HbA1c) was collected in an EDTA tube. The HBA1C level was measured using the turbidimetric immunoassay method. Using fasting glucose and insulin levels, the Homeostasis Model Assessment of Insulin Resistance (HOMA-IR) was computed to assess the level of insulin resistance in accordance with the following equations: (13,14)

HOMA-IR = (Fasting Insulin $[\mu U/mL] \times$ Fasting Glucose [mg/dL]) / 405.

While TyG and TyG-BMI were calculated by the following equations (13,14): TyG index = $\ln [Triglycerides (mg/dL) \times Fasting Glucose (mg/dL) / 2$

TyG-BMI = TyG index \times BMI The cutoff for HOMA-IR is 2 (15)

Statistical Analysis

Data were analyzed using SPSS 26.0. The normality of data distribution in both the patient and control groups was evaluated using the Kolmogorov-Smirnov test. Variables were classified as parametric or nonparametric based on their distribution characteristics. Group comparisons were performed using the Student's t-test for normally distributed data and the Mann-Whitney U test for nonparametric data. Continuous variables were presented as mean ± standard deviation (SD), and differences between groups were assessed using Student's t-test or Mann-Whitney U test, depending on data distribution. Correlation between neudesin and insulin resistance markers was determined using Pearson's correlation or Spearman's rank correlation for non-parametric data. A logistic regression model was employed to determine independent predictors of GDM. Logistic regression was employed to identify independent predictors of group classification, and two models were constructed. Model 1 included

neudesin alone. Model 2incorporated anthropometric and laboratory-related parameters. The diagnostic performance of serum neudesin in predicting GDM was evaluated using ROC curve analysis, which provides for AUC, ideal cutoff value, sensitivity, and specificity. Statistical significance was set at p < 0.05.

Results

Demographic and clinical characteristics of the studied population: Table 1 presents the demographic and clinical characteristics of the control and GDM groups, with comparable ages and gestational ages between groups (p > 0.05). Significant differences were observed in BMI, FBG, HbA1C, insulin levels, and HOMA-IR, all of which were markedly elevated in the GDM group (p < 0.001), indicating metabolic dysregulation.

Serum neudesin levels and insulin resistance markers: Table 2 compares serum neudesin levels and insulin resistance markers between healthy pregnant women and those with GDM. Neudesin levels were significantly higher in the GDM group (p < 0.001), alongside elevated HOMA-IR, TyG index, and TyG-BMI index, suggesting a strong association between neudesin and insulin resistance.

Table 1. Comparisons of the demographic and clinical characteristics of the studied population.

	Control Group	GDM Group	p-value
Age(year)	28.65 ± 6.51	29.72 ± 5.68	0.351
Body Mass Index (kg/m ²)	31.47±	36.38 ± 3.95	0.000
FBG (mg/dL)	88.82 ± 11.34	143.38 ± 30.77	0.000
HbA1c %	4.98 ± 0.57	7.49 ± 1.125	0.000
Insulin(µIU/mL)	3.117 ± 0.87	7.56 ± 1.23	0.000
HOMA IR	0.667 ± 0.21	2.67 ± 0.74	0.000
Total Cholesterol(mg/dL)	213.21 ± 48.86	232.99 ± 60.26	0.085
Triglycerides(mg/dL)	177.24 ± 65.36	180.45 ± 49.81	0.745
Gestational age(weeks)	30.6 ± 3.31	31.41 ± 3.36	0.260

Table 2. Comparisons of the serum level of neudesin and the markers of Insulin resistance between the

control and pregnant women with GDM.

	Control	Pregnant with GDM	p-value
Serum Neudesin (ng/ml)	0.919 ± 0.061	2.372 ± 0.051	0.000
HOMA IR	0.667 ± 0.21	2.67 ±0.74	0.000
TyG-index	8.9148 ± 0.344	9.417 ± 0.32	0.000
TyG-BMI index	283.18 ± 27.151	342.76 ± 40.93	0.000

Serum neudesin level by body mass index in women with gestational diabetes:

Table 4 examines serum across BMI categories in women with GDM. Although BMI and HbA1c increased significantly across groups (p< 0.001 and p = 0.008,

respectively), serum neudesin levels did not differ significantly (p = 0.699), suggesting that neudesin may be independent of BMI in this population.

Table 3. Comparison of serum neudesin levels based on gestational age in women with GDM.

	Gestational age less than 24-30 weeks	Gestational age more than 30 weeks	p-value
Number	41	79	
Serum Neudesin (ng/ml)	2.407 ± 0.603	2.354 ± 0.39	0.641

Correlation between serum neudesin and various metabolic parameters in GDM:

Table 5 shows the correlation between serum neudesin and various metabolic parameters in GDM patients. Neudesin was positively correlated with BMI, FBG, HbA1C, insulin, and HOMA-IR in both Pearson and Spearman analyses (p < 0.05), reinforcing its potential role in glucose metabolism and insulin resistance.

Neudesin as a predictor of GDM:

Table 6 summarizes logistic regression models predicting the development of GDM based on serum neudesin and other clinical parameters. In Model 1, neudesin was a strong

independent predictor (OR = 3.83, 95% CI: 2.01–7.28, p < 0.001). In Model 2, which included additional covariates, neudesin remained significant (OR = 2.51, 95% CI: 0.38–16.78, p = 0.034).

Table 4. Comparisons of the serum level of neudesin according to the body mass index in women with GDM.

	BMI less than 35 (kg/m2)	BMI 35-40 (kg/m2)	BMI more than 40 (kg/m2)	p-value
	N=49	N= 40	N=31	
Body Mass Index (kg/m2)	32.34± 1.706	37.14 ± 1.24	42.44 ± 3.61	0.000
Age (Years)	29.88 ± 5.87	29.6 ± 5.56	29.76 ± 6.08	0.979
FBG (mg/dL)	140.77 ± 24.21	141.01 ± 28.95	157.15 ± 44.59	0.208
HbA1c %	7.20 ± 1.08	7.40 ± 1.01	8.35± 1.19	0.008
Insulin(µU/mL)	7.45 ± 1.28	7.53 ± 1.34	7.89 ± 0.63	0.562
HOMA IR	2.66 ± 0.74	2.55 ± 0.64	3.05 ± 0.92	0.108
Total Cholesterol (mg/dL)	219.42± 64.16	234.58 ± 56.68	256.25 ± 59.51	0.109
Triglycerides (mg/dL)	183.82 ± 56.09	174.46 ± 40.57	191.91 ± 62.28	0.505
Serum Neudesin (ng/ml)	2.325 ± 0.53	2.417 ± 0.42	2.332 ± 0.46	0.699

Table 5. Correlation of the serum neudesin level with other parameters in pregnant women with gestational Diabetes.

	Pearson Correlation		Spearmen Corre	lation
	R	P	R	P
Age (Years)	0.032	0.726	0.052	0.572
Body Mass Index (kg/m2)	0.474	0.000	0.473	0.000
FBG (mg/dL)	0.606	0.000	0.636	0.000
HbA1c %	0.616	0.000	0.233	0.037
Insulin (µU/mL)	0.718	0.000	0.560	0.000
HOMA- IR	0.682	0.000	0.606	0.000
TyG index	0.505	0.000	0.117	0.301
TyG- BMI index	0.542	0.000	0.045	0.691
Gestational age (weeks)	0.138	0.132	0.074	0.421

Table 6. Combined Logistic Regression Results: Model 1 versus Model 2 for predicting neudesin in GDM development.

Predictor	Model 1 OR (95%	Model 1 p-value	Model 2 OR (95%	Model 2 p-		
	CI)		CI)	value		
Neudesin(ng/ml)	3.83 (2.01–7.28)	< 0.001	2.51 (0.38–16.78)	0.034		
Age (years)		_	1.11 (0.92–1.35)	0.269		
BMI (kg/m2)	_	_	1.07 (0.83–1.38)	0.608		
FBG (mg/dL)	_	_	2.45 (0.34–17.88)	0.377		
HbA1c%		_	0.87 (0.38–1.99)	0.740		
Cholesterol (mg/dL)	_	_	0.99 (0.98-1.01)	0.418		
Triglycerides	_	_	1.01 (0.99–1.03)	0.241		
(mg/dL)						

Diagnostic performance of serum neudesin for GDM:

ROC curve analysis demonstrated excellent diagnostic performance of serum neudesin for GDM prediction (AUC = 0.986) (Figure 1). The optimal cutoff of 1.1185 ng/ml provided 1005 sensitivity and 86.7% specificity, with a Youden index of 0.867 (Table 7).

Table 7 provides the optimal cutoff value for serum neudesin in distinguishing GDM from controls. A threshold of 1,1185 ng/ml yielded 100% sensitivity and 86.7% specificity, with a Youden index of 0.867 and a 95% confidence interval ranging from 1.050 to 1,19, highlighting its strong predictive utility.

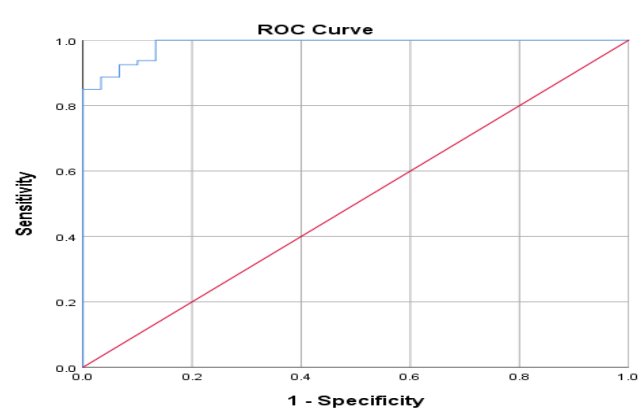


Figure 1. ROC curve analysis of neusidin for predicting GDM.

Table 7. The cut-off value of serum neusidin level that best predicts GDM versus the control.

	AUC	Cutoff value	Sensitivity	specificity	Youden Index	95% Confidence interval
Serum Neudesin (ng/ml)	0.986	1.1185 ng/ml	100 %	86.7%	0.867	1.050- 1.19

Discussion

Gestational diabetes mellitus (GDM) is a multifactorial condition characterized by glucose intolerance and insulin resistance during pregnancy. This study investigated the clinical and biochemical profiles of pregnant women with GDM with a particular focus on serum neudesin levels and their association with metabolic parameters. The findings provide compelling evidence for the role of neudesin as a potential biomarker and contributor to the pathophysiology.

As shown in Table 1, women with GDM exhibited significantly higher BMI, FBG, HbA1C, insulin levels, and HOMA-IR compared to controls (p< 0.001), consistent with previous studies that underscore insulin resistance as a hallmark of GDM (16,17). These alterations reflect the metabolic stress imposed by pregnancy, which is exacerbated in GDM due to impaired insulin signaling and signaling pathways. The lack of significant difference in age and gestational age between groups suggests that these metabolic changes are intrinsic to the disease process rather than confounded by demographic variables.

Table 2 revealed markedly elevated serum neudesin levels in the GDM group (p < 0.001), alongside increased HOMA-IR and TyG index-BMI. These findings suggest a strong association between neudesin and insulin resistance. Neudesin has been implicated in energy homeostasis and the regulation of the sympathetic system (18). Ohta et al. demonstrated that neudesin-deficient mice were resistant to diet-induced obesity and exhibited enhanced thermogenesis, suggesting that neudesin plays a role in metabolic suppression (19). The current data support a pathogenic role for neudesin in GDM, potentially through modulation of insulin sensitivity and energy expenditure.

In the current study, Table 3 showed no significant difference in neudesin levels between GDM patients below and above 30 weeks of gestation, indicating that neudesin expression remains stable across late pregnancy. This contrasts with other biomarkers such as leptin and CRP, which fluctuate with gestational age (20). The temporal stability of neudesin enhances its utility as a diagnostic marker, particularly for early screening Despite significant increases in BMI and HbA1c across BMI categories (Table 4), serum neudesin levels did not differ

significantly. This suggests that neudesin may be independent of adiposity in GDM, unlike adipokines such as adiponectin and resistin, which are closely linked to fat mass (21). The lack of correlation with BMI implies that neudesin reflects intrinsic metabolic dysfunction rather than being a secondary consequence of obesity.

In previous studies, Karatas et al. reported elevated neudesin levels in individuals with Type 2DM and obesity, with significant associations to insulin resistance markers (22). Our study mirrors these findings in a gestational context, suggesting that neudesin 's role in metabolic dysfunction may extend across different physiological states, including pregnancy.

Table 5 demonstrates strong positive correlations between neudesin and BMI, FBG, HbA1C, insulin, and HOMA-IR in both Pearson and Spearman analyses (p < 0.05), reinforcing its role in glucose metabolism. Interestingly, neudesin showed weaker or non-significant correlations with TyG indices and gestational age, suggesting specificity for insulin-related pathways. These findings are consistent with prior research linking neudesin to insulin resistance in both animal and human models (11, 23).

Logistic confirmed regression analysis significant independent neudesin as a predictor of GDM. In Model 1, neudesin had an odds ratio of 3.83 (p < 0.001) and remained important in Model 2 after adjusting for confounders (OR 2.51, p = 0.034). These results highlight the robustness of neudesin as The predictor marker. consistent significance across models supports the clinical relevance of this finding.

A pilot study by Eren et al. explored neudesin levels in pregnant women and found modest elevation in those with impaired glucose tolerance. However, their sample size was

limited (24). The current study builds upon this by demonstrating robust diagnostic performance with an AUC of 0.986, as illustrated in Figure 1 and Table 7, and identifying a precise cutoff value (1.1185 ng/mL) with high sensitivity and specificity, which was not previously established. The high odds ratio observed in this study suggests that a higher level of neudesin is a strong predictor of GDM, making it an effective marker for early risk stratification. Additionally, the excellent area under the curve further supports its diagnostic value.

If validated in larger cohorts, serum neudesin could be integrated into routine prenatal screening to identify women at high risk for GDM before onset. Adding neudesin to current tests, such as OGTT, fasting glucose, and HbA1c, may improve diagnostic precision and reduce false negatives. Incorporating this biomarker into AI-driven platforms could further enhance early prediction by analyzing complex biochemical patterns and enabling timely, personalized interventions, ultimately leading to improved maternal-fetal outcomes.

Conclusion

The findings of this study support the use of neudesin as a predictive tool for GDM. Its independent elevation in GDM, strong correlation with insulin resistance, and excellent AUC indicate it holds promise for clinical application. Moving forward, validating Neudesin through longitudinal studies, mechanistic investigations, and interventional trials will be crucial in determining its full potential, ultimately benefiting maternal and fetal health outcomes.

Source of funding: No source of funding.

Ethical clearance: The study received ethical approval from the Ethics Committee of the College of Science for Women, University of Baghdad (No. 22/8691, dated 16/12/2024). All information was used exclusively for scientific study, and participant confidentiality and data privacy were rigorously upheld. All participants provided written informed

consent, and confidentiality of medical records was maintained in accordance with ethical guidelines.

Conflict of interest: None.

Use of Artificial Intelligence (AI): The authors state they did not use any generative AI tools for creating or editing manuscript's language.

Acknowledgments: The authors thank the Department of Chemistry at the College of Science for Women, University of Baghdad, and the Department of Obstetrics and Gynecology at Al-Yarmouk **Teaching** Hospital for their support in completing this work

References

- 1. Baz B, Riveline JP, Gautier JF. Endocrinology of pregnancy: gestational diabetes mellitus: definition, aetiological and clinical aspects. European journal endocrinology. 2016 Feb;174(2):R43-51. https://doi.org/10.1530/EJE-15-0378.
- 2. Osmulski ME, Yu Y, Kuang A, Josefson JL, Hivert MF, Scholtens DM, Lowe Jr WL. Subtypes of gestational diabetes mellitus are differentially associated with newborn and childhood metabolic outcomes. Diabetes care. 2025 Mar 1;48(3):390-9. https://doi.org/10.2337/dc24-1735.
- 3. Sweeting A, Wong J, Murphy HR, Ross GP. A clinical update on gestational diabetes Oct mellitus. Endocrine reviews. 2022 1:43(5):763-93.

https://doi.org/10.1210/endrev/bnac003.

Haleem SA, Hamzah MI, Khudhair MS, Deli EQ. Assessment of Meteorin-like

Protein Serum Levels in Pre-diabetes and Newly Diagnosed Type 2 Diabetes Mellitus. AL-Kindy College Medical Journal. 2024 Apr 1;20(1):27-3.

https://doi.org/10.47723/vmsq2630.

5. Khashan IS, Majeed MJ. The Role of GABA and Insulin Regulated

Aminopeptidase on Insulin Resistance and GLUT4 in Prediabetes and Type 2 Diabetes Mellitus. AL-Kindy College Medical Journal. 2024 Apr 1;20(1):65-70.

https://doi.org/10.47723/6b3yqa81

6.Powe CE, Hivert MF, Udler MS. Defining heterogeneity among women with gestational diabetes mellitus. Diabetes. 2020 Oct 1:69(10):2064-74.

https://doi.org/10.2337/dbi20-0004

7. Ghildayal N, Allard C, Blais K, Doyon M, Arguin M, Bouchard L, Perron P, Hivert MF. Associations of maternal insulin sensitivity during pregnancy with childhood central adiposity in the Genetics of Glucose regulation in Gestation and Growth Pediatric (Gen3G) cohort. obesity. 2023 Feb:18(2):e12982.

https://doi.org/10.1111/ijpo.12982

8. Kimura I, Nakayama Y, Zhao Y, Konishi M, Itoh N. Neurotrophic effects of neudesin in the central nervous system. Frontiers in neuroscience. 2013 Jun25;7:111.

https://doi.org/10.3389/fnins.2013.00111

- 9. Ohta H, Konishi M, Kobayashi Y, Kashio A, Mochiyama T, Matsumura S, Inoue K, Fushiki T, Nakao K, Kimura I, Itoh N. Deletion of the neurotrophic factor neudesin prevents diet-induced obesity by increased sympathetic activity. Scientific reports. 2015 May 8;5(1):10049. https://doi.org/10.1038/srep10049
- 10.Bozkaya G, Fenercioglu O, Demir İ, Guler A, Aslanipour B, Calan M. Neudesin: a neuropeptide hormone decreased in subjects with polycystic ovary syndrome. Gynecological Endocrinology. 2020 Oct 2;36(10):849-53.

https://doi.org/10.1080/09513590.2020.1751106

11.Ohta H, Kimura I, Konishi M, Itoh N. Neudesin as a unique secreted protein with multi-functional roles in neural functions, energy metabolism, and tumorigenesis. Frontiers in molecular biosciences. 2015 May 19:2:24.

https://doi.org/10.3389/fmolb.2015.00024

12. Nakayama Y, Masuda Y, Mukae T, Mikami T, Shimizu R, Kondo N, Kitagawa H, Itoh N, Konishi M. A secretory protein neudesin regulates splenic red pulp macrophages in erythrophagocytosis and iron recycling. Communications Biology. 2024 Jan 25;7(1):129.

https://doi.org/10.1038/s42003-024-05802-9

13. Hameed EK, Al-Ameri LT, Hasan HS,

Abdulqahar ZH. The cut-off values of triglycerides-glucose index for metabolic syndrome associated with type 2 diabetes mellitus. Baghdad Science Journal. 2022;19(2):7.

https://doi.org/10.21123/bsj.2022.19.2.0340

14.Hameed EK. TyG index a promising biomarker for glycemic control in type 2 Diabetes Mellitus. Diabetes and Metabolic Syndrome: Clinical Research and Reviews. 2019 Jan 1;13(1):560-3. https://doi.org/10.1016/j.dsx.2018.11.030

15.Gayoso-Diz P, Otero-González A, Rodriguez-Alvarez MX, Gude F, García F, De Francisco A, Quintela AG. Insulin resistance (HOMA-IR) cut-off values and the metabolic syndrome in a general adult population: effect of gender and age: EPIRCE cross-sectional study. BMC endocrine disorders. 2013 Oct 16;13(1):47.

https://doi.org/10.1186/1472-6823-13-47

16. Plows JF, Stanley JL, Baker PN, Reynolds CM, Vickers MH. The pathophysiology of gestational diabetes mellitus. International journal of molecular sciences. 2018 Oct 26;19(11):3342.

https://doi.org/10.3390/ijms19113342

17. Hassan HJ, Mohammad TU, Hameed EK. Assessment of serum metalloendopeptidase level in patients with double diabetes. AL-Kindy College Medical Journal. 2023 Dec 30;19(3):21-5.

https://doi.org/10.47723/kcmj.v19i3.999

18.Kimura I, Yoshioka M, Konishi M, Miyake A, Itoh N. Neudesin, a novel secreted protein with a unique primary structure and neurotrophic activity. Journal of neuroscience research. 2005 Feb 1;79(3):287-94.

https://doi.org/10.1002/jnr.20356

19. Bahar S, Özgen İT, Cesur Y, Yıldız C, Özer ÖF, Kaplan EH, Sütçü ZK. Serum

Neudesin Levels in Patients with Congenital Hypothyroidism. Journal of clinical research in pediatric endocrinology. 2025 Jan 24. https://doi.org/10.4274/jcrpe.galenos.2025.2024-1-14

20.Catalano PM, Hauguel-De Mouzon S. Is it time to revisit the Pedersen hypothesis in the face of the obesity epidemic? American journal of obstetrics and gynecology. 2011 Jun 1;204(6):479-87. https://doi.org/10.1016/j.ajog.2010.11.039

21.Retnakaran R, Hanley AJ, Raif N, et al. Adiponectin and resistin in pregnancy. *J Clin Endocrinol Metab.* 2004;89(3):1174–1178.

22.Karatas O, Calan M, Yuksel A, Chousein R, Bozkaya G, Karatas M, Uslu A, Tatar E. The level of the neudesin in type-2 diabetic patients and the relationship between the metabolic parameters and carotid intima-media thickness. Minerva Endocrinology. 2021 Jan 12;48(3):288-94. https://doi.org/10.23736/s2724-6507.20.03217-4

23. Vergani E, Bruno C, Cipolla C, Currò D, Mancini A. Plasma levels of neudesin and glucose metabolism in obese and overweight children. Frontiers in Endocrinology. 2022 Jul 14;13:881524. https://doi.org/10.3389/fendo.2022.881524

24. Eren EÇ, Kaya S, Argun D. The assessment of maternal and umbilical cord neudesin levels in pregnancies with gestational diabetes mellitus. Journal of Obstetrics and Gynaecology. 2022 Oct 3;42(7):2941-5.

https://doi.org/10.1080/01443615.2022.2114328

مستوى النيوديسين في مصل الدم لدى النساء المصابات بسكري الحمل: علامة حيوية محتملة للتنبؤ بالمرض

ا الاء جمعة إسماعيل، الريج شوكت حميد، الخلاص خالد حميد

الملخص

الخلفية: يعد التصنيف الدقيق لخلايا الدم أمرًا بالغ الأهمية لتشخيص وإدارة اضطرابات الدم. حيث أن التقييمات اليدوية التقليدية لمسحات الدم تتطلب جهدًا كبيرًا وتخضع للتباين بين المختصين، مما قد يهدد موثوقية التشخيص. يُعد داء السكري الحملي (GDM) من الاضطرابات الأيضية الشائعة المرتبطة بالحمل، ويرتبط بمقاومة الإنسولين وضعف تحمل الجلوكوز. يُعتقد أن نيوديسين، وهو ببتيد تنظيمي يشارك في عملية أيض الجلوكوز، قد يكون علامة حيوية جديدة لداء السكري الحملي، إلا أن دوره لا يزال غير واضح.

الأهداف: تقييم القيمة التنبؤية لنيوديسين في داء السكري الحملي، ودراسة ارتباطه بمؤشرات مقاومة الإنسولين ومؤشرات التحكم في سكر الدم..

المواد والطرق: تم إجراء دراسة حالة ضبط شملت ٢٠٠ امرأة حامل، من بينهن ١٢٠ مصابة بداء السكري الحملي و ٨٠ من الأصحاء كمجموعة ضابطة. تم قياس المؤشرات الجسمانية، وسكر الدم الصائم (FBG)، والهيمو غلوبين السكري (HbA1c)، والإنسولين، ومؤشر TyG-BMI، ومؤشر TyG-BMI، أجريت تحليلات الارتباط والانحدار ومؤشر TyG، ومؤشر TyG-BMI. أجريت تحليلات الارتباط والانحدار اللوجستي لاستخدام تقنية العلاقات والقيمة التنبؤية.

النتائج: أظهرت النساء المصابات بداء السكري الحملي مستويات أعلى بشكل ملحوظ من نيوديسين في الدم مقارنةً بالمجموعة الضابطة (7,707 و7,707 بنانوغرام/مل، 1,707 بنانوغرام/مل، 1,707 بكانت مستويات نيوديسين مرتبطة ارتباطًا إيجابيًا بمؤشر كتلة الجسم (1,707 والإنسولين، ومؤشر (1,700 Homa-IR)، وسكر الدم الصائم، و1,700 Hbeats والإنسولين، ومؤشر (1,700 Hbeats)، ومؤشر الدم الصائم، و1,700 Hbeats والإنسولين، ومؤشر (1,700 Hbeats)، مع قيمة قطع تبلغ أن نيوديسين يُعد مؤشرًا مستقلًا للتنبؤ بـ 1,700 كما أظهرت تحليلات منحنى 1,700 دقة تشخيصية عالية (1,700 Auc على مما يوفر حساسية بنسبة 1,700 وخصوصية بنسبة 1,700 بيكوغرام/مل، مما يوفر حساسية بنسبة 1,700 وخصوصية بنسبة 1,700

الاستنتاج : ترتفع تركيزات نيوديسين في الدم بشكل ملحوظ لدى المصابات بداء السكري الحملي، وترتبط ارتباطًا قويًا بدرجة مقاومة الإنسولين وضعف التحكم في سكر الدم. وقد يُعد نيوديسين علامة حيوية واعدة للتشخيص المبكر وهدفًا محتملاً لإدارة داء السكري الحملي.

الكلمات المفتاحية: سكري الحمل، نيوديسين، مقاومة الإنسولين، العلامات الحيوية.

المؤلف المراسل: إخلاص خالد حميد

ikhlaskhalid@yahoo.com الايميل:

تاريخ الاستلام: ٩ تموز ٢٠٢٥

تاریخ القبول: ۸ أیلول ۲۰۲۵

تاريخ النشر: ٢٠ تشرين الأول ٢٠٢٥

ا قسم الكيمياء، كلية العلوم للبنات، جامعة بغداد، بغداد، العراق. كلية الطب الكندي، جامعة بغداد، بغداد، العراق.

Association Between Uremic Pruritus and Differential Leukocyte Counts Among Hemodialysis Patients in Ibn Sina Dialysis Center

Hiba M. Al-Darraji (1)¹, Ismail Ibrahim Latif (1)¹, Fatimah khazaal khamees Al-majmaie (1)², Nabeel Khalid Al Wandi (1)³

OPEN ACCESS

Correspondence: Hiba M. Al-Darraji Email: hiba.m@uodiyala.edu.iq Copyright: ©Authors, 2025, College of Medicine, University of Diyala. This is an open

access article under the CC BY 4.0 license (http://creativecommons.org/licenses/by/4.0/) Website:

https://djm.uodiyala.edu.iq/index.php/djm

Received: 30 September 2024 Accepted: 02 June 2025 Published: 25 October 2025

Abstract

Background: Pruritus is a common and bothersome symptom of chronic kidney disease (CKD). According to the most recent epidemiologic data, about 40% of patients with end-stage renal disease (ESRD) experience moderate to severe pruritus. The reason for uremic pruritus remains poorly understood, but recent studies suggest a strong association with the inflammatory process and elevated white blood cell (WBCs).

Objectives: This study aims to investigate the correlation between uremic pruritus (UP) and differential leukocyte levels in patients with CKD undergoing dialysis (Hemodialysis patients), and to examine the potential role of inflammation in the severity of pruritus.

Patients and Methods: A study was conducted at Ibn Sina Dialysis Center, Diyala Governorate, Iraq. The study involved 150 hemodialysis (HD) patients, divided into two groups: 75 patients with UP and 75 without UP. The control group consisted of 26 healthy individuals. Out of 226 HD patients at the Dialysis Center, those under 20 years old, as well as patients with hepatitis C or hepatitis B, were excluded. From each patient and control in this study, 3 ml of venous blood was collected before dialysis, placed in an ethylene diamine tetraacetic acid (EDTA) tube for leukocyte differential count, and analyzed at the educational laboratory of Baqubah Teaching Hospital.

Results: The results showed that 33.8% of HD patients had uremic pruritus and had a significantly higher eosinophil level when compared with patients without UP and controls. While basophil and neutrophil showed no significant difference in patients with UP and without UP when compared with the control. When compared to patients without UP, HD patients with UP had higher lymphocyte counts; however, there was no discernible difference between the control group, hemodialysis patients with UP, and patients without UP.

Conclusion: It was shown that eosinophils may play an essential role in the pathogenesis of UP by inducing and secreting materials that exacerbate its severity. Lymphocytes can also play a role in the pathogenesis of UP by secreting cytokines.

Keywords: Uremic pruritus, Leukocytes, Hemodialysis, Diyala, Eosinophil.

Introduction

Uremic pruritus is a common, unpleasant symptom of CKD, and it's linked to a lower quality of life and bad outcomes. It's now widely acknowledged as a major research priority (1). Chargin and Keil

¹ Department of Microbiology, College of Medicine, University of Diyala, Diyala, Iraq.

² Çankırı karatekin üniversitesi, Çankırı, Turkey.

³ Directorate of Health, Baqubah teaching hospital, Diyala, Iraq.

ORIGINAL RESEARCH Published: 25 October 2025

DOI: 10.26505/djm.v29i1.1121

first reported on uremic pruritus in 1932 (2). It occurs as a frequent or near-daily incidence of itch that spans large bilaterally symmetrical surface areas (3). It is an unpleasant sensation that has been recognized as a frequent complication in patients with chronic kidney disease (4,5). One of the most common and burdensome dermatological symptoms affecting patients undergoing dialysis is CKD-associated pruritus (CKD-aP) (6). Skin pruritus can affect any part of the body and last for various durations, resulting in secondary scratches. Nodular prurigo, for example, is a moss-like skin condition that has a significant impact on the patient's physical and mental health (7). It affects more than one-third of dialysis patients and has an incidence of 15% to 49% (5). Thirty percent to sixty percent of patients in this group had symptoms for more than a year (8). As CKD progresses and the incidence of pruritus increases, the patient's quality of life deteriorates. According to some studies, uremic pruritus is linked to a greater risk of mortality in patients with chronic kidney disease (9). CKD was recognized as a cause of immune dysfunction that arises from a combination of factors, including uremia, malnutrition, chronic inflammation, and mineral bone disease (10). The toxic metabolic wastes accumulate in uremic states, promoting cytokine accumulation and persistent systemic inflammation, which causes acquired immune suppression due to the depletion of immune cells from low-grade persistent inflammation (11). The immune dysfunction is a risk factor for progression and mortality of CKD (12). Since a high total white blood cell (WBC) count often indicates inflammation and a low lymphocyte count indicates immune suppression, a high WBC count and a low lymphocyte count in patients with CKD are associated with a worse prognosis (13,14).

Another study has highlighted the immunological mechanisms contributing to uremic pruritus,

indicating that it is closely related to systemic immune dysregulation and not merely a dermatologic or neurological condition. Patients on hemodialysis who experience pruritus have been found to have elevated white blood cell (WBC) counts, specifically eosinophils, basophils, and neutrophils. This suggests an inflammatory state that could play a role in the pathophysiology of the uremic pruritus (15). The interaction between uremic toxins and immune cells leads to chronic immune activation, promoting pruritogenic signaling (16). These findings suggest a possible inflammatory or immunological role in the pathogenesis of uremic pruritus, and understanding these immunological contributors is essential for developing targeted therapies (17).

Patients and Methods

Study design: This study was conducted on HD patients to assess the levels of different leukocytes in those with uremic pruritus. It took place at Ibn Sina Dialysis Center in Diyala, Iraq. During this period, the center had 226 patients. Patients under 20 years old, as well as those with hepatitis C and hepatitis B, were excluded, resulting in a study group of 150 patients (75 with UP and 75 without UP).

Questionnaire: A questionnaire was prepared, distributed, and collected from each patient and control group. Patients answered the questions in the Dialysis Center. For each case of uremic pruritus, a questionnaire was used to gather demographic information about age, sex, duration of dialysis, number of dialysis sessions per week, number of hours per dialysis session per day, and the severity of uremic pruritus.

Visual analyze scale: A VAS was used, which is a technique for converting non-numeric values into numeric values. It is a 10-point scale, with 0 indicating no pruritus and 10 indicating severe pruritus. One-centimeter intervals differentiate the numerical values. The categorization by Reich et al. was used as a reference when

relationship between variables.

classifying the VAS score. They classified the severity of pruritus as follows: < 4 points was considered mild; ≥ 4 points but < 7 points was moderate; ≥ 7 points but < 9 points was severe; and ≥ 9 points was very severe pruritus (18).

Sample preparation and storage: All patients were examined by a dermatologist referred from Ibn Sina Dialysis Center. From each patient and control in this study, 3 ml of venous blood was collected before dialysis under complete aseptic conditions and put in an ethylene diamine tetraacetic (EDTA) tube (to prevent coagulation) for leukocyte differential. We utilized the DxH 520 Hematology Analyzer to measure white blood cell (WBC) counts in whole blood samples. The reference range for WBC counts in this analysis was established between 4,000 and 11,000 cells per microliter. **Differential** leukocytes were recorded: eosinophils, basophils, neutrophils, and lymphocytes. These measurements are performed in educational Laboratories in Baqubah Teaching Hospital.

Statistical Analysis

The data processing software package is used (SPSS, 2020) for Windows. Data are expressed as mean \pm standard error (M \pm SE). Differences between the means of the two major groups are analyzed using a t-test, and significance is tested at a two-tailed P-value. However, differences among subgroups are analyzed using one-way analysis of variance (ANOVA). If a significant difference is found, it is further analyzed using the least significant difference test (LSD). The Pvalue of differences <0.05 is considered significant. The Pearson correlation (R) accounted for the type and strength of the

Results

Characterization of patients with pruritus under hemodialysis session: Table 1 shows the demographic and clinical characteristics of 75 patients undergoing hemodialysis with uremic pruritus. The age of the participants ranged from 20 to 70 years. Regarding the duration of hemodialysis, a higher proportion of patients (56%) had been on dialysis for more than 6 months, while 44% had been receiving treatment for less than 6 months. The data also show a male predominance among the pruritus cases, with 60% of patients being male and 40% female. In terms of itch distribution, 65.3% of patients reported localized pruritus, whereas 34.6% experienced generalized itching. Concerning the severity of itch, most patients (56%) reported moderate pruritus, followed by severe itching in 26.6%, and mild symptoms in 17.3% of the cases. The table also outlines the main risk factors associated with chronic kidney disease (CKD) in these patients. Hypertension was the most commonly reported risk factor (32%), followed by diabetic mellitus (17.3%) and kidney stones (17.3%).Chronic glomerulonephritis accounted for 12%, interstitial nephritis and unknown causes each for 8%, and polycystic kidney disease was identified in 5.3% of the cases. This data provides an overview of the key demographic, clinical, and etiological features of uremic pruritus in hemodialysis patients.

Table 1. Characterization of uremic pruritus patients under hemodialysis treatments.

Age (year)	Range (20-70)			
Duration of Hamadialysis	More than 6 months	N= 42		
Duration of Hemodialysis	Less than 6 months	N= 33		
Corr	Men	N= 45	(60 %)	
Sex	Women	N= 30	(40 %)	
Tyme of itah	Localize	N= 49	(65.3 %)	
Type of itch	Generalize	N= 26	(34.6 %)	
	Mild	N= 13	(17.3 %)	
Severity of itch	Moderate	N= 42	(56 %)	
	Sever	N= 20	(26.6 %)	
	Hypertension	N= 24	(32 %)	
	Diabetic Mulitas	N= 13	(17.3 %)	
	Kidney Stone	N=13	(17.3 %)	
Risk factor of CKD	Chronic Glomerulonephritis	N= 9	(12 %)	
	Interstitial Nephritis	N= 6	(8 %)	
	Polycystic Kidney Disease	N= 4	(5.3 %)	
	Unknown	N= 6	(8 %)	
Characteristics of Patients with	Pruritus under hemodialysis treatn	nents $N = 75$		

Differential leukocytes among patients with uremic pruritus and without uremic pruritus: Eosinophils increased significantly in hemodialysis patients with uremic pruritus $(0.24 \pm 0.02 \times 10^9 L)$ when compared with control $(0.14 \pm 0.02 \times 10^{9})$ (p-value= 0.010), and patients without uremic pruritus (0.09 \pm $0.00 \times 10^9 / L$) (p-value= 0.000), but the results showed no any significant differences between hemodialysis patients without uremic pruritus and control group (p-value= 0.137). Basophils and neutrophils cells showed a significant increase in hemodialysis patients with pruritus $(0.04 \pm 0.00 \times 10^{9} / L, \text{ and } 4.29)$ \pm 0.17 x 10⁹ /L, respectively) (p-value= 0.000 and 0.001, respectively) and patients without pruritus $(0.04 \pm 0.00 \times 10^{9} / L)$, and

 $4.29 \pm 0.17 \text{ x } 10^9 \text{ /L}$, respectively) (p-value= 0.000 and 0.005, respectively) when compare with control ($0.02 \pm 0.00 \text{ x } 10^9 \text{ /L}$, and $3.17 \pm 0.19 \text{ x } 10^9 \text{ /L}$, respectively). At the same time, it did not show any significant differences between hemodialysis patients with and without uremic pruritus (p-value= 0.051 and 0.376).

Lymphocytes increased significantly in hemodialysis patients with uremic pruritus (1.77 \pm 0.06 x 10^9 /L) when compared with patients without uremic pruritus (1.60 \pm 0.04 x 10^9) (p-value 0.002). The results showed non-significant differences between hemodialysis patients with uremic pruritus and the control group (p-value = 0.094) and patients without uremic pruritus and the control group (p-value = 0.938) (Table 2).

Table 2. Differential leukocytes among patients with uremic pruritus, without uremic pruritus, and controls.

Groups	Eosinophils x10^9 /L (Mean ± SE)	Basophils x10^9/L (Mean ± SE)	Neutrophils x10^9 /L (Mean ± SE)	Lymphocytes x10^9 /L (Mean ± SE)
Patients with uremic Pruritus (N=75)	0.24 ± 0.02	0.04 ± 0.00	4.54 ± 0.24	1.77 ± 0.06
Patients Without Uremic Pruritus (N=75)	0.09 ± 0.00	0.04 ± 0.00	4.29 ± 0.17	1.60 ± 0.04
Control (N=26)	0.14 ± 0.02	0.02 ± 0.00	3.17 ± 0.19	1.59 ± 0.08
P-value*	P vs W, P= 0.000 C vs P, p= 0.010 C vs W, P= 0.137	P vs W, P= 0.051 C vs P, p= 0.000 C vs W, P= 0.000	P vs W, P= 0.376 C vs P, p= 0.001 C vs W, P=0.005	P vs W, P= 0.002 C vs P, p= 0.094 C vs W, P= 0.938
P value <0.05, SE: standar	d error, C: control, P:	pruritus, and W.P: w	ithout pruritus.	

Differential leukocytes among mild, moderate, and severe itch groups: Eosinophils showed no significant difference among patients with mild, moderate, and severe itch $(0.28 \pm 0.07, 0.20 \pm 0.02, \text{ and } 0.29)$ \pm 0.06, respectively), with p-values of 0.341, 0.901, and 0.181, respectively. Additionally, basophils showed non-significant differences among patients with mild, moderate, and severe itch $(0.04 \pm 0.00, 0.04 \pm 0.00, \text{ and } 0.04)$ \pm 0.02, respectively), with p-values of 0.351,

0.639, and 0.634, respectively. Neutrophils showed no significant difference among patients with mild, moderate, and severe itch $(4.36 \pm 0.48, 4.78 \pm 0.35, \text{ and } 4.13 \pm 0.42, \text{ respectively})$, with p-values of 0.530, 0.762, and 0.261, respectively. Lymphocytes showed no significant differences among patients with mild, moderate, and severe itch $(1.68 \pm 0.12, 1.79 \pm 0.88, \text{ and } 1.92 \pm 0.15, \text{ respectively})$, with p-values 0.551, 0.253, and 0.421, respectively (Table 3).

Table 3. Leukocytes and differential among mild, moderate, and severe itch groups.

Groups	Basophils x10^9 /L (Mean ± SE)	Neutrophils x10^9 /L (Mean ± SE)	Eosinophils x10^9 /L (Mean ± SE)	Lymphocytes x10^9/L (Mean ± SE)	
Patients with mild itch (N=13)	0.04 ± 0.00	4.36 ± 0.48	0.28 ± 0.07	1.68 ± 0.12	
Patients with moderate itch (N=42)	0.04 ± 0.00	4.78 ± 0.35	0.20 ± 0.02	1.79 ± 0.88	
Patients with severe (N=20)	0.04 ± 0.02	4.13 ± 0.42	0.29 ± 0.06	1.92 ± 0.15	
P-value*	MI vs MO, p= 0.351 MI vs S, p= 0.639 MO vs S, p= 0.634	MI vs MO, p= 0.530 MI vs S, p= 0.762 MO vs S, p= 0.261	MI vs MO, p= 0.314 MI vs S, p= 0.901 MO vs S, p= 0.181	MI vs MO, p= 0.551 MI vs S, p= 0.253 MO vs S, p= 0.421	
P value <0.05, MI mild, MO moderate, and S severe.					

Discussion

this study, eosinophils increased significantly in hemodialysis patients with uremic pruritus compared to the control group patients without uremic pruritus. and However, there were no significant differences between hemodialysis patients without uremic pruritus and the control group. According to another study, an increase in eosinophils caused by various conditions facilitates the recruitment of type 2 helper T (Th2) cells and cytokine-induced activation of eosinophils, resulting in the release of these molecules and subsequent effects on the affected tissues (19). Kojima et al demonstrated that an allergic reaction to HDmaterials related may have induced eosinophilia, and the resultant increase in eosinophils might cause allergic symptoms such as itching (20). Keithi-Reddy et al described a case of uremic pruritus in which the eosinophil count in the peripheral blood was 24 percent and the skin biopsy revealed eosinophil infiltration. The authors stated that the uremic condition most likely caused the eosinophilia, and that histamine release was involved in the pathogenesis (21). In another study, it was reported that eosinophil levels increase in patients who suffer from pruritus. The increase in eosinophils is standard in Hemodialysis patients and is mainly induced by allergy to material of the dialysis circuit (22). In this study, Basophils and neutrophil cells showed a significant increase in hemodialysis patients with pruritus, as well as in those without pruritus, compared to controls. However, there were no significant differences between hemodialysis patients with and without uremic pruritus. A study by Pisonin et al also showed that no significant relationship was seen between neutrophil counts or neutrophil percentage and pruritus (23). This study agrees with the results

obtained by Diehn and Tefferi, who found no significant correlation between pruritus and basophil count (24). In this study, lymphocytes increased significantly in hemodialysis patients with UP compared to those without UP. However, the results showed no significant differences between hemodialysis patients with uremic pruritus and the control group, nor between patients without uremic pruritus and the control group. The alterations in host immune response have primarily been studied in ESRD patients. The function of lymphocytes, monocytes, and polymorphonuclear white blood cells is altered, resulting in an impaired host response to infection (25). In a study by Alshafei and Nour, it was shown that the total number of lymphocytes significantly decreased in patients with pruritus compared to control patients (those without uremic pruritus under hemodialysis) (26). The same result was found in a study by Litjens et al, which suggested that patients with CKD suffer from inflammation and low levels of lymphocytes (27). The result was also supported by a study by Ommen et al, who found that lymphopenia in ESRD patients (28). Vaziri indicates that the accumulation of uremic toxins could lower the number of T-lymphocytes (29). In Turkey, a study by Ozen et al found that a WBC count was a risk factor for UP development in HD patients, with elevated WBC levels (30). A previous study showed that inflammation and proinflammatory factors are essential in development of UP (31). Ghassan et al indicate that there is no significant difference in WBC count was found in the patients who had no pruritus compared with patients with mild, moderate and severe pruritus (32), similar to the results of a study to Chiu et al which found there was no significant difference in WBC count between patients with uremic pruritus and patients without pruritus (33). In a recent study, Rowee and Yosipovitch found that Cutaneous T-cell lymphoma may cause unmanageable pruritus and may have the cytokine interleukin 31 as a mediator of itching (34). In this

study, eosinophils showed no significant differences among patients with mild, moderate, and severe itching. Also, basophils, neutrophils, and lymphocytes showed no significant differences among patients with mild, moderate, and severe itching. A study in Baghdad by Ghassan et al found that there is no significant correlation between the severity of pruritus in pruritic patients and both WBC and neutrophil counts (32). This may be attributed to the fact that WBC and neutrophil counts were within the normal range in most patients involved in the study. eosinophil levels are linked to more severe pruritus and a lower quality of life, according to a strong association between the absolute eosinophil count (AEC) and the Dermatology Life Quality Index (DLQI). Eosinophils are implicated in pruritic dermatoses (35).

Conclusion:

Uremic pruritus is a complex condition influenced by multiple factors, including inflammation and WBC counts. The result showed that eosinophils may play an important role in the pathogenesis of uremic pruritus by inducing and secreting materials that increase the severity of UP. Lymphocytes can also play a role in the pathogenesis of UP by secreting and inducing cytokines that cause UP. Further research is needed to explain the mechanisms and develop effective treatments.

Source of funding: No source of funding.

Ethical clearance: The patients and control participants completed the questionnaire in the study and provided a blood sample. The Ethical Approval Committee at the College of Medicine, University of Diyala, approved this study (Code no. 2025HMJ900).

Conflict of interest: None.

Use of Artificial Intelligence: The authors declare that they did not use generative artificial intelligence for the creation or preparation of this manuscript.

Acknowledgments: The author would like to thank the Health and Education Directorates of Diyala for their support and assistance in conducting this study. The author appreciates the cooperation of patients who agree to participate in the study.

References

- 1. Trachtenberg AJ, Collister D, Rigatto C. Recent advances in the treatment of uremic pruritus. Current opinion in nephrology and hypertension. 2020 Sep 1;29(5):465-70. https://doi.org/10.1097/MNH.000000000000000055
- 2. CHARGIN L, KEIL H. Skin diseases in nonsurgical renal disease. Archives of Dermatology and Syphilology. 1932 Aug 1;26(2):314-35. https://doi.org/10.1001/archderm.1932.014500303 11010
- 3. Simonsen E, Komenda P, Lerner B, Askin N, Bohm C, Shaw J, Tangri N, Rigatto C. Treatment of uremic pruritus: a systematic review. American Journal of Kidney Diseases. 2017 Nov 1;70(5):638-55. https://doi.org/10.1053/j.ajkd.2017.05.018
- 4. Okada K, Matsumoto K. Effect of skin care with an emollient containing a high water content on mild uremic pruritus. Therapeutic Apheresis and Dialysis. 2004 Oct;8(5):419-22. https://doi.org/10.1111/j.1526-0968.2004.00175.x
- 5. Narita I, Iguchi S, Omori K, Gejyo F. Uremic pruritus in chronic hemodialysis patients. Journal of nephrology. 2008 Mar 1;21(2):161-5.
- Białynicki-Birula Świerczyńska K, Szepietowski JC. Chronic intractable pruritus in chronic kidney disease patients: prevalence, impact, and management challenges—a narrative review. Therapeutics and Clinical Risk Management. 2021 Nov 30:1267-82. https://doi.org/10.2147/TCRM.S310550
- 7. Min JW, Kim SH, Kim YO, Jin DC, Song HC, Choi EJ, Kim YL, Kim YS, Kang SW, Kim NH, Yang CW. Comparison of uremic pruritus between patients undergoing hemodialysis and peritoneal dialysis. Kidney research and clinical practice. 2016 Jun 1;35(2):107-13. https://doi.org/10.1016/j.krcp.2016.02.002

8. Ko MJ, Wu HY, Chen HY, Chiu YL, Hsu SP, Pai MF, Lai CF, Lu HM, Huang SC, Yang SY, Wen SY. Uremic pruritus, dialysis adequacy, and metabolic profiles in hemodialysis patients: a prospective 5-year cohort study. PloS one. 2013

Aug6;8(8):e71404.

https://doi.org/10.1371/journal.pone.0071404

- 9. Adejumo OA, Akinbodewa AA, Okaka EI, Alli OE, Ibukun IF. Chronic kidney disease in Nigeria: Late presentation is still the norm. Nigerian Medical Journal. 2016 May 1;57(3):185-9. https://doi.org/10.4103/0300-1652.184072
- 10. Fernandes SC, Ferreira AC. Immune dysfunction in chronic kidney disease. Port J Nephrol Hypert. 2021 Dec;35(4):247-50. http://doi.org/10.32932/pjnh.2021.12.159
- 11. Kurts C, Panzer U, Anders HJ, Rees AJ. The immune system and kidney disease: basic concepts and clinical implications. Nature Reviews Immunology. 2013 Oct;13(10):738-53. https://doi.org/10.1038/nri3523
- 12. Silverstein DM. Inflammation in chronic kidney disease: role in the progression of renal and cardiovascular disease. Pediatric nephrology. 2009 Aug;24(8):1445-52. https://doi.org/10.1007/s00467-008-1046-0
- 13. Kovesdy CP, George SM, Anderson JE, Kalantar-Zadeh K. Outcome predictability of biomarkers of protein-energy wasting and inflammation in moderate and advanced chronic kidney disease. The American journal of clinical nutrition. 2009 Aug 1;90(2):407-14. https://doi.org/10.3945/ajcn.2008.27390
- 14. Kim SM, Kim HW. Relative lymphocyte count as a marker of progression of chronic kidney disease. International urology and nephrology. 2014 Jul;46(7):1395-401. https://doi.org/10.1007/s11255-014-0687-0
- 15. Ko MJ, Peng YS, Chen HY, Hsu SP, Pai MF, Yang JY, Wen SY, Jee SH, Wu HY, Chiu HC. Interleukin-31 is associated with uremic pruritus in patients receiving hemodialysis. Journal of the American Academy of Dermatology. 2014 Dec 1;71(6):1151-9. https://doi.org/10.1016/j.jaad.2014.08.004
- 16. Schricker S, Kimmel M. Unravelling the pathophysiology of chronic kidney disease-associated pruritus. Clinical Kidney Journal. 2021 Dec;14(Supplement_3):i23-31. https://doi.org/10.1093/ckj/sfab200
- 17. Verduzco HA, Shirazian S. CKD-associated pruritus: new insights into diagnosis, pathogenesis, and management. Kidney International Reports. 2020 Sep

1;5(9):1387-402.

https://doi.org/10.1016/j.ekir.2020.04.027

18. Reich A, Heisig M, Phan NQ, Taneda K, Takamori K, Takeuchi S, Furue M, Blome C, AUgUSTIN M, STäNDER S, SzEPIETOWSKI JC. Visual analogue scale: evaluation of the instrument for the assessment of pruritus. Acta dermatovenereologica. 2012;92(5):497-501.

https://doi.org/10.2340/00015555-1265

- 19. Hogan SP, Rosenberg HF, Moqbel R, Phipps S, Foster PS, Lacy P, Kay AB, Rothenberg ME. Eosinophils: biological properties and role in health and disease. Clinical & Experimental Allergy. 2008 May;38(5):709-50. https://doi.org/10.1111/j.1365-2222.2008.02958.x
- 20. Kojima K, Oda K, Homma H, Takahashi K, Kanda Y, Inokami T, Uchida S. Effect of vitamin E-bonded dialyzer on eosinophilia in haemodialysis patients. Nephrology Dialysis Transplantation. 2005 Sep 1;20(9):1932-5. https://doi.org/10.1093/ndt/gfh912
- 21. Keithi-Reddy SR, Patel TV, Armstrong AW, Singh AK. Uremic pruritus. Kidney international. 2007 Aug 1;72(3):373-7. https://doi.org/10.1038/sj.ki.5002197
- 22. Hildebrand S, Corbett R, Duncan N, Ashby D. Increased prevalence of eosinophilia in a hemodialysis population: Longitudinal and case control studies. Hemodialysis International. 2016 Jul:20(3):414-20.

https://doi.org/10.1111/hdi.12395

23. Pisoni RL, Wikström B, Elder SJ, Akizawa T, Asano Y, Keen ML, Saran R, Mendelssohn DC, Young EW, Port FK. Pruritus in haemodialysis patients: International results from the Dialysis Outcomes and Practice Patterns Study (DOPPS). Nephrology Dialysis Transplantation. 2006 Dec 1;21(12):3495-505.

https://doi.org/10.1093/ndt/gfl461

- 24. Diehn F, Tefferi A. Pruritus in polycythaemia vera: prevalence, laboratory correlates and management. British journal of haematology. 2001 Dec;115(3):619-21. https://doi.org/10.1046/j.1365-2141.2001.03161.x
- 25. Minnaganti VR, Cunha BA. Infections associated with uremia and dialysis. Infectious Disease Clinics. 2001 Jun 1;15(2):385-406. https://doi.org/10.1016/S0891-5520(05)70152-5
- 26. KAMAL AL SHAFEI N, NOUR A. CBC, serum proteins, and Immunoglobulins in chronic

hemodialysis patients with or without pruritus in Egypt. Biochemistry & Analytical Biochemistry. 2016;5(01):1-7. https://doi.org/10.4172/2161%E2%80%9010 09.1000246

- 27. Litjens NH, van Druningen CJ, Betjes MG. Progressive loss of renal function is associated with activation and depletion of naive T lymphocytes. Clinical immunology. 2006 Jan 1;118(1):83-91. https://doi.org/10.1016/j.clim.2005.09.007
- 28. Ommen SR, Hodge DO, Rodeheffer RJ, McGregor CG, Thomson SP, Gibbons RJ. Predictive power of the relative lymphocyte concentration in patients with advanced heart failure. Circulation. 1998 Jan 13;97(1):19-22. https://doi.org/10.1161/01.CIR.97.1.19
- 29. Vaziri ND. Oxidative stress in uremia: nature, mechanisms, and potential consequences. InSeminars in nephrology 2004 Sep 1 (Vol. 24, No. 5, pp. 469-473). WB Saunders.

https://doi.org/10.1016/j.semnephrol.2004.06.

30. Ozen N, Cinar FI, Askin D, Mut D. Uremic pruritus and associated factors in hemodialysis patients: A multi-center study. Kidney research and clinical practice. 2018 Jun 30;37(2):138.

https://doi.org/10.23876/j.krcp.2018.37.2.138

- 31. Suzuki H, Omata H, Kumagai H. Recent advances in treatment for uremic pruritus. Open Journal of Nephrology. 2015 Mar 13;5(1):1-3. https://doi.org/10.4236/ojneph.2015.51001
- 32. Ghassan B, Alalsaidissa JN, Al-Saedi AJ, Alawchi SN. Relationship of Pruritus with Biochemical and Haematological Parameters in Haemodialysis Patients (A Single Center Study). Journal of the Faculty of Medicine Baghdad. 2015;57(4):306-11.

https://doi.org/10.32007/jfacmedbagdad.574396

- 33. Chiu YL, Chen HY, Chuang YF, Hsu SP, Lai CF, Pai MF, Yang SY, Peng YS. Association of uraemic pruritus with inflammation and hepatitis infection in haemodialysis patients. Nephrology Dialysis Transplantation. 2008 Nov 1;23(11):3685-9. https://doi.org/10.1093/ndt/gfn303
- 34. Rowe B, Yosipovitch G. Malignancy-associated pruritus. European Journal of Pain. 2016 Jan;20(1):19-23. https://doi.org/10.1002/ejp.760
 35. Joshi VD, Belgaumkar VA, Pradhan SN. Peripheral Eosinophilia as an Ominous Marker of Poor Quality of Life: A Cross-Sectional Study Evaluating the Correlation Between Absolute Eosinophilia and Dermatology Life Quality Index in Various Pruritic Dermatoses. Journal of Skin and Stem

 Cell. 2023;10(3).

https://doi.org/10.5812/jssc-139132

العلاقة بين الحكة البولية وعدد كريات الدم البيضاء التفاضلي لدى مرضى غسيل الكلى في مركز ابن سينا لغسيل العلاقة بين الحكة البولية وعدد كريات الدم البيضاء الكلى

' هبة محمد الدراجي، السماعيل إبراهيم لطيف، الفاطمة خزعل خميس المجمعي، البيل خالد الوندي

الملخص

الخلفية: : الحكة الجلدية عرض شائع ومزعج لمرض الكلى المزمن. ووفقًا لأحدث البيانات الوبائية، يعاني حوالي ٤٠٪ من مرضى الفشل الكلوي في مرحلته النهائية من حكة جلدية تتراوح بين المتوسطة والشديدة. لا يزال سبب الحكة الجلدية اليوريمية غير مفهوم جيدًا، لكن الدراسات الحديثة تشير إلى ارتباطها القوي بالعملية الالتهابية وارتفاع عدد خلايا الدم البيضاء.

الأهداف: تهدف هذه الدراسة إلى دراسة العلاقة بين الحكة اليوريمية (UP) ومستويات الكريات البيضاء التفاضلية في المرضى الذين يعانون من مرض الكلى المرمن الذين يخضعون لغسيل الكلى (مرضى غسيل الكلى)، وفحص الدور المحتمل للالتهاب في شدة الحكة.

المواد والطرق: أُجريت دراسة في مركز ابن سينا لغسيل الكلى، محافظة ديالى، العراق. شملت الدراسة ١٥٠ مريضًا يخضعون لغسيل الكلى، محافظة ديالى، العراق. شملت الدراسة ١٥٠ مريضًا يخضعون لغسيل الكلى المزمن (UP) و ٧٥ مريضًا غير مصاب به. تألفت المجموعة الضابطة من ٢٦ فردًا سليمًا. من بين ٢٢٦ مريضًا يخضعون لغسيل الكلى في مركز غسيل الكلى، استبعد من تقل أعمار هم عن ٢٠ عامًا، بالإضافة إلى مرضى التهاب الكبد الوبائي (B) أو التهاب الكبد الوبائي (B). من كل مريض ومجموعة ضابطة في هذه الدراسة، جُمِع ٣ مل من الدم الوريدي قبل غسيل الكلى، ووُضِع في أنبوب حمض إيثيلين ديامين رباعي الأسيتيك (EDTA) لعد كريات الدم البيضاء التفاضلي، وخُلِل في المختبر التعليمي بمستشفى بعقوبة التعليمي.

النتائج: أظهرت النتائج أن ٣٣,٨٪ من مرضى غسيل الكلى يعانون من حكة بولية، وأن مستوى الخلايا الحمضية لديهم أعلى بشكل ملحوظ مقارنةً بالمرضى بالمرضى غير المصابين بالتهاب الكلى المزمن ومجموعة الضبط. بينما لم يُظهر مستوى الخلايا القاعدية والعدلات فرقًا كبيرًا بين المرضى المصابين بالتهاب الكلى المزمن، كان لدى مرضى غسيل الكلى المصابين بالتهاب الكلى المزمن عاد أعلى من الخلايا الليمفاوية؛ ومع ذلك، لم يكن هناك فرق ملحوظ بين المجموعة الضابطة، ومرضى غسيل الكلى المرصابين بالتهاب الكلى المزمن، والمرضى غير المصابين بالتهاب الكلى المزمن، والمرضى غير المصابين بالتهاب الكلى المزمن.

الاستنتاج: وقد تبين أن الخلايا الحمضية قد تلعب دورًا أساسيًا في التسبب بالتهاب البنكرياس المزمن، وذلك من خلال تحفيز وإفراز مواد تُفاقم شدته. كما يمكن للخلايا الليمفاوية أن تلعب دورًا في التسبب بالتهاب البنكرياس المزمن من خلال إفراز السيتوكينات.

الكلمات المفتاحية: حكة بولية، كريات الدم البيضاء، غسيل الكلي، ديالا، الحمضات.

المؤلف المراسل: هبة محمد الدراجي

الايميل: hiba.m@uodiyala.edu.iq

تاريخ الاستلام: ٣٠ ايول ٢٠٢٤

تاریخ القبول: ۲ حزیران ۲۰۲۵

تاريخ النشر: ٢٥ تشرين الأول ٢٠٢٥

فرع الأحياء المجهرية، كلية الطب، جامعة ديالى، ديالى، العراق.
 ٢ جامعة تشانكيري كاراتكين، تشانكيري، تركيا.
 ٣ مديرية الصحة، مستشفى بعقوبة التعليمى، ديالى، العراق

The Efficacy and Safety of Using a Stone Cone During Ureteroscopic Pneumatic Lithotripsy

Waleed Kh. Mohammed (1), Issam S. AL-Azzawi (1), Yousif S. Khalaf (1), Athanasios Papatsoris (1)

OPEN ACCESS

Correspondence: Waleed Kh. Mohammed Email: waleed@uodiyala.edu.iq
Copyright: ©Authors, 2025, College of Medicine, University of Diyala. This is an open access article under the CC BY 4.0 license (http://creativecommons.org/licenses/by/4.0/)

https://djm.uodiyala.edu.iq/index.php/djm

Received: 20 February 2025 Accepted: 19 August 2025 Published: 25 October 2025

Website:

Abstract

Background: Ureteroscopic fragmentation and extraction of ureteric stones is one of the most efficient minimal invasive treatment modalities. One of the drawbacks of this procedure, which occurs mainly during the fragmentation of upper ureteric stones, is the migration of proximal stones.

Objectives: To study the efficacy and safety of the Stone cone in preventing proximal stone migration during ureteroscopic pneumatic lithotripsy.

Patients and Methods: A retrospective data set of forty patients (25 male and 15 female), with symptomatic upper ureteral stones of greater than 7 mm in size, was collected from patients' records. Patients were allocated into two equal groups: Group A (interventional group) underwent ureteroscopic pneumatic fragmentation using a stone cone, and Group B (control group) underwent ureteroscopic fragmentation without using a stone cone. The data on pre-operative patients, the stones dealt with, and the results of the procedure in both groups were all stated.

Results: Pre-treatment patients and stone data (including patient age, gender, stone size, opacity, laterality, duration of symptoms, and degree of pelvicalyceal system dilatation) were comparable in both groups, with no statistically significant difference. The mean stone size was 12.7 mm in group A and 12.5 mm in group B. Stone migration occurred in 0 % in group A and 35% in group B (p=0.004), which led to a stone-free rate of 90% in group A and 60% in group B (p=0.028). Complications were minimal and comparable in both groups, and they were all amenable to conservative treatment.

Conclusion: Use of a stone cone as a ureteric occlusive device was reasonably safe, helped prevent proximal stone migration, and led to statistically significant improvement in stone-free rate during pneumatic lithotripsy.

Keywords: Ureteroscope, Renal Stone, Pneumatic Lithotripsy, Efficacy, Safety.

Introduction

The urinary tract consists of four parts, including the kidneys, ureters, bladder, and urethra. The ureters act as narrow muscular channels that transport urine from the renal pelvis to the bladder. This narrow and delicate anatomy contributes to the deposition and formation of urinary tract stones (1). Urinary tract stones affect 5–12% of people throughout their lives, and recurrence rates are close to 50.0%. Stone development is more than twice as common in males as in males (2). Ureteric stone usually presents with a sudden onset of severe flank pain, which is colicky in nature, and most

¹ Surgery Department, College of Medicine, University of Diyala, Diyala, Iraq.

² Urology department, College of Medicine, Mustansiriya University, Baghdad, Iraq.

³ Department of Surgery, College of Medicine, Ibn Sina University of Medical and Pharmaceutical Sciences, Baghdad, Iraq.

⁴ Department of Urology, Sismanoglio General Hospita, Athens, Greece.

commonly presents in emergency rooms. Intracorporeal lithotripsy via ureteroscopy has become the preferred treatment for ureteric stones during the past three decades (3,4). The preferred method for surgically treating ureteric stones has historically ureteroscopy. A safer and more effective method for treating stones in any part of the ureter has emerged with the invention of small-caliber semirigid and flexible ureteroscopies, along with the introduction of better equipment. Global complication rates, particularly those of ureteral perforations, have decreased to less than 5% due to growing experience, and the incidence of long-term issues like stricture formation is 2.0% or lower (5). The development of intracorporeal lithotripters, such as ultrasonic, electrohydraulic, pneumatic, and laser lithotripters, coincided with advancements in rigid and flexible ureteroscopies. These advancements allowed for effective stone fragmentation using contemporary ureteroscopic equipment. **Among** indications for using URS for a ureteric stone are the stone is larger than 7 mm, insufficient pain alleviation even with analgesics, the stone is less than 7 mm, when the medical expulsive therapy has failed, the possibility of sepsis or pyonephrosis, and unilateral obstruction in a single kidney or bilateral ureteric obstruction. After ureteroscopic

Patients and Methods

Study design: In this retrospective study, medical records of forty patients (25 males, 15 females) were reviewed over a period of 2 years. All patients were assessed by history taking, physical examination, and laboratory investigations (urinalysis, complete blood count, blood sugar, and renal function tests). Imaging studies, including KUB, ultrasound, and native computerized tomography (CT) scan, helped

removal, the predicted stone-free percentage is 90-100% for distal ureter stones and 74.0% for proximal ureter stones. The development of innovative gripping tools, pneumatic and laser lithotripters, and efficient semi-rigid and flexible ureteroscopes is responsible for the high success rate of ureteroscopic stone extraction (6,7). Nevertheless, the irrigant's propulsion effect or, more commonly, the application of kinetic energy employed for stone breakdown are two minor concerns that restrict the success of ureteroscopic stone manipulation. These issues include the possibility of upward migration or retropulsion of the stone (7). Retropulsion rates range from 2 to 60.0% (8,9,10). Furthermore, because proximal ureteric stones have a larger retropulsion rate than those placed distally in the ureter, this large variance in migration rate is mainly attributable to the stone's location. Stone cones and N-traps are examples of ureteric occlusion devices that have been developed as a remedy for this retropulsion. During intracorporeal lithotripsy, the stone cone and N-Trap are intended to prevent the retropulsion of ureteric calculi and facilitate the secure removal of stone fragments. Furthermore, the ureteric guide wire can be replaced with a stone cone, preserving continuous ureteric access and reducing the need for extra disposables (11,12). This study aimed to study the efficacy and safety of the stone cone in preventing ureteral stone migration during ureteroscopic pneumatic lithotripsy.

assess stone size, site, opacity, and degree of hydronephrosis.

Inclusion and exclusion criteria: The

inclusion criteria were being older than 20 years and having a stone with a longest diameter of more than 7 mm located in the upper ureter. The Exclusion criteria include the presence of ureteral stricture distal to the stone, clinical evidence of sepsis, coexistence of kidney stones, lower ureteric stone, ureteric stone in a single kidney,

and significant renal impairment.

Procedures: Patients were distributed

equally into two groups. Group A (interventional group) underwent ureteroscopic fragmentation using a stone cone, and Group B (control group) underwent ureteroscopic fragmentation without using a stone cone. In both groups, an 8-9.5 Fr semi-rigid ureteroscope with a 5 Fr working channel was used, a pneumatic lithotripter was employed for stone fragmentation, and the stone cone used in group A was 3 Fr in size.

Stone cone technique: All patients underwent ureteroscopy under general or spinal anesthesia, and all of them received a single dose of broadspectrum antibiotics parenterally at the time of induction of anesthesia. Patients were placed in lithotomy position; the ureteroscope was passed into the ureter with the aid of a 0.035-inch guide wire. After reaching the stone with the semi-rigid ureteroscope, in group A patients, the stone cone was advanced through the working channel of the ureteroscope until it reached beyond the stone, and the stone should be seen between the two black lines on the Stone Cone sheath. Coaxial traction on the Stone Cone sheath allows the cone to reform, and it should act as a barrier between the stone and the pelvicalyceal system. The ureteroscope is then taken out and reinserted beside the Stone Cone device to the level of the calculus, and the pneumatic lithotripsy probe is introduced to fragment the stone. Once the stone has been sufficiently fragmented, residual fragments are removed by a ureteric grasper. Continuous low-pressure fluid irrigation was necessary to maintain visibility of the stone and was used in both groups. In group B patients, fragmentation of the stone was also performed using the pneumatic lithotripter, but without the Stone cone. At the end of the procedure, a 5 Fr JJ stent was inserted over the guide wire and left indwelling for 4-6 weeks. A Foley catheter was inserted for all the patients and kept for 2 days. Parenteral antibiotics were continued for two

days postoperatively, and if no fever occurred, they were replaced by oral antibiotics for 5-7 days. KUB was taken on the same or next day (before discharge) to check the state of stone fragmentation and the position of the JJ stent. Most of our patients were discharged on the same operation day (after complete recovery) and asked to return after two weeks for followup. This follow-up usually includes a history review, physical examination, and an ultrasound or KUB or native CT scan to check for any residual stone pieces & complications. The procedure was considered successful in either group if no proximal stone migration occurred and if the stone was fragmented completely. Stone-free status is defined as complete clearance of stone fragments at the time of JJ stent removal, without the need for auxiliary procedure. The recorded post-operative data were: the degree of fragmentation (complete or incomplete), stone-free rate, proximal stone migration, and any complications related to the intracorporeal lithotripsy or Stone cone.

Statistical Analysis

The data were analyzed using Epi InfoTM version 7, a statistical software developed by the Centers for Disease Control and Prevention (CDC), Atlanta, USA

[https://www.cdc.gov/epiinfo/index.html].

Continuous data are presented as means and standard deviations. Student's t-test (two-tailed) was used to compare them between study groups. Categorical data are shown in frequency and percentage tables. Pearson's chi—squared test was used to assess the statistical association between categorical variables. A p-value less than 0.05 was considered significant.

Results

Demographics and clinical characteristics: Pre-treatment parameters, including the demographic and clinical characteristics, were compared between Group A (interventional group) and Group B (control group) (Table 1).

The mean age (\pm SD) of total respondents was 35.2 (\pm 7.6). The mean age in Group B (36.4 \pm 8.6 years) was higher than that in Group A (33.9 \pm 6.5 years). Most of the participants were males, with a higher percentage in Group A (65%) compared to Group B (60%). The Majority of stones were radio-opaque (87.5%), and Right-sided (22, 55.0%), especially among the interventional group (13, 65% vs. 9, 45%). The mean duration of impaction was longer among the Group A individuals (10.1 \pm 20.5 weeks vs. 5.2 \pm 3.3 weeks in Group B), with an overall mean of 7.7 \pm 14.7

weeks. Both interventional and control groups similarly exhibit mild and moderate P.C.S. dilatation. Findings of the independent t-test (t) and chi-square test showed that all parameters had no statistically significant differences when compared between the two groups (Table 1).

Table 1. Pre-treatment parameters, comparison between study groups (Number = 40).

Parameters	Categories	Group A	Group B	Total	p- value
Age (years), Mean ± SD		33.9±6.5	36.4±8.6	35.2±7.6	0.306 t
	<30 years	5 (20.0)	3(20.0)	8 (20.0)	
Age groups, No. (%)	30 - 39 years	12 (48.0)	9 (60.0)	21(52.5)	0.688
	40+ years	8 (32.0)	3 (20.0)	11(27.5)	
Gender, No. (%)	Male	13 (65)	12 (60)	25 (62.5)	0.744
Gender, No. (70)	Female	7 (35)	8 (40)	15 (37.5)	0.744
Stone laterality, No. (%)	Left	7 (35)	11 (55)	18 (45)	0.204
Stone fateranty, No. (%)	Right	13 (65)	9 (45)	22 (55)	
Stone opacity, No. (%)	Radio-opaque	17 (85)	18 (90)	35 (87.5)	0.633
Stone opacity, No. (%)	Radio-lucent	3 (15)	2 (10)	5 (12.5)	
Duration of impaction (weeks), Mean ± SD		10.1 ± 20.5	5.2±3.3	7.7±14.7	0.304 ^t
	Mild	7 (35)	7 (35)	14 (35)	
Degree of P.C.S. dilatation, No. (%)	Moderate	9 (45)	10 (50)	19 (47.5)	0.907
	Sever	4 (20)	3 (15)	7 (17.5)	
PCS: pelvicalyceal system, SD: standard devia	ntion, t independer	nt t-test, chi-squ	are test.		

The outcomes of the intervention procedure: Average stone size was compared between Group A (12.7 ± 3 mm) and Group B (12.5 ± 3.2 mm) using an independent t-test prior to surgical intervention (Table 2). Findings were almost similar in both groups, with no statistically significant difference (0.841).

Table 2 illustrates the outcomes of the intervention procedure among patients in group A and group B. Chi-square tests showed that the successful fragmentation was higher

(90%) in group A compared to group B (60%), with a statistically significant difference (p-value = 0.028). Stone migration was reported only in group B (35%), with a significant difference (p-value = 0.004). The highest stone-free rate (90.0%) was in group A compared to 60.0% in group B, indicating a significant difference (p-value = 0.028). However, complications were similar between groups (30% in group A vs. 25% in group B) with no significant difference (p-value = 0.723). Out of forty cases, 11 (27.5%) were reported complications, mainly bleeding and post-operative fever (Table 3).

Table 2: Results of treatment with comparison between study groups (Number = 40).

Parameters	Group A	Group B	Total	p-value
Average Stone size (mm), Mean ± SD	12.7±3	12.5±3.2	12.6±3.1	0.841 ^t
Successful fragmentation, No. (%)	18 (90)	12 (60)	30 (75)	0.028*
Stone migration, No. (%)	0 (0)	7 (35)	7 (17.5)	0.004*
Stone free rate, No. (%)	18 (90)	12 (60)	30 (75)	0.028*
Complications, No. (%)	6 (30)	5 (25)	11 (27.5)	0.723
* Significant by chi-square test.				

Table 3. Complications of treatment according to study groups (Number = 40).

Complication	Group A	Group B	Total
Bleeding	3 (15)	2 (10)	5 (12.5)
Perforation	1 (5)	0 (0)	1 (2.5)
Post-Operative Fever	2 (10)	3 (15)	5 (12.5)
Total	6 (30%)	5 (25%)	11 (27.5%)

Findings of bivariate analysis: Bivariate analysis was performed to assess the relationship between stone migration and various studied parameters. A significant reduction in stone migration was seen when using the stone cone (no cases of stone migration), compared to 35% of cases had migration when stone cone was not used, with

a statistically significant correlation (p-value = 0.004) suggesting that using a stone cone significantly reduces the risk of stone migration. Other parameters, including the stone size (p-value = 0.426), PCS dilatation (p-value = 0.101), and duration of impaction (p-value = 0.772), did not show significant correlations (Table 4).

Table 4. Correlations between stone migration and different parameters (Number = 40).

Parameters	Categories		p-value		
Observation No. (%)		Yes 7(17.5)	No 33(82.5)	Total	
Stone size (mm), Mean ± SD		13.7±4	12.4±2.9	12.6±3	0.426 ^t
Degree of PCS dilatation, No. (%)	Mild	0 (0)	14 (100)	14 (100)	0.101
	Moderate	5 (26.3)	14 (73.7)	19 (100)	
	Sever	2 (28.6)	5 (71.4)	7 (100)	
Duration of impaction (weeks), Mean ± SD		6.9±4.6	7.8±16.1	7.7±14.7	0.772 ^t
Use of stone cone, No. (%)	Used	0 (0)	20 (100)	20 (100)	0.004*
	Not used	7 (35)	13 (65)	20 (100)	
PCS: pelvicalyceal system, mm: millimeter, SD: standard deviation, * significant by chi-square test, t independent t-test.					

Association between stone-free rate and different parameters: The chi-square test and the independent t-test were employed to find out the relationship between the stone-free rate and different parameters (Table 5). The stone-free rate was 95.5% in the right kidney compared to 50.0% in the left kidney,

with a statistically significant difference (p-value = 0.001), indicating that kidney stones in the left kidney were harder to clear than those in the right kidney. In terms of stone migration, about 90.9% of non-migrated stones succeeded in becoming stone-free, while 100% of cases with stone migration were unsuccessful in becoming stone-free,

suggesting a highly significant correlation (p-value < 0.001). The stone-free rate was significantly higher among patients who underwent a stone cone procedure (90.0%) compared to those without a stone cone procedure (p-value = 0.028), indicating the

effectiveness of the stone cone procedure in improving kidney stone clearance. Sociodemographic factors (age, gender), stone size, stone opacity, duration of impaction, and PCS dilatation showed no significant difference (Table 5).

Table 5. Association between stone-free rate and selected clinical parameters (Number = 40).

	Yes			p-value
	108	No	Total	
	30 (75)	10 (25)	40 (100)	
	34.1±6.5	38.3±10.1	35.2±7.6	0.242^{t}
Male	18 (72)	7 (28)	25 (100)	0.572
Female	12 (80)	3 (20)	15 (100)	
Left	9 (50)	9 (50)	18 (100)	0.001*
Right	21 (95.5)	1 (4.5)	22 (100)	
	12.5±2.8	12.8±3.9	12.6±3.1	0.845 ^t
Radio-opaque	26 (74.3)	9 (25.7)	35 (100)	0.783
Radio-lucent	4 (80)	1 (20)	1 (20) 5 (100)	
	8.2±16.8	5.9±4.2	7.7±14.7	0.490 t
Mild	13 (92.9)	1 (7.1)	14 (100)	0.146
Moderate	12 (63.2)	7 (36.8)	19 (100)	
Sever	5 (71.4)	2 (28.6)	7 (100)	
Yes	0 (0)	7 (100)	7 (100)	<0.001*
No	30 (90.9)	3 (9.1)	33 (100)	
Yes	18 (90)	2 (10)	20 (100)	0.028*
No	12 (60)	8 (40)	20 (100)	
	Female Left Right Radio-opaque Radio-lucent Mild Moderate Sever Yes No Yes No	Male 18 (72) Female 12 (80) Left 9 (50) Right 21 (95.5) 12.5±2.8 Radio-opaque 26 (74.3) Radio-lucent 4 (80) 8.2±16.8 Mild 13 (92.9) Moderate 12 (63.2) Sever 5 (71.4) Yes 0 (0) No 30 (90.9) Yes 18 (90)	Male 18 (72) 7 (28) Female 12 (80) 3 (20) Left 9 (50) 9 (50) Right 21 (95.5) 1 (4.5) 12.5±2.8 12.8±3.9 Radio-opaque 26 (74.3) 9 (25.7) Radio-lucent 4 (80) 1 (20) 8.2±16.8 5.9±4.2 Mild 13 (92.9) 1 (7.1) Moderate 12 (63.2) 7 (36.8) Sever 5 (71.4) 2 (28.6) Yes 0 (0) 7 (100) No 30 (90.9) 3 (9.1) Yes 18 (90) 2 (10) No 12 (60) 8 (40)	Male 18 (72) 7 (28) 25 (100) Female 12 (80) 3 (20) 15 (100) Left 9 (50) 9 (50) 18 (100) Right 21 (95.5) 1 (4.5) 22 (100) 12.5±2.8 12.8±3.9 12.6±3.1 Radio-opaque 26 (74.3) 9 (25.7) 35 (100) Radio-lucent 4 (80) 1 (20) 5 (100) 8.2±16.8 5.9±4.2 7.7±14.7 Mild 13 (92.9) 1 (7.1) 14 (100) Moderate 12 (63.2) 7 (36.8) 19 (100) Sever 5 (71.4) 2 (28.6) 7 (100) Yes 0 (0) 7 (100) 7 (100) No 30 (90.9) 3 (9.1) 33 (100) Yes 18 (90) 2 (10) 20 (100) No 12 (60) 8 (40) 20 (100)

Discussion

The past three decades have witnessed noticeable developments in the field of renal ureteral stone management. procedures ranged from simple medical treatment to relief of pain, open surgery intervention, to more advanced, specific, and minimally invasive techniques such as the extracorporeal shock wave lithotripsy (ESWL) and the Ureteroscopy (URS) (13,14). Several studies confirm the highly effective achievement of stone-free rates up to 95.0% using the URS technique (14,15,16). Although the success rate differs with the size and position of the stone (14), one of the main

challenges in the upper ureter stones were the proximal migration during fragmentation,

especially when processing pneumatic lithotripsy (15,16). To alleviate this, urologists have adopted the Lithotripsy laser instead of pneumatic and ureteral occlusive devices, which improve the outcomes by preventing the stone migration in the renal pelvis (12). This study evaluated the effectiveness of using a stone cone as an occlusive device to prevent stone migration in a trial to improve the stone-free rate. To reduce the cost and also due to the lack of a laser machine or flexible URS, the stone cone was preferred. The results of the surgical intervention, indicated a significantly higher successful fragmentation (90.0% versus 60.0%, p=0.028), stone migration (0.0% versus

35.0%, p=0.004), and stone free rate (90.0%) versus 60.0%, p=0.028) among patients who had underwent ureteroscopic pneumatic fragmentation with using of stone cone compared to without using stone cone suggesting a strong protective effect. These findings are consistent with recent evidence reported by Saeed Pansota et al. (11), who conducted a prospective study among 94 patients with proximal ureteric stones sized 7— 15 mm. They reported a significantly higher stone clearance using the Stone Cone (93.6% vs. 70.2%, p = 0.003). Raphael and Danagogo (17) reported a 100% stone clearance after lithotripsy for proximal ureteric stone under ureteroscopy, indicating that the stone cone is a safe device. The mean stone size in our samples was 12.6 ± 3.1 mm, which was comparable to those reported by Raphael and Danagogo (17), and less than those reported by Alameddine et al. (18). The more the duration of stone impaction, the more inflammatory process around the stone, which usually leads more difficult stone manipulation. Consequently, the above-mentioned histological changes most likely affect ureteroscopy instrumentation, leading to an inability to deal with stones proximal to the level of ureteric obstruction. Ansari et al. (19) reported that the stone-free rate was improved among stented patients compared to those who had not been stented. Moreover, the duration of stone impaction was neither a statistically significant factor affecting stone migration nor affecting the stone-free rate between the two groups. Furthermore, we studied the factors affecting stone migration, and the main correlation was obviously with the use of the stone cone in group A. All cases with migration failed to become stone-free, whereas 90.9% of non-migrated stones were successfully cleared (p < 0.001). Although there was a difference in stone migration

regarding the degree of PCS dilatation, it was statistically nonsignificant. Overall stone free rate was 75.0% in our series (90.0% in group A versus 60.0% in group B), while it was 95.0% to 100% in Raphael and Danagogo (17), 89.0% in Alameddine et al. (18), 100.0% in Kapoor et al. (20) and 95.5% in Sen et al. (21) and related to the high incidence of stone migration in group B (35.0%). In this study, there was a statistically significant stone-free rate in the right kidney (95.5%) compared to the left-sided (50.0%) (p = 0.001), raising the challenge to clear stones from the left kidney. However, this positive correlation between stone-free rate and stone laterality is actually of no clinical importance. The use of the stone cone and its introduction through URS was easy and safe, especially with building experience, and the whole procedure, with or without using the stone cone, was, in general, with minimal complications. Although the sample size was relatively small, the study showed statistically significant differences in the main results, such as stone-free rates and stone migration between patients who received the stone cone and those who did not. These findings suggest that the study has sufficient power to identify clinically related effects, especially concerning the interest of using the stone cone in improving the success of the surgical procedure. Additionally, retrospective studies often serve as a basis for future prospective studies or help guide hypothesis generation and design for larger randomized trials. This study contributes to real evidence of the effectiveness and safety of the stone cone devices during ureteroscopy.

Conclusion

The study demonstrates that the use of a stone cone significantly improves stone-free rates and reduces stone migration. Patients in the interventional group (Group A) had a higher stone-free rate compared to the control group. Stone migration was reported exclusively in the control group, reinforcing the role of the stone cone in preventing migration. Other factors, including age, gender, stone size, and

duration of impaction, were not significantly associated with treatment success. Ureteroscopic pneumatic lithotripsy for ureteric stones is still a valid treatment option. Use of a stone cone as a ureteric occlusive device was reasonably safe and was helpful in preventing proximal stone migration, and led to statistically significant improvement in stone-free rate during pneumatic lithotripsy.

Source of funding: No source of funding. **Ethical clearance:** This study was conducted following the Declaration of Helsinki. The ethical committee approval was obtained from the Iraqi Board for Medical Specialization, Ministry of Higher Education and Scientific Research, Iraq (Reference No. 3712).

Conflict of interest: None.

Use of Artificial Intelligence: The authors declare that they did not use artificial intelligence for creating or preparing this manuscript.

Acknowledgments: The authors sincerely thank the reviewers and editors for their valuable comments and support. The authors also acknowledge their institution for providing the necessary support and resources for this work.

References

- 1. Wandile PM. Complexity and management of chronic kidney disease. Open Journal of Nephrology. 2023 Jul 31;13(3):280-91. https://doi.org/10.4236/ojneph.2023.133027
- 2. Patti L, Leslie SW. Acute renal colic. InStatPearls [Internet] 2024 Jun 6. StatPearls Publishing.

https://www.ncbi.nlm.nih.gov/books/NBK43 1091/?utm_source=chatgpt.com

3. Raynal G, Malval B, Panthier F, Roustan FR, Traxer O, Meria P, Almeras C, lithiasis committee of the French Association of Urology (CLAFU. 2022 Recommendations of the AFU Lithiasis Committee: Ureteroscopy and ureterorenoscopy. Progrès

- en Urologie. 2023 Nov 1;33(14):843-53. https://doi.org/10.1016/j.purol.2023.08.016
- 4. Buzescu B, Cozma C, Geavlete P, Multescu R, Georgescu D, Ene C, Bulai C, Geavlete B. Laser Lithotripsy in Renal Lithiasis—2023 Update—a Narative Review. Maedica. 2024 Jun;19(2):388. https://doi.org/10.26574/maedica.2024.19.2.388
- 5. Wu W, Wan W, Yang J, Amier Y, Li X, Zhang J, Yu X. For upper ureteral stone, semirigid ureteroscopy or flexible ureteroscopy? Strengths and weaknesses. BMC urology. 2024 Nov 29;24(1):261. https://doi.org/10.1186/s12894-024-01647-w
- 6. Ordon M, Andonian S, Blew B, Schuler T, Chew B, Pace KT. CUA Guideline: Management of ureteral calculi. Canadian Urological Association Journal. 2015 Dec 14;9(11-12):E837. https://doi.org/10.5489/cuaj.3483
- 7. Irsayanto D, Yatindra IB, Setiawan MR, Salsabila S, Renaldo J, Wirjopranoto S. Efficacy and Safety of Pneumatic Lithotripsy with Laser Lithotripsy in The Treatment of Ureteral Stones
 20 Millimeters in Children: A Systematic Review and Meta-Analysis. Journal of Ayub Medical College Abbottabad. 2024 Apr 17;36(1):202-9. https://doi.org/10.55519/JAMC-01-12288
- 8. Shalaby EA, Abdelhalim KM, Bakr M, El-Lilly AA, Elkoushy MA. Impact of forced diuresis on retropulsion of disintegrated ureteral calculi during semi-rigid ureteroscopy: a double-blind randomized-controlled study. Urolithiasis. 2022 Aug;50(4):465-72. https://doi.org/10.1007/s00240-022-01324-3
- 9. Anastos H, Yaghoubian AJ, Khusid JA, Chandhoke RA, Lundon DJ, Sadiq AS, Bamberger JN, Gallante B, Shimonov R, Atallah WM, Gupta M. Reverse trendelenburg positioning minimizes stone retropulsion during ureteroscopic laser lithotripsy: a prospective randomized study. Journal of Endourology. 2023 Jun 1;37(6):660-6. https://doi.org/10.1089/end.2022.0701
- 10. Almusawi FF. The Safety and Efficiency of Percutaneous Nephrolithotomy in Managing Renal

Stones in A Single Solitary Kidney. Divala Journal of Medicine. 2024 Dec 25:27(2):103-13. https://doi.org/10.26505/djm.v27i2.1229

- 11. Pansota MS, Saleem MS, Barkat B, Aleem A, Rasool M. Evaluating the Efficacy of Ureteroscopic Management of Proximal Ureteric Calculi using Stone Cone Entrapment Device. Journal of Saidu Medical College Swat. 2025 Jan 29;15(1):56-60. https://doi.org/10.52206/jsmc.2025.15.1.982
- 12. Wetherell DR, Ling D, Ow D, Koonjbeharry B, Sliwinski A, Weerakoon M, Papa N, Lawrentschuk N, Bolton DM. Advances in ureteroscopy. Translational Andrology and Urology. 2014 Sep;3(3):321.

https://doi.org/10.3978/j.issn.2223-4683.2014.07.05

- 13. Yaseen SM, Jadoo SA, Abdullah AA, Mahmood AS. Abd Al-wahaab Predictive factors of successful extracorporeal shockwave lithotripsy (ESWL) for renal stones: evidence of retrospective study. Journal of Ideas in Health. 2019 May 17;2(1):60-4.
- 14. Sadeeg KJ. Extracorporeal Shock Wave Lithotripsy success rate for upper and lower ureteric stones in Azadi-teaching (Dohuk) hospital in Kurdistan Region-Iraq. Diyala Journal of Medicine. 2017;13(2):48-55.
- 15. Gharib TM, Abdel-Al I, Elmohamady BN, Deif H, Haty AA, Shebl SE, Safar O, Hassan GM, Haggag YM, Elatreisy A. Ultrathin semirigid retrograde ureteroscopy versus antegrade flexible ureteroscopy in treating proximal ureteric stones 1–2 cm, a prospective randomized multicenter study. Urolithiasis. 2024 Sep 19;52(1):131.

https://d`10i.org/10.1007/s00240-024-01626-8

16. Wagenius M, Rydberg M, Popiolek M,

Forsvall A, Stranne J, Linder A. Ureteroscopy: a populationbased study of clinical complications and possible risk factors for stone surgery. Central European journal of urology. 2019 Sep 2;72(3):285. https://doi.org/10.5173/ceju.2019.1951

17. Raphael JE, Danagogo O. The ureteral stone cone is a useful device for the prevention of calculi retropulsion during holmium laser lithotripsy for proximal and mid-ureteric stones. a Nigerian experience. Saudi Journal of Biomedical Research. 2022;7(2):90-4.

https://doi.org/10.36348/sjbr.2022.v07i02.004

- 18. Alameddine M, Azab MM, Nassir AA. Semirigid ureteroscopy: Proximal versus distal ureteral stones. Urology annals. 2016 Jan 1;8(1):84-6. https://doi.org/10.4103/0974-7796.171495
- 19. Ansari MI, Khan SA, Thakur DK, Agrawal CS. Comparative efficacy of pre-stented versus nonstented retrograde intrarenal surgery: A randomized Medicine. controlled trial. 2025 May 30;104(22):e42659.

https://doi.org/10.1097/MD.0000000000042659

20. Kapoor R, Mane D, Singh SJ, Satav V, Sabale V, Ranjan P. Relevance of Guy's stone score in and outcome evaluation of percutaneous nephrolithotomy. Current Urology. 2024 Dec 1;18(4):287-90.

https://doi.org/10.1097/CU9.0000000000000165

21. Sen H, Bayrak O, Erturhan S, Urgun G, Kul S, Erbagci A, Seckiner I. Comparing of different methods for prevention stone migration during ureteroscopic lithotripsy. Urologia Internationalis. 2014 Jul 4;92(3):334-8. https://doi.org/10.1159/000351002.

فعالية وسلامة استخدام Stone Cone أثناء تفتيت الحصوات الهوائي بالمنظار

ا وليد خالد محمد، ٢ عصام العزاوي، "يوسف خلف، أثناسيوس باباتسوريس

الملخص

الخلفية: يُعدّ تفتيت واستخراج حصوات الحالب باستخدام المنظار من أكثر طرق العلاج طفيفة التوغل كفاءة. ومع ذلك، فإنّ أحد العيوب الرئيسية لهذا الإجراء، خاصة أثناء تفتيت الحصوات في الجزء العلوي من الحالب، هو هجرة الحصوات إلى الأعلى.

الأهداف: دراسة فعالية وسلامة استخدام Stone Cone في منع هجرة الحصوات العلوية أثناء تفتيت الحصوات الهوائي بالمنظار.

المواد والطرق: تمّ إدراج أربعين مريضًا (٢٥ ذكرًا و١٥ أنثى) يعانون من حصوات علوية في الحالب يزيد حجمها عن 7 مم في هذه الدراسة. تمّ تقسيم المرضى عشوائيًا إلى مجموعتين متساويتين:

- المجموعة (A) المجموعة التدخلية : خضع المرضى لتفتيت الحصوات الهوائي بالمنظار باستخدام . Stone Cone
- المجموعة (B) مجموعة الضبط: خضع المرضى لتقتيت الحصوات الهوائي بالمنظار دون استخدام .Stone Cone

تمّ تسجيل البيانات الأولية للمرضى، وخصائص الحصوات، ونتائج الإجراء لكلا المجموعتين.

النتائج: كانت البيانات الأولية للمرضى وخصائص الحصوات (بما في ذلك عمر المريض، الجنس، حجم الحصوة، الكثافة الشعاعية، الجهة المصابة، مدة الأعراض، ودرجة توسع حوض الكلية) متشابهة في كلا المجموعتين دون فروق ذات دلالة إحصائية. بلغ متوسط حجم الحصوات A0,7 مم في المجموعة A1,7 مم في المجموعة A2 مما أدى إلى تحقيق معدل خلو من الحصوات بنسبة A4, في المجموعة A4 مقارنة بA5 في المجموعة A5 كانت المضاعفات طفيفة ومتماثلة في كلا المجموعتين، وتمّت معالجتها جميعًا بشكل تحفظي.

الاستنتاج :يُعتبر استخدام Stone Cone كجهاز انسداد للحالب آمنًا إلى حدٍ كبير، ويساعد في منع هجرة الحصوات العلوية، مما يؤدي إلى تحسن ملحوظ من الناحية الإحصائية في معدل خلو المرضى من الحصوات أثناء التفتيت الهوائي بالمنظار.

الكلمات المفتاحية: منظار الحالب، حصى الكلي، تفتيت الحصوات الهوائي، الفعالية، السلامة

المؤلف المراسل: وليد خالد محمد

waleed@uodiyala.edu.iq الايميل:

تاريخ الاستلام: ٢٠ شباط ٢٠٢٥

تاريخ القبول: ١٩ أب ٢٠٢٥

تاريخ النشر: ٢٠ تشرين الأول ٢٠٢٥

' فرع الجراحة، كلية الطب، جامعة ديالى، ديالى، العراق.
' فرع جراحة المسالك البولية، كلية الطب، الجامعة المستنصرية، بغداد، العراق.
' فرع الجراحة، كلية الطب، جامعة ابن سينا للعلوم الطبية والصيدلانية، بغداد، العراق.
' فرع جراحة المسالك البولية، مستشفى سيسمانوجليو العام، أثينا، اليونان.

Pentraxin-3 Level Assessment Among Ischemic Stroke Patients with Polycystic Ovarian Syndrome

Mufeed Akram Taha (1)¹, Sahar A. Taha (1)², Esraa Abdulkareem Mohammed (1)³

- ¹ Department of Medicine, College of Medicine, University of Kirkuk, Kirkuk, Iraq.
- ² Department of Biology, College of Sciences, University of Kirkuk, Kirkuk, Iraq.
- ³ Department of Obstetrics and Gynecology, College of Medicine, University of Kirkuk, Kirkuk, Iraq.

Correspondence: Mufeed Akram Taha Email: mufeedakram@uokirkuk.edu.iq Copyright: ©Authors, 2025, College of Medicine, University of Diyala. This is an open access article under the CC BY 4.0 license (http://creativecommons.org/licenses/by/4.0/) Website:

OPEN ACCESS

https://djm.uodiyala.edu.iq/index.php/djm

Received: 02 April 2025 Accepted: 21 July 2025 Published: 25 October 2025

Abstract

Background: Pentraxin-3 (PTX3) is an important component of the innate immune system, playing a significant role in the inflammatory process and tissue damage. Assessing its levels in different clinical conditions may offer insights into its diagnostic and prognostic significance.

Objectives: This study aims to evaluate whether PTX3 levels are elevated in ischemic stroke patients with PCOS and whether increased PTX3 is linked to greater stroke risk and worse outcomes.

Patients and Methods: A case-control study was conducted in the neurology and obstetrics & gynecology clinics at Azadi Teaching Hospital in Kirkuk starting from 1st February 2023 to 1st March 2024. Women diagnosed with polycystic ovarian syndrome (PCOS) according to Rotterdam criteria were divided into three groups: the first group had PCOS with stroke, while the second group had PCOS without stroke; and the third group was considered an age matching control group with age ranges between 18 and 50 years. Blood samples were withdrawn in the morning to determine the levels of PTX3, C-reactive protein (CRP), triglyceride/ high density lipoprotein (TG/HDL) ratio, and homeostatic model assessment for insulin resistance (HOMA-IR) and measured in all studied groups.

Results: The level of PTX3 was significantly higher in patients with PCOS with stroke group (5.717 \pm 1.172 ng/mL) than those without Stroke (3.665 \pm 1.085 ng/mL) and Control (2.377 \pm 0.740 ng/mL) groups (p < 0.001). Pentraxin3 levels positively correlated with stroke severity (r = 0.42, p < 0.001), while there was no significant correlation with CRP, TG/HDL Ratio, and HOMA-IR.

Conclusion: Pentraxin-3 levels are markedly higher in PCOS patients who have had an ischemic stroke, and the level is in proportion to the severity of the stroke. This means that PTX3 could potentially be used as a biomarker for risk assessment.

Keywords: Polycystic ovarian syndrome, Ischemic stroke, Pentraxin 3, CRP, PCOS.

Introduction

Stroke is one of the emergent neurological disorders that is common with high morbidity and mortality rates in the world (1). Despite advances in the medical field, the incidence of ischemic stroke is still a major health problem in the world (2). However, the condition may worsen if it occurs in association with other metabolic and inflammatory disorders that increase the severity of stroke and chances of a good outcome (3). Among these conditions is polycystic ovarian syndrome (PCOS), which is one of the endocrine disorders that is more predominant in females of childbearing age and is characterized

by hormonal, inflammatory, and metabolic manifestations **(4)**. However, since inflammatory disorders are one of the constituents of PCOS, their role in ischemic strokes has become an essential topic of this study. Pentraxin-3 (PTX3) is one of the newly discovered acute-phase inflammatory glycoprotein markers that may be useful in the diagnosis and prognosis. PTX3 plays a key role in vascular inflammation and endothelial dysfunction by affecting nitric oxide synthesis, cell proliferation, and matrix metalloproteinase production. It is linked to arterial hypertension and may serve as a potential biomarker (5). Furthermore, it has been identified as a potential biomarker for cardiovascular and cerebrovascular diseases, and further studies were recommended in this direction to improve awareness and treatment of these conditions (6). The role of PTX3 in patients with ischemic stroke focuses on the inflammatory responses to blood vessel damage due to cerebral ischemia. It's a glycoprotein that has been rapidly produced in response to proinflammatory cytokines like TNF-α and IL-1. High PTX3 levels can be seen after cerebrovascular disease like myocardial infarction, signifying its role in the inflammatory responses that occur after tissue injury. Also, PTX3 accelerates the activation of complement pathways and the attraction of immune cells, thus connecting innate immunity to vascular pathology (7). However, the specific role of PTX3 concentrations in ischemic stroke outcomes is still unclear. The various studies are inconsistent in regarding

Patients and Methods

Study design: A case-control study was conducted at Azadi Teaching Hospital in Kirkuk, starting from 1st February 2023 to 1st March 2024. The study was conducted in the neurology, obstetrics, and gynaecology clinics, and the

its possibility as a disease severity marker for stroke and its failure as a predictor of stroke events (8, 9). Despite the fact that some research has reported increased PTX3 levels in stroke patients (10, 11), this has raised questions about its clinical significance. The complexity of the issue is amplified when considering patients with PCOS. condition is also characterized hyperandrogenism, insulin resistance, and lowgrade chronic inflammation, all of which are known to be metabolically associated with cardiovascular disease risk factors, including stroke Women with PCOS have been noted to have more cardiovascular disease complications and mortality than women without PCOS (12), with significantly increased levels of inflammatory markers such as C-reactive protein (CRP) (13). However, the relationship between the protein PTX3 and ischemic stroke within the PCOS population has not been well explored. Research suggests that the persistent inflammatory state that is characteristic of PCOS may regulate PTX3 production, which in turn may influence the risk of stroke. Thus, the investigation of the role of PTX3 in ischemic stroke in the context of PCOS may open up new possibilities for treatment and risk assessment, given the possible consequences of these associations. This study aims to evaluate whether PTX3 levels are elevated in ischemic stroke patients with PCOS and whether increased PTX3 is linked to greater stroke risk and worse outcomes. The results may help to improve understanding of the mechanisms inflammation in ischemic stroke in patients with PCOS and, therefore, to develop more specific approaches to stroke prevention and treatment

women who had polycystic ovarian syndrome (PCOS) with and/or without stroke, as well as healthy women, were included in the study.

Data collection, participants, and clinical assessment: Patients were screened for eligibility according to the relevant diagnostic criteria after obtaining written informed consent from the

participants and were divided into three groups: the first group had PCOS with stroke, while the second group had PCOS without stroke; and the third group was considered an age-matching control group with age ranges between 18 and 50 years.

The inclusion criteria include enrolling cases of PCOS diagnosed according to Rotterdam criteria and ischemic stroke diagnosed by a neurologist, depending on clinical manifestation radiological imaging studies. The data were collected according a to standardized questionnaire that contains general information, medical history, and drug history. Blood samples were withdrawn in the morning after an overnight fast.

Exclusion criteria: The exclusion criteria included patients with other types of cerebrovascular diseases, malignant conditions, hemorrhagic stroke, severe systemic diseases, autoimmune or other chronic inflammatory diseases, or the use of immunosuppressive or anti-inflammatory drugs.

Laboratory investigations: The levels of Pentraxin-3 (PTX3) and C-reactive protein (CRP) were measured using a quantitative sandwich enzyme-linked immunosorbent assay (ELISA) technique, following the manufacturer's instructions. PTX3 was calculated using the Human Pentraxin 3/TSG-14 Quantikine ELISA Kit (R&D Systems, Catalog # DPTX30). CRP was measured using the Human CRP ELISA Kit (Abcam, Catalog # ab260058). The standard reference ranges are 2-5ng/mL and 0-10mg/dL, respectively. The triglyceride/high-density lipoprotein (TG/HDL) ratio was measured depending on the fasting lipid profile. Fasting blood samples were analyzed for serum triglycerides and HDL-C levels using enzymatic colorimetric methods with an automated chemistry analyzer (Roche Cobas c311), and reagents supplied by Roche (Triglycerides Gen.2, Catalog # 20767107322; HDL-Cholesterol

Gen.4, Catalog # 05168538190). The TG/HDL-C ratio was determined by dividing the triglyceride concentration (mg/dL) by the HDL-C concentration (mg/dL).

Insulin resistance was assessed by calculating the Homeostatic Model Assessment for Insulin Resistance (HOMA-IR) index using following formula: homeostatic model assessment for insulin resistance (HOMA-IR) = fasting insulin (μ U/mL) × fasting glucose (mg/dL) and dividing by 405 (14). Fasting glucose was measured using the Roche Glucose Hexokinase reagent (Catalog # 04404483 190), and fasting insulin was measured using the Human Insulin ELISA Kit (Abcam, Catalog # ab100578). The severity of stroke was assessed by the National Institutes of Health Stroke Scale (NIHSS) (15).

Statistical Analysis

Statistical analyses were conducted using SPSS version 26. For descriptive and continuous data, the means and standard deviations were calculated. The normal distribution of the data was measured using the Shapiro-Wilk test. For comparing the biomarker levels between the three groups, analysis of variance (ANOVA) was used, and Tukey's post-hoc test was performed for pairwise comparisons if the ANOVA results were significant. To determine the relationship between PTX3, CRP, TG/HDL ratio, HOMA-IR, and stroke severity measured by the NIHSS, the Pearson correlation was applied. The set of statistical tests consisted of ANOVA for the comparison of the levels of biomarkers among the three groups, the post-hoc Tukey test for the determination of the specific differences between the pairs of groups, the correlation coefficient Pearson for the assessment of the relationships between the biomarkers and stroke severity, and regression analysis in the evaluation of the predictive value of the biomarkers with respect to stroke severity.

A p-value of less than 0.05 was considered significant.

Results

Study design: The study was carried out, and the participants were divided into three categories according to their medical history and status: the PCOS with Stroke Group, the polycystic ovarian syndrome (PCOS) without Stroke Group, and the healthy control Group.

Demographic and biomarker variables across the studied groups:

There was no apparent statistical disparity in the mean age of the groups. The pentraxin-3 (PTX3) levels were greatly increased in the PCOS with stroke group as compared to the PCOS without Stroke and the healthy control group. The mean PTX3 concentration was quite striking and was seen to be highest at 5.717 ± 1.172 ng/mL in the PCOS stroke group, while those with PCOS without stroke had a mean PTX3 level of $3.665 \pm$ 1.085 ng/mL, and the healthy controls had a mean PTX3 level of 2.377 ± 0.740 ng/ml. This difference was statistically highly significant (p < 0.001). When CRP levels were further checked there was an increase in both PCOS groups when compared to the healthy control group. The mean C-reactive protein (CRP) level of the PCOS Stroke group was 8.043 ± 2.102 mg/L while that of the PCOS without Stroke group was 5.448 \pm 1.532 mg/L compared to the healthy controls who had a lower mean CRP level of 3.037 ± 0.959 mg/L. However, the CRP values were higher than the normal values in both groups, but the difference in the stroke and non-stroke subgroups was not statistically significant (p = 0.651).

The triglyceride/high-density lipoprotein (TG/HDL) ratio and homeostatic model assessment for insulin resistance (HOMA-IR) values were also higher in both groups of patients with PCOS when compared with the healthy control group. Specifically, the TG/HDL ratio was found to be 4.297 ± 0.935 in the PCOS stroke group, while the PCOS without stroke group had

a ratio of 3.719 ± 0.863 . Nonetheless, the mean TG/HDL Ratio of Healthy Controls was considerably lower at 2.203 ± 0.585 . Also, the HOMA-IR values of the groups were 3.547 ± 0.949 for the PCOS stroke group, 3.194 ± 1.034 for the PCOS without Stroke group, and 1.771 ± 0.492 for the healthy controls; however, there was no statistically significant difference in the TG/HDL ratio and HOMA-IR values between the groups, as seen by the p-values of 0.189 and 0.148, respectively.

An analysis of variance (ANOVA) was done to compare the mean biomarker levels over three groups. The results showed a highly significant difference in the mean PTX3 levels, with a p-value of less than 0.001. This meant that the group called PCOS with Stroke had the highest levels and thus was confirmed to be the group with the highest levels. On the other hand, there was no statistically significant difference in the CRP levels (p = 0.651). Similarly, there was no statistical significance in the comparison of the TG/HDL ratio and HOMA-IR between the groups, as shown in Table 1.

Correlation of markers with stroke severity:

A Pearson correlation analysis was performed to determine the correlation of PTX3, CRP, TG/HDL ratio, and HOMA-IR with the severityof strokes as determined by the NIH Stroke Scale. The results showed a positive correlation between the NIH Stroke Scale scores and the PTX3 levels (r = 0.42, p < 0.001). It means that there is an association between raised levels of PTX3 and increased severity of stroke. However, the results of the analysis failed to show a correlation between CRP, TG/HDL Ratio, and HOMA-IR with the severity of strokes Table 2.

Table 1. Comparison of demographic and biomarker variables across three distinct studied groups.

Variables	PCOS w	with Stroke PCOS without Stroke		ithout Stroke	Healthy Control		P-Value
variables	Mean	SD	Mean	SD	Mean	SD	P-value
Age (Years)	33.160	8.931	33.720	9.170	32.893	9.258	0.852†
PTX3 (ng/mL)	5.717	1.172	3.665	1.085	2.377	0.740	<0.001*
CRP (mg/L)	8.043	2.102	5.448	1.532	3.037	0.959	0.651†
TG/HDL Ratio	4.297	0.935	3.719	0.863	2.203	0.585	0.189†
HOMA-IR	3.547	0.949	3.194	1.034	1.771	0.492	0.148†
NIHSS	14.507	7.119	N/A	N/A	N/A	N/A	N/A

[†] Anova, *Post-hoc Tukey test (PCOS with stroke group as reference), PTX3= Pentraxin-3, HOMA-IR= Homeostatic model assessment for insulin resistance, CRP= C-reactive protein, TG/HDL= Triglyceride/ high density lipoprotein, NIHSS= National Institutes of Health Stroke Scale.

Table 2. Pearson Correlation Coefficients between Biomarkers and Stroke Severity (NIH Stroke Scale).

Variable	Pearson's r	p-value
PTX3 (ng/mL)	0.429	< 0.001
HOMA-IR	-0.115	0.520
CRP (mg/L)	-0.097	0.595
TG/HDL Ratio	-0.030	0.796
DELLO D O IVO		

PTX3= Pentraxin-3, HOMA-IR= Homeostatic model assessment for insulin resistance, CRP= C-reactive protein, TG/HDL= Triglyceride/ high density lipoprotein.

Relation of various biomarkers with NIH stroke scale severity in PCOS: Figure 1 demonstrates the relationship of 4 biomarkers namely PTX3, CRP, TG/HDL ratio, and HOMA-IR, with stroke severity as measured by the NIH Stroke Scale in patients with PCOS who have had a stroke. Each plot shows a regression line that represents the average trend and a 95% confidence interval that surrounds the line. The relationship between the levels of PTX3 and the severity of stroke is positive and statistically significant. This can be seen from the positively inclined regression line which has a distinct slope. This

finding indicated that increased levels of

PTX3 are associated with more severe strokes in PCOS patients, signifying its possibility as a predictor of stroke severity. On the other hand, the scatter plot that associates CRP levels to the NIH Stroke Scale is almost horizontal, indicating a low correlation between CRP and stroke severity. Moreover, the TG/HDL Ratio has a mild increase with the NIH Stroke Scale that indicates a weak relationship.

Finally, the relation between HOMA-IR and stroke scale severity shows weakly negative trend, signifying that HOMA-IR has a poor correlation with stroke severity.

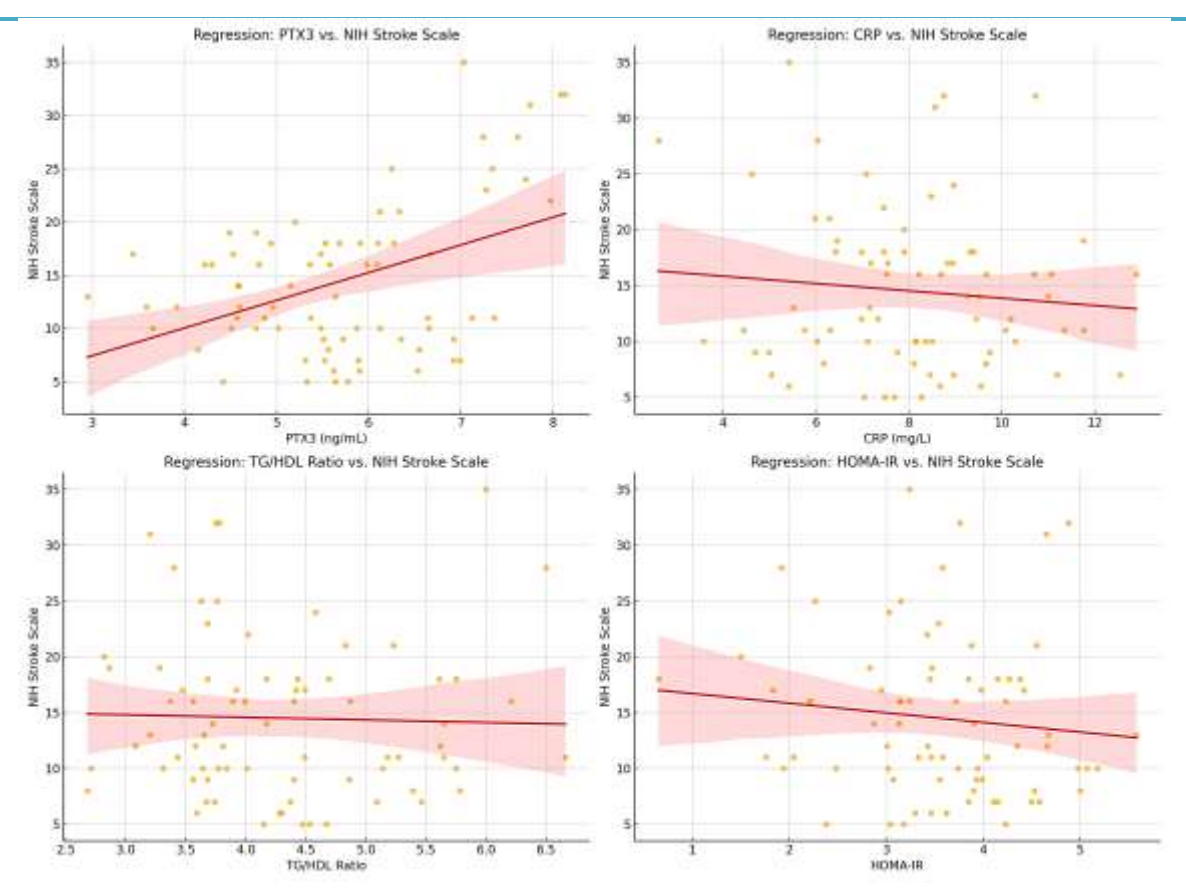


Figure 1. Regression line analysis shows the relation of various biomarkers with NIH stroke scale severity in PCOS.

Discussion

Ischemic stroke is one of the emergent neurological disorders that are common with high morbidity and mortality rate in the world (16). It's important to manage this condition to minimize the morbidity and mortality rate. Currently, biomarkers that are related to inflammatory and metabolic changes are considered as markers of the risk of ischemic stroke especially in people with other diseases like polycystic ovarian syndrome (PCOS).

PCOS is defined by a disturbance of hormone secretion, which may involve elevated androgen production and the attenuation of the effectiveness of insulin, as well as lowered levels of inflammation – all of which are known to be the risks for various conditions, including strokes (17). A major problem in managing strokes among PCOS patients is to determine the effect of each biomarker on the severity and progression of the stroke.

The present study examined the biomarkers such as pentraxin-3 (PTX3), C-reactive protein (CRP), triglyceride/high density lipoprotein (TG/HDL) ratio, and homeostatic model assessment for insulin resistance (HOMA-IR) together to capture the inflammatory interconnected and metabolic pathways that may raise ischemic stroke risk in PCOS patients: PTX3 reflects local vascular **CRP** inflammation. indicates systemic inflammation. the TG/HDL-C ratio atherogenic dyslipidemia, and HOMA-IR measures insulin resistance, factors that collectively contribute to vascular dysfunction and stroke development in this population.

The current study showed an increase in PTX3 levels among individuals in the PCOS with Stroke group compared to those in both the PCOS without Stroke and the Healthy Control groups (p < 0.001). This finding aligns with the Ye, X., et al. study that has linked PTX3 levels to vascular inflammatory and ischemic events of cardiovascular disease (18).

The strong connection between PTX3 levels and NIH Stroke Scale ratings (correlation coefficient of 0.429 with a p-value less than 0.001) indicates that PTX3 could serve as an indicator for estimating stroke severity in patients with PCOS. It's crucial to mention that the examination results related to CRP, TG/HDL ratio, and HOMA IR present a more complex scenario. CRP levels were higher in both PCOS groups compared to the healthy controls group; however, the variance between the PCOS with and without Stroke groups did not reach statistical significance (p=0.651). This finding challenges the Biya A. study that highlighted CRP as an indicator of stroke severity (19). In our study, the findings did not show a link between factors, possibly due to the nature of inflammation in PCOS conditions. This suggests that CRP alone might not be sensitive enough to identify the precise vascular inflammatory processes linked to strokes. In a way, the TG/HDL ratio and HOMA IR levels in both groups, with PCOS compared to healthy controls, suggest the metabolic issues commonly seen in PCOS cases. There were no variances found in either the TG/HDL ratio or HOMR index between the groups with PCOS Stroke and those without (with p-values of 0.189 for the TG/HDL ratio and 0.148 for the HOMA IR index). This finding differs from studies that suggest high TG/HDL ratios may be indicative of a problem like strokes (20, 21). One way to understand this situation is that dyslipidemia might not affect stroke severity on its own but could also be influenced by factors such as endothelial dysfunction and chronic inflammation, rather than just lipid metabolism (22).

The connection between PTX3 and ischemic stroke has been extensively studied by researchers who believe it could serve as an indicator of prognosis. For instance, Zhu Y et al. study found that higher PTX3 levels are independently associated with increased mortality after ischemic stroke (23). However, conflicting results come from Zhang CY. et al. study, which showed no link between PTX3 and the severity of stroke (24). The variation in results could be due to the variations in the characteristics of patients and their current health conditions. Our research concentrates on patients diagnosed with PCOS, providing a distinct viewpoint on how metabolic and hormonal aspects impact PTX3 expression levels in relation to CRP, TG/HDL ratio, and HOMA-IR. The lack of findings could be attributed to the range of PCOS presentations. Some individuals may exhibit more pronounced metabolic issues than others do. Furthermore, the association between stroke severity and HOMA IR, a metric for insulin resistance, was not found to be statistically significant. This observation aligns with the study conducted by Gu T. et al. In a survey conducted in 2020 (25), it was found that although insulin resistance is recognized, the exact link between it and the seriousness of ischemic stroke remains unclear. Our results indicate that even though insulin resistance is common among those with PCOS, it may not be directly associated with increasing the risk of stroke unless accompanied by other risk factors. The specific roles of the biomarkers studied in this study highlight the process of developing stroke in patients with PCOS. Our research has certain limitations that need to be considered. Firstly, the structure of our study makes challenging to establish cause-and-effect relationships between biomarkers and stroke severity clearly. Long-term studies are necessary to how these understand biomarkers evolve. Additionally, although our sample size is adequate for statistical analysis, it may not represent all PCOS types. Furthermore, exploring the metabolic

aspects in more detail could illuminate the connection between biomarkers and stroke outcomes.

Conclusion

Pentraxin-3 levels are markedly higher in PCOS patients who have had an ischemic stroke, and the level is in proportion to the severity of the stroke. This means that PTX3 could be potentially used as a biomarker for risk Nevertheless, assessment. other biomarkers such as CRP, the TG/HDL ratio, and HOMA-IR did not show significant differences when compared between stroke and non-stroke patients, which suggests that PTX3 may be a better predictor than the conventional markers. Further work is needed to determine the relationship between PTX3 and stroke-related complications in PCOS and to confirm these results in larger, multicenter studies.

Source of funding: No source of funding. **Ethical clearance:**

The study was conducted ethically and followed the guidelines of the Declaration of Helsinki; ethical clearance was obtained from the Research Ethics Committee of the University Of Kirkuk College Of Medicine (Document no.70, date May 14, 2025). Anonymity and confidentiality were maintained at all times during the study, and written informed consent was obtained from all participants before they were enrolled without any other sources.

Conflict of interest: None.

Use of Artificial Intelligence (AI): The authors state they did not use any generative AI tools for creating or editing the manuscript's language.

Acknowledgments: The authors would like to express their sincere appreciation to all individuals and institutions that provided valuable support and guidance during the development of this research. Their

contributions have been essential to the successful completion of this work.

References

- 1. Taha MA, Shukur AS. Effect of Aspirin and Clopidogrel on C-Reactive Protein in Acute Ischemic Stroke. International Journal of Pharmaceutical Research (09752366). 2019 Jan 1:11(1).
- 2. Taha, M., Gümüş, H. Shaping the Future of Stroke Management: Latest Innovations and Discoveries. Kirkuk Journal of Medical Sciences, 2025; 13(2): 1-3. doi: 10.32894/kjms.2025.161005.1162.

https://doi.org/10.32894/kjms.2025.161005.1162

3. Pacinella G, Ciaccio AM, Tuttolomondo A. Molecular links and clinical effects of inflammation and metabolic background on ischemic stroke: an update review. Journal of Clinical Medicine. 2024

Dec 10;13(24):7515.

https://doi.org/10.3390/jcm13247515

- 4. Ibrahim RO, Omer SH, Fattah CN. The correlation between hormonal disturbance in PCOS women and serum level of kisspeptin. International journal of endocrinology. 2020;2020(1):6237141. https://doi.org/10.1155/2020/6237141
- 5. Haseeb NM, Mohammed EA, Ibrahem S. Significance of maternal serum pentraxin-3 level in assessment of severity of pre-eclampsia and its effect on neonatal outcome. Medical Journal of Babylon. 2023 Dec 1;20(Supplement 1):S88-94. https://doi.org/10.4103/MJBL_MJBL_30_23
- 6. Banfi C, Brioschi M, Vicentini LM, Cattaneo MG. The Effects of Silencing PTX3 on the Proteome of Human Endothelial Cells. International Journal of Molecular Sciences. 2022 Nov 3;23(21):13487.

https://doi.org/10.3390/ijms232113487

7. Shindo A, Takase H, Hamanaka G, Chung KK, Mandeville ET, Egawa N, Maki T, Borlongan M, Takahashi R, Lok J, Tomimoto H. Biphasic roles of pentraxin 3 in cerebrovascular function after white matter stroke. CNS Neuroscience & Therapeutics. 2021

Jan;27(1):60-70.

https://doi.org/10.1111/cns.13510

8. Ceylan M, Yalcin A, Bayraktutan OF, Atis O, Acar E. Serum pentraxin-3 levels in acute stroke: No association with stroke prognosis. Atherosclerosis. 2015 Dec 1;243(2):616-20.

 $\frac{https://doi.org/10.1016/j.atherosclerosis.2015}{.10.089}$

9. Violi F, Pastori D. Pentraxin 3–A Link Between Obesity, Inflammation and Vascular Disease?—. Circulation Journal. 2016 Jan 25;80(2):327-8.

https://doi.org/10.1253/circj.CJ-15-1303

10. Ryu WS, Kim CK, Kim BJ, Kim C, Lee SH, Yoon BW. Pentraxin 3: a novel and independent prognostic marker in ischemic stroke. Atherosclerosis. 2012 Feb 1;220(2):581-6.

https://doi.org/10.1016/j.atherosclerosis.2011 .11.036

11. Cao Z, Chen Z, Yang J, Shen X, Chen C, Zhu X, Fang Q. Prediction Value of High Serum Pentraxin-3 for Short-Term Recurrence of Cerebral Infarction in Patients Accompanied with Intracranial Atherosclerotic Stenosis Within One Year. International Journal of General Medicine. 2024 31:6029-35. Dec https://doi.org/10.2147/IJGM.S491039

- 12. Dubey P, Reddy S, Sharma K, Johnson S, Hardy G, Dwivedi AK. Polycystic ovary syndrome, insulin resistance, and cardiovascular disease. Current Cardiology Reports. 2024 Jun;26(6):483-95. https://doi.org/10.1007/s11886-024-02050-5
- 13. Abdalla MA, Shah N, Deshmukh H, Sahebkar A, Östlundh L, Al-Rifai RH, Atkin SL, Sathyapalan T. Effect of pharmacological interventions on lipid profiles and C-reactive protein in polycystic ovary syndrome: A systematic review and meta-analysis. Clinical Endocrinology. 2022 Apr;96(4):443-59. https://doi.org/10.1111/cen.14636
- 14. Lu Q, Chen B, Li A, Liang Q, Yao J, Tao Y, Dai F, Hu X, Lu J, Liu Y, Liu Y. The correlation between HOMA-IR and cardiometabolic risk index among different metabolic adults: a cross-sectional study. Acta Diabetologica. 2025 Jan;62(1):49-57. https://doi.org/10.1007/s00592-024-02332-y
- 15. Koka A, Stuby L, Carrera E, Gabr A, O'Connor M, Missilier Peruzzo N, Waeterloot O, Medlin F, Rigolet F, Schmutz T, Michel P. Asynchronous Distance Learning Performance and Knowledge Retention of the National Institutes of Health Stroke Scale

Among Health Care Professionals Using Video or e-Learning: Web-based Randomized Controlled Trial. Journal of medical Internet research. 2025 Mar 4;27:e63136. https://doi.org/10.2196/63136
16. Ganti L. Management of acute ischemic stroke in the emergency department: optimizing the brain. International Journal of Emergency Medicine. 2025 Jan 7;18(1):7. https://doi.org/10.1186/s12245-024-

17. Su P, Chen C, Sun Y. Physiopathology of polycystic ovary syndrome in endocrinology, metabolism and inflammation. Journal of ovarian research. 2025 Feb 20;18(1):34. https://doi.org/10.1186/s13048-025-01621-6

00780-5

- 18. Ye X, Wang Z, Lei W, Shen M, Tang J, Xu X, Yang Y, Zhang H. Pentraxin 3: A promising therapeutic target for cardiovascular diseases. Ageing research reviews. 2024 Jan 1;93:102163. https://doi.org/10.1016/j.arr.2023.102163
- 19. Biya A. The role of high sensitivity C-reactive protein level in predicting stroke and other cardiovascular events: a meta-analysis review. Int J Health Pharm. 2024;9(4):104-28. https://doi.org/10.56201/ijhpr.v9.no4.2024.pg104.128
- 20. Zhang S, Cao C, Han Y, Hu H, Zheng X. A nonlinear relationship between the triglycerides to high-density lipoprotein cholesterol ratio and stroke risk: an analysis based on data from the China Health and Retirement Longitudinal Study. Diabetology & Metabolic Syndrome. 2024 Apr 27;16(1):96. https://doi.org/10.1186/s13098-024-01339-3
- 21. Han Y, Huang Z, Zhou J, Wang Z, Li Q, Hu H, Liu D. Association between triglyceride-to-high density lipoprotein cholesterol ratio and three-month outcome in patients with acute ischemic stroke: a second analysis based on a prospective cohort study. BMC neurology. 2022 Jul 16;22(1):263. https://doi.org/10.1186/s12883-022-02791-2
- 22. Tuttolomondo A, Daidone M, Pinto A. Endothelial dysfunction and inflammation in ischemic stroke pathogenesis. Current Pharmaceutical Design. 2020 Sep 1;26(34):4209-19.

https://doi.org/10.2174/1381612826666200417154

23. Zhu Y, Fan K, Zhao X, Hou K. The Association Between Serum Pentraxin-3 Level at Admission

and the Functional Outcome of Patients After Acute Ischemic Stroke: A Meta-Analysis. Balkan Medical Journal. 2025 May 5;42(3):201.

https://doi.org/10.4274/balkanmedj.galenos.2 025.2025-1-36

24. Zhang CY, Han HD, Wang SY, Huang SR, Deng BQ. Pentraxin-3 in thrombolytic therapy for acute ischemic stroke: no relation with curative effect and prognosis. Medical science monitor: international medical journal of experimental and clinical research. 2018 Jun 27:24:4427.

https://doi.org/10.12659/MSM.909015

25. Gu T, Yang Q, Ying G, Jin B. Lack of association between insulin resistance as estimated by homeostasis model assessment and stroke risk: A systematic review and meta-analysis. Medical hypotheses. 2020 Aug 1;141:109700. https://doi.org/10.1016/j.mehy.2020.109700

تقییم مستوی البنتراکسین ۳ بین مرضی الجلطة الدماغیة الاقفاریة المصابین بمتلازمة تکیس المبایض المبایض المبایض المناد اکرم طه، المدراء عبد الکریم محمد

الملخص

الخلفية: يُعد البنتراكسين-٣ (Pentraxin 3) مكونًا هامًا من مكونات جهاز المناعة الفطرية، ويلعب دورًا مهمًا في العمليات الالتهابية وتلف الأنسجة. قد يوفر تقييم مستوياته في الحالات السريرية المختلفة رؤى حول أهميته التشخيصية والتنبؤية.

الأهداف: تقييم العلاقة بين مستويات البنتر اكسين-٣ وحدوث السكتة الدماغية الإقفارية بين المريضات المصابات بمتلازمة تكيس المبايض.

المواد والطرق: تم إجراء دراسة الحالات والشواهد في عيادات الأعصاب والتوليد وأمراض النساء في مستشفى آزادي التعليمي في كركوك، ابتداءً من ١ شباط ٢٠٢٣ وحتى ١ آذار ٢٠٢٤. تم تشخيص النساء المصابات بمتلازمة تكيس المبايض وفقًا لمعايير روتردام، وقسمن إلى ثلاث مجموعات: المجموعة الأولى ضمت مريضات لديهن تكيس المبايض مع سكتة دماغية، والمجموعة الثانية ضمت مريضات لديهن تكيس المبايض بدون سكتة دماغية، والمجموعة الثالثة كانت مجموعة ضابطة مطابقة بالعمر تتراوح أعمار المشاركات فيها بين ١٨-٥٠ سنة. تم سحب عينات الدم في الصباح لتحديد مستويات PTX3 و تسبة TG/HDL ومؤشر مقاومة الإنسولين (HOMA-IR) وتم قياسها في جميع المجموعات المدروسة.

النتائج: كانت مستويات PTX3 أعلى بشكل ملحوظ في مجموعة مريضات تكيس المبايض المصابات بالسكتة الدماغية (0,V1V + 0,V1V أناوغرام/مل) مقارنة بالمصابات بتكيس المبايض بدون سكتة دماغية (0,V1V + 0,V1V نانوغرام/مل) (0,V2V والمجموعة الضابطة (0,V1V + 0,V2V) بينما لم تكن هناك علاقة ذات دلالة إحصائية مع CRP أو نسبة TG/HDL أو TG/HDL.

الاستنتاج :مستويات البنتر اكسين-٣ مرتفعة بشكل ملحوظ لدى المريضات المصابات بمتلازمة تكيس المبايض واللواتي تعرضن لسكتة دماغية إقفارية، وترتبط هذه المستويات بشدة السكتة. مما يشير إلى إمكانية استخدام PTX3 كواسم حيوي لتقييم خطر الإصابة بالسكتة الدماغية.

الكلمات المفتاحية: متلازمة تكيس المبايض؛ السكتة الدماغية الإقفارية؛ البنتر اكسين-٣. CRP, PCOS

المؤلف المراسل: مفيد أكرم طه

mufeedakram@uokirkuk.edu.iq الايميل:

تاريخ الاستلام: ٢ نيسان ٢٠٢٥

تاریخ القبول: ۲۱ تموز ۲۰۲۰

تاريخ النشر: ٢٠ تشرين الأول ٢٠٢٥

ا فرع الباطنية، كلية الطب، جامعة كركوك، كركوك، العراق.

٢ قسم علوم الحياة، كلية العلوم، جامعة كركوك، كركوك، العراق.

" فرع النسائية والتوليد، كلية الطب، جامعة كركوك، كركوك، العراق.

Interplay Between Biometric Profiles, Biomarkers, Body Fat, and Bone Health: A Statistical and Machine Learning Approach

Jawad Kadhum Abass (b), Wisam A. Hussein (b), Ahmed Naseer Kaftan (b)

OPEN ACCESS

Correspondence: Wisam A. Hussein Email: wisam.allami@uokufa.edu.iq
Copyright: ©Authors, 2025, College of Medicine, University of Diyala. This is an open access article under the CC BY 4.0 license (http://creativecommons.org/licenses/by/4.0/)
Website:

https://djm.uodiyala.edu.iq/index.php/djm

Received: 19 April 2025 Accepted: 24 August 2025 Published: 25 October 2025

Abstract

Background: Obesity and metabolic disorders are increasingly prevalent public health concerns. Excess adiposity, particularly visceral fat, is associated with metabolic dysfunction, whereas regional fat depots, such as gynoid fat, may confer protective benefits on skeletal integrity.

Objectives: This study aimed to examine the intricate relationship between biometric profiles, biochemical markers, body fat distribution, and bone health.

Patients and Methods: Data were obtained from the National Health and Nutrition Examination Survey (NHANES), including adult participants with complete measurements on body composition (total, visceral, and subcutaneous fat; BMI; waist circumference), biochemical markers (lipid profiles, fasting glucose, insulin, hormonal regulators), and bone health metrics (bone mineral density and content via DXA). Correlation and multivariate regression analyses were conducted to identify predictors among demographic, biometric, and biochemical variables. Machine learning techniques, specifically Random Forest Regression, were employed to enhance predictive modeling of fat indices and bone health outcomes.

Results: BMI and waist circumference emerged as robust predictors of total and visceral fat, with significant gender and age disparities noted. Women exhibited higher total and subcutaneous fat, whereas men demonstrated increased visceral fat. Biochemical markers, notably insulin and glucose, correlated strongly with adiposity indices. Furthermore, bone health was positively associated with BMI and specific biomarkers (testosterone, Creatinine phosphokinase (CPK) and negatively associated with Sex Hormone-Binding Globulin (SHBG) and Alkaline Phosphatases (ALP). Moderate to high predictive accuracy was observed for the machine learning models, confirming the supporting role of predictive analytics in understanding these relationships.

Conclusion: The combination of anthropometric measures, biochemical markers, fat and bone density, and machine learning offers a comprehensive understanding of their correlation. Such insights can inform the design of targeted clinical decision-making strategies and highlight the feasibility of using simple, non-invasive measurements to assess metabolic and skeletal risks.

Keywords: biometric profile, bone health, body fat, machine learning approach.

¹Department of Medicine, college of Medicine, Kufa University, Najaf, Iraq.

² Department of Surgery, college of Medicine, Kufa University, Najaf, Iraq.

³ Department of Biochemistry, college of Medicine, Kufa University, Najaf, Iraq.

Introduction

Metabolic health and obesity are emerging as major healthcare challenges, mainly due to the role of body fat distribution in contributing to associated health risks.

Metabolic health and obesity are becoming major health care problems, which are linked to the distribution of body fat that contributes to disorders, associated risks. Metabolic cardiovascular disease, and impaired bone health are related to fat accumulation, particularly visceral adiposity. To determine individuals at risk for these disorders and provide further preventive actions, we must understand the interplay between body fat distribution, bone integrity, and biochemical markers; the way our bodies store fat is becoming a central issue in healthcare, linking obesity to significant health dangers. Health complications like metabolic syndromes, heart conditions, and even weakened bones are increasingly tied to where fat accumulates, with fat around the organs—known visceral adiposity—being particularly problematic. To effectively prevent these conditions, it's essential that we gain a deeper insight into how body fat location, bone strength, and various blood markers are all interconnected (1).

These relationships are as intricate as those between fat distribution and bone health. For example, while increased body weight is traditionally seen as protective for bone density due to mechanical loading, excessive adiposity, particularly visceral fat, is increasingly recognized as a potential negative factor in bone metabolism. This is caused by the damaging effects of inflammatory cytokines, hormonal shifts, and metabolic disturbances resulting from fat overload. The negative influence of visceral fat on the skeleton goes down to the cellular level, disrupting the delicate balance between bone creation and breakdown. Fat cells are not inert;

produce hormones like leptin thev adiponectin. While leptin can sometimes support bone formation, in states of obesity, the body can become leptin-resistant, nullifying any benefits. At the same time, the chronic inflammation driven by excess visceral fat directly encourages the cells that dissolve bone (osteoclasts) while hindering the cells that build new bone (osteoblasts). This creates an environment where the skeleton is constantly being weakened from within, even while it's carrying a heavier load (2). Conversely, certain types of regional fat distribution, especially gynoid fat, have been linked to positive effects on bone mass, which also highlights the importance of differentiating various fat depots. Unlike the inflammatory nature of deep abdominal fat, the fat stored on the hips, thighs, and buttocks—known as gynoid fat—has a much healthier metabolic profile. This type of fat depot is more stable and less likely to release inflammatory substances into the bloodstream. Instead, it's better at safely storing fatty acids for the long term. It is known to secrete beneficial hormones like adiponectin, which improves the body's sensitivity to insulin and has antiinflammatory effects. This creates a systemic environment that is much more conducive to healthy bone maintenance, supporting the activity of bone-building cells (3).

Adiposity and bone health have determinants, with key biomarkers such as lipid profiles, glucose metabolism indicators, and hormonal regulators serving as biochemical markers. Fat storage patterns resulting from insulin resistance, dyslipidemia, and hormonal imbalances, along with their impact on bone mineralization changes, warrant concern. This underscores the need for a highly integrated approach to bone health; Beyond their role in cardiovascular risk, specific components of a person's lipid profile have a direct and damaging effect on the bone's internal

environment. When levels of triglycerides and "bad" LDL cholesterol are high, fatty acids can accumulate within the bone marrow. This lipotoxicity is directly poisonous to the bonebuilding osteoblast cells and creates a shift in the bone marrow's cellular development. encourages stem cells to become fat cells (adipocytes) rather than bone cells, effectively "crowding out" the machinery needed for skeletal repair. This results in a bone structure that is not only less dense but is also filled with inflammatory fat tissue, weakening it from the inside out (4,5). The relationship among these factors can be explored more deeply using advanced statistical techniques, such regression analysis and machine learning models, which will aid in risk stratification and predictive modeling.

This study aims to investigate the relationship between the distribution of body fat, biomarkers, body measurements, and metrics of bone health (density and content) using correlation, regression, and machine learning analysis methods. It aims to explore the crucial relationships between adiposity and bone health, which may aid in developing clinical evaluation and customized treatment strategies using data from the National Health and Nutrition Examination Survey (NHANES) (if any) data set.

Patients and Methods

Study design and data source: The study was conducted using data from the National Health and Nutrition Examination Survey (NHANES), which is a nationwide, cross-sectional survey program sponsored by the U.S. Centers for Disease Control and Prevention (CDC). NHANES collects data across multiple U.S. locations, representing the non-institutionalized U.S. civilian population. The analysis was performed on a cohort of approximately 8,000 adults aged 18 years and older, selected from the NHANES dataset (2017-2018 cycle), with

complete data on body fat indices, biometric markers, biochemical markers, and bone health parameters. The study period spanned from 2013 to 2016, based on data from two consecutive NHANES cycles (2013-2014 and 2015-2016). This study utilizes publicly accessible information from the National Health and Nutrition Examination Survey (NHANES), a cross-sectional survey sponsored by the Centers for Disease Control and Prevention (CDC) under the American Government, NHANES collects comprehensive data for the entire nation, encompassing health information such as demographics, biometrics, biochemistry, body composition, and other data gathered through interviews, physical assessments, and laboratory investigations.

Study population: The study sample comprises all adult respondents aged 18 years and older who have complete information on body fat indices, biometric, lipid, and metabolic markers, as well as bone health parameters. Exclusion criteria included individuals with missing data for key variables, those with diagnosed metabolic or skeletal disorders that could confound the results, and pregnant women.

Variables and measurements body distribution and biometric measures: Total fat mass, measured in grams, was determined using Dual-Energy X-ray Absorptiometry (DXA), a validated imaging method that provides precise assessments of body composition (6). Visceral fat mass, also in grams, was calculated through proprietary DXA-based algorithms specifically designed to estimate fat within the abdominal cavity (7). Subcutaneous fat mass, similarly measured in grams, was estimated using DXA's regional fat segmentation capabilities, which distinguish it from visceral fat (6). The android fat percentage indicates fat accumulation in the abdominal region and is obtained through regional analysis of DXA scans (8). In contrast, the gynoid fat



percentage reflects fat distribution in the hips and thighs (9). Total body fat percentage was calculated as the ratio of total fat mass to total body weight (8). Body Mass Index (BMI), expressed in kg/m², was derived from directly measured body weight and height (9,10). Waist circumference was measured in centimeters at the level of the iliac crest using a standardized tape measure protocol (11). Age was self-reported by participants, and gender was recorded as male or female (9).

Biochemical markers: Lipid profile assessments included total cholesterol and triglyceride levels, both measured in milligrams per deciliter (mg/dL) using standardized enzymatic assays (12). Metabolic biomarkers included fasting glucose and fasting insulin, measured in milligrams per deciliter (mg/dL) and micro-units per milliliter (µU/mL), (12). Additional biomarkers respectively relevant to metabolic and hormonal status were analyzed through blood samples. These included alkaline phosphatase (ALP) (13,14) and creatine phosphokinase (CPK) (15,16), reported in units per liter (U/L), as well as phosphorus (mg/dL), which plays a role in bone mineralization (17). Vitamin D levels were assessed as serum 25-hydroxyvitamin D [25(OH)D], measured in nanograms per milliliter (ng/mL), serving as an indicator of vitamin D status (18). Sex hormones were also quantified: estradiol (19), testosterone (20), and sex hormone-binding globulin (SHBG) (21, 22), which were reported in appropriate standardized units.

Bone health metrics: Bone health was evaluated using two primary DXA-derived indicators. Bone Mineral Density (BMD), expressed in grams per square centimeter (g/cm²), represents the concentration of mineral content in bone and is a widely used metric for assessing osteoporosis and fracture risk (23, 24, 20). Bone Mineral Content (BMC), measured in

grams, reflects the total amount of mineral present in the scanned bone area, complementing BMD in characterizing overall bone strength (17,18,25). Additional associations with bone metabolism include the influence of obesity (23), testosterone (20), SHBG (22), and biochemical markers such as ALP (13) and CPK (15, 16).

Statistical Analysis

To examine the relationships among fat distribution, biometric characteristics, and biochemical rank markers, Spearman's correlation analysis was employed in R (2). This non-parametric method was chosen to capture both linear and non-linear associations between variables that may not follow distributions, including fat indices, metabolic biomarkers, and anthropometric measures.

Multivariate linear regression models were constructed to further evaluate the predictive capacity of demographic, biometric, and biochemical variables on outcomes such as fat indices, bone health parameters, and lipid metabolism indicators. These models accounted for potential confounding variables, including age and gender, to isolate the independent effects of the predictors. The goal was to identify key determinants of body composition and bone status within a multifactorial framework.

In addition to classical statistical methods, machine learning approaches were employed to enhance prediction accuracy and uncover complex, non-linear relationships. Random Forest Regression models (3) were developed using the Scikit-learn library in Python (v1.0.2) (1) to predict total fat mass using age, BMI, and waist circumference; visceral fat mass using cholesterol, triglycerides, glucose, and insulin; and bone mineral density and content using a range of metabolic and hormonal biomarkers. Model performance was evaluated using standard metrics: the coefficient of

determination (R²), root mean squared error (RMSE), and mean absolute error (MAE), providing insight into both accuracy and model robustness.

All statistical analyses and data preprocessing were conducted using R version 4.1.2 (2) and Python version 3.8. Machine learning models were implemented using the Scikit-learn library (1). The NHANES dataset was accessed, cleaned, and manipulated using Pandas (4) and NumPy (5). Visualization of the analytical results, including correlations, model performance, and feature importance, was performed using Matplotlib (24) and Seaborn (25), allowing for precise and interpretable graphical representation of findings.

Results

Biometric variables and fat indices: The relationship between biometric variables and fat indices revealed consistent patterns across both correlation and regression analyses (Table 1, Figure 1). BMI and waist circumference emerged as the strongest predictors of fat accumulation, with Spearman's correlation coefficients exceeding 0.8 when compared to total fat. Gender-based differences were pronounced: women exhibited significantly higher total and subcutaneous fat, while men showed greater visceral fat accumulation. Age was positively associated with visceral fat but showed a slight negative association with total fat percentage. Regression models (Table 2) supported these findings; total fat was highly predictable ($R^2 = 0.923$) using BMI and waist circumference, with women having approximately 5.7 kg fatter than men. Total percent fat was also well explained ($R^2 = 0.784$), with a clear gender gap ($\beta = 11.61\%$, p < 0.001). Visceral fat was most strongly associated with waist circumference and age ($R^2 = 0.677$), and

men had significantly higher values. The Random Forest model predicting total fat using age, BMI, and waist circumference yielded robust performance ($R^2 = 0.85$, RMSE = 4.5 kg, MAE = 3.5 kg) (Table 3), highlighting the dominant role of anthropometric predictors. However, the inclusion of biochemical markers could further improve model accuracy. The feature importance from this model is shown in Figure 2.

Biochemical markers and fat indices:

In examining the influence of biochemical markers on fat indices, correlations revealed modest but significant relationships (Figure 3). Total cholesterol showed weak-to-moderate associations with total and subcutaneous fat, while triglycerides correlated moderately with android, gynoid, and total fat. Glucose demonstrated similar correlations, particularly with android and visceral fat. Insulin was the strongest biochemical predictor, showing moderate-to-strong correlations ($\rho \approx 0.5-0.6$) across all fat measures. Regression models (Table 4) confirmed insulin's dominant role, especially in predicting total fat ($R^2 = 0.196$) and visceral fat $(R^2 = 0.281)$, with glucose contributing as a secondary predictor. Total percent fat was more weakly explained by biomarkers alone ($R^2 = 0.095$). In machine learning models predicting visceral fat using cholesterol, triglycerides, glucose, and insulin, the model achieved limited performance (R^2 = 0.33) (Table 3), reinforcing that lipid and glucose metabolism markers, while important, are insufficient as standalone predictors of fat accumulation, likely due to missing physiological or genetic variables.

ORIGINAL RESEARCH

Published: 25 October 2025 DOI: 10.26505/djm.v29i1.1415

Table 1. Correlation between biometric variables and fat indices (spearman's ρ).

Fat Index	Age	Gender (M=0, F=1)	BMI	Waist Circumference
Total Fat (g)	-0.18	0.62	0.85	0.83
Visceral Fat (g)	0.42	-0.51	0.65	0.77
Subcutaneous Fat (g)	-0.05	0.59	0.79	0.76
Android Fat (%)	0.21	0.10	0.68	0.72
Gynoid Fat (%)	-0.12	0.48	0.63	0.54

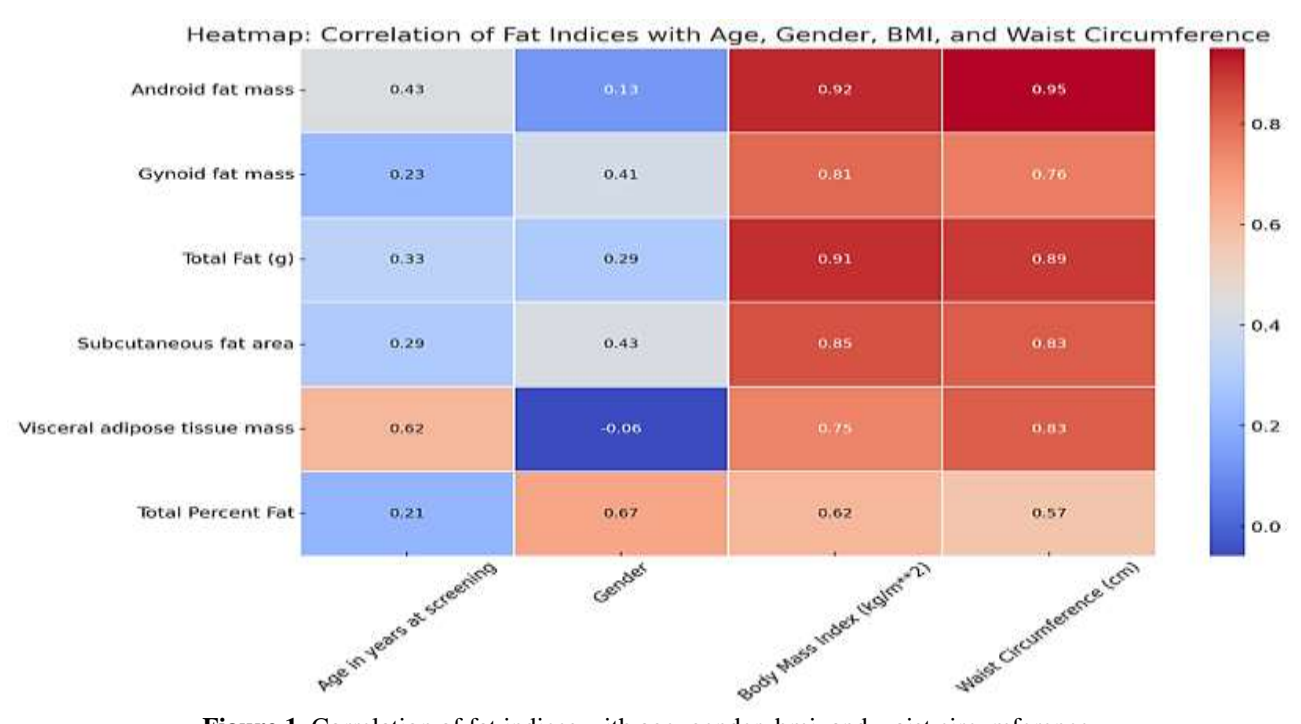


Figure 1. Correlation of fat indices with age, gender, bmi, and waist circumference.

Table 2. Regression results for predicting fat indices.

Dependent Variable	Predictor	β (Coefficient)	p-value	\mathbb{R}^2
Total Fat (g)	BMI	841.64	< 0.001	0.923
	Waist Circumference	328.41	< 0.001	
	Gender (F)	5726.02	< 0.001	
Total Fat (%)	Waist Circumference	0.25	< 0.001	0.784
	BMI	0.16	< 0.001	
	Age	-0.027	< 0.001	
	Gender (F)	11.61	< 0.001	
Visceral Fat (g)	Age	6.59	< 0.001	0.677
	Waist Circumference	11.01	< 0.001	
	Gender (F)	-28.79	< 0.001	

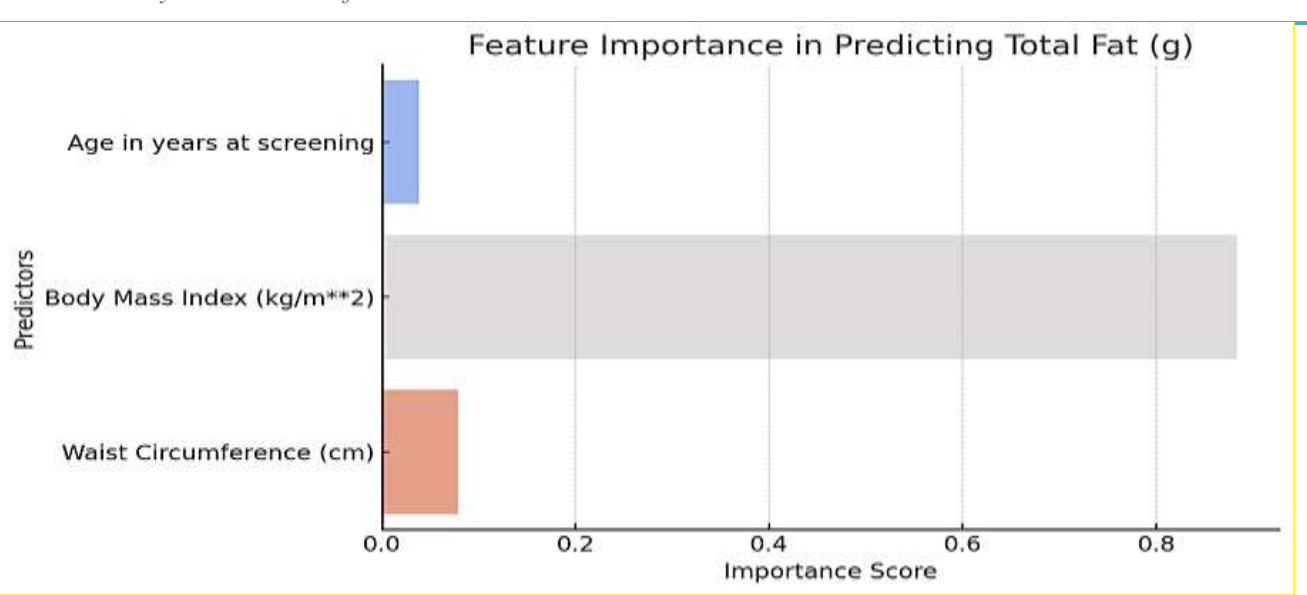


Figure 2. Feature importance in predicting total fat (g).

Table 3. Machine learning model performance summary.

Outcome	Model	\mathbb{R}^2	RMSE	MAE
Total Fat (g)	Random Forest	0.85	4.5 kg	3.5 kg
Visceral Fat (g)	Random Forest	0.33	229.1 g	171.1 g
Bone Density (g/cm²)	Random Forest	0.24	0.105 g/cm ²	0.084 g/cm ²
Bone Content (g)	Random Forest	0.36	379.42 g	302.95 g

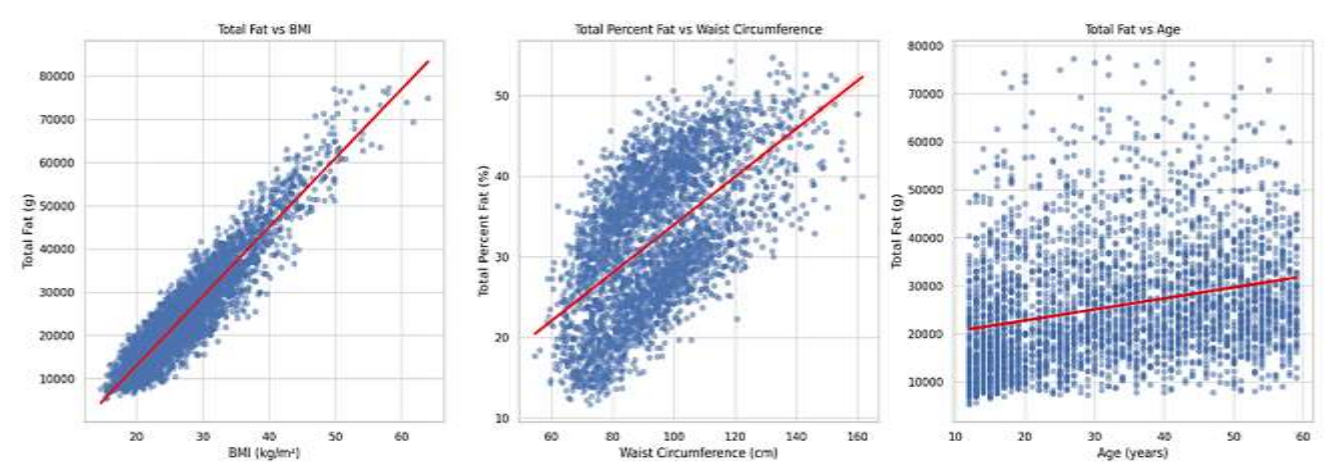


Figure 3. Regression of biomarkers with fat indices.

Table 4. Machine learning model performance summary.

Dependent Variable	Predictor	В	p-value	R ²
Total Fat (g)	Insulin	318	< 0.001	0.196
	Glucose	48.8	< 0.001	
Total Fat (%)	Insulin	0.165	< 0.001	0.095
Visceral Fat (g)	Insulin	4.74	< 0.001	0.281
	Glucose	1.99	< 0.001	

Bone health and biometric characteristics:

The association between bone health and biometric characteristics revealed both intuitive and novel findings (Figure 4, Figure 5). Age, BMI, and waist circumference were all positively associated with bone density and bone content, though gender differences were notable, with women displaying significantly lower values in

both metrics. Regression analysis (Table 5). Showed that BMI and age positively predicted bone mineral density (BMD), whereas waist circumference had a small but negative association ($R^2 = 0.131$). For bone mineral content (BMC), BMI, age, and waist circumference were all positive predictors,

explaining a larger portion of variance ($R^2 = 0.338$). Machine learning models showed moderate predictive power for bone density ($R^2 = 0.17$) and stronger performance for bone content ($R^2 = 0.37$) (Table 3), suggesting anthropometric data are more effective at capturing skeletal mass rather than bone mineral quality.

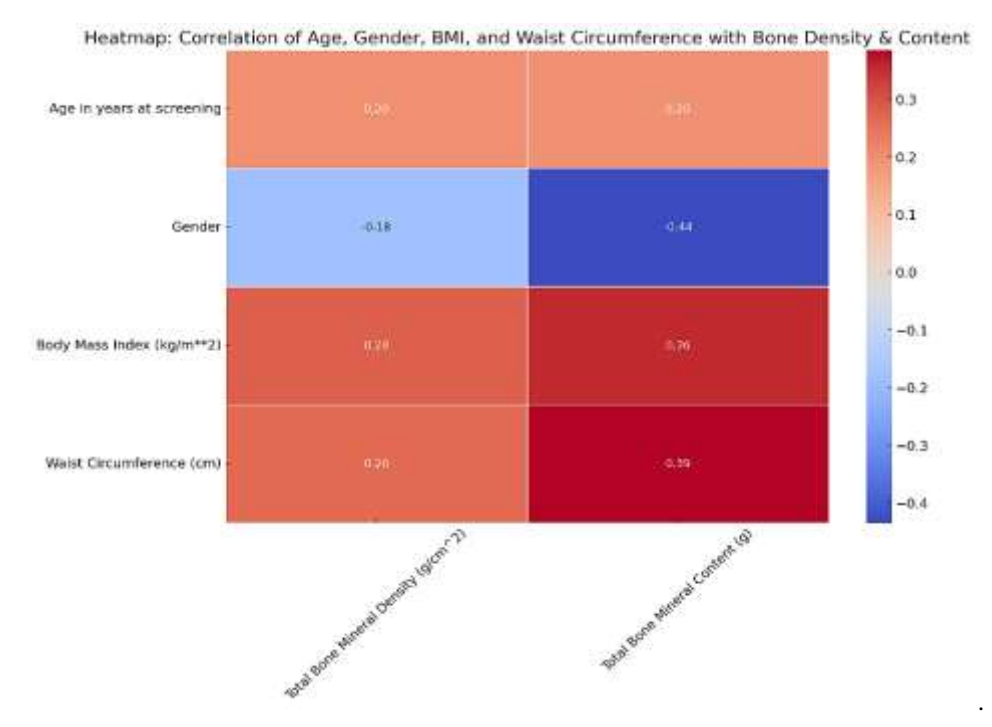


Figure 4. Correlation of bone health markers with Age, Gender, BMI, and Waist Circumference.

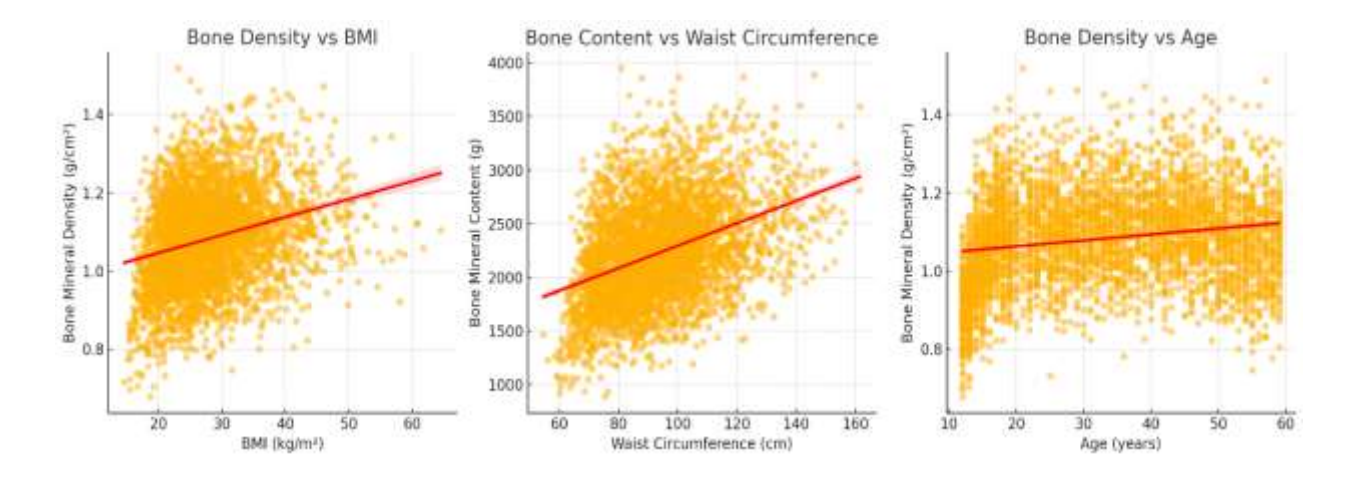


Figure 5. Regression of biometrics with bone health markers.

Table 5. Biometric predictors of bone health metrics.

Bone Metric	Predictor	В	p-value	\mathbb{R}^2
Bone Density	BMI	0.0071	< 0.001	0.131
	Age	0.0012	< 0.001	
	Waist Circumference	-0.0012	< 0.001	
	Gender (F)	-0.0541	< 0.001	
Bone Content	BMI	16.75	< 0.001	0.338
	Waist Circumference	3.28	0.004	
	Age	2.24	< 0.001	
	Gender (F)	-420.27	< 0.001	

Hormonal and biochemical contributions **bone health:** Further analysis biochemical markers in relation to bone health highlighted hormonal and metabolic contributions. Testosterone was strongly and positively associated with both BMD and BMC, while SHBG demonstrated an inverse relationship. Muscle-related enzyme CPK also had a positive impact, reinforcing the mechanical linkage between muscle and bone health. In contrast, alkaline phosphatase (ALP) and phosphorus were negatively associated with bone health metrics, suggesting a role in bone turnover or mineral imbalance. Estradiol had a moderate but statistically significant positive effect. supporting its known protective role in bone metabolism. Regression models (Table 6) showed that testosterone, CPK, and estradiol were the strongest positive predictors of bone density ($R^2 = 0.242$) and bone content ($R^2 =$ 0.358), while ALP, SHBG, and phosphorus were negative contributors. Machine learning models incorporating these biochemical predictors yielded similar results to traditional regression, with R² values of 0.24 and 0.36 for BMD and BMC, respectively (Table 6). The

feature importance for these models is detailed in Figure 6. Fat Indices and Bone Health Interactions The interaction between fat indices and bone health metrics demonstrated both positive and negative associations (Figure 6, Figure 7). Total fat showed a strong positive correlation with bone content ($\rho =$ 0.21) and a moderate one with BMD ($\rho = 0.16$), suggesting that higher overall fat mass may support bone maintenance to some extent. Conversely, higher gynoid fat was negatively associated with BMC ($\rho = -0.32$), while android fat showed a weak negative association with BMD ($\rho = -0.04$). Total percent fat and subcutaneous fat area were also negatively linked to bone content and density, albeit modestly. Regression analysis indicated that total fat and gynoid fat had positive contributions to BMD, while total percent fat and subcutaneous fat area had minor adverse effects ($R^2 = 0.371$). BMC was more strongly explained ($R^2 = 0.689$), with android and gynoid fat being strong positive predictors, though higher overall fat percentage and subcutaneous fat were negatively associated. Machine learning models reflected these patterns, with better performance in predicting bone content ($R^2 = 0.65$) than bone density ($R^2 = 0.31$, Table 3), underscoring the complexity of fat-bone interactions (Figure 8, and Figure 9).

ORIGINAL RESEARCH Published: 25 October 2025

DOI: 10.26505/djm.v29i1.1415

Table 6. Hormonal and biochemical predictors of bone health metrics.

Bone Metric	Predictor	В	p-value	\mathbb{R}^2
Bone Density	Testosterone	8.85e-05	< 0.001	0.242
	SHBG	-0.0002	< 0.001	
	CPK	9.42e-05	< 0.001	
	ALP	-0.0007	< 0.001	
	Estradiol	0.0021	0.004	
Bone Content	Testosterone	0.6634	< 0.001	0.358
	SHBG	-1.6952	< 0.001	
	CPK	0.3703	< 0.001	
	ALP	-2.4138	< 0.001	
	Estradiol	3.2147	0.001	
	Phosphorus	-52.0294	< 0.001	
	Vitamin D	0.6459	0.027	

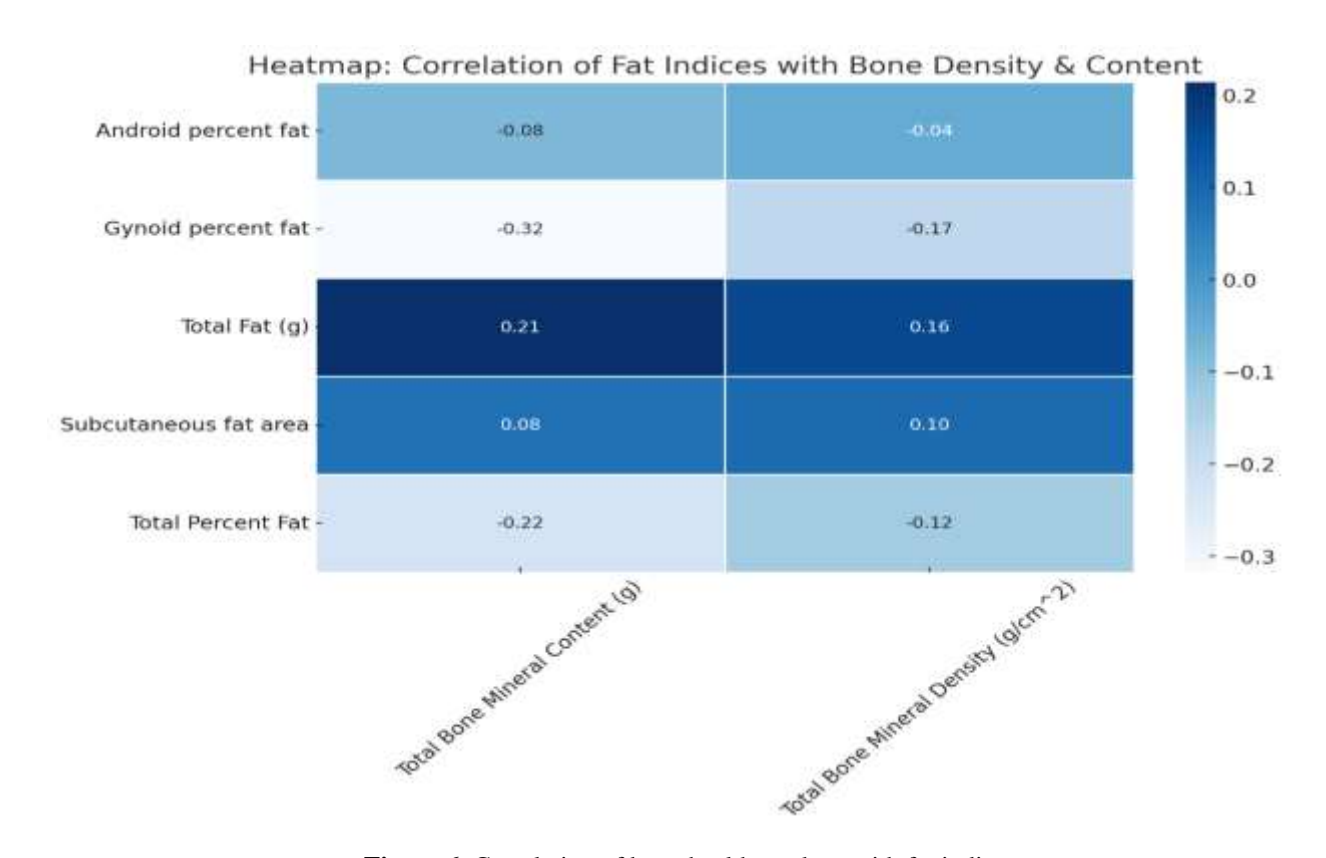


Figure 6. Correlation of bone health markers with fat indices.

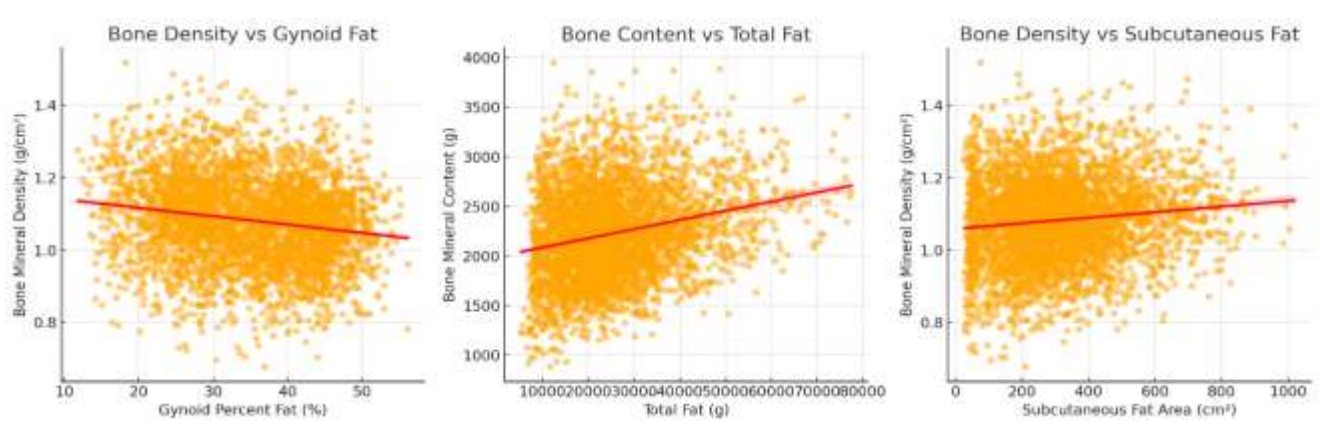


Figure 7. Regression of fat indices with bone health markers.

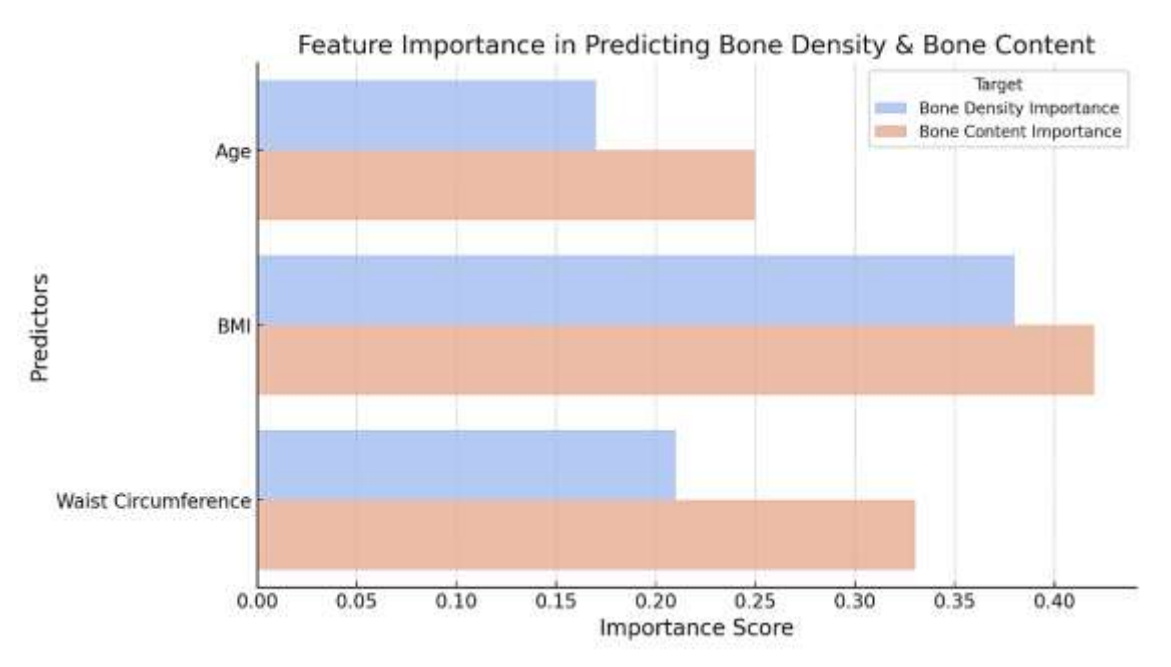


Figure 8. Feature importance in BMD and BMC.

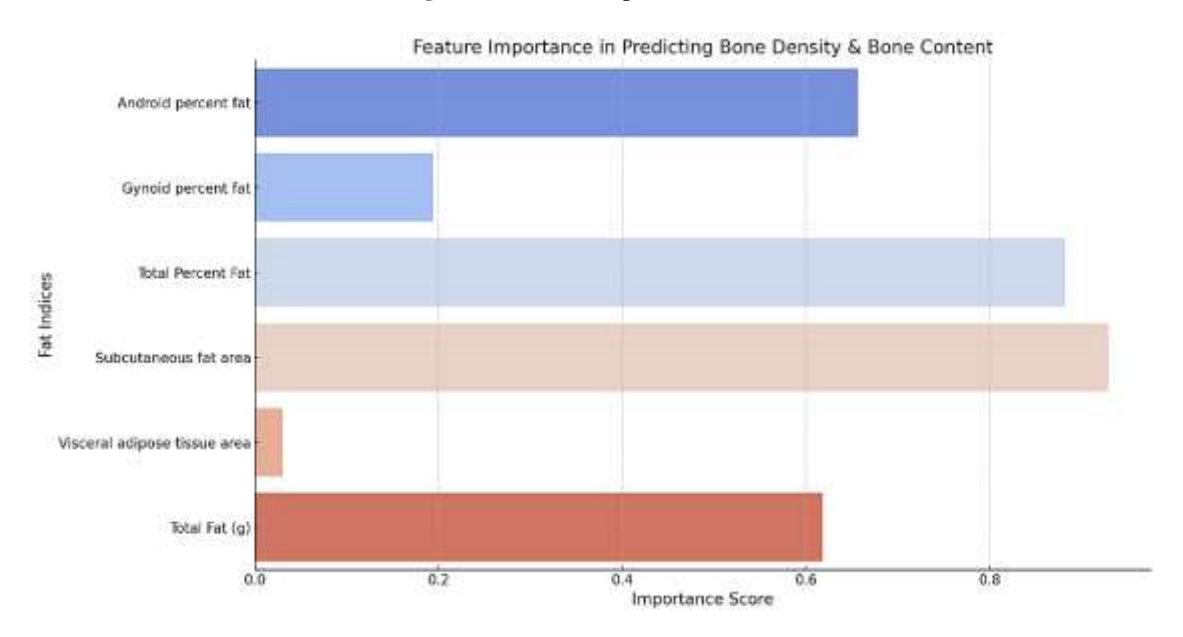


Figure 9. Feature importance in predicting bone density and bone content using fat indices

Discussion

This study provides a comprehensive analysis of the complex relationships between body fat distribution, demographic and biometric factors, and a broad range of lipid and hormonal biomarkers in influencing bone health. By integrating correlation, regression, and machine learning analyses, the findings reveal critical insights that hold significant clinical and research implications.

The study highlights how specific anthropometric measures, particularly body mass index and waist circumference, are key predictors of both fat accumulation bone mineral and metrics. Measurement of waist circumference is essential to understand central fat accumulation, which is strongly linked to various metabolic problems and complications (2). The remarkable observed associations highlight the importance of these variables as simple, easy-to-apply, and non-invasive



methods for measuring or mapping body fat dispersal in medical practice. The potential of these measurements suggests a possible replacement or enhancement for more accurate existing radiological or analytical methods for detecting people at risk of metabolic disturbances.

There is an apparent difference in body fat distribution among males & females, with males prone to metabolic syndrome, insulin resistance, and cardiovascular disease because of high visceral fat accumulation. In contrast, females have total and subcutaneous fat in a more obvious distribution (3). These gender differences would highlight the known biological variances in the pattern of fat distribution and necessitate a gender-specific approach to handle such risks (4).

The study indicates that body fat distribution is further influenced by age differences, with a trend toward increased fat accumulation in belly area, particularly in older the individuals, regardless of total fat amounts, consistent with previous observations (5). This distribution will explain the relatively high cardio-metabolic risk in old-age patients. This will highlight the importance of preventive strategies such as directed exercises and dietary adjustments to minimize this noncorrectable risk factor.

The results underscore the value customized (gender & age) specific strategies in handling body fat distributions and bone well-being. For males, controlling visceral fat is vital to minimize associated cardiometabolic risks through lifestyle interventions such as resistance exercise, dietary changes, or medications according to the guidelines (24). In females, maintaining good bone health is essential, especially for postmenopausal women. This can be achieved through simple screening using dual-energy X-ray absorptiometry (DXA) scans, along with

proper instructions on weight-bearing exercises, vitamin D and calcium

prescriptions, or even hormone replacement therapy when necessary (25). A wise gathering and interpretation of anthropometric variables, biomarker readings, and body composition is a fundamental observation from this study to measure related risks and implement designed interventions. The waist circumference measurements should be routinely done in metabolic risk calculations to improve the early recognition of those at risk for cardio-metabolic disorders, given their high association with visceral fat (2).

The association between fat maps and lipid profiles provides further understanding of metabolic health. Glucose and insulin levels are now considered essential predictors of regional fat distribution, with high levels linked to increased total and abdominal fat and insulin resistance. Nevertheless, lipid profiles alone partially explain the uneven fat distributions throughout the body, highlighting the possible effects of other important factors such as genetic issues, chronic inflammation, and lifestyle attitudes (6). The modest prognostic ability of these biomarkers recommends an integrated approach, combining anthropometric and metabolic values for a complete evaluation of health risks related to fat disorders.

Bone metrics are significantly influenced by body mass index, gender, and age, with a high body mass index linked to good bone mineral density and bone mineral constituents. These positive associations may be explained by the intermittent mechanical loading effect of high body weight, which in turn stimulates new bone formation and strengthens skeletal integrity (11). Differences in bone health by gender are remarkable. In general, Women exhibit low bone mineral density and bone mineral content. This may explain the high prevalence of osteoporosis in women, especially after menopause, when there is a sharp decline in estrogen levels (9).

Central obesity seems to hurt bone density despite its good contribution to overall bone content. This Divala Jou

ORIGINAL RESEARCH Published: 25 October 2025 DOI: 10.26505/djm.v29i1.1415

complex relationship may be better understood when we recognize that the metabolic penalties of central adiposity, such as chronic inflammation and hormonal inequities, can negatively affect bone quality despite the mechanical support provided to bones by high body weight (23).

Hormones have a fundamental effect in maintaining adequate bone health. Testosterone has been recognized to have a positive influence on bone mineral density and bone mineral content (20). This observation repeats the well-documented positive effects of testosterone in maintaining and improving bone and skeletal integrity. On the other hand, Sex hormone-binding globulin is associated with a negative contribution to bone health, possibly due to its effect in reducing the essential anabolic hormones like testosterone and estradiol (21). Evaluation of bone turnover markers also provides insight into the biological mechanisms controlling skeletal health. Creatine phosphokinase, which is a muscle enzyme reflecting muscle function, shows a positive effect on bone health in contrast to alkaline phosphatase, a marker of high bone turnover, which is associated with low bone mineral density; this observation confirmed the previous reports regarding the effects of alkaline phosphatase & creatine phosphokinase on bone health (13,16). Phosphorus level imbalances, caused by excessive intake or other factors, may affect bone mineralization and bone contents, stressing the need for vigilant checking of dietary and metabolic factors in bone health evaluations.

The complex interplay between fat profiles and bone health shows a characteristic association. Regional fat accumulation has divergent influences, with fat depositions in specific areas such as the thighs and hips being linked to higher bone mineral content. In

contrast, total body fat and subcutaneous fat show negative contributions. This complexity highlights the need to consider fat distribution

rather than total fat mass alone when evaluating bone health risks. The predictive models established in this topic perform well in approximating bone mineral content over bone mineral density, indicating that bone density is influenced by a broader range of factors beyond adiposity, even though fat indices help predict overall bone mass (26).

Nevertheless, the study has remarkable limitations. It was a cross-sectional study that precludes causal extrapolations, mainly concerning the unanticipated positive relationship between age and bone health, which reverses the traditional trends of age-related bone loss. This incongruity may arise from untested confounders such as the level of physical activity, diet, or survival bias, emphasizing the need for longitudinal research to elucidate these associations. The limited descriptive efficacy of lipid profiles in estimating fat accumulation suggests that other important factors, such as genetics, lifestyle, or inflammation, are absent, which restricts model accuracy. Moreover, the study's dependence on a particular population may limit the generalizability of conclusions, especially the age-bone health relationship, which might be affected by cohort properties. Incorporating other variables such as muscle mass, hormonal variations, or genetic tendencies will enhance the predictive power of machine learning models (27).

To interpret these results practically, physicians should integrate body mass index measurements with waist circumference in routine evaluations to address possible metabolic risks. DXA scans should be utilized for bone health proactive screening, especially in high-risk groups, including middle-aged women, postmenopausal women, and those with high total or subcutaneous fat, alongside lifestyle assessments. Consideration of testosterone replacement therapy with careful supervision should be discussed in patients with low bone mass after

checking and monitoring testosterone levels. Measuring fasting insulin and glucose levels to identify possible abnormal metabolic functions is also recommended. Future studies should embrace longitudinal strategies to establish causality and consider factors such as genetic issues, chronic inflammation, and lifestyle to improve predictive models. These understandings recommend multidimensional, evidence-based methodology, balancing integrated evaluations and customized interventions to enhance conclusions on metabolic and skeletal health (28).

Conclusion

This study highlights the complex interplay composition, between body metabolic biomarkers, and health. bone Waist circumference and BMI are strong, noninvasive predictors of both fat distribution and skeletal metrics, with apparent variations by age and gender. Hormonal and biochemical markers, particularly insulin, testosterone, SHBG, and CPK, significantly influence adiposity and bone outcomes. Machine learning models show moderate predictive accuracy, suggesting room for enhancement through the inclusion of additional factors such as muscle mass and genetics. These findings support comprehensive, a individualized approach to assessing metabolic and bone health, emphasizing the utility of simple clinical measures in guiding risk stratification and intervention strategies. It recommended that routine was Measurement of Waist Circumference and BMI should be integrated into clinical assessments to estimate fat distribution and associated risks. In addition, hormonal Evaluations, including testosterone SHBG, should be considered in bone health assessments, especially in aging men and women with low bone mass.

Source of funding: No source of funding.

Ethical clearance: This study utilized data from the National Health and Nutrition Examination Survey (NHANES), which is publicly available and fully deidentified in accordance with the Health Insurance. Portability and Accountability Act (HIPAA) Privacy Rule. As such, the analysis of this secondary data does not constitute human subjects research and does not require additional Institutional Review Board (IRB) approval. All NHANES study protocols were reviewed and approved by the National Center for Health Statistics (NCHS) Research Ethics Review Board under Protocol #2011-17, and written informed consent was obtained from all participants before data collection. The study adheres to the ethical standards outlined in the Declaration of Helsinki and complies with U.S. federal regulations governing research using publicly available datasets.

Conflict of interest: None.

Use of Artificial Intelligence: The authors declare that they did not use generative artificial intelligence for creating or preparing the manuscript.

Acknowledgments: The authors would like to express their deep thanks to all those who aided in the completion of this work, especially our families and colleagues, for their continuous encouragement and understanding during the period of this study.

References

- 1. Pedregosa F, Varoquaux G, Gramfort A, Michel V, Thirion B, Grisel O, Blondel M, Prettenhofer P, Weiss R, Dubourg V, Vanderplas J. Scikit-learn: Machine learning in Python. the Journal of machine Learning research. 2011 Nov 1;12:2825-30.
- 2. R Core Team. R: A language and environment for statistical computing. R Foundation for Statistical Computing, Vienna, Austria. http://www. R-project. org/. 2016.
- 3. Breiman L. Random forests. Machine learning. 2001Oct;45(1):5-32.

https://doi.org/10.1023/A:1010933404324

4. McKinney W. Data structures for statistical computing in Python. scipy. 2010 Jun 28;445(1):51-6.

 $\underline{https://doi.org/10.25080/Majora-92bf1922-00a}$

5. Harris CR, Millman KJ, Van Der Walt SJ,

Gommers R, Virtanen P, Cournapeau D, Wieser E, Taylor J, Berg S, Smith NJ, Kern R. Array programming with NumPy. nature. 2020 Sep 17;585(7825):357-62. https://doi.org/10.1038/s41586-020-2649-2

6. Alser M, Naja K, Elrayess MA. Mechanisms of body fat distribution and gluteal-femoral fat protection against metabolic disorders. Frontiers in Nutrition. 2024 Mar 25;11:1368966. https://doi.org/10.3389/fnut.2024.1368966

7. Yang Y, Xie M, Yuan S, Zeng Y, Dong Y, Wang Z, Xiao Q, Dong B, Ma J, Hu J. Sex differences in the associations between adiposity distribution and cardiometabolic risk factors in overweight or obese individuals: a cross-sectional study. BMC Public Health. 2021 Jun 26;21(1):1232.

https://doi.org/10.1186/s12889-021-11316-4

8. Kang SM, Yoon JW, Ahn HY, Kim SY, Lee KH, Shin H, Choi SH, Park KS, Jang HC, Lim S. Android fat depot is more closely associated with metabolic syndrome than abdominal visceral fat in elderly people. PloS one. 2011 Nov11;6(11):e27694.

https://doi.org/10.1371/journal.pone.0027694

9. Kantowski T, Schulze zur Wiesch C, Aberle J, Lautenbach A. Obesity management: sexspecific considerations. Archives of Gynecology and Obstetrics. 2024 May;309(5):1745-52.

https://doi.org/10.1007/s00404-023-07367-0

10. Fan Z, Chiong R, Hu Z, Keivanian F, Chiong F. Body fat prediction through feature extraction based on anthropometric and laboratory measurements. Plos one. 2022 Feb 22;17(2):e0263333.

https://doi.org/10.1371/journal.pone.0263333

11. Ross R, Neeland IJ, Yamashita S, Shai I, Seidell J, Magni P, Santos RD, Arsenault B, Cuevas A, Hu FB, Griffin BA. Waist circumference as a vital sign in clinical practice: a Consensus Statement from the IAS

and ICCR Working Group on Visceral Obesity. Nature Reviews Endocrinology. 2020 Mar;16(3):177-89. https://doi.org/10.1038/s41574-019-0310-7

- 12. Modi A, Gadhavi R, Pérez CM, Joshipura K. Longitudinal association between adiposity measures and regression of prediabetes/diabetes. Nutrition, Metabolism and Cardiovascular Diseases. 2021 Oct 28;31(11):3085-94. https://doi.org/10.1016/j.numecd.2021.07.005
- 13. Tariq S, Tariq S, Lone KP, Khaliq S. Alkaline phosphatase is a predictor of Bone Mineral Density in postmenopausal females. Pakistan journal of medical sciences. 2019 May;35(3):749. https://doi.org/10.12669/pjms.35.3.188
- 14. Wang Z, Du W, Han M, He L, Zhang H, Hu J, Quan R. Association between creatine phosphokinase level within normal range and bone mineral density in adolescents. Medicine. 2023 Aug 11;102(32):e34724.

https://doi.org/10.1097/MD.000000000034724

- 15. Echegaray M, Rivera MA. Role of creatine kinase isoenzymes on muscular and cardiorespiratory endurance: genetic and molecular evidence. Sports Medicine. 2001 Nov;31(13):919-34. https://doi.org/10.2165/00007256-200131130-00003
- 16. Lee AW, Cho SS. Association between phosphorus intake and bone health in the NHANES population. Nutrition journal. 2015 Mar 21;14(1):28. https://doi.org/10.1186/s12937-015-0017-0
- 17. Dai X, Liu C, Bi W, Zheng G, Lv K, Xia Z. Estradiol and vitamin D exert a synergistic effect on preventing osteoporosis via the miR-351-5p/IRS1 axis and mTOR/NFκB signaling pathway. Scientific Reports. 2025 May 28;15(1):18678. https://doi.org/10.1038/s41598-025-02808-z
- 18. Kiel DP, Felson DT, Anderson JJ, Wilson PW, Moskowitz MA. Hip fracture and the use of estrogens in postmenopausal women. New England Journal of Medicine. 1987 Nov 5;317(19):1169-74. https://doi.org/10.1056/NEJM198711053171901
- 19. Shigehara K, Izumi K, Kadono Y, Mizokami A.

Testosterone and bone health in men: a narrative review. Journal of Clinical Medicine. 2021 Feb 2;10(3):530. https://doi.org/10.3390/jcm10030530

20. Narinx N, David K, Walravens J, Vermeersch P, Claessens F, Fiers T, Lapauw B, Antonio L, Vanderschueren D. Role of sex hormone-binding globulin in the free hormone hypothesis and the relevance of free testosterone in androgen physiology. Cellular and Molecular Life Sciences. 2022 Nov;79(11):543.

https://doi.org/10.1007/s00018-022-04562-1

21. Yakout SM, Khattak MN, Al-Daghri NM, Al-Masri AA, Elsaid MA. Associations of bone mineral density with sex hormone-binding globulin (SHBG) and testosterone in middle-aged Saudi men: a cross-sectional study. Frontiers in Endocrinology. 2023 Nov 24:14:1230279.

https://doi.org/10.3389/fendo.2023.1230279

22. Gkastaris K, Goulis DG, Potoupnis M, Anastasilakis AD, Kapetanos G. Obesity, osteoporosis and bone metabolism.

Journal of musculoskeletal and neuronal interactions. 2020;20(3):372.

https://www.ncbi.nlm.nih.gov/pmc/articles/PMC7493444/

23. Hunter JD. Matplotlib: A 2D graphics

environment. Computing in science and engineering. 2007 May 1;9(03):90-5. https://doi.ieeecomputersociety.org/10.1109/MCSE. 2007.55

24. Waskom ML. Seaborn: statistical data visualization. Journal of open source software. 2021 Apr 6;6(60):3021.

https://doi.org/10.21105/joss.03021

25. Greenblatt MB, Tsai JN, Wein MN. Bone turnover markers in the diagnosis and monitoring of metabolic bone disease. Clinical chemistry. 2017 Feb1;63(2):464-74.

https://doi.org/10.1373/clinchem.2016.259085

26. Hilton C, Vasan SK, Neville MJ, Christodoulides C, Karpe F. The associations between body fat distribution and bone mineral density in the Oxford Biobank: a cross sectional study. Expert Review of Endocrinology & Metabolism. 2022 Jan 2;17(1):75-81. https://doi.org/10.1080/17446651.2022.2008238
27. Özmen S, Kurt S, Timur HT, Yavuz O, Kula H, Demir AY, Balcı A. Prevalence and risk factors of osteoporosis: a cross-sectional study in a tertiary center. Medicina. 2024 Dec 23;60(12):2109. https://doi.org/10.3390/medicina60122109

28. Leslie WD. Estimating waist and hip circumference from routine clinical DXA. Journal of Clinical Densitometry. 2020 Oct 1;23(4):582-7. https://doi.org/10.1016/j.jocd.2019.08.001

التفاعل بين الملامح الحيوية والعلامات الحيوية ونسبة الدهون في الجسم وصحة العظام: نهج احصائي وتعلّم الني

ا جواد كاظم عباس ، وسام على حسين ، احمد نصير قفطان

الملخص

الخلفية: السمنة واضطرابات التمثيل الغذائي هي مخاوف صحية عامة منتشرة بشكل متزايد. ترتبط السمنة الزائدة ، وخاصة الدهون الحشوية ، بخلل التمثيل الغذائي ، في حين أن مستودعات الدهون الإقليمية مثل الدهون الجينويد قد تمنح فوائد وقائية على سلامة الهيكل العظمي

ا**لأهداف:** هدفت هذا الدراسة إلى دراسة العلاقة المعقدة بين الملامح الحيوية والعلامات الكيميائية الحيوية وتوزيع الدهون في الجسم وصحة العظام

المواد والطرق: تم الحصول على البيانات من المسح الوطني لفحص الصحة والتغذية (NHANES) ، بما في ذلك المشاركين البالغين الذين لديهم قياسات كاملة لتكوين الجسم (الدهون الكلية ، الحشوية ، وتحت الجلد. مؤشر كتله الجسم; محيط الخصر) ، والعلامات الكيميائية الحيوية (ملامح الدهون ، والجلوكوز الصائم ، والأنسولين ، والمنظمين الهرمونيين) ، ومقاييس صحة العظام (كثافة المعادن في العظام ومحتواها عبر DXA). تم إجراء تحليلات الارتباط والانحدار متعدد المتغيرات لتحديد المتنبئين بين المتغيرات الديموغرافية والقياسية الحيوية والكيميائية الحيوية. تم استخدام تقنيات التعلم الألي ، وتحديدا الانحدار العشوائي، لتعزيز النمذجة التنبؤية لمؤشرات الدهون ونتائج صحة العظام.

النتائج: ظهر مؤشر كتلة الجسم ومحيط الخصر كتنبؤات قوية للدهون الكلية والحشوية ، مع ملاحظة تفاوتات كبيرة بين الجنسين والعمر. أظهرت النساء دهونا إجمالية وتحت الجلد أعلى ، بينما أظهر الرجال زيادة في الدهون الحشوية. ترتبط العلامات الكيميائية الحيوية ، ولا سيما الانسولين والجلوكوز ، ارتباطا وثيقا بمؤشرات السمنة. علاوة على ذلك ، ارتبطت صحة العظام بشكل إيجابي بمؤشر كتلة الجسم والمؤشرات الحيوية المحددة (التستوستيرون ، CPK) وبشكل سلبي مع SHBG و ALP. لوحظت دقة تنبؤية متوسطة إلى عالية لنماذج التعلم الآلي ، مما يؤكد المساهمة الداعمة للتحليلات التنبؤية في فهم هذه العلاقات.

الاستنتاج: يقدم الجمع بين المقاييس الأنثروبومترية والعلامات الكيميائية الحيوية والدهون والعظام مع التعلم الألي شرحا شاملا لارتباطها وارتباطها. يمكن لمثل هذه الأفكار أن توجه تصميم استراتيجيات محددة لاتخاذ القرار السريري والتأكيد على جدوى استخدام قياسات بسيطة غير جراحية لتقييم مخاطر التمثيل الغذائي والهيكل العظمي.

الكلمات المفتاحية: الملف الحيوي، صحة الهيكل العظمي، نسبة الدهون في الجسم، منهج التعلم الألى.

المؤلف المراسل: وسام على حسين

wisam.allami@uokufa.edu.iq الإيميل:

تاريخ الاستلام: ١٩ نيسان ٢٠٢٥

تاریخ القبول: ۲۰۲۰ أب

تاريخ النشر: ٢٥ تشرين الأول ٢٠٢٥

'فرع الطب الباطني، كلية الطب، جامعة الكوفة، النجف، العراق. 'فرع الجراحة، كلية الطب، جامعة الكوفة، النجف، العراق. "فرع الكيمياء الحيوية، كلية الطب، جامعة الكوفة، النجف، العراق.

Classification and Prediction of Human Blood Cells Using Artificial Intelligence and Advanced Image Processing Techniques

Ahmad S. Lateef (1), Ahmed J. M. Al-Zuhairi (1), Mohammed Y. Kamil (1)

- ¹ Mustansiriyah University, College of Science, Baghdad, Iraq.
- ² Department of Physiology and Medical Physics, College of Medicine, University of Diyala, Diyala, Iraq.

Abstract

Background: Accurate blood cell classification is essential for diagnosing and monitoring blood disorders. Manual blood evaluation is cumbersome and subject to disagreement among specialists, which can negatively impact diagnostic reliability.

Objectives: This study aims to develop an automated deep learning framework for accurate classification of major blood cell types, especially basophils, red blood cells, and bone marrow cells, to enhance the accuracy and efficiency of clinical diagnosis.

Patients and Methods: A set of publicly available, high-resolution blood smear images obtained from a specific patient cohort with distinct genetic properties was analyzed, with standardized preprocessing applied to address variance. Multiple AI-based classification strategies were developed, and all models were evaluated on an independent test set using overall accuracy, precision, recall, and F1 score.

Results: Wavelet scattering combined with an SVM delivered the strongest overall performance, surpassing both the custom CNN and ResNet variants. It achieved a near-perfect separation of basophils and erythroblasts and only occasional confusion with myeloblasts. These results highlight the sensitivity of the wavelet scattering method to subtle morphological differences in blood cells.

Conclusion: This study highlights how machine learning-based image analysis techniques can reliably and accurately classify blood cells, reducing the need for the subjective manual interpretation that characterizes traditional microscopy. There is potential for increasing the accuracy of early diagnosis and simplifying patient treatment plans for hematological disorders by integrating these automated systems into standard clinical practice.

Keywords: Hematological Diagnostics, Blood Cell Classification, Wavelet Scattering Transform, Transfer Learning.

OPEN ACCESS

Correspondence: Ahmad S. Lateef Email: a97s21@uomustansiriyah.edu.iq Copyright: ©Authors, 2024, College of Medicine, University of Diyala. This is an open access article under the CC BY 4.0 license (http://creativecommons.org/licenses/by/4.0/) Website:

https://djm.uodiyala.edu.iq/index.php/djm

Received: 10 May 2025 Accepted: 16 September 2025 Published: 25 October 2025

Introduction

The diagnosis and treatment of blood disorders, such as leukemia and bone marrow dysplasia, rely on blood cell classification; however, traditional microscopic examination remains time-consuming and subject to interdisciplinary variation. Advanced artificial intelligence and image processing techniques can overcome these limitations by providing objective and reproducible analyses of cellular characteristics, enabling early detection of subtle morphological changes, and helping guide individual treatment decisions. To demonstrate better outcomes, accuracy and consistency than

traditional microscopy, we create and validate an AI-driven framework in this study for the automated classification of basophils, erythroblasts, and myeloblasts in high-resolution blood smear images (1-3).

Deep learning frameworks and sophisticated computational techniques have emerged as potent remedies for these problems in recent years (4). For various tasks in biomedical image analysis, CNNs, transfer learning frameworks, and autoencoder-based cascades have been widely utilized (5-8). These methodologies have achieved high precision in recognizing the populations of various leukocytes, providing more objective and reproducible alternatives to manual methods. Even with these advances, the classification of basophils, erythroblasts, and myeloblasts remains challenging because their histological features are very delicate, as there are no comprehensive, properly cataloged data sets (9-16). Consequently, a successful computerized classification scheme would significantly enhance diagnostic precision, ultimately leading to earlier diagnosis and more targeted therapies (17-20).

This work primarily aims to address this shortcoming by developing and validating a custom-designed deep learning algorithm for classifying basophils, erythroblasts, and myeloblasts from microscopic images. By embracing the latest image processing methodologies and advanced neural network designs, the strategy aims to minimize subjectivity in morphological evaluation and enhance consistency during cell classification. In the process, we confront the specific challenges related to these cells while building upon the promising results from the most recent studies. Following this introductory section, the paper proceeds as outlined below.

First, a comprehensive review of related work is provided, summarizing current methodologies and their inherent limitations. Next, the proposed methodology, including the network design and data augmentation strategies employed to address data scarcity and morphological overlap, is described in detail. Finally. we present results validate experimental that the effectiveness of our approach and discuss the potential implications for clinical hematological diagnostics and future research directions. Arabyarmohammadi et al. (2022) trained a deep model to segment myeloblast chromatin and extracted 214 texture/shape features. After LASSO and Cox regression refinement, their risk score correlated with relapse-free survival (AUC 0.71) in AML and MDS post-transplant patients, demonstrating a reproducible alternative to manual cytology (21). In addition, Guo et al. (2022) developed a deep classifier with a "rejected option" to flag ambiguous bone marrow images. By quantitatively measuring morphological features, the system abstains from uncertain cases, reducing misclassification and directing them to expert review (22). Jarjees et al. (2022) developed a VGG-19 transfer-learning pipeline using an augmented dataset comprising seven blood cell classes. Their CNN achieved 98 % overall accuracy, standardizing leukocyte classification and minimizing dependence on expert interpretation (23). Tarquino et al. (2023) introduced a cascade of one-class variational autoencoders to distinguish four pathological bone marrow subtypes. Trained on 26,000 openaccess images, the model achieved 93.8% accuracy, outperforming benchmarks ResNext, ResNet-50, Xception, and CoAtNet (24). Consensus criteria for acute and chronic basophilic leukemias were established, defining "hyperbasophilia" (≥1,000 basophils/µL) and standardizing diagnoses to enhance clinical reproducibility across hematologic malignancies (25). A CNN with specialized layers and data augmentation was designed to detect AML in high-resolution images. The system delivered high accuracy and reliability, demonstrating

versatility for other overlapping cell types and accelerating diagnostic workflows (26).

Patients and Methods

Dataset description: A portion of a publicly available Kaggle dataset was utilized in this study. The dataset comprises 5,000 high-resolution microscopic blood cell images evenly distributed across five classes (1,000 images per class) from different countries. Each image meets the following technical specifications:

minimum resolution of 1024×1024 pixels, Wright-Giemsa staining, acquisition at 100× oil immersion (equivalent to 1000× total magnification), 24-bit RGB color, and multiple focal planes per sample. Given the computational demands associated with training AI algorithms on such high-resolution data, only a subset of the dataset was employed for training, specifically, three classes with 100 images per class. A portion of the dataset is depicted in Figure 1.

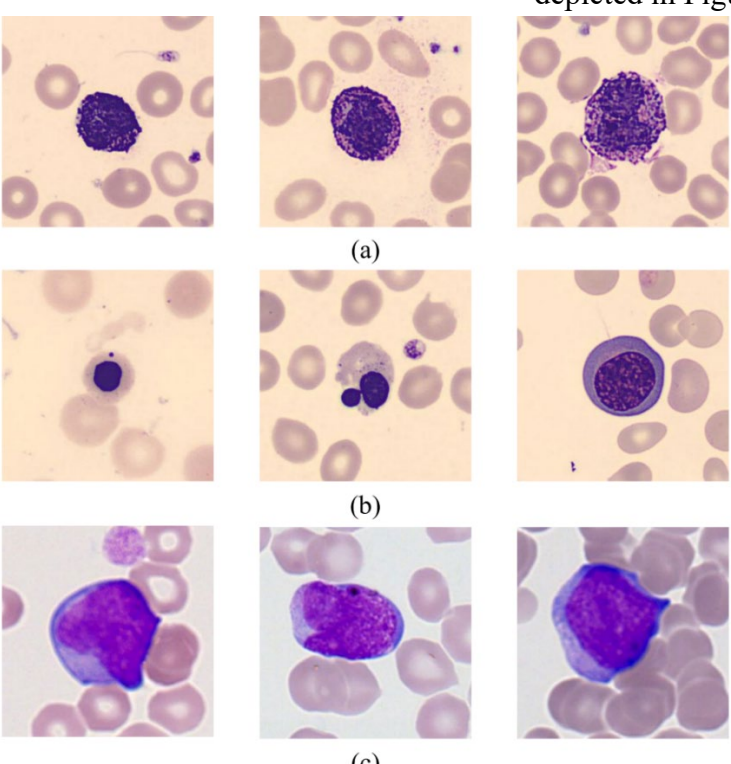


Figure 1. Samples of the dataset: (a) Basophil cells; (b) Erythroblast; and (c) Myeloblast.

Data preparation: The study employed a publicly available dataset of blood smear images. The original dataset was provided as a compressed archive (e.g., BloodSmearImages.zip) and was extracted to a designated working directory. The images are in RGB format with a common size of 1024×1024 pixels, which leads to resizing the images to 400×400 pixels. To facilitate data management and ensure proper labeling, an Image Datastore was created; labels were automatically assigned based on the folder

names. The dataset comprises 100 images uniformly distributed across three classes corresponding to specific parasitic infections (basophil, erythroblast, and myeloblast), with 100 images per class.

To ensure balanced class representation, the dataset was split into training and hold-out (test) sets using a 70:30 ratio. Randomization was controlled via a fixed random seed to guarantee reproducibility. The entire set of training and test images was loaded into memory, which permitted rapid access during feature extraction and classifier training.

Feature extraction using wavelet scattering technique: Accurate feature extraction is crucial due to the dataset's small size and diversity. To address this challenge, a twolayer wavelet dispersion transform was applied to extract low-contrast, translationinvariant feature descriptors from highresolution images. The network was designed to accommodate input images of 400 × 400 pixels, with a 40-pixel invariance scale selected to ensure robustness against subtle translational shifts and shape distortions. Two wavelets per octave were used in the first dispersion layer to capture fine details. In contrast, one wavelet per octave was employed in the second layer to downscale the resolution hierarchically. To enable the model to adapt to angular variations in cellular structures, two rotational transforms were incorporated into each dispersion layer to account for orientation diversity. The outcome of these stages is a robust set of dispersion parameters, including successive wavelet convolutions. nonlinear parameter transformations, and local averaging via lowpass filtering. These parameters serve as highlevel discriminative representations enhance the model's ability to distinguish between normal and pathological cell types, even in images exhibiting subtle variations that complicate discrimination.

Classification using support vector machine (SVM): Following feature extraction, the scattering coefficients were used as inputs to a Support Vector Machine (SVM) classifier. Recognized for their effectiveness in high-dimensional spaces and limited-sample scenarios, SVMs were chosen to robustly discriminate among the classes. In our implementation, a multiclass SVM was constructed using the one-vs-all strategy (or error-correcting output codes) to generalize the binary decision-making process inherent

in SVMs to a multiclass classification problem.

Hyperparameters for the SVM, including the choice of kernel (e.g., linear or radial basis function), regularization parameters, and other tuning parameters, were optimized using cross-validation on the training set. This approach ensured that the classifier maintained high generalizability and minimized the risk of overfitting. The classifier's performance was subsequently assessed on the reserved test set using standard metrics, including accuracy, precision, recall, and F1-score. Table 1 shows the hyperparameters of the SVM algorithm.

Table 1. Properties of the Wavelet feature extraction method.

Parameter	value
KernelFunction	cubic polynomial kernel
PolynomialOrder	3
KernelScale	1
BoxConstraint	314
Standardize	True
KFold	5

Deep convolutional neural network: The results of the Water sorption of the zirconium mixed with PVA decreased in the study group compared to the control group, as shown in Table 2. It was demonstrated that water sorption results show

a significant difference in the study group at all curing times (1-2-5-10-15-20 sec), while showing a non-significant difference in the control group at all curing time intervals.

Deep convolutional neural network: The custom Convolutional Deep Network is engineered to learn discriminative features directly from input images by employing a structured architecture that begins with an input layer where images are resized to a fixed resolution (e.g., 300×300 pixels) and accepted in 24-bit RGB format. The network then utilizes a series of convolutional blocks for feature extraction; each block typically comprises a convolutional layer with small receptive fields (such as 3×3 filters) to scan the input feature maps, followed by batch normalization layers to stabilize and accelerate training, ReLU

activation functions to introduce non-linearity, and max pooling layers to down sample the feature maps- thereby reducing spatial dimensions and capturing translational invariance. After several such blocks, a global average pooling layer aggregates these high-level features, summarizing the learned spatial representations into a fixed-length feature vector. This vector is further processed

through one or two fully connected dense layers that incorporate dropout to prevent overfitting, given the high capacity of the network relative to the dataset size. Finally, the architecture culminates in a fully connected SoftMax output layer, which maps the refined features to class probabilities corresponding to the various blood cell categories.

Table 2. Architecture of the custom deep CNN.

Layer (type)	Output Shape	Number of parameters
conv2d_4 (Conv2D)	(None, 400, 400, 16)	2368
batch normalization 4	(None, 400, 400, 16)	64
re_lu_4 (ReLU)	(None, 400, 400, 16)	0
conv2d 5 (Conv2D)	(None, 400, 400, 20)	2900
batch normalization 5 (Batch)	(None, 400, 400, 20)	80
re_lu_5 (ReLU)	(None, 400, 400, 20)	0
max pooling2d 2 (MaxPooling2)	(None, 100, 100, 20)	0
flatten_2 (Flatten)	(None, 200000)	0
dense_2 (Dense)	(None, 3)	600003
softmax_2 (Softmax)	(None, 3)	0
Total params: 605415, Traina	able params: 605343, No	n-trainable params: 72

The network was trained using stochastic gradient descent (or an alternative optimizer such as Adam) with appropriate learning rate scheduling and weight regularization (e.g., L2 weight decay). Hyperparameters, including mini-batch size, learning rate, dropout ratio, and number of epochs, were empirically set, followed by cross-validation to ensure robust performance and mitigate overfitting. Data augmentation techniques (e.g., rotation, scaling, or flipping) were applied during training to expand the effective dataset and further enhance the model's generalization.

ResNet network: ResNet, or Residual Network, is a highly effective deep learning model known for its ability to train very deep neural networks by addressing the vanishing gradient problem through skip connections. In our work, we used a pretrained version of ResNet, specifically ResNet-50, because of its strong performance in image classification

tasks. The core idea behind ResNet lies in its residual blocks, which include shortcut connections (also called identity mappings) that skip over one or more layers. These connections allow the network to learn residual functions relative to the input, making it easier to train deeper models by reducing the degradation problem.

Stacking multiple residual blocks can enable the network to obtain high-level representations from low-level textures progressively. This functionality is very effective for recognizing faint blood cell morphology cues. Transfer learning was used to allow the pretrained ResNet model to learn blood cell classification. It allowed us to leverage strong feature representations learned on the vast ImageNet dataset. Early layers of the network extract general visual features that are widely applicable, so we left most of them unchanged.

For a certain number of classes in the dataset, we replaced the classification layer with a different fully connected softmax layer, and we then adjusted the learning rate. By doing this, it was able to stay close

$$P = \frac{\text{TP}}{\text{TP} + \text{FP}}$$

- Recall (R) measures the ability of the model to capture all actual positive instances (27):

$$R = \frac{\text{TP}}{\text{TP} + \text{FN}}$$

- F1-Score is the harmonic mean of precision and recall, providing a balanced measure (27):

$$F1 = 2 \times \frac{P \times R}{P + R}$$

A confusion matrix was constructed during the qualitative analysis to assess the performance of the models in each category, which helps identify patterns of misclassification and highlights areas that require improvement in each model.

Results

Study design:

Both models were implemented in MATLAB. The custom network was constructed using the deep learning primitives available in the MATLAB Deep Learning Toolbox, while the pretrained ResNet model was adapted using MATLAB's transfer learning capabilities. The environment facilitated rapid prototyping, hyperparameter exploration, and performance evaluation using standard metrics such as accuracy, precision, recall, and F1-score.

Classification via wavelet scattering features using SVM: Figure 2 shows the confusion matrix obtained from the wavelet scattering feature extraction and SVM classification approach, which reveals an overall high performance discriminating blood cell types. For the three classes under investigation- basophils, erythroblasts, and myeloblasts- the classifier achieved near-perfect Specifically, both accuracy. basophils erythroblasts were classified with 100% accuracy, indicating that the scattering coefficients extracted from these cell images capture their distinctive morphological features very effectively. Myeloblasts, while also largely well-classified with

to the original and preserve only limited, yet significant, modifications introduced by the model's retraining for the particular domain. To enhance the model's resilience and generalization capabilities, we also employed regularization and data augmentation techniques. This led to the development of a functional and precise blood type classification system.

Evaluation: To conduct a comprehensive performance comparison of the methods adopted in this study, we ran each technique on a hold-out test dataset comprising 30% of the entire dataset. To evaluate the developed model, we used accuracy, precision, recall, and F1-score classification metrics. We computed each metric for each class and then averaged it with the macro average across all classes to obtain an overall assessment of the model's performance across all classes.

For reference:

- True Positives (TP): The number of samples correctly predicted as belonging to a given class.
- False Positives (FP): The number of samples incorrectly predicted to belong to the class.
- True Negatives (TN): The number of samples correctly identified as not belonging to the class.
- False Negatives (FN): The number of samples that were actually in the class but were misclassified as something else.

The evaluation metrics were computed using the following equations:

- Accuracy measures the proportion of all correct predictions (24):

$$Accuracy = \frac{TP + TN}{TP + TN + FP + FN}$$

- Precision (P) quantifies the correctness of positive predictions for a class (27):

29 out of 30 instances correctly identified, exhibited a single misclassification (incorrectly labeled as an erythroblast),

resulting in a slight reduction in metrics such as recall and F1-score for this class.

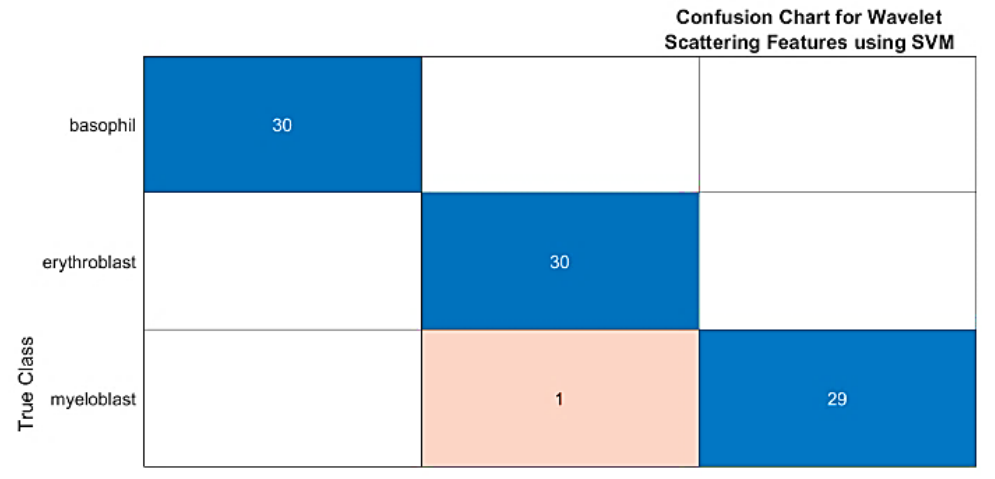


Figure 2. Confusion chart of Wavelet features using SVM.

The excellent performance for basophils and erythroblasts suggests that the wavelet scattering transform is successful in deriving translation-invariant and discriminative features that robustly represent morphological characteristics of these cells. The minor overlap observed between myeloblasts and erythroblasts, however, implies that in certain cases, the feature space representations of these two cell types may become similar. Such subtle overlaps are not entirely unexpected, given the inherent complexity in distinguishing cells that share comparable structural and textural attributes. The SVM classifier, when provided with these high-quality features, demonstrates effective discrimination across classes. Its decision boundaries appear to be well-calibrated, as evidenced by the high class-wise accuracies. the misclassification of one myeloblast highlights a potential area for

further refinement. Future work could explore more sophisticated feature fusion techniques that integrate additional descriptors (e.g., color histograms or morphological measurements) into the classification pipeline, or consider threshold adjustments and ensemble learning methods to more reliably resolve borderline cases.

Classification via deep CNN: The training of the deep CNN model was characterized by steady improvements in both accuracy and loss over successive epochs, as illustrated in Figure 3. Initially, the model achieved around 60% accuracy, and within several epochs, it rapidly improved, eventually stabilizing between 90% and 100%. Concurrently, the training loss started from a high value (approximately 9) and consistently decreased toward near-zero levels, reflecting effective optimization of network weights and a substantial reduction in the difference between predicted outputs and true labels.

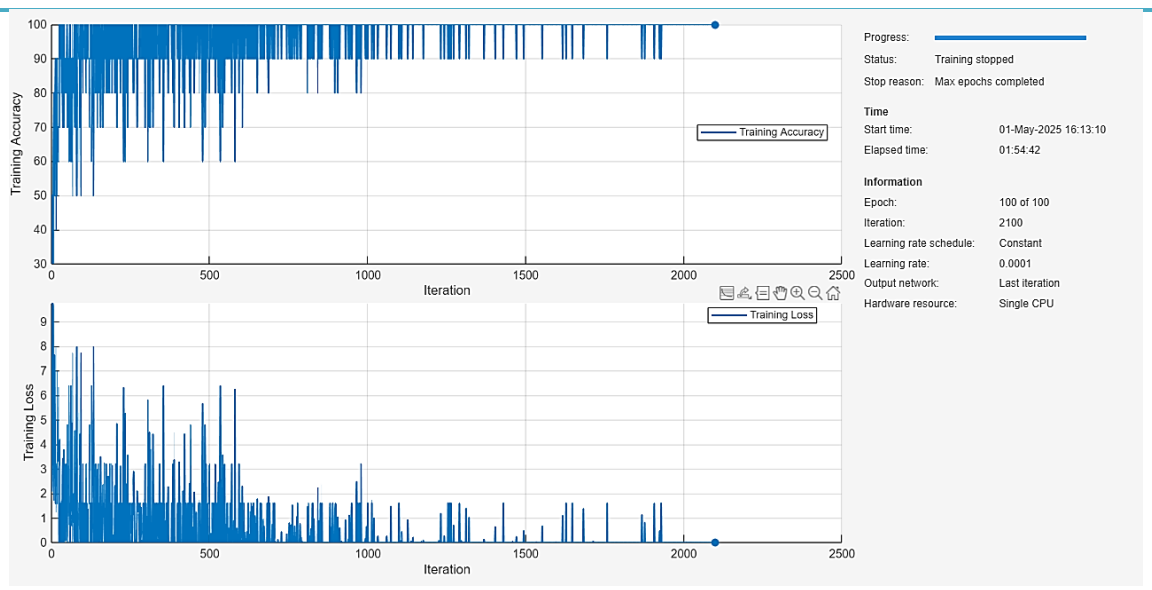


Figure 3. Training process of the deep CNN.

The network was trained for a total of 100 epochs, encompassing approximately 2100 iterations. A constant learning rate of 0.0001 was chosen, which contributed to the stable convergence observed, as it ensured gradual weight adjustments without causing erratic behavior in the loss or accuracy metrics. Notably, the training was executed on a single CPU, which may indicate either the modest scale of the dataset or a scenario where highend GPUs were not available. Despite these hardware constraints, the learning curves demonstrate that the model was able to effectively capture the morphological nuances in the blood cell images.

While minor fluctuations in training accuracy are common in mini-batch gradient descent due to inherent stochasticity, the overall upward trend in accuracy and corresponding decline in loss confirm the model's ability to learn relevant features. The training process was allowed to complete all 100 epochs, reaching a point of convergence where the loss stabilized and the accuracy plateaued, without the implementation of early stopping mechanisms.

The confusion matrix for the deep CNN model reveals near-perfect classification performance overall, with 100% accuracy for both basophils and myeloblasts. In comparison, erythroblasts show a slightly lower accuracy of 86.7% (26 out of 30 correctly classified, with 4 misclassified as basophils), as illustrated by Figure 4. When normalized by true class, basophils and myeloblasts maintain perfect recognition. In contrast, the rowwise accuracy for erythroblasts indicates that a small subset is misinterpreted, likely due to subtle morphological similarities to basophils, despite their distinctive features. Analysis of column-wise normalization shows that approximately 88.2% of samples predicted as basophils are indeed basophils, with the remainder being erythroblasts, underscoring a slight overlap in the feature space between these two classes. These observations suggest that while the deep CNN effectively distinguishes the majority of blood cell types, there remains an opportunity for further refinement, potentially through enhanced feature engineering, increased data augmentation, or additional model tuning to differentiate erythroblasts from basophils better and improve the overall robustness of the classifier in clinical diagnostics.

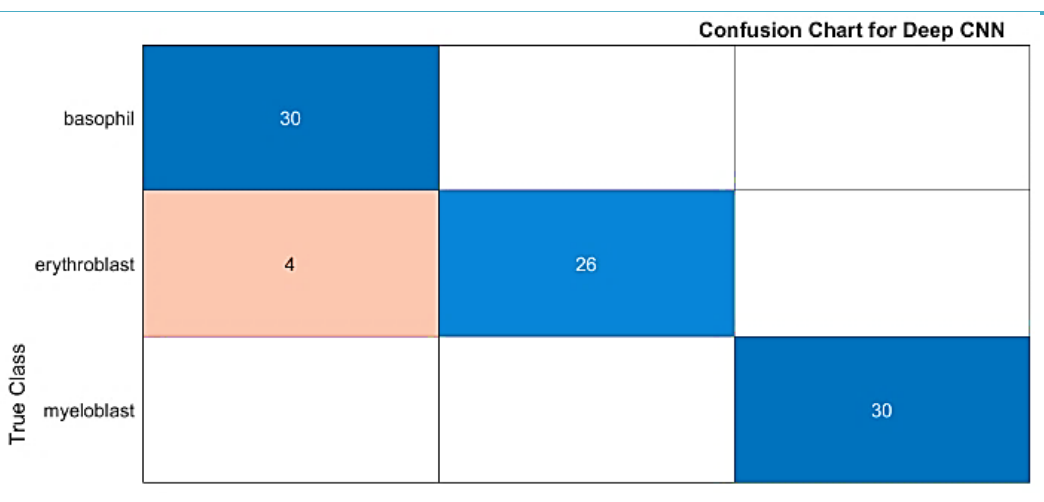


Figure 4. Confusion chart of the deep CNN.

Classification via transfer learning using **ResNet:** The training process of the ResNet model was both robust and efficient, as demonstrated by the steady evolution of key performance metrics over 2100 iterations and 100 epochs, as shown in Figure 5. Initially, the training accuracy rapidly increased from a moderate value, quickly approaching and then maintaining near 100% accuracy, indicating that the network's residual connections were highly effective in facilitating deep feature extraction and mitigating the vanishing gradient problem. Concurrently, the training loss decreased sharply from an initial high value and plateaued at very low levels, with only minor fluctuations that are typical in mini-batch optimization. This convergence was achieved using a constant learning rate of 0.0001, ensuring gradual yet consistent weight updates that contributed to the model's stable performance over time. Notably, the entire training process was executed on a single CPU, suggesting an efficient use of computational resources despite the complexity of the ResNet architecture. Overall, the training results indicate that the

The ResNet model successfully learned the underlying patterns in the data, as reflected in its high accuracy and low loss by the end of training, thereby affirming its potential for effective generalization to unseen samples.

Figure 6 displays the confusion matrix for the ResNet model, indicating a high level classification accuracy across the three blood cell categories. Specifically, basophils and myeloblasts classified with 100% are accuracy, while erythroblasts achieve a slightly lower accuracy of 90%, with 3 out of 30 instances misclassified as basophils. This pattern suggests that although the deep architecture of ResNet effectively captures the discriminative features necessary for accurate classification, there exists a subtle overlap between the feature representations of erythroblasts and basophils. Such overlaps may be due to inherent morphological similarities in the texture or structure of the cells. Overall, these results attest to the robustness of the transfer learning approach using ResNet while also highlighting an opportunity for further refinement in distinguishing closely related cell types.

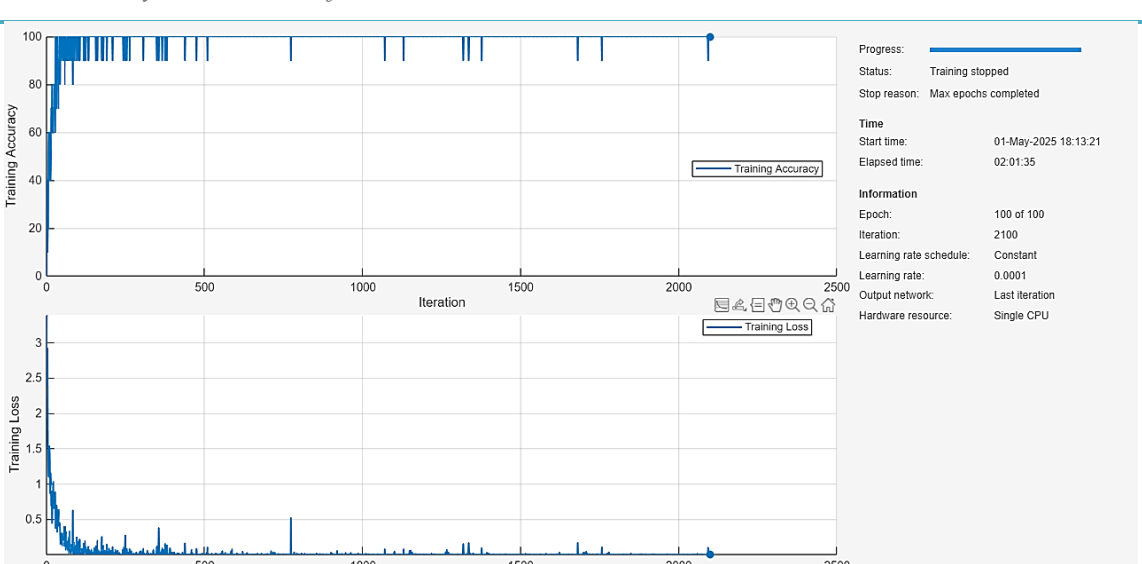


Figure 5. Training process of the ResNet method.

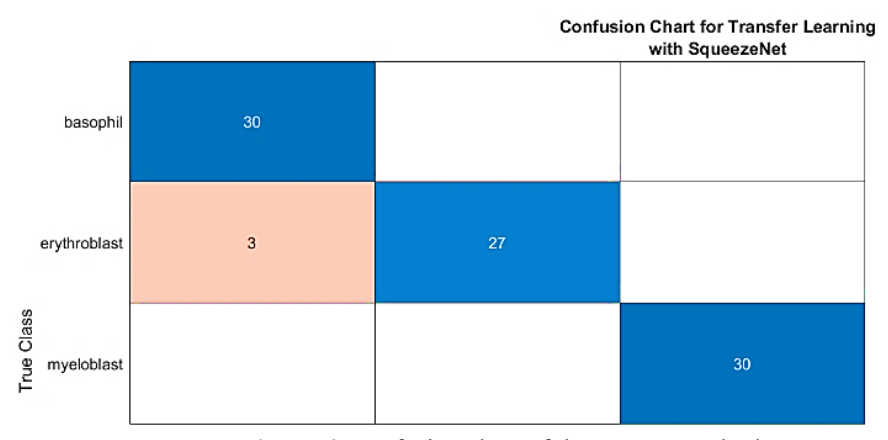


Figure 6. Confusion chart of the ResNet method.

Clinical integration and validation: To transition from a research prototype to a routine diagnostic tool, our AI framework must be embedded seamlessly within existing digital pathology infrastructures. In a typical laboratory workflow, blood smear slides scanned by high-throughput slide scanners will be automatically conveyed to the AI engine through the Laboratory Information System (LIS). The model's cell-type predictions-including confidence scores-will be overlaid on the digital-pathology viewer, pathologists visualize enabling to annotations alongside their manual assessments. This integration minimizes

additional workflow steps and ensures that AI outputs augment, rather than disrupt, established diagnostic practices.

Effective adoption also hinges on user training and feedback mechanisms. Laboratory staff will participate in structured workshops and e-learning modules to learn how to interpret AI annotations, manage low-confidence or "rejected" outputs, and reconcile discrepancies between model predictions and expert opinions. Regular feedback sessions will capture user experiences and inform iterative refinements of both the AI model and the user interface, ensuring that the system evolves in alignment with clinical needs.

Finally, safeguarding patient data and ensuring long-

term performance stability is paramount. All image transfers will adhere to HIPAA and GDPR standards, employing end-to-end encryption and de-identification protocols. Post-deployment, a continuous monitoring framework will track metrics such as false-positive and false-negative rates, model drift, and override frequencies. These indicators will trigger scheduled retraining with newly annotated cases, guaranteeing that the AI system maintains its accuracy and reliability over time.

Discussion

Our findings demonstrate that all three approaches-wavelet scattering with SVM, custom deep CNN, and ResNet transfer learning-achieved strong performance in distinguishing between basophils, erythroblasts, and myeloblasts. However, important performance differences emerged among the methods. The wavelet scattering with the SVM approach achieved the highest overall accuracy (~98.9%), with perfect classification of basophils and erythroblasts and only a single misclassification among myeloblasts. The deep CNN achieved 95.6% overall accuracy, with slightly reduced performance for erythroblasts (86.7%), while the ResNet model performed between the two methods, reaching 96.7% accuracy with 90% correct classification of erythroblasts. These differences highlight that while deep learning architectures are effective, handcrafted feature extraction using wavelet scattering remains highly competitive in scenarios with limited datasets.

Comparing these results with prior studies underscores their significance. Jarjees *et al.* (23) reported 98% accuracy using a VGG-19 transfer learning pipeline for leukocyte classification, which is comparable to our

ResNet model but slightly lower than the wavelet scattering + SVM approach. Similarly, Khanam et al. (26) demonstrated high performance of CNNs in acute myeloid leukemia detection, yet their work also noted challenges in separating morphologically similar cell types-a limitation mirrored in our between misclassifications erythroblasts and basophils. Tarquino et al. (24) achieved 93.8% accuracy with a variational autoencoder cascade for bone marrow cell classification, which is lower than all three methods in our study. This indicates that both conventional machine learning (wavelet scattering + SVM) and transfer learning approaches are advantageous for small, specialized datasets.

Other investigations have also confirmed the challenge of differentiating morphologically overlapping cells. Arabyarmohammadi *et al.* (21) utilized texture-based deep models to stratify myeloblasts in AML and MDS, reporting strong prognostic accuracy while also highlighting issues with feature overlap. Likewise, Guo *et al.* (22) proposed a rejection-based classifier for bone marrow cells to handle ambiguous cases, which aligns with our observation that a small subset of erythroblasts was misclassified as basophils.

Our results, therefore, support the notion that robust, handcrafted descriptors, such as wavelet scattering coefficients, outperform deep CNNs and even transfer learning models when dataset size is constrained, as they capture subtle morphological patterns without requiring massive annotated datasets (28). At the same time, the promising results of ResNet (96.7% accuracy) suggest that deep hierarchical feature extraction can achieve reliable performance and may surpass handcrafted features when larger datasets and additional augmentation strategies are available.

Taken together, this study contributes to the growing evidence that AI-driven image analysis can enhance hematological diagnostics by providing high accuracy and reducing inter-observer variability. While some misclassifications remain, particularly between erythroblasts and basophils, our

comparative analysis shows that integrating wavelet-based descriptors with traditional classifiers remains a viable and powerful approach. Future work should investigate hybrid feature fusion strategies, as well as enriched datasets, to further improve erythroblast recognition and achieve robust, clinically deployable diagnostic support systems.

Conclusion

Our findings demonstrate that AI can effectively automate blood cell classification, reducing the subjectivity of manual microscopy. All three models-wavelet scattering with SVM, a custom CNN, and ResNet-achieved high accuracy (>95%), with the wavelet-SVM combination performing best (~98.9%). However, a limitation of this study is the genetic properties of our dataset, which differs from others and may impact model generalizability. Future research should expand datasets and incorporate genetic variability to strengthen clinical applicability. Despite this, our work confirms that AI-driven frameworks are promising tools for enhancing hematological diagnostics

Source of funding: This research did not receive any specific grant from funding agencies in the public, commercial, or not-forprofit sectors.

Ethical clearance: Ethical approval for this study was obtained from the Ethics Committee of the College of Science, Mustansiriyah University.

Conflict of interest: The authors declare that they have no known competing financial interests or personal relationships that could have appeared to influence the work reported in this paper.

Use of Generative Artificial Intelligence (AI): The authors state that they did not utilize any generative AI tools for creating or editing the language of the manuscript.

Acknowledgments: The authors would like to thank Mustansiriyah University, Baghdad, Iraq, for supporting the presented work.

References

- 1. Aby AE, Salaji S, Anilkumar KK, Rajan T. Classification of acute myeloid leukemia by pretrained deep neural networks: A comparison with different activation functions. Medical Engineering & Physics. 2025;135:104277. doi: https://doi.org/10.1016/j.medengphy.2024.104277.
- 2. He J, Xu X, Zhang Y, Jiang S, Lin Q, Zhang H, et al. Photoelectrochemical aptasensing and fluorescence imaging co-joint detecting MCF-7 cells in whole blood via an inertial separation microfluidic chip. Talanta. 2025;286:127488. doi: https://doi.org/10.1016/j.talanta.2024.127488.
- 3. Zhang X, Zhao Q, Zhu W, Liu T, Xie SH, Zhong LX, et al. The Association of Telomere Length in Peripheral Blood Cells with Cancer Risk: A Systematic Review and Meta-analysis of Prospective Studies. Cancer Epidemiology,

Biomarkers & Prevention. 2017;26(9):1381–90. doi: https://doi.org/10.1158/1055-9965.EPI-16-0968.

4. Li Y, Cai L, Lu Y, Lin C, Zhang Y, Jiang J, et al. Domain-invariant representation learning via SAM for blood cell classification. Pattern Recognition. 2026;170:112000.

 $\underline{https://doi.org/10.1016/j.patcog.2025.112000}.$

- 5. AlKindy B, Jamil OB, Al-Nayyef H, Alkendi W. A Machine Learning Approach for Identifying Five Types of Horizontal Ocular Disorders Using Haar Features. Al-Mustansiriyah Journal of Science. 2025;36(1):69–83. doi: https://doi.org/10.23851/mjs.v36j1.1597.
- 6. Lakshmi Narayanan K, Santhana Krishnan R, Harold Robinson Y, Vimal S, Rashid TA, Kaushal C, et al. Enhancing acute leukemia classification through hybrid fuzzy C means and random forest methods. Measurement: Sensors. 2025;39. doi: https://doi.org/10.1016/j.measen.2025.101876.
- 7. Radhi E, Kamil M. An Automatic Segmentation of Breast Ultrasound Images Using U-Net Model. Serbian Journal of Electrical Engineering. 2023;20(2):191–203. doi:

https://doi.org/10.2298/SJEE2302191R.

8. Radhi EA, Kamil MY. Breast tumor segmentation in mammography image via Chan-Vese technique. Indonesian Journal of Electrical Engineering and Computer Science. 2021;22(2):809–17. doi:

http://doi.org/10.11591/ijeecs.v22.i2.pp809-817.

- 9. Das S, Padmanaban K. Incremental learning for acute lymphoblastic leukemia classification based on
- hybrid deep learning using blood smear image. Computational Biology and Chemistry. 2025;118. doi: https://doi.org/10.1016/j.compbiolchem.2025. 108456.
- 10. Fukuyama S, Kumamoto S, Nagano S, Hitotsuya S, Yasuda K, Kitamura Y, et al. Detection of cancer cells in whole blood using a dynamic deformable microfilter and a nucleic acid aptamer. Talanta. 2021;228:122239. doi: https://doi.org/10.1016/j.talanta.2021.122239. 11. Igbal A, Ahmed MF, Suvon MNI, Shuvho SD. Fahmin A. Towards Efficient Segmentation and Classification of White Blood Cell Cancer Using Deep Learning. 2021 Emerging Technology in Computing, Communication and Electronics (ETCCE)2021. p. 1-6.
- 12. Kamil M, Hashem S. Segmentation of Chest X-Ray Images Using U-Net Model. Mendel. 2022;28(2):49-3.. doi: https://doi.org/10.13164/mendel.2022.2.049.
- 13. Keller A, Leidinger P, Borries A, Wendschlag A, Wucherpfennig F, Scheffler M, et al. miRNAs in lung cancer studying complex fingerprints in patient's blood cells by microarray experiments. BMC Cancer. 2009;9:353. doi: https://doi.org/10.1186/1471-2407-9-353.
- 14. Muduli D, Parija S, Kumari S, Hassan A, Jangwan HS, Zamani AT, et al. Deep learning-based detection and classification of acute lymphoblastic leukemia with explainable AI techniques. Array. 2025;26. doi: https://doi.org/10.1016/j.array.2025.100397.
- 15. Rahman SIU, Abbas N, Salman M, Ali S, Alkhayat A, Khan J, et al. Deep Learning and Artificial Intelligence-Driven Advanced Methods for Acute Identification Leukemia Lymphoblastic and Classification: **Systematic** Review. Computer Modeling Engineering Sciences. 2025;142(2):1199–231. doi:

http://dx.doi.org/10.32604/cmes.2025.057462.

- 16. Yasui K, Saito T, Ueda S, Shinohara K, Fukami Y, Sano T, et al. Sequential Changes in Circulating Tumor Cells in the Peripheral
- Blood of Pancreatic Cancer Patients with Preoperative Chemotherapy Using a New Immunocytology-Based, Light Microscopic CTC Detection Platform. Diagnostics (Basel). 2025;15(6). doi: https://doi.org/10.3390/diagnostics15060752.
- 17. Alsamri J, Alqahtani H, Al-Sharafi AM, Darem AA, Nazim K, Sattar A, et al. Computer-aided diagnosis of Haematologic disorders detection based on spatial feature learning networks using blood cell images. Scientific Reports. 2025;15(1):12548. doi: https://doi.org/10.1038/s41598-025-85815-4.
- 18. Chola C, Muaad AY, Bin Heyat MB, Benifa JVB, Naji WR, Hemachandran K, et al. BCNet: A Deep Learning Computer-Aided Diagnosis Framework for Human Peripheral Blood Cell Identification. Diagnostics. 2022;12(11):2815. doi: https://doi.org/10.3390/diagnostics12112815.
- 19. Mohamed H, Omar R, Saeed N, Essam A, Ayman N, Mohiy T, et al. Automated detection of white blood cells cancer diseases. 2018 First International Workshop on Deep and Representation Learning (IWDRL)2018. p. 48–54.
- 20. Radhi EA, Kamil MY. Anisotropic Diffusion Method for Speckle Noise Reduction in Breast Ultrasound Images. International Journal of Intelligent Engineering and Systems. 2024;17(2):621–31. doi: https://doi.org/10.22266/ijies2024.0430.50.
- 21. Arabyarmohammadi S, Leo P, Viswanathan VS, Janowczyk A, Corredor G, Fu P, et al. Machine Learning to Predict Risk of Relapse Using Cytologic Image Markers in Patients With Acute Myeloid Leukemia Posthematopoietic Cell Transplantation. JCO Clinical Cancer Informatics. 2022(6):e2100156. doi: https://doi.org/10.1200/cci.21.00156.
- 22. Guo L, Huang P, He H, Lu Q, Su Z, Zhang Q, et al. A method to classify bone marrow cells with rejected option. Biomedical Engineering / Biomedizinische Technik. 2022;67(3):227–36. doi: https://doi.org/10.1515/bmt-2021-0253.
- 23. Jarjees MS, Sheet SSM, Ahmed BT. Leukocytes identification using augmentation and transfer learning based convolution neural network. Telkomnika (Telecommunication Computing Electronics and Control).

2022;20(2):314–20. doi:http://doi.org/10.12928/telkomnika.v 20i2.23163.

24. Tarquino J, Rodriguez J, Alvarez-Jimenez C, Romero E. A One-Class Variational Autoencoder (OCVAE) Cascade for Classifying Atypical Bone Marrow Cell Sub-types. Cham: Springer Nature Switzerland; 2023. p. 725–34.

25. Valent P, Sotlar K, Blatt K, Hartmann K, Reiter A, Sadovnik I, et al. Proposed diagnostic criteria and classification of basophilic leukemias and related disorders. Leukemia. 2017;31(4):788–97. doi: https://doi.org/10.1038/leu.2017.15.

26. Khanam AS, Khan MH, Tabassum F, Ripa TA, Jabid T, Ali MS, et al. Classification of acute myeloid leukemia using convolutional neural network. International Conference on Green Energy, Computing and Intelligent Technology (GEn-CITy 2023)2023. p. 253–8.

27. Al-Obaidi FEM, Al-Saeed AJMA, Al-Zuhairi AJM. Self-Automatic Threshold Technique For Eye Pupil Detection. Journal of Optics (India). 2025. doi: https://doi.org/10.1007/s12596-025-02529-6.

28. Hindi RJ. Ensemble Machine Learning Approach for Anemia Classification Using Complete Blood Count Data. Al-Mustansiriyah Journal of Science. 2025;36(3):51–70. doi: https://doi.org/10.23851/mjs.v36i3.1709.

تصنيف وتنبؤ خلايا الدم البشرية باستخدام الذكاء الاصطناعي وتقنيات معالجة الصور المتقدمة

الحمد سعيد لطيف، ٢ احمد جبار محمد، المحمد يوسف كامل

الملخص

الخلفية: يعد التصنيف الدقيق لخلايا الدم أمرًا بالغ الأهمية لتشخيص وإدارة اضطرابات الدم. حيث أن التقييمات اليدوية التقليدية لمسحات الدم تتطلب جهدًا كبيرًا وتخضع للتباين بين المختصين، مما قد يهدد موثوقية التشخيص.

ا**لأهداف:** تهدف هذه الدراسة إلى تطوير والتحقق من إطار عمل آلي يعتمد على التعلم العميق لتصنيف أنواع خلايا الدم الرئيسية بدقة، وتحديدًا الخلايا القاعدية، والخلايا الأرومية الحمراء، والخلايا الأرومية النقوية، لتعزيز دقة وكفاءة التشخيص في الإعدادات السريرية.

المرضى والطرق: قمنا بتحليل مجموعة فرعية مختارة من صور مسحات الدم عالية الدقة المتاحة publicly ، مع تطبيق معالجة مسبقة موحدة لمعالجة مشكلة التباين. تم تطوير واستعراض استراتيجيات تصنيف متعددة مدعومة بالذكاء الاصطناعي، حيث تم تقييم جميع النماذج على مجموعة اختبار مستقلة باستخدام مقاييس الدقة الشاملة، والدقة، والاستدعاء، ودرجة F1.

النتائج: أظهرت تقنية "تبعثر الموجهات (Wavelet Scattering) "المقرونة بآلة المتجهات الداعمة (SVM) أقوى أداءً إجمالي، متجاوزة أداء كل من شبكة CNN المخصصة والنماذج المشتقة من .ResNet حيث حققت هذه الطريقة فصلًا شبه كامل للخلايا القاعدية والخلايا الأرومية المحراء، واقتصر ارتباكها النادر على الخلايا الأرومية النقوية. تؤكد هذه النتائج على حساسية طريقة تبعثر الموجهات للفروق الشكلية الدقيقة في خلايا الدم.

الاستنتاج: تسلط هذه الدراسة الضوء على كيفية قدرة تقنيات تحليل الصور القائمة على التعلم الآلي على تصنيف خلايا الدم بشكل موثوق ودقيق، مما يقلل من الاعتماد على التفسير اليدوي الذاتي الذي يميز الفحص المجهري التقليدي. يوجد إمكانية لزيادة دقة التشخيص المبكر وتبسيط خطط علاج المرضى الذين يعانون من اضطرابات دموية من خلال دمج هذه الأنظمة الآلية في الممارسة السريرية القياسية.

الكلمات المفتاحية: التشخيص الدموي، تصنيف خلايا الدم، تحويل تبعثر الموجهات، التعلم بالانتقال.

المؤلف المراسل: احمد سعيد لطيف

a97s21@uomustansiriyah.edu.iq الايميل:

تاريخ الاستلام: ١٠ أيار ٢٠٢٥

تاريخ القبول: ١٦ ايلول ٢٠٢٥

تاريخ النشر: ٢٠ تشرين الاول ٢٠٢٥

العلوم، الجامعة المستنصرية، بغداد، العراق. 2 قسم الفسلجة والفيزياء الطبية، كلية الطب، جامعة ديالي، ديالي، العراق.

Interleukin-20 Gene Polymorphism and Serum Levels of Interleukin-20 and Interleukin-23 in Rheumatoid Arthritis

Iman Najat Ali (1) Najat Jabbar Ahmed Berwary (1)

¹ Department of Medical Laboratory Technology, Erbil Health and Medical Technical College, Erbil Polytechnic University, Erbil, Iraq.

OPEN ACCESS

Correspondence: Iman Najat Ali Email <u>iman.ali@epu.edu.iq</u>

Copyright: ©Authors, 2025, College of Medicine, University of Diyala. This is an open access article under the CC BY 4.0 license (http://creativecommons.org/licenses/by/4.0/)

Website:

https://djm.uodiyala.edu.iq/index.php/djm

 Received:
 05
 May
 2025

 Accepted:
 18
 August
 2025

 Published:
 25
 October
 2025

Abstract

Background: Rheumatoid arthritis (RA) is an autoimmune disease marked by complex causes and ongoing joint inflammation. Recently, more efforts have been directed at finding new non-invasive prognostic biomarkers for RA, which can help in disease monitoring.

Objectives: To investigate the circulatory levels of IL-20 and IL-23 in RA patients relative to healthy volunteers and to evaluate their correlation with disease activity. Additionally, to explore the association between IL-20 genetic polymorphism and RA susceptibility.

Patients and Methods: The study comprised a total of 85 individuals with RA and 45 healthy subjects. IL-20 and IL-23 concentrations were measured using ELISA, and disease activity was assessed using the DAS-28 score. The IL-20 rs2981573 polymorphism was genotyped using Amplification Refractory Mutation System-Polymerase Chain Reaction.

Results: The study found that RA participants exhibited significantly elevated serum IL-23 levels compared to controls (P = 0.0347), while IL-20 levels did not differ (P = 0.6354). Correlations between IL-20 and IL-23 with DAS-28 were significant (P = 0.0021 and P = 0.0030, respectively). Regarding the IL-20 gene polymorphism, no significant association was found between the rs2981573 gene polymorphism and RA susceptibility

Conclusion: This study demonstrated that IL-23 levels were significantly higher in RA patients and may have diagnostic value. Although IL-20 levels were not significantly different between groups, both cytokines showed a positive correlation with disease activity and could be valuable markers. Furthermore, the IL-20 gene polymorphism showed no association with rheumatoid arthritis susceptibility.

Keywords: IL-20 Genetic polymorphism, DAS-28, rheumatoid arthritis, IL-20, IL-23.

Introduction

Rheumatoid arthritis (RA) is an autoimmune condition that leads to chronic joint inflammation, progressive joint damage, impairment, and reduced quality of life. The pathogenesis of RA is complicated, including a delicate interplay of environment and genes that eventually result in the dysregulation of the immune system (1). Cytokines, which are small proteins that mediate various cellular functions, have been recognized as significant factors in the development of RA (2).

Diyala Journal of Medicine

ORIGINAL RESEARCH Published: 25 October 2025 DOI: 10.26505/djm.v29i1.1451

Interleukin-20 is a cytokine within the IL-10 family that mediates complex immune and inflammatory responses (3). It binds to the IL-20RA or IL-20RB ligand, triggering intracellular signaling pathways. Primarily produced by activated macrophages and neutrophils infiltrating the synovial tissue (4). IL-20 induces the production of fibroblasts in the synovium, the proliferation of proinflammatory cytokines that amplify inflammation. and the recruitment additional immune cells to the affected tissue. further exacerbating the condition (5). IL-23 also plays a role in the inflammatory response associated with RA. This cytokine consists of two subunits forming a heterodimer, primarily induced through active macrophages and dendritic cells (6, 7). IL-23 stimulates and maintains T helper 17 cells, which induce proinflammatory cytokine IL-17, crucial for RA pathogenesis (7). Additionally, IL-23 can directly stimulate other immunocytes, for example, neutrophils and macrophages, further contributing to the inflammatory process in RA (8). Furthermore, there is a growing trend toward identifying new prognostic biomarkers for RA that could aid in monitoring disease improvement or guiding decisions regarding subsequent treatment. A 2010 study by Lindstrom and Robinson. Found that cytokine biomarkers in RA are more accurate in determining disease activity outcomes than other biomarkers, such as autoantibodies and acute-phase reactants, which may be less reliable (9). High levels of both interleukin-20 and interleukin-23 have been observed within the joint fluid and serum of RA individuals, suggesting they are likely laboratory markers for disease activity and progression (5, 10).

The genes that encode IL-20 are in a designated area on chromosome 1 (11). Previous studies have revealed correlations

between specific polymorphisms in the IL-10 group as well as an elevated risk for the development of numerous autoimmune, infectious, and malignant disorders (12, 13). The results presented thus far suggest that IL-20 is a key gene in the understanding of RA. But no research has looked at the function of IL-20 gene polymorphisms in RA till now. The objective of this study was to investigate the association of the IL-20 rs2981573 polymorphism with RA susceptibility, to assess IL-20 and IL-23 serum levels in RA patients and healthy controls, and to elucidate their correlation with disease activity.

Patients and Methods

Study design: This case-control investigation was performed on 45 healthy controls and 85 patients confirmed to have RA using the classification criteria of 2010 set by the ACR/EULAR (14). RA patients were taken from the private clinics and inpatient units of the Rheumatology departments at Rizgary Teaching Hospital and Hawler Teaching Hospital between September 2024 and December 2024. The criteria for excluding patients encompassed individuals under 18 years old, those who were pregnant, and those with any malignancy or other autoimmune diseases. For RA patients and healthy controls, demographic data were collected, including age, sex, and body mass index (BMI). The healthy volunteers ' sex, age, and BMI matched those of RA patients who participated in the research. In RA patients, additional clinical information, such as disease duration and disease activity score (DAS28), was documented.

Data collection and laboratory investigations: After obtaining informed consent, blood was taken from every individual. A sample of blood was deposited in EDTA-coated tubes for genetic investigation. The residual blood samples were subsequently gathered in plain tubes and separated at 3000 rpm for fifteen minutes to get serum, and then frozen at -20°C for future investigations. The disease activity in patients was assessed using the Disease Activity Score (DAS28), calculated using

C-reactive protein the (CRP) serum concentration. All RA participants underwent comprehensive medical history taking, detailed physical examination, and laboratory tests such as CRP, Anti-Cyclic Citrullinated Peptide (Anti-CCP), rheumatoid factor (RF), Complete Blood Count (CBC), Rate (ESR). Erythrocyte Sedimentation Serum CRP levels were assessed using the Cobas c 111 (Roche Diagnostics, Germany), Anti-CCP antibodies were quantified using Alegria® system (ORGENTEC the Diagnostika, Germany), and RF levels were determined using the Cobas 6000 analyzer (Roche Diagnostics, Germany). **CBC** parameters were assessed using the Convergys® X3 NG hematology analyzer (Roche Diagnostics, Switzerland). Platelet-to-Lymphocyte Ratio (PLR) and Neutrophil-to-Lymphocyte Ratio (NLR) were calculated manually. And ESR was determined using the Westergren method. Both IL-20 and IL-23 concentrations were assessed in RA participants and controls using ELISA kits from Sun Long Biotech Co., LTD. IL-20 (catalogue number: SL1907HU) and IL-23 (catalogue number: SL0989Hu) followed the same sandwich ELISA procedure.

DNA extraction: DNA has been isolated from the samples of patients and healthy individuals using the Blood DNA Preparation-Solution Kit (Jenabioscience/Germany), following the manufacturer's instructions. DNA concentrations were measured by Nanodrop. The absorbance ratio at 260 nm to 280 nm was employed to check the purity of the extracted DNA.

Genotyping polymorphism by ARMS-PCR: Genotyping of the IL-20 rs2981573 polymorphism was done for all participants using the Amplification Refractory Mutation

System–Polymerase Chain Reaction (ARMS-PCR) technique as designated by Kingo and colleagues (15). The PCR process was performed in a reaction containing 25 microliters, consisting of 12.5 µL of master mix (Go TagGreen Master Mix/ Promega/ USA), 1 µL of each primer (Table 1), 3 microliters of the DNA, and 5.5 microliters of free DNase water. The cycling conditions included a starting denaturation phase at 95°C for five minutes, then ten cycles of 95 degrees Celsius for thirty seconds, 60°C in thirty seconds, and 72°C for 1 minute. This was succeeded by 30 cycles at 58°C in 30 seconds each, concluding with 72°C for 1 minute. A finalizing extension phase at 72°C in 10 minutes was incorporated. PCR amplicons were viewed, and their sizes were assessed using 2% agarose gel electrophoresis.

Statistical Analysis

The data was examined with the help of GraphPad Prism 8.0.2. Frequencies and percentages were used to represent categorical data, whereas means and medians with ranges were used to represent quantitative data. The Shapiro-Wilk and D'Agostino tests were performed to determine normality. The results showed that IL-20, IL-23, Anti-CCP, RF, CRP, ESR, Hb, PLR, NLR, neutrophil count, and lymphocyte count were not normally distributed, whereas DAS28 and platelet count were normally distributed. Mann-Whitney Utest performed for comparison. For comparisons involving categories, Fisher's exact and chi-square tests were utilized. For correlations, Spearman's correlation is used. When the p-value was less than 0.05, all tests were deemed to have statistical significance. p < 0.05 (*): statistically significant, p < 0.01 (**): highly significant, p < 0.001 (***): highly significant, p < 0.0001extremely significant, $p \ge 0.05$ (NS): not significant

Table 1. Primers for amplifying polymorphism.

Genetic polymorphism	Primer sequence	Amplicon size
	Forward inner primer, (A allele),	181 base pairs A allele
IL-20 1380 A/G rs2981573	CCTCTCCTAGCTGATGATGAACTGAA	
	Reverse inner primer, (G allele),	255 base pairs G allele
	CTCTTTCAGACCTCACATTTGGAATAAC	
	Forward outer primer,	382 base pairs control
	TCTGAATAGGACCTAGGAATTCAATTCTTT	

Results

Basic characteristics of study participants:

The age distribution among RA patients and controls was comparable, with the RA cohort averaging 48.92 ± 10.69 years and the control group averaging 47.67 ± 8.555 years, showing no differences (p = 0.4989). The percentage of female participants in the RA and control groups was 89.41% and 91.11%, respectively. The body mass index was recorded for each participant, with a mean Body Mass Index (BMI) of 29.85 ± 5.756 kg/m² in rheumatoid arthritis patients and 31.03 ± 4.613 kg/m² in the controls (p = 0.0782). The mean duration of disease in patients with rheumatoid arthritis was 8.61 years. Rheumatoid arthritis patients had markedly elevated CRP (p = 0.0039), ESR (p < 0.0001), and neutrophil counts levels (p = 0.0009), and reduced hemoglobin

levels (p < 0.0001) than healthy subjects. The basic characteristics and lab parameters of the study cohorts are delineated in Tables 2 and 3. Comparing serum IL-20 and IL-23 levels in RA patients with healthy controls: The healthy group exhibited a mean IL-20 serum level of 80.45 ± 15.11 pg/ml, whereas the RA individuals presented a mean of 97.22 ± 97.07 pg/ml (p = 0.6354), indicating a nonsignificant difference. The two groups demonstrated significant distinction in IL-23 levels (p = 0.0347). The mean serum IL-23 level in those with RA was 61.70 ± 51.39 pg/ml, compared to 49.39 ± 10.34 pg/ml in the healthy group. Table 4 summarizes the comparison of serum IL-20 and IL-23 levels between the patient and control subjects.

Table 2. Demographic and Clinical Data of Patient and Control Group.

Variables Mean ± SD (range), n (%)	RA patients (n=85)	Healthy subjects (n=45)	p-value
A /	48.92 ± 10.69	47.67 ± 8.555	0.4989
Age/year	(24-74)	(30-65)	NS
Gender			
Female	76 (89.41%)	41 (91.11%)	>0.9999 NS
Male	9 (10.59%)	4 (8.89%)	NS
DMI (log/m²)	29.85 ± 5.756	31.03 ± 4.613	0.0782
BMI (kg/m²)	(18.90-44.80)	(19.90-42)	NS
Disease duration/Year	8.61 ± 7.81 (0.08 - 30)	N/A	
Tender Joints Count	14.98 ± 9.838 (0-28)	N/A	
Swollen Joints Count	2.294 ± 2.979 (0-12)	N/A	
DAS-28	4.651 ± 1.477 $(1.19-7.41)$	N/A	
Family history			
No	42 (49.4%)	N/A	
Yes	43 (50.6%)		
Hypertension			
No	64 (75.29%)	N/A	
Yes	21 (24.71%)		
Smoking			
No	77 (90.59%)	N/A	
Yes	8 (9.41%)		
Medications			
csDMARDs	76 (89.4%)		
Biologic agents	37 (43.5%)		
Corticosteroids	58 (68.2%)	N/A	
NSAIDs	23 (27.1%)	1 1/ / 1	

Rheumatoid arthritis (RA); body mass index (BMI); disease activity score (DAS28); conventional synthetic disease-modifying anti-rheumatic drugs (csDMARD); nonsteroidal anti-inflammatory drugs (NSAID); SD: standard deviation; not applicable (N/A). A p-value exceeding 0.05 suggests non-significance (NS); p < 0.05 is considered significant.

Table 3. Laboratory Characteristics of Patient and Healthy Subjects.

Variables Mean ± SD (range)	RA patients n=85	Controls n=45	p-value
CRP (mg/L)	12.71 ± 28.38 (0.20-244.5)	3.936 ± 3.549 (0.18-16)	0.0039**
ESR (mm/1h)	31.62 ± 21.33 (2-111)	17.09 ± 10.79 (1-43)	<0.0001****
RF (IU/ml)	119.5 ± 248.8 (0.1-1314)	N/A	
Anti-CCP (U/ml)	248.6 ± 345.7 (0.1-1000)	N/A	
Hb (g/dl)	12.41 ± 1.657 (7-16.30)	13.64 ± 1.368 (9.5-18.20)	<0.0001****
Lymphocytes (10 ⁹ /L)	2.209 ± 0.8042 (0.60 - 4.790)	2.009 ± 0.6254 (0.44 - 3.580)	0.2455 NS
Neutrophils (10 ⁹ /L)	5.096 ± 2.073 (1.4 - 13)	3.981 ± 1.114 (2.29 - 7.17)	0.0009***
Platelets (10 ⁹ /L)	278.2 ± 79.51 (115 - 471)	241.6 ± 49.01 (131 - 361)	0.0057**
NLR	2.632 ± 1.593 (0.5833 - 9.5)	2.204 ± 1.137 (1.081 - 7.886)	0.1985 NS
PLR	148.4 ± 93.06 (55.11 - 555)	132.8 ± 53.69 (62.57 - 361.4)	0.8378 NS

Rheumatoid factor (RF), hemoglobin (Hb), platelet-to-lymphocyte ratio (PLR), neutrophil-to-lymphocyte ratio (NLR), erythrocyte sedimentation rate (ESR), C-reactive protein (CRP), anti-cyclic citrullinated peptide (Anti-CCP), and DAS28: disease activity score, not applicable (N/A). A p-value exceeding 0.05 suggests non-significance (NS); p < 0.05 is considered significant.

Table 4. Comparison of IL-20 and IL-23 between the control and study groups.

Variables	mean ± SD median (ranges) Study (n=85)	mean ± SD median (ranges) Control (n=45)	p-value
IL-20 (pg/ml)	97.22 ± 97.07 80.09 (23.08-900)	80.45 ± 15.11 80.71 (54.26-120.4)	0.6354 NS
IL-23 (pg/ml)	61.70 ± 51.39 52.63 (40.89-500)	49.39 ± 10.34 49.20 (24.09-63.13)	0.0347*

Correlation of IL-20 and IL-23 with clinical and laboratory variables: A positive relationship between DAS-28 and IL-20 and IL-23 was found (p=0.0021, p=0.0030, respectively), the number of tender joints (p=0.0061, p=0.0126, respectively), and the number of swollen joints (p=0.0238, p=0.0401, respectively). However, hemoglobin and IL-23 levels were inversely

correlated (p = 0.0462). Furthermore, other parameters did not correlate with both IL-20 and IL-23 (Table 5).

Correlation between NLR and PLR with RA disease activity: Platelet-to-Lymphocyte Ratio (PLR) revealed a statistically significant correlation with DAS-28 (r = 0.2158, p = 0.0473), while Neutrophil-to-Lymphocyte Ratio (NLR) did not (r = 0.1751, p = 0.1089) (Figure 1).

Table 5. Spearman's correlation between serum concentrations of IL-20 and IL-23 and the clinical and laboratory variables in RA participants.

Variables	IL-20 level r	p-value	IL-23 level r	p-value
Age	-0.08295	0.4504 NS	0.05875	0.5933 NS
Disease duration(years)	0.0589	0.5923 NS	-0.04735	0.6669 NS
Tender Joints Count	0.2951	0.0061**	0.2696	0.0126*
Swollen Joints Count	0.2450	0.0238*	0.2231	0.0401*
CRP (mg/L)	0.1460	0.1825 NS	0.08871	0.4195 NS
ESR (mm/1h)	0.08111	0.4606 NS	0.09735	0.3754 NS
Hb (g/dl)	0.04512	0.6818 NS	-0.2169	0.0462*
Lymphocytes (10 ⁹ /L)	-0.03380	0.7588 NS	0.02525	0.8186 NS
Neutrophils (10 ⁹ /L)	-0.1535	0.1606 NS	-0.07112	0.5178 NS
Platelets (10 ⁹ /L)	0.1293	0.2382 NS	0.1619	0.1387 NS
NLR	-0.09102	0.4074 NS	-0.08072	0.4627 NS
PLR	0.1067	0.3311 NS	0.08512	0.4386 NS
RF level (IU/ml)	0.02295	0.8349 NS	0.1755	0.1082 NS
Anti-CCP level (U/ml)	0.09672	0.3785 NS	0.03235	0.7688 NS
DAS28-CRP	0.3290	0.0021**	0.3182	0.0030 **

C-reactive protein (CRP), erythrocyte sedimentation rate (ESR), hemoglobin (Hb), neutrophil-to-lymphocyte ratio (NLR), platelet-to-lymphocyte ratio (PLR), rheumatoid factor (RF), anti-cyclic citrullinated peptide (Anti-CCP), DAS28: disease activity scorer, and r: correlation. Not significant (NS), and p < 0.05 is considered significant, and biochemical predictors of bone health metrics.

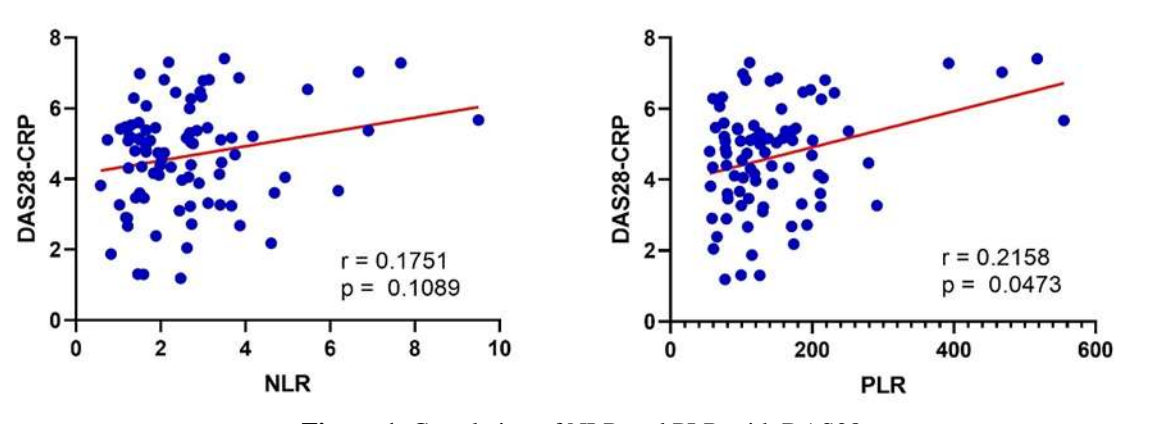


Figure 1. Correlation of NLR and PLR with DAS28.

Genotypic distribution and allele frequency of IL20 rs2981573 polymorphisms in the RA patients and control groups: The genotype distribution of the IL-20 rs2981573 SNP among the control group (n=45) was evaluated for Hardy-Weinberg equilibrium (HWE). The analysis showed a significant deviation from HWE ($\chi^2 = 45.37$, p < 0.0001), which may reflect a small sample size, population substructure, or the nature of the studied variant.

The AA genotype exhibited the highest prevalence in both patient and control groups, observed in 94.1% of RA patients and 95.6% of the healthy group. The AG genotype was detected in 1.2% of RA patients, while it was absent in the healthy group. The GG genotype was found in 4.7% of RA patients and 4.4% of the control group. The study could not identify a statistically significant correlation between the IL-20 rs2981573 polymorphism and susceptibility to RA (p > 0.9999). Similarly, allele frequency analysis

revealed no significant differences, with the A allele accounting for 94.7% in RA patients and 95.6% in control group and the G allele representing 5.3% in RA patients and 4.4% in controls (p = 0.7649) as in (Table 6).

Figures 2 and 3 illustrate the agarose gel electrophoresis results for IL-20 1380 A/G (rs2981573) polymorphism analysis. The gel images confirm the successful amplification of the target 181 bp (A allele) and 255 bp (G allele) fragments, along with the 382 bp internal control band.

Receiver operating characteristic (ROC) curve analysis: The ROC analysis for IL-20

revealed a non-significant discriminative value. A serum IL-20 level >79.99 pg/ml resulted in an AUC of 0.5255 (95% CI: 0.4272–0.6238; p = 0.6333), with a sensitivity of 50.59% and a specificity of 48.89%. In contrast, the analysis of the ROC curve revealed that a serum IL-23 level more than 49.27 pg/ml can significantly differentiate rheumatoid arthritis patients from healthy subjects (AUC=0.613; 95% CI: 0.5064–0.7189; p=0.0349), demonstrating a 51.11% specificity and 65.88% sensitivity (Figure 4).

Table 6. Genotypic and allelic frequencies of IL20 rs2981573 in rheumatoid arthritis patients and controls.

Genotype/Allele	Cases (n=85) N (%)	Control (n=45) N (%)	OR	CI (95%)	p-value
Genotype					
AA	80 (94.1%)	43 (95.6%)	Ref	-	-
AG	1 (1.2%)	0 (0%)	-	-	-
GG	4 (4.7%)	2 (4.4%)	0.93	(0.1716 - 4.130)	>0.9999
Allele					
A	161 (94.7%)	86 (95.6%)	Ref	-	-
G	9 (5.3%)	4 (4.4%)	0.83	(0.2767 - 2.729)	0.7649

Confidence interval (CI); odds ratio (OR); A p-value that is lower than 0.05 is considered to be statistically significant.

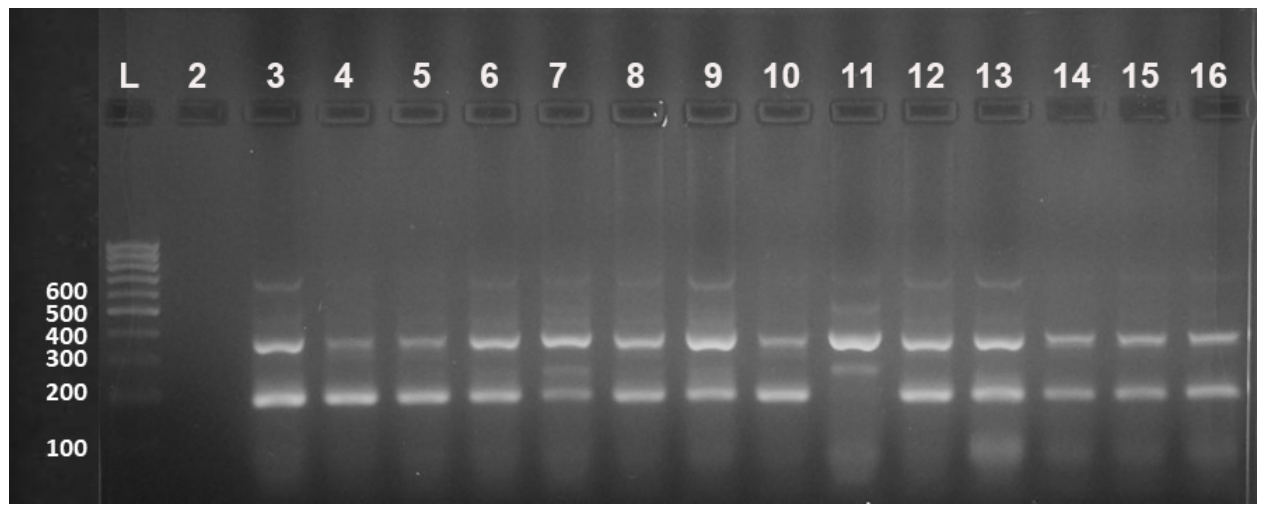


Figure 2. Agarose gel electrophoresis showing IL-20 1380 A/G rs2981573: Lane 1: Ladder of 100bp. Lane 2: Negative control. The 382bp is an internal positive control. Lane 7: Amplified both alleles A/G (181/255) bp, Lane 11: Amplified allele G 255bp. The remaining samples: Allele A target amplification (181bp).

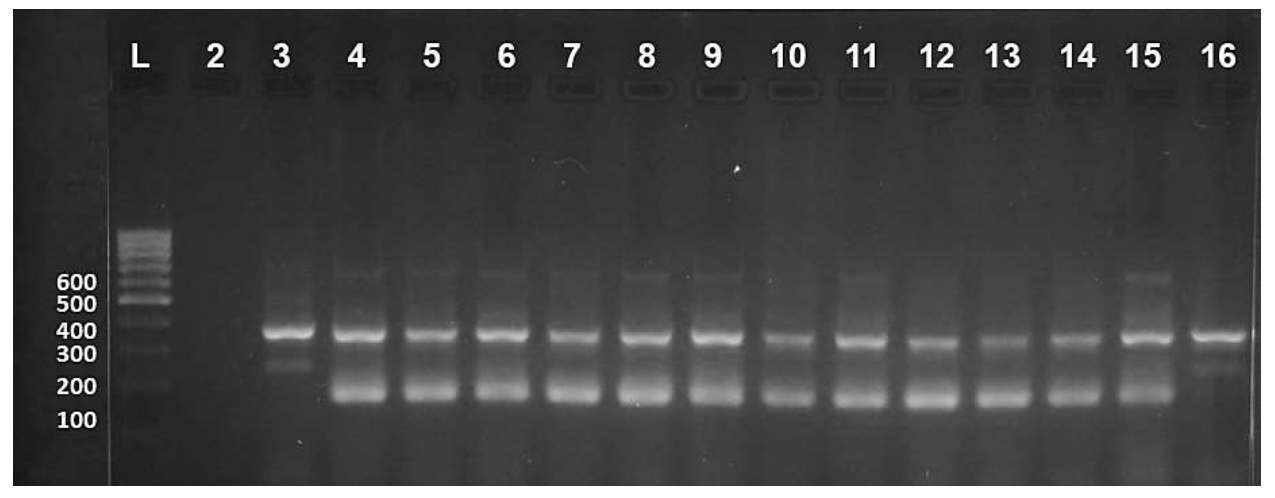


Figure 3. Agarose gel electrophoresed showing IL-20 1380 A/G rs2981573: Lane 1: Ladder of 100bp. Lane 2: Negative control. The 382bp is an internal positive control. Lanes 3 and 16 show the amplified allele G (255) bp. The remaining samples: Allele A target amplification (181bp).

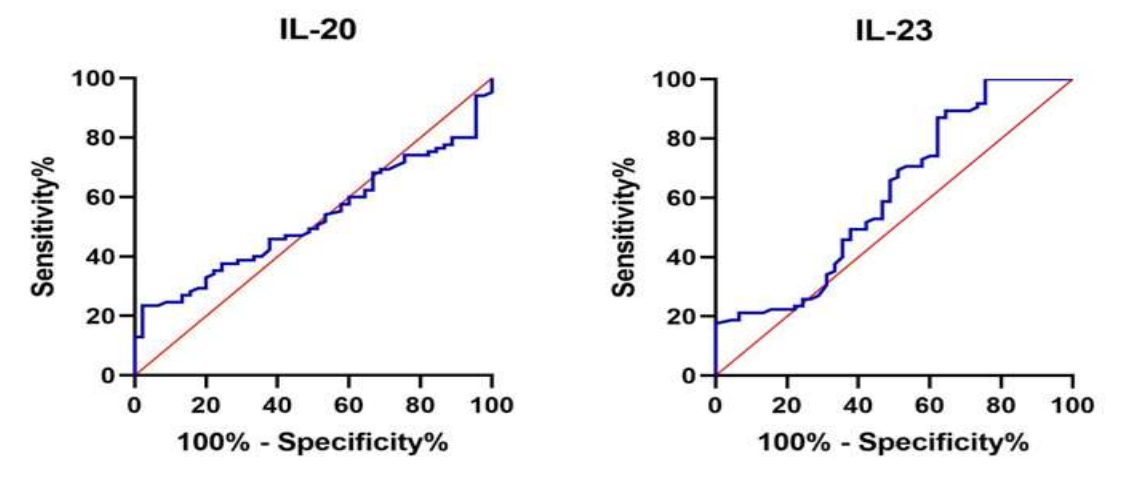


Figure 4. ROC curve of IL-20 and IL-23 levels.

Discussion

This study investigated the levels of IL-20 and IL-23 in rheumatoid arthritis participants, their association with clinical and laboratory assessments, and analyzed the genotypic distribution of the IL-20 rs2981573 polymorphism. Recent study aids identifying potential indications of disease activity and offers significant insights into the inflammatory profile of rheumatoid arthritis patients. The age, sex distribution, and Body Mass Index (BMI) of the RA and control groups were analogous, with no statistically significant differences detected. As anticipated, RA patients demonstrated

markedly elevated levels of C - C-reactive protein (CRP), Erythrocyte Sedimentation Rate (ESR), and neutrophil counts, in addition hemoglobin (Hb) levels relative to controls. These findings correspond with prior demonstrating that systemic inflammation and anemia are prevalent characteristics of rheumatoid arthritis resulting from persistent inflammation and bone marrow suppression (16). Serum IL-20 concentrations were not significantly higher in RA patients compared to healthy individuals, according to this study's results. This finding aligns with studies reporting that IL-20 was not increased in the serum of RA patients, suggesting a localized rather than systemic role in RA inflammation (5, 17). In contrast, IL-20 serum levels were found to be

considerably higher in RA patients compared to control groups in multiple investigations (18-20). Kragstrup et al. (19) specifically observed that IL-20 was elevated in early RA but normalized after six months of treatment. Despite these differences, IL-20's function in neutrophil chemotaxis, endothelial proliferation, and synovial fibroblast migration is still crucial to its role in the pathophysiology of RA (17). The present investigation found that serum IL-23 levels were considerably greater in RA patients compared to healthy individuals. observation aligns with previous research documenting increased IL-23 concentrations in individuals with RA compared to nonindividuals, affected highlighting significance as a key proinflammatory cytokine in disease pathogenesis (21, 22). The growth and proliferation of Th17 cells, which generate IL-17 and other inflammatory mediators that promote chronic inflammation, joint degradation, and the progression of illness, are greatly aided by the cytokine IL-23 (7). The observed elevation of IL-23 in this study reinforces its involvement in the dysregulated immune response characteristic of RA. It validates its prospective utility as an indicator for disease identification progression.

This study found a favorable relationship between serum IL-20 and IL-23 and disease activity indices such as the Disease Activity Score (DAS28), tender joint count (TJC), and swollen joint count (SJC). Therefore, it can be inferred that elevated levels of these cytokines are linked to more active disease in RA patients. Consistent with the current findings, Hussien et al. (20) identified a high association between blood IL-20 levels and DAS28, SJC, TJC, ESR, and CRP. Similarly, Šenolt et al. (5) demonstrated robust associations between IL-20 levels in the blood and TJC, SJC, CRP,

and DAS-28 in RA subjects, thus confirming IL-20's involvement in disease progression. In contrast, Kragstrup et al. (23) documented no significant correlation in IL-20 serum levels with disease activity. The findings of this study support previous research on IL-23, which has shown a strong association between serum IL-23 levels and disease activity. The fact that IL-23 promotes Th17 cell development and the generation of inflammatory cytokines lends credence to the concept that it is crucial in the pathophysiology of RA (21, 22). However, Zaky and El-Nahrery's investigation indicated an insignificant association between IL-23 and DAS28. (10). The disparities in findings between research may be attributed to variances in patient demographics, sample sizes, and other participant factors. The inverse relationship between concentration of IL-23 and hemoglobin levels demonstrated by this study suggests a possible contributory role for IL-23 in the development of anemia related with RA, which may in turn be facilitated by chronic inflammatory pathways that impair erythropoiesis. While Alsheikh et al. (22) did not documented association between hemoglobin and IL-23. This study also investigated the relationship between Neutrophilto-Lymphocyte Ratio (NLR), Platelet-to-Lymphocyte Ratio (PLR) and DAS28 in patients with RA. The analysis showed a statistically significant positive relationship between PLR and DAS-28 scores, indicating its potential as an accessible and cost-effective biomarker for evaluating disease activity in RA. NLR, on the other hand, showed no significant correlation. This is in line with the results from Du et al. (24), who also reported a significant relationship between PLR and disease activity score 28 (DAS28), while the association between NLR and DAS28 was not Similarly, Gökmen et significant. al. discovered that NLR was not associated with DAS-28. In contrast, several other studies reported that both NLR & PLR correlated with DAS-28 (16, 26). Taken together, these findings suggest that PLR is

likely a reliable and informative biomarker in the context of RA. In contrast, the utility of NLR may be more heterogeneous, related to the specific patient cohort, disease duration, and type of treatment (in particular immunotherapy). Meng et al. (26) documented that NLR and PLR were considerably lowered in RA patients after therapy. The use of NLR as an indicator of disease activity may be limited due to methotrexate-induced neutropenia and thrombocytopenia in their patient population (27).

According to the literature review, this is the first study investigating the IL-20 rs2981573 polymorphism in rheumatoid arthritis, which will provide further insights into the potential involvement of IL-20 in the disease's susceptibility. Another way of looking at this is that there were no differences in genotypic distribution. Similarly, the A allele was the most prevalent in both groups, and no statistically significant differences were observed in allele frequency analysis between the control group and RA patients. Although in this study population, there was no relationship established between this genetic variant and RA susceptibility, IL-20 is known to contribute to synovial inflammation, immune cell recruitment, and joint damage (4). This suggests that genetic variations in IL-20 may still influence RA pathogenesis. Since this is the first study examining rs2981573 in RA, direct comparisons with previous research are not available. This emphasizes the novelty of these findings and the need for further investigations in broader and more varied communities to elucidate the potential role of IL20 polymorphisms in RA. In the present study, the ROC curve analysis demonstrated that IL-23 levels above 49.27 pg/ml could distinguish RA patients from controls. Although the AUC value for IL-23 was statistically significant, its diagnostic

accuracy (AUC = 0.613) was relatively weak, indicating limited clinical usefulness when used alone as a diagnostic marker, its combination with other inflammatory markers could enhance diagnostic accuracy. A post hoc power analysis indicated that the study may have been underpowered to detect small differences in IL-20 levels due to the sample size, which could explain the non-significant findings for this cytokine. Future studies with larger and more balanced sample sizes are recommended to validate these results.

Conclusion

This study demonstrated that serum IL-23 levels were significantly elevated in RA patients compared to healthy controls, and ROC analysis revealed a modest diagnostic utility for IL-23. While no significant difference was found in IL-20 levels between the groups, correlation analysis revealed positive associations between both IL-20 and IL-23 with DAS-28, tender joint count, and swollen joint count. Notably, IL-23 levels showed an inverse correlation with hemoglobin levels. These findings suggest that IL-23 may play a role in the pathogenesis of RA and could be a useful marker of disease activity. Regarding the IL-20 gene polymorphism, no statistically significant differences in genotype and allele distribution were observed between RA patients and healthy controls, suggesting that this polymorphism is not associated with increased susceptibility to RA. Further research is recommended to examine IL-20 and IL-23 concentrations in the synovial fluid, as well as to evaluate other relevant cytokines. Additional research with larger sample sizes and more thorough analyses is needed to clarify the roles of IL-20 and IL-23 in rheumatoid arthritis.

Source of funding: No source of funding.

Ethical clearance: The study protocol was authorized by the Medical Ethics Committee of Erbil Polytechnic University (permit No.: 24/0044 HRE).

Conflict of interest: None.

Use of Artificial Intelligence: The authors declare that they did not use generative artificial intelligence the for creation or preparing of this manuscript.

Acknowledgments: The authors are grateful for the rheumatology department staff at both Rizgary Teaching Hospital and Hawler Teaching Hospital for their support and assistance throughout this research project.

References

- 1. Gravallese EM, Firestein GS. Rheumatoid arthritis—common origins, divergent mechanisms. New England Journal of Medicine. 2023 Feb 9;388(6):529-42. https://doi.org/10.1056/nejmra2103726
- 2. Kondo N, Kuroda T, Kobayashi D. Cytokine networks in the pathogenesis of rheumatoid arthritis. International journal of molecular sciences. 2021 Oct 10;22(20):10922.

https://doi.org/10.3390/ijms222010922

3. Ni S, Shan F, Geng J. Interleukin-10 family members: Biology and role in the bone and joint diseases. International immunopharmacology. 2022 Jul 1;108:108881.

https://doi.org/10.1016/j.intimp.2022.108881

- 4. Kragstrup TW, Andersen T, Heftdal LD, Hvid M, Gerwien J, Sivakumar P, Taylor PC, Senolt L, Deleuran B. The IL-20 cytokine family in rheumatoid arthritis and spondyloarthritis. Frontiers in immunology. 2018 Sep 25;9:2226. https://doi.org/10.3389/fimmu.2018.02226
- 5. Šenolt L, Prajzlerová K, Hulejová H, Šumová B, Filková M, Veigl D, Pavelka K, Vencovský J. Interleukin-20 is triggered by TLR ligands and associates with disease activity in patients with rheumatoid arthritis. Cytokine. 2017 Sep 1;97:187-92. https://doi.org/10.1016/j.cyto.2017.06.009
- 6. Yago T, Nanke Y, Kawamoto M, Kobashigawa T, Yamanaka H, Kotake S. IL-

- 23 and Th17 disease in inflammatory arthritis. Journal of clinical medicine. 2017 Aug 29;6(9):81. https://doi.org/10.3390/jcm6090081.
- 7. Schinocca C, Rizzo C, Fasano S, Grasso G, La Barbera L, Ciccia F, Guggino G. Role of the IL-23/IL-17 pathway in rheumatic diseases: an overview. Frontiers in immunology. 2021 Feb 22;12:637829.

https://doi.org/10.3389/fimmu.2021.637829.

8. McHugh J. IL-23 promotes arthritic and inflammatory pain. Nature Reviews Rheumatology. 2020Aug;16(8):409-.

https://doi.org/10.1038/s41584-020-0460-y.

- 9. Lindstrom TM, Robinson WH. Biomarkers for rheumatoid arthritis: making it personal. Scandinavian Journal of Clinical and Laboratory Investigation. 2010 Jan 1;70(sup242):79-84. https://doi.org/10.3109/00365513.2010.493406
- 10. Zaky DS, El-Nahrery EM. Role of interleukin-23 as a biomarker in rheumatoid arthritis patients and its correlation with disease activity. International immunopharmacology. 2016 Feb 1;31:105-8.

https://doi.org/10.1016/j.intimp.2015.12.011.

11. Galimova E, Rätsep R, Traks T, Kingo K, Escott-Price V, Kõks S. Interleukin-10 family cytokines pathway: genetic variants and psoriasis. British Journal of Dermatology. 2017 Jun 1;176(6):1577-87.

https://doi.org/10.1111/bjd.15363

- 12. Trifunović J, Miller L, Debeljak Ž, Horvat V. Pathologic patterns of interleukin 10 expression—a review. Biochemia medica. 2015 Feb 15;25(1):36-48. https://doi.org/10.11613/bm.2015.004.
- 13. Liu Q, Yang J, He H, Yu Y, Lyu J. Associations between interleukin-10 polymorphisms and susceptibility to rheumatoid arthritis: a meta-analysis and meta-regression. Clinical rheumatology. 2018 Dec;37(12):3229-37. https://doi.org/10.1007/s10067-018-4329-2
- 14. Aletaha D, Neogi T, Silman AJ, Funovits J, Felson DT, Bingham III CO, Birnbaum NS, Burmester GR, Bykerk VP, Cohen MD, Combe B.

2010 rheumatoid arthritis classification criteria: an American College of Rheumatology/European League Against Rheumatism collaborative initiative. Arthritis & rheumatism. 2010 Sep;62(9):2569-81. https://doi.org/10.1002/art.27584

15. Kingo K, Koks S, Nikopensius T, Silm H, Vasar E. Polymorphisms in the interleukin-20 gene: relationships to plaque-type psoriasis. Genes & Immunity. 2004 Mar;5(2):117-21. https://doi.org/10.1038/sj.gene.6364046

16. Uslu AU, Küçük A, Şahin A, Ugan Y, Yılmaz R, Güngör T, Bağcacı S, Küçükşen S. Two new inflammatory markers associated with Disease Activity Score-28 in patients with rheumatoid arthritis: neutrophillymphocyte ratio and platelet-lymphocyte ratio. International journal of rheumatic diseases. 2015 Sep;18(7):731-5. https://doi.org/10.1111/1756-185X.12582

17. Hsu YH, Li HH, Hsieh MY, Liu MF, Huang KY, Chin LS, Chen PC, Cheng HH, Chang MS. Function of interleukin-20 as a proinflammatory molecule in rheumatoid and arthritis. experimental Arthritis & Rheumatism. 2006 Sep;54(9):2722-33. https://doi.org/10.1002/art.22039

18. Scrivo R, Conigliaro P, Riccieri V, Di Franco M, Alessandri C, Spadaro A, Perricone R, Valesini G. Distribution of interleukin-10 family cytokines in serum and synovial fluid of patients with inflammatory arthritis reveals different contribution to systemic and joint inflammation. Clinical & Experimental Immunology. 2015 Feb;179(2):300-8. https://doi.org/10.1111/cei.12449

19. Kragstrup TW, Greisen SR, Nielsen MA, Rhodes C, Stengaard-Pedersen K, Hetland ML, Hørslev-Petersen K, Junker Østergaard M, Hvid M, Vorup-Jensen T. The interleukin-20 receptor axis in early rheumatoid arthritis: novel links between disease-associated autoantibodies and radiographic progression. Arthritis research

& 2016 therapy. Mar 11;18(1):61. https://doi.org/10.1186/s13075-016-0964-7

20. Hussien DT, Shabana AA, Hassan AS, Elmarghany EB. Assessment of serum interleukin-20 level in rheumatoid arthritis patients: Relation to disease activity and ultrasound measures. The Egyptian Rheumatologist. 2022 Apr 1;44(2):181-6. https://doi.org/10.1016/j.ejr.2022.01.002

21. Alsheikh MM, El-Shafey AM, Gawish HH, El-Desoky ET. Serum interleukin-23 level in rheumatoid arthritis patients: Relation to disease activity severity. and The Egyptian Rheumatologist. 2019 Apr 1;41(2):99-103. https://doi.org/10.1016/j.ejr.2018.07.001

22. Alsheikh MM, El-Shafey AM, Gawish HH, El-Desoky ET. Serum interleukin-23 level in rheumatoid arthritis patients: Relation to disease activity severity. Egyptian and The 1;41(2):99-103. Rheumatologist. 2019 Apr https://doi.org/10.1016/j.ejr.2018.07.001

23. Kragstrup TW. The IL-20 receptor axis in immune-mediated inflammatory arthritis: novel links between innate immune recognition and bone homeostasis. Scandinavian Journal Rheumatology. 2016 Aug 1;45(sup128):53-7. https://doi.org/10.1080/03009742.2016.1203022

24. Du J, Chen S, Shi J, Zhu X, Ying H, Zhang Y, Chen S, Shen B, Li J. The association between the lymphocyte-monocyte ratio and disease activity in rheumatoid arthritis. Clinical rheumatology. 2017 Dec;36(12):2689-95.

https://doi.org/10.1007/s10067-017-3815-2

25. Gökmen F, Akbal A, Resorlu H, Binnetoğlu E, Cevizci S, Gökmen E, Köse MM, Türkyılmaz AK, Akbal E. Mean platelet volume and neutrophil lymphocyte ratio as related to inflammation markers and anti-CCP in rheumatoid arthritis. Aktuelle Rheumatologie. 2016 Dec;41(06):488-91. http://dx.doi.org/10.1055/s-0034-1374605

26. Meng Y, Cai XL, Cong S, Sun J, Hu YW, Gu YQ, Ma XM, Luo L. Role of platelet/lymphocyte, neutrophil/lymphocyte, and interleukin-37/Interleukin-17 ratios in the occurrence and treatment of rheumatoid arthritis. Immunological Investigations. 2024 Apr 2;53(3):464-74. https://doi.org/10.1080/08820139.2023.2299687

27. Hosseini E, Shahbazi F. Methotrexate-induced Severe Pancytopenia in a Patient with Rheumatoid Arthritis: A Case Report and Review of Literature. Current Drug Safety. 2024 May 1;19(2):224-35. https://doi.org/10.2174/1574886318666230516115737

في مصل مرضى التهاب المفاصل الروماتويدي 23-IL و10 وتركيز 20-IL تعدد أشكال جين

ا إيمان نجاة علي ، ا نجاة جبار أحمد برواري

الملخص

الخلفية: : التهاب المفاصل الروماتويدي (RA) هو حالة مناعية ذاتية تتميز بتعقيد في المسببات والتهاب مزمن في المفاصل. ومؤخرًا، ظهرت توجهات جديدة تهدف إلى تحديد مؤشرات حيوية تنبؤية غير جراحية يمكن أن تساعد في مراقبة المرض.

الأهداف: التحقيق في مستويات L-20 وL-23 في الدم لدى مرضى RA مقارنة بالأشخاص الأصحاء، وتقييم ارتباطها بنشاط المرض. بالإضافة إلى ذلك، دراسة العلاقة بين تعدد الأشكال الجيني لـ L-20 وقابلية الإصابة بـ RA.

المواد والطرق: شملت الدراسة ٨٥ مريضًا يعانون من RA و ٤٥ شخصًا سليمًا. تم قياس تراكيز 20-LL و 23-IL باستخدام تقنية ELISA، وتم تقييم نشاط المرض باستخدام مقياس DAS-28. كن المرض باستخدام تقنية ARMS-PCR.

النتائج: أظهرت الدراسة أن المشاركين المصابين بـ RA لديهم ارتفاع ملحوظ في مستويات IL-23 في الدم مقارنةً بالأصحاء (القيمة الاحتمالية IL-23 و IL-20 في حين لم تكن مستويات 20-LL و IL-23 و (p=0.6354). كما وُجد ارتباط معنوي بين كل من p=0.0031 و p=0.0021 مختلفة بشكل معنوي التوالي). أما بالنسبة لتعدد الأشكال الجيني لجين p=0.0021، فلم يكن هناك ارتباط معنوي بين تعدد الأشكال p=0.0021 و p=0.0031 و p=0.0

الاستنتاج: على الرغم من أن تعدد الأشكال الجيني لـ 12-LL قد لا يكون عاملًا مسببًا للإصابة بـ RA، فإن كل من 20-LL و 23-LL قد يكونان مؤشر بن مهمين لنشاط المرض.

الكلمات المفتاحية: تعدد الأشكال الجيني لـ DAS-28 ، IL-20 ، النهاب المفاصل الروماتويدي، LL-23 ، IL-23 ، IL-29 ، التهاب المفاصل الروماتويدي، DAS-28 ، المفاصل الروماتويدي، الكلمات المفتاحية المفاصل الروماتويدي، المفاصل الروماتويدي، المفاصل الروماتويدي، الله على المفاصل الروماتويدي، الله على المفاصل الروماتويدي، الله على المفاصل الروماتويدي، الله على المفاصل الروماتويدي، الله على المفاصل الروماتويدي، الله على المفاصل الروماتويدي، الله على المفاصل الروماتويدي، الله على الل

المؤلف المراسل: إيمان نجاة علي

iman.ali@epu.edu.iq الايميل:

تاريخ الاستلام: ٥ أيار ٢٠٢٥

تاریخ القبول: ۱۸ أب

تاريخ النشر: ٢٠ تشرين الأول ٢٠٢٥

اقسم تكنولوجيا المختبرات الطبية، كلية أربيل الصحية والتقنية الطبية، جامعة أربيل التقنية، أربيل، العراق.

Prevalence of Oral Aphthous Stomatitis and Recurrent Herpes Labialis Among Dental Students

Hayder Mahdi Idan (b), Ghasaq Abdullah Mahmood (b), Ibtehal Qhtan Othman (b)

OPEN ACCESS

Correspondence: Hayder Mahdi Idan
Email: haider.m@uodiyala.edu.iq
Copyright: ©Authors, 2025, College of
Medicine, University of Diyala. This is an open
access article under the CC BY 4.0 license
(http://creativecommons.org/licenses/by/4.0/)
Website:

https://djm.uodiyala.edu.iq/index.php/djm

Received: 09 November 2024 Accepted: 28 February 2025 Published: 25 October 2025

Abstract

Background: The most frequent oral mucosal lesion is recurrent aphthous stomatitis. It first appears in childhood or adolescence and is evident as many tiny, recurrent, or ovoid ulcers with yellow floors and erythematous haloes. A widespread viral infection, herpes labialis, is characterized by recurrent vesicular lesions, frequently on the lips and perioral tissue.

Objectives: To find the prevalence of oral aphthous stomatitis and recurrent herpes labialis among dental students of Bilad Alrafidain University.

Patients and Methods: A cross-sectional study was conducted among 187 dental students of Bilad Alrafidain University, who are in the fourth and fifth stages of the dental department. The data were collected using questionnaires. Questionnaires required two sections. The first section restricted personal information. The second section involved questions related to aphthous ulcers and recurrent herpes labialis, including the duration and site of the ulcer after examination.

Results: In the present study, the number of students with aphthous ulcers in the fourth stage is 13 (14.1%), and in the fifth stage, 24 (25.3%), with a highly statistically significant difference. Out of 187 students, 10 (10.9%) had recurrent herpes labialis in the fourth stage, while 15 (15.8%) were in the fifth stage, indicating a highly significant statistical relationship. The number of students with recurrent aphthous stomatitis and recurrent herpes labialis in the fifth stage is 24 (25.3%) and 15 (15.8%), respectively, which is higher than in the fourth stage, where the numbers are 13 (14.1%) and 10 (10.9%), respectively, indicating a significant relationship.

Conclusion: Recurrent aphthous stomatitis is a lesion with a higher prevalence in females than in males. Stress during the period of academic examinations is one of the reasons for recurrent eruption of aphthous stomatitis and reactivation of recurrent herpes labialis.

Keywords: Aphthous stomatitis, Herpes labialis, Dental, Students, and Oral.

Introduction

The Greek word "aphtha," which means ulcer, is where the word "aphthous" was created. Recurrent aphthous stomatitis (RAS), also identified as aphthous ulcers, is a benign ulcerated lesions that usually develop on the mouth. The cause of these lesions is unknown, and treatment options are still controversial (1,2).

The oral mucosa is usually affected by inflammatory diseases such as aphthous ulcers or recurrent aphthous stomatitis. Aphthous ulcers are the most prevalent, affecting up to 25% of people worldwide,

¹ Department of Clinical Dental Sciences, College of Dentistry, University of Diyala, Diyala, Iraq.

² College of Dentistry, University of Bilad Alrafidain, Diyala, Iraq.

³ Diyala Health Directorate, Diyala, Iraq.

with an estimated 4% frequency of oral ulcers (3). Hippocrates initially used the term "aphthae" to describe mouth disorders, and canker sores are another name for ulcers, or aphthae (4,5).

RAS was divided into three classes: herpetiform, minor, and major ulcers. Minor or mild aphthous ulcers account for 80% of RAS. These are minute ulcers, 1 to 5 in number, measuring 8 to 10 mm in diameter, that affect the nonkeratinized oral mucosa and heal in 10 to 14 days without leaving any scars. Large aphthous ulcers (10–15% of RAS cases) can affect the keratinized oral mucosa, including the hard palate, and are bigger than minor ones (>1 cm). They frequently leave a scar and might take up to 6 weeks to heal. There are clusters of 1-3 mm-diameter tiny ulcers that number more than 10 and may number up to 100 in herpetiform ulceration (3).

Both environmental and genetic variables are associated with the development of RAS. Stress, chemical or physical trauma, illness, allergy, a genetic susceptibility, or nutritional inadequacies are some of the triggering reasons (6, 7).

In general, symptoms may comprise prodromal sensations like burning, itching, or stinging that may happen hours before any lesion manifests itself, and pain that is frequently exaggerated and associated with the degree of ulceration and is made worse by physical contact, especially with firm foods and beverages (e.g., if they are abrasive or acidic). The first few days after the ulcer forms are the most painful, but as the ulcer heals, the pain diminishes (8). Speaking and chewing may be uncomfortable if the tongue is affected, and swallowing may be painful if the soft palate, throat, or esophagus is affected by an ulcer (8).

Stress impacts the immune system, which could help explain why some conditions are directly related to stress. It is frequently said that in training sessions for students with the illness, ulceration worsens during exam times and improves during rest times (9,10). As an

alternative, it has been proposed that during stressful times, oral parafunctional behaviors such as chewing on the lips or cheeks become more evident, which may trigger the mucosa to experience less severe damage (11). The primary type of herpetic stomatitis has systemic involvement, such as fever, and can be confused with RAS and recurrent in its intraoral form. On the oral mucosa, the vesicle phase can be detected. When it establishes as an ulcer, it's more diffuse and erythematous in many places, especially on keratinized mucosa, which is uncommon in RAS (2,6).

Herpes (genital or oral) and fulminant human encephalitis are illnesses brought on by the herpes simplex viruses 1 and 2 (HSV-1, HSV-2). These DNA-based viruses are members of the Herpesviridae family (12).

Recurrent herpes labialis (RHL) is a herpes simplex virus infection that often affects the lip (13). A burning ache as symptoms frequently follow little blisters or sores (13). Fever, sore throat, and swollen lymph nodes may also exist during the initial episode (13,14). The virus remains dormant in the trigeminal ganglion, even though the rash typically disappears after 10 days (13). Periodically, the virus can reactivate and cause another occurrence of sores on the lips or mouth (13). Between 15 and 40 percent of those who contract the HSV-1 infection, and 98% of the world's population, may go on to get RHL (15).

The present study aimed to determine the prevalence of oral aphthous stomatitis and recurrent herpes labialis among dental students following academic exams at Bilad Alrafidain University in Diyala, Iraq.

Patients and Methods

Study design: A cross-sectional study was conducted among 187 dental students of Bilad Alrafidain University, who are in the fourth and fifth stages of the dental department. After receiving ethical clearance, a well-versed

recurrent herpes labialis 2(8%) were males, and 8(32%) were females, as shown in Table 2.

The second group (fifth stage), students with recurrent aphthous ulcers, consisted of 3 males (8%) and 21 females (56.8%). In contrast, five males (20%) and 10 females (40%) had recurrent herpes labialis, as shown in Table 2.

Distribution of aphthous ulcer and recurrent herpes labialis according to academic stage: The number of students with aphthous ulcers in the fourth stage is 13 (14.1%), and in the fifth stage is 24 (25.3%), with a highly statistically significant level as shown in Table 3.

consent was obtained from the participants. Questionnaires required two sections. The first section restricted personal information. The second section is associated with aphthous ulcers and recurrent herpes labialis, such as duration (0-5 days) and site of ulcer after academic exams. In addition, photos of the students' aphthous ulcers were taken to determine the distribution of infection across different sites in the mouth.

Inclusion criteria: The students included in this study were divided into two groups as follows: 1-Group 1 (fourth stage): Ninety-two students (33 male and 59 female). 2-Group 2 (fifth stage): Ninety-five students (34 male and 61 female).

Exclusion criteria: Students taking medication that causes immunosuppression, such as steroids, or those with systemic diseases, were excluded from the study. Data were collected using questionnaires.

Statistical Analysis

The program employed to distinguish the outcome of alteration factors in study variances is the Statistical Analysis System (SAS 2018). A chi-square test was run to determine whether there is a significant difference between expected frequencies and observed frequencies in one or more classes.

Results

Distribution of the studied groups according to gender: The total number of participants in the research was 187 students; 67 (35.8%) were males, and 120 (64.2%) were females. Regarding the first group (fourth stage), which consisted of 92 students (49.2%), 33 were males (17.6%) and 59 were females (31.6%), as shown in Table 1. The second group (fifth stage) included 95(50.8%) students, 34(18.2%) were males, and 61(32.6%) were females, as shown in Table 1. Regarding the first group (fourth stage), students with a recurrent aphthous ulcer, 4 (10.8%) were males and 9 (24.3%) were females. In contrast,

Table 1. Distribution of the studied groups according to gender.

	N	Male		Female		T	otal					
Stage	No.	%	No.	%	P-value	No.	%					
Forth	33	17.6	59	31.6	0.0067 **	92	49.2					
Fifth	34	18.2	61	32.6	0.0056 **	95	50.8					
Total	67	35.8	120	64.2	0.0001 **	187	100					
P-value	0.90	02 NS	0.855	NS		0.82	26 NS					
		:	** (P≤0.01), NS	** (P≤0.01), NS: Non-Significant.								

Table 2. Distribution of aphthous ulcer and recurrent herpes parameters among the studied groups.

Aphthous ulcer							Recui	rrent	herpes			
Stage	Male	%	Female	%	Total	%	Male	%	Female	%	Total	%
Forth	4	10.8	9	24.3	13	35.1	2	8	8	32	10	40
Fifth	3	8	21	56.8	24	64.9	5	20	10	40	15	60
Total	7	19	30	81	37	100	7	28	18	72	25	100
P-value	P-value 0.0001 ** 0.0			0.000	0.0004 ** 0.0004 ** 0.0074 **				.0074 **			
	** (P≤0.01).											

Table 3. Distribution of the observed frequencies in the two categories, none and present, of aphthous ulcer in different samples.

Store	Count & noncontages	Aphth	ous ulcer	Total	P-value	
Stage	Count & percentages	None	Present	Totai	P-value	
Eouth	Count	79	13	92	0.0001 **	
Forth	% within group	85.9%	14.1%	100.0%	0.0001 **	
Fifth	Count	71	24	95	0.0001 **	
FIIII	% within group	74.7%	25.3%	100.0%	0.0001 **	
Total	Count	150	37	187	0.0001 **	
Total	% within group	80.2%	19.8%	100.0%	0.0001 **	
	**	(P≤0.01)				

Out of 187 students, 10 (10.9%) had recurrent herpes labialis in the fourth stage, and 15 (15.8%) in the fifth stage, with a statistically highly significant relationship as shown in Table 4. The number of students with RAS and RHL in

the fifth stage is 24 (25.3%), 15(15.8%), respectively, more than in the fourth stage, 13(14.1%), 10(10.9%), respectively, with a significant relationship as shown in tables (3,4,5).

Table 4. The distribution of the observed frequency in two categories, none and present, of recurrent herpes labialis in different samples.

Store		Recurr	ent herpes	Total			
Stage		None	Present	Total			
Fourth	Count	82	10	92	0.0001 **		
rourth	% within group	89.1%	10.9%	100.0%	0.0001 **		
Fifth	Count	80	15	95	0.0001 **		
riitii	% within group	84.2%	15.8%	100.0%	0.0001 **		
Total	Count	162	25	187	0.0001 **		
Total	% within group	86.6%	13.4%	100.0%	0.0001		
** (P≤0.01)							

Distribution of aphthous ulcers according to the infection site: The lower lip was the most frequently affected anatomical region,

with 15 students, followed by the cheek, with nine students, and then the upper lip, with five students, as shown in Table 5.

picture shows a male from the fifth stage of the Dentistry College, age 23 years old, with recurrent herpes labialis on the left side of his lower lip, as shown in Figure 1.

The pictures show recurrent aphthous

stomatitis in the lower lip (A) of a 22-year-old female from the fourth stage of Dentistry College, and (B) of a 23-year-old male from the fifth stage of Dentistry College, as shown in Figure 2.

Table 5. Distribution of aphthous ulcers according to infection site and gender.

		Distribution by infection site									
	Aphtho	us ulcer		Aphtho	us ulcer						
	Fourtl	h stage		Fifth	stage						
Parameters	Male	Female	Total	Male	Female	Total	Total				
	No.	No.		No.	No.						
Lower lip	2	4	6	1	8	9	15				
Cheek	0	2	2	1	6	7	9				
Tongue	1	1	2	0	1	1	3				
Floor of the mouth	0	1	1	0	0	0	1				
Upper lip	0	1	1	0	4	4	5				
Palate	1	0	1	1	2	3	4				
Total	4	9	13	3	21	24	37				
P-value	0.04	19 *	0.0271*	0.003	52 **	0.0038**	0.0007**				
		*	(P≤0.05), *:	* (P≤0.01)	•						



Figure 1. A male with recurrent herpes labialis at the age of 23 years from the fifth stage of the Dentistry College.



Figure 2. Recurrent aphthous stomatitis in the lower lip: (A) Female of age 22 years old from the fourth stage of Dentistry College, (B) Male of age 23 years old from the fifth stage of Dentistry College.

Discussion

The oral mucosa is frequently affected by recurrent aphthous stomatitis, primarily affecting non-keratinized tissues. It typically initiates in childhood, is symptomatic, recurrent, and presents clinically as ulcers, which may seem like a single or many lesions (1,13). It is a widespread illness that affects 20% of the general population and 9% of children, according to estimates (16).

Communal illness is herpes labialis (cold sore, fever blister). It's a rash that marks lips and other mucous membranes, and it's notable by blisters and erythema that are associated with a burning sensation (17). It is triggered by the reactivation of latent infection of virus-1 of herpes simplex (HSV-1) (15).

In the present study, it is interesting to find that 150 individuals do not have recurrent aphthous stomatitis, and 162 individuals do not have recurrent herpes labialis. This could be explained by the fact that stress does not always affect the oral cavity.

Although the exact reason for RAS is still unidentified, Sawair (17) noted in 2010 that the disorder can be made more likely to recur by stress, dietary sensitivity, physical or chemical harm, and genetic susceptibility (2,17,18).

The present study showed that the prevalence of RAS is 14.1% in the fourth stage and 25.3% in the fifth stage, with a highly statistically significant association recognized. This may be explained by the fact that stress has diverse adverse effects on health, many of which are facilitated by its action on the immune system. According to research, stress can trigger type 1- type 2 cytokine-mediated or proinflammatory immune responses, making it hard to control innate and adaptive immune responses (18). This study supports the idea that stress and anxiety play a role in the

development of RAS in educated patients, particularly during the examination.

Our study agrees with the studies of Gallo et al. (7) and Sharma et al. (19), which showed the relation between RAS and stress. Al-Omiri et al. (20) researched 50 RAS patients' psychological profiles and found that either stressful circumstances or anxiety can encourage recurring sessions of this illness. According to the scientists, while under stress, salivary cortisol concentration increases, stimulating the immune system to attract leukocytes to sites of inflammation and playing a crucial part in the condition's pathophysiology (17,20).

Our study agrees with the studies of another researcher, who describes RAS as a lesion with high prevalence in females (21,22). Whereas we disagree with other studies that don't approve of the theory of the presence of an association between this condition and gender, such as Leonardo et al. (23) and Chattopadhyay and Shetty (24), who confirmed a lack of a relationship between RAS and gender. This high prevalence in females is indicated by women seeking additional medical attention.

The prevalence of RHL and RAS was higher in women than in men, which correlated with the fact that women experience more hormonal changes.

George and Joseph (3) supposed that the duration of an aphthous ulcer (0–2 days) was 17%, (3-5 days) was 38.7%, and that stress and examinations were responsible for 41.1% and 22.6% of cases, respectively. These results are similar to the results of the present study, which reported that the prevalence of aphthous ulcer in duration (0-5 days) is 19.8% in both stages related to examination.

Areas like the buccal and labial mucosa, the floor of the mouth, the ventral surface of the tongue, and the soft palate are often affected by recurrent aphthous ulcers (25). In the present study, the lower lip was the most commonly affected anatomical region, with 15 students, followed by the cheek with nine students, then the upper lip with five students.

The present study exhibited that the prevalence of

RAS and RHL in the fifth stage is (25.3% 15.8% respectively) more than in the fourth stage (14.1% 10.9% respectively), with a significant relationship. This may be explained by the fact that students in the fifth stage are more anxious because they are in the final stage and about to graduate from college. Our study agrees with the study of Faulkner and Smith (25). They noted that recurrent HSV-1 reactivation was connected to higher levels of psychological stress. This could be clarified by the fact that stress elevates cortisol levels, which depress the immune system and contribute to the reactivation of viral latency (26).

Regarding RHL, the present study showed that the prevalence of RHL is 10.9% in the fourth stage and 15.8% in the fifth stage, with a highly statistically significant connection identified. This may be clarified by the fact that individuals who commonly experience HSV-1 reactivation are more susceptible to the adverse effects of stress on the immune system. The central nervous system, endocrine system, and immune system are just a few examples of the body's mechanisms that can be altered by stress, defined as a force that creates a somatic reaction outside of normal bodily processes (27,28).

Conclusion

Recurrent aphthous stomatitis is a lesion with a higher prevalence in females than in males. Stress during the period of academic examinations is one of the reasons for recurrent eruption of aphthous stomatitis and reactivation of recurrent herpes labialis. It was recommended to conduct a new study involving a large number of Iraqi students during the academic examination period and to study immune dysregulation during the stress period.

Source of funding: No source of funding.

Ethical clearance: This study received approval from the Scientific and Ethical Committee of the College of Medicine at the University of Diyala, in collaboration with Bilad Alrafidain University. The approval code is 2024HMI868.

Conflict of interest: None.

Use of Artificial Intelligence (AI): The authors declare that they were not using generative artificial intelligence for the preparation, creation, or language editing of this manuscript.

Acknowledgments: Many thanks to everyone who contributed and cooperated in completing this research, as well as to all dental students of Bilad Alrafidain University in Diyala city, Iraq.

References

1. Alves PM, Ramalho LD, Oliveira RS, Cavalcanti AL, Queiroz LM. Fatores de risco da ulceração aftosa recorrente—uma revisão dos achados atuais.

https://repositorio.ufba.br/handle/ri/20521

2. Hamedi S, Sadeghpour O, Shamsardekani MR, Amin G, Hajighasemali D, Feyzabadi Z. The most common herbs to cure the most common oral disease: stomatitis recurrent aphthous ulcer (RAU). Iranian Red Crescent Medical Journal. 2016 Feb 13;18(2):e21694.

https://doi.org/10.5812/ircmj.21694

- 3. George S, Joseph BB. A study on aphthous ulcer and its association with stress among medical students of an Indian medical institution. International Journal of Contemporary Medical Research. 2016 Jun;3(6):1692-5.
- 4. Jurge S, Kuffer R, Scully C, Porter SR. Number VI recurrent aphthous stomatitis. Oral diseases. 2006Jan;12(1):1-21.

https://doi.org/10.1111/j.1601-0825.2005.01143.x

- 5. Chavan M, Jain H, Diwan N, Khedkar S, Shete A, Durkar S. Recurrent aphthous stomatitis: a review. Journal of oral pathology & medicine. 2012 Sep;41(8):577-83. https://doi.org/10.1111/j.1600-0714.2012.01134.x
- 6. Natah SS, Konttinen YT, Enattah NS, Ashammakhi N, Sharkey KA, Häyrinen-

Immonen R. Recurrent aphthous ulcers today: a review of the growing knowledge. International journal of oral and maxillofacial surgery. 2004 Apr 1;33(3):221-34. https://doi.org/10.1006/ijom.2002.0446

- 7. Gallo CD, Mimura MA, Sugaya NN. Psychological stress and recurrent aphthous stomatitis. Clinics. 2009;64:645-8. https://doi.org/10.1590/S1807-59322009000700007
- 8. Bruch JM, Treister NS. Clinical oral medicine and pathology. New York: Humana Press; 2010. https://doi.org/10.1007/978-3-319-29767-5
- 9. Neville BW, Damm DD, Allen CM, Chi AC. Oral and maxillofacial pathology. Elsevier Health Sciences; 2015 May 13.
- 10. Scully C. Oral and maxillofacial medicine: the basis of diagnosis and treatment. Elsevier Health Sciences; 2013 Jan 15.
- 11. Preeti L, Magesh KT, Rajkumar K, Karthik R. Recurrent aphthous stomatitis. Journal of oral and maxillofacial pathology. 2011 Sep 1;15(3):252-6. https://doi.org/10.4103/0973-029X.86669
- 12. Лупу ДВ, Давиденко OM. АКТУАЛЬНІСТЬ ПРОБЛЕМАТИКИ ГЕРПЕСВІРУСНИХ ІНФЕКЦІЙ 6-ГО ТА 7-ГО ТИПІВ З РІЗНИМИ КЛІНІЧНИМИ ФОРМАМИ (ОГЛЯД ЛІТЕРАТУРИ). Іп the 2 nd International scientific and practical conference "Modern research in science and education" (October 12-14, 2023) BoScience Publisher, Chicago, USA. 2023. 498 p. 2023 Oct 12 (p. 68). https://doi.org/10.3390/idr13020049
- 13. Opstelten W, Neven AK, Eekhof J. Treatment and prevention of herpes labialis. Canadian Family Physician. 2008 Dec 1;54(12):1683-7.

https://www.ncbi.nlm.nih.gov/pmc/articles/PMC2602638/

14. Stoopler ET, Sollecito TP. Oral mucosal

diseases: evaluation and management. Medical Clinics. 2014 Nov 1;98(6):1323-52. https://doi.org/10.1016/j.mcna.2014.08.006

- 15. Fatahzadeh M, Schwartz RA. Human herpes simplex virus infections: epidemiology, pathogenesis, symptomatology, diagnosis, and management. Journal of the American Academy of Dermatology. 2007 Nov 1;57(5):737-63. https://doi.org/10.1016/j.jaad.2007.06.027
- 16. Tofiq SH, Idan HM. Hematological Assessments of Children with Oral Aphthous Ulcer in Diyala Governorate, Iraq. Journal of Applied Hematology. 2024 Apr 1;15(2):111-5. https://doi.org/10.4103/joah.joah 23_24
- 17. Sawair FA. Does smoking really protect from recurrent aphthous stomatitis. Therapeutics and clinical risk management. 2010 Nov 22:573-7. https://doi.org/10.2147/TCRM.S15145
- 18. Scully C, Porter S. Oral mucosal disease: recurrent aphthous stomatitis. British Journal of Oral and Maxillofacial Surgery. 2008 Apr 1;46(3):198-206.

https://doi.org/10.1016/j.bjoms.2007.07.201

- 19. Sharma M, Gupta R, Singh S. Correlation of psychological stress with recurrent aphthous stomatitis among dental students in an educational institution. International Journal of Applied Dental Sciences. 2017;3(4):455-8.
- 20. Al-Omiri MK, Karasneh J, Lynch E. Psychological profiles in patients with recurrent aphthous ulcers. International journal of oral and maxillofacial surgery. 2012 Mar 1;41(3):384-8. https://doi.org/10.1016/j.ijom.2011.12.024
- 21. Handa R, Bailoor DN, Desai VD, Sheikh S, Goyal G. A study to evaluate the impact of examination stress on recurrent aphthous ulceration in professional college students in Jaipur district. Minerva Stomatologica. 2012 Nov 1;61(11-12):499-507.
- 22. Singh A, Chopra M, Adiba S, Mithra P, Bhardwaj A, Arya R, Chikkara P, Rathinam RD, Panesar S. A descriptive study of perceived stress among the North Indian

undergraduate students. Iranian nursing journal of nursing and midwifery research. 2013 Jul 1;18(4):340-2.

- 23. C Jr AF, C Jr LG, Silva BS. Prevalence and risk factors for the development of recurrent aphthous stomatitis. Revista de Cirurgia e Traumatologia Buco-maxilo-facial. 2010 Jun; 10(2):61-6.
- 24. Chattopadhyay A, Shetty KV. Recurrent aphthous stomatitis. Otolaryngologic Clinics of North America. 2011 Feb 1;44(1):79-88. https://doi.org/10.1016/j.otc.2010.09.003
- 25. Faulkner S, Smith A. A prospective diary study of the role of psychological stress and negative mood in the recurrence of herpes simplex virus (HSV1). Stress and Health: Journal of the International Society for the Investigation of Stress. 2009 Apr;25(2):179

87. https://doi.org/10.1002/smi.1235

26. Hasanah NT, Hidayat W. Stress as trigger factor of HSV-1 reactivation causing recurrent intraoral mimicking HAEM: a case report. International Medical Case Reports Journal. 2022 Jan1:699-706.

https://doi.org/10.2147/IMCRJ.S388708

27. Sainz B, Loutsch JM, Marquart ME, Hill JM. Stress-associated immunomodulation and herpes simplex virus infections. Medical hypotheses. 2001 Mar1;56(3):348-56.

https://doi.org/10.1054/mehy.2000.1219

28. Goswami P, Ives AM, Abbott AR, Bertke AS. Stress hormones epinephrine and corticosterone selectively reactivate HSV-1 and HSV-2 in sympathetic and sensory neurons. Viruses. 2022 May23;14(5):1115.

https://doi.org/10.3390/v14051115

انتشار التهاب الفم القلاعى الفموي والهربس الشفوي المتكرر بين طلاب طب الاسنان

الحيدر مهدي عيدان، اغسق عبد الله محمود، البتهال قحطان عثمان

الملخص

الخلفية: : آفة الغشاء المخاطي للفم الأكثر شيوعا هي التهاب الفم القلاعي المتكرر. يظهر لأول مرة في مرحلة الطفولة أو المراهقة ويظهر على شكل العديد من القرح الصغيرة أو المتكررة أو البيضاوية ذات الأرضيات الصفراء والهالات الحمامية. تتميز العدوى الفيروسية واسعة النطاق بالهربس الشفهي بآفات حويصلية متكررة، في كثير من الأحيان على الشفاه والأنسجة المحيطة بالفم.

الأهداف: معرفة مدى انتشار التهاب الفم القلاعي الفموي والهربس الشفوي المتكرر بين طلاب طب الأسنان في جامعة بلاد الرافدين.

المواد والطرق: تمت الموافقة على دراسة مقطعية بين ١٨٧ طالبا من طلاب طب الأسنان من جامعة بلاد الرافدين، الذين هم في المرحلتين الرابعة والخامسة من قسم طب الأسنان. وتم جمع البيانات باستخدام الاستبيانات. تتطلب الاستبيانات قسمين. القسم الأول المعلومات الشخصية. أما القسم الثانى فيشمل الأسئلة المرتبطة بالقرح القلاعية والهربس الشفوي المتكرر، مثل مدة القرحة وموقعها بعد الفحص.

النتائج: في الدراسة الحالية بلغ عدد الطلاب المصابين بالقرحة القلاعية في المرحلة الرابعة ١٣ ((١ , ٤ ١))، وفي المرحلة الخامسة ٢٤ (٢ , ٥ ١))، بمستوى دال إحصائياً. من بين ١٨٧ طالبا، كان ١٠ ((, ١٠ , ١)) مصابين بالهربس الشفوي المتكرر في المرحلة الرابعة، في حين كان ١٥ ((, ١٠) في المرحلة الخامسة، مع وجود علاقة ذات دلالة إحصائية عالية. بلغ عدد الطلاب المصابين بالتهاب الفم القلاعي المتكرر والهربس الشفوي المتكرر في المرحلة الخامسة ٢٤ (, ١٠ , ١))، و ١٥ (, ١٥ , ١)) على التوالي، مع وجود علاقة معنوية.

الاستنتاج :التهاب الفم القلاعي المتكرر هو آفة أكثر انتشارا في الإناث مقارنة بالذكور. يعد الإجهاد خلال فترة الامتحانات الأكاديمية أحد أسباب الطفح المتكرر لالتهاب الفم القلاعي وإعادة تنشيط الهربس الشفوي المتكرر.

الكلمات المفتاحية: التهاب الفم القلاعي، الهربس الشفوي، الأسنان، الطلاب، والفم.

المؤلف المراسل: حيدر مهدي عيدان

الايميل: haider.m@uodiyala.edu.iq

تاريخ الاستلام: ٩ تشرين الثاني ٢٠٢٤

تاریخ القبول: ۲۸ شباط ۲۰۲۵

تاريخ النشر: ٢٠ تشرين الأول ٢٠٢٥

ا كلية طب الاسنان، جامعة ديالى، ديالى، العراق. 2 كلية طب الاسنان، جامعة بلاد الرافدين، ديالى، العراق. ٣ دائرة صحة ديالى، ديالى، العراق.

Investigation of Methylglyoxal, soluble Receptor for Advanced Glycation End-products, and Malondialdehyde in Type 2 Diabetes Mellitus with and Without Cardiovascular Risk Factors

Weaam F. Hussien (b), Estabraq A. R. Al-Wasiti (b) Mahood. Sh. Khudair (b), Hayder A. AL-Aubaidy (b)

- ² Department of Chemistry and Biochemistry, Collage of Medicine, AL_Nahrain University, Baghdad, Iraq.
- ³ Department of Internal Medicine, Collage of Medicine, AL_Nahrain University, Baghdad, Iraq.
- ⁴ New Medical Education Australia, Brisbane QLD 4000. Australia.

Abstract

Background: Type 2 diabetes mellitus is a chronic metabolic illness that significantly increases the probability of cardiovascular disorders among individuals with type 2 diabetes. Oxidative stress represents a central pathophysiological connection between type 2 diabetes mellitus and cardiovascular complications. Hyperglycemia in type 2 diabetes mellitus elevates oxidative stress through multiple pathways, including the production of advanced glycation end products and methylglyoxal, which interact with their receptor advanced glycation end product (sRAGE). These processes enhance the generation of reactive oxygen species, which leads to lipid peroxidation with malondialdehyde serving as a biomarker.

Objectives: To investigate the levels of methylglyoxal, sRAGEs, and malondialdehyde in type 2 diabetes patients with and without cardiovascular risk factors.

Patients and Methods: The cross-sectional study involved eighty patients with type 2 diabetes diagnosed with and without cardiovascular risk factors. The study used high-performance liquid chromatography (HPLC) to measure serum methylglyoxal and an ELISA kit (Sun Long Biotech, China) to measure serum sRAGE. Malondialdehyde levels were assessed by spectrophotometry. Moreover, measured parameters included FBS, HbA1c, CRP, and lipid profile by the Cobas system using a kit from Roche, Germany.

Results: Type 2 diabetes patients with cardiovascular risk factors had significantly higher serum methylglyoxal, sRAGE, and malondialdehyde compared to those without CV risk factors. Furthermore, fasting blood glucose, HbA1c, lipid profile, and CRP are higher in diabetes with CV risk factors compared to those without.

Conclusion: The patients with type 2 diabetes and cardiovascular risk factors showed an increase in methylglyoxal, sRAGE, and Malondialdehyde, which are considered useful biomarkers for the indication of T2DM with cardiovascular risk.

Keywords: Methylglyoxal, sRAGE, Cardiovascular risk.

OPEN ACCESS

Correspondence: Weaam F. Hussien
Email: dr.weaamfadhil@gmail.com
Copyright: ©Authors, 2025, College of
Medicine, University of Diyala. This is an open
access article under the CC BY 4.0 license
(http://creativecommons.org/licenses/by/4.0/)
Website:

https://djm.uodiyala.edu.iq/index.php/djm

Received: 31 May 2025 Accepted: 19 September 2025 Published: 25 October 2025

¹ Collage of Pharmacy, AL_Nahrain University, Baghdad, Iraq.

Introduction

Type 2 diabetes mellitus (T2DM) is one of the most common metabolic disorders worldwide, accounting for approximately 90% of all diabetes cases (1). It developed due to the inability of insulin-sensitive tissues to respond as well as a defect in insulin secretion (2). Therefore, this dysfunction leads to hyperglycemia, which microvascular and macrovascular causes (3).complications Chronic hyperglycemia contributes to endothelial dysfunction and oxidative stress, which is considered a key to cardiovascular risk (4). Common factors include hypertension, hyperlipidemia, and obesity with type 2 diabetes mellitus (5). These factors accelerate the development of cardiovascular complications (6). Early identification and management of cardiovascular risk in T2DM are essential for preventing long-term complications (7). Persistent hyperglycemia promotes highly reactive intermediates such advanced as glycation end products(AGEs)(8). A precursor to these intermediates is a dicarbonyl compound called methylglyoxal (MGO), which is produced mostly during carbohydrate, lipid, and protein metabolism (9). Accumulation of MGO and advanced glycation end products (AGEs) plays a role in the development of type 2 diabetes mellitus (T2DM) and its complications (10,11). Chronic hyperglycemia in diabetes causes the formation of AGEs, which accumulate in tissues and contribute to vascular damage. The receptor for Advanced Glycation End Products (RAGE) is a interacts with a varied range of ligands and a member of the immunoglobulin superfamily that mediates interaction between the advanced glycation end-products (AGEs) and endothelial cells. RAGE is considered a membrane-bound immunoglobulin surface (12,13). Moreover, when AGEs bind to RAGE causes the development of reactive oxygen species (ROS) and the stimulation of transcription factors like nuclear factor- κB (NF- κB) and resulting in the

expression involved vascular inflammation and endothelial dysfunction (14). Elevated levels of binding AGEs with RAGE are linked to the development of macrovascular microvascular complications in diabetes, such as atherosclerosis, nephropathy, and retinopathy (15). The soluble receptor advanced glycation end product (sRAGE) acts as a decoy receptor that binds to AGEs, preventing their interaction with membrane-bound RAGE. This interaction triggers oxidative stress typically and inflammation pathways. By sequestering AGEs, sRAGE reduces these harmful effects (16,17). Moreover, sRAGE plays an essential role in modulating the effects of AGEs in diabetes. It is a valuable biomarker and a potential medicinal target in dealing with diabetes and its associated cardiovascular risks (18). The development and progression of diabetes, alongside complications, are largely caused by oxidative stress, which is typically associated with increased free radical production or defective antioxidant defenses. Reactive oxygen species ROS attack lipids, and the major consequence of oxidative stress is lipid peroxidation, leading to the generation of malondialdehyde (MDA), a well-established biomarker of oxidative damage (19,20). Therefore, Oxidative stress, as indicated by elevated MDA, and linked to pancreatic betacell dysfunction and impaired insulin secretion.

Patients and Methods

Study design: This cross-sectional study design included 80 Iraqi individuals, of whom 40 had DM without CVR Factors and 40 were in the DM with CVR Factors. It was conducted from January 2024 to June 2024. The age of the participants ranged from 40 to 60 years at Al-Imamin Alkadmeen City Hospital, Baghdad, Iraq. Prediabetic patients received a consultant's examination by a specialist and were approved by the institutional ethical review committee.

Inclusion criteria: This study involves two groups: Group 1: 40 patients with Type 2

diabetes mellitus without cardiovascular risk factors.

Group 2:40 patients with Type 2 diabetes mellitus with cardiovascular risk factors.

Exclusion criteria: This study exclude the following patients:

- a. Patients were excluded if they were aged < 40 years or more than 60 years.
- b. Type 1 diabetes patients
- c. Pregnant females
- d. Patients with a history of cardiovascular disease.
- e. Patients receiving insulin treatment.
- f. Individuals with anemia
- g. Patients with kidney, liver, or thyroid disorders
- h. Known case of carcinoma anywhere
- i. Autoimmune diseases

Blood collection and procedures: All blood samples were collected from fasting participants during their hospital visit. The diagnosis of type 2 diabetes mellitus was based on the American Diabetes Association (ADA) guidelines (21). Body mass index (BMI) measurements were recorded. A total of 7 mL of whole blood was collected and divided into two tubes; the first tube was an EDTA tube for HbA1c measurement, and the second was a gel tube allowed to coagulate for 15 minutes. The samples were centrifuged at 5500 rpm for 15 minutes at room temperature to separate the serum for measuring fasting blood glucose, CRP, and lipid profile. and stored at -20 c to measure serum MDA, methylglyoxal (MG), and soluble receptor advanced glycation endproducts (sRAGE).

Measurement of chemical parameters:

Methylglyoxal (MG): Methylglyoxal (MG) levels were determined using high-performance liquid chromatography (HPLC) with a standard solution obtained from Mvcklin (China). The derivatization reagent used was 1,2-diamino-4,5-methylenedioxybenzene (DMP). The mobile phase consisted of acetonitrile, methanol, and

distilled water. Separation was performed on a C18 Octadecyl-silica (ODS) column (250 mm × 4.6 mm) with a flow rate of 1 mL/min. Detection was carried out by a fluorescence detector at an excitation wavelength of 355 nm and an emission wavelength of 393 nm.

Sample preparation: Serum samples (100 μl) were centrifuged at 10,000 rpm for 5 minutes to remove cellular components. The supernatant was filtered using a 10 kDa centrifugal ultrafiltration device to eliminate proteins. Subsequently, 50 μL of serum was mixed with 50 μL of DMP (0.7 mM) and incubated at 60°C for 40 minutes to form the MG-DMP derivative. A 10 μL aliquot of the derivatized solution was injected into the HPLC system for analysis. (22).

Soluble receptor for advanced glycation endproducts (sRAGE): Soluble receptor for advanced glycation end-products (sRAGE) was quantified with an ELISA kit according to the manufacturer's protocols, according to the manufacturer's protocol NO.:SL0036Ra (Sun Long Biotech, China).

Malondialdehyde: Serum MDA levels were determined using the thiobarbituric acid reactive substances (TBARS) method. In this assay, lipid peroxidation end products, mainly MDA, react with thiobarbituric acid (TBA) under acidic conditions and heating in a boiling water bath (100 °C) to form a pink chromogen. After cooling and centrifugation, the absorbance of the clear supernatant was measured spectrophotometrically at 532 nm against a The concentration of MDA was calculated using the molar extinction coefficient of the MDA-TBA adduct $(1.56 \times 10^5 \text{ cm}^{-1})$ mol⁻¹), and the results were expressed in μmol/L (23).

Additional tests: HbA1c, fasting blood glucose (FBG), lipid profile, and C-reactive protein (CRP) were measured using the Cobas c111 fully automated analyzer (Roche Diagnostics, Germany), following the manufacturer's

standard protocols.

Statistical Analysis

To analyze the data, GraphPad Prism (version 10.3.1) and MedCalc software were used to create the ROC curve. date the expression as mean, standard deviation (SD), mean \pm SD. Comparison between the two groups used an unpaired t-test with a p-value < 0.05 was considered statistically significant, and very small p-values were reported as p < 0.001.

Results

Demographic and diabetes-associated characteristics of the study cohort eighty patients with type 2 diabetes mellitus with and without cardiovascular risk factors. The study groups were divided into smaller groups based on age, gender, and BMI (Table 1). The study included 25 females (62.5%) and 15 males (37.5%), as shown in Table 1.

Table 1. Descriptive features of the study population (Number = 80).

Parameters	DM without CVR Factors Mean±SD. No.= 40	DM with CVR Factors Mean±SD. No.=40	p-value
Age (years)	48.87±9.3	56.94±4.17	<0.001 (S)
Sex	M 15 (37.5%) F 25 (62.5%)	M 15 (37.5%) F 25 (62.5%)	
BMI (kg/m²)	29.88±5.782	30.18±3.209	0.775 (NS)
Duration of type 2 DM	6.15±5.38	9.25±2.38	0.0013 (S)

T-test: significant at p < 0.05, SD: standard deviation; S: significant; NS: non-significant DM: diabetes Mellitus CVR: cardiovascular risk factors

Measurement of glucose profile, methylglyoxal, sRAGE, MDA, and CRP in the patients' groups: The high level of average serum fasting blood glucose (FBS) and HbA1c in diabetes with CV risk factors was (238.0±34.35 mg/dL and 10.03±1.30%), respectively, and when compared with diabetes without CV risk factors (175.4±76.28 mg/dl, 7.86±1.28%) (p < 0.001). The Methylglyoxal level (1.235±0.256 μg/mL) was significantly higher (p < 0.001) in

diabetes with CV risk factors patients when compared to those without $(0.9139\pm0.046~\mu g/mL)$. The high level of sRAGE in diabetes with CV risk factors $(699.8\pm86.78~pg/mL)$ compared to without $(542.2\pm72.96~pg/mL)$ (p < 0.001). The MDA level was higher in diabetes with CV risk factors $(5.726\pm0.82~(\mu mol/L)~)$ compared to without (p < 0.001). CRP levels were higher in T2DM patients with CV risk $(10.81\pm0.76~mg/l)$ than without $(7.50\pm0.296~mg/l)$, with p value < 0.001as shown in Table 2.

Table 2. The mean difference of biomarkers for patients with type 2 diabetes mellitus with and without cardiovascular risk factors.

Parameters	DM without CVR Factors Mean±SD. N= 40	DM with CVR Factors Mean±SD. N=40	P - value
FBS (mg\dL)	175.4±76.28	238.0±34.35	<0.001 (S)
HbA1c %	7.86±1.28	10.03±1.30	<0.001(S)
MGO (μg/mL)	0.9139±0.046	1.235±0.256	<001 (S)
sRAGEs (pg/mL)	542.2±72.96	699.8±86.78	<0.001 (S)
MDA (μmol/L)	3.509±0.42	5.726±0.82	<0.001 (S)
CRP (mg/l)	7.50±0.296	10.81±0.76	<0.001 (S)

T-test: significant at p < 0.05, SD: standard deviation; S: significant.

NS= non-significant DM: diabetes Mellitus CVR: cardiovascular risk factors.

Measurement of lipid profile and atherogenic index in the patients groups: The total cholesterol level was higher in T2DM with CV risk factors (284.5±34.44 mg/dL) than without CV risk $(241.3\pm77.32 \text{ mg/dL})$, and the p < 0.001. In contrast, the level of HDL cholesterol was lower in T2DM with CV risk factors (27.19±5.686 mg/dL) compared to those without CV risk $(36.62\pm4.89 \text{ mg/dL})$, p < 0.001. While LDL cholesterol was significantly increased in T2DM with CV risk factors (131.7±20.65 mg/dL) as compared to those without CV risk $(121.4\pm14.13 \text{mg/dL})$, the p-value was < 0.05. The level of VLDL cholesterol was significantly higher (p < 0.001) in patients with T2DM and CV risk factors (50.11±5.69 mg/dL) compared to those without CV risk (40.42±11.42 mg/dL).

Triglyceride levels were significantly higher in T2DM with CVrisk factors (250.0±26.91mg/dL) as compared to without CV risk (241.3±77.32mg/dL), and the p-value was p < 0.001. Furthermore, the high level of Atherogenic Index of Plasma (AIP) in T2DM with CV risk factors (0.97±0.1) as compared to those without CV risk (0.733 ± 0.12) , the p-value was p < 0.0001, Additionally, the cardiac Risk Index 1 (CRI-1) level was significantly higher in T2DM with CV risk factors (10.91±2.71) as compared to those without CV risk (6.856 ± 3.07) , with p < 0.001. The Cardiac Risk Index 2 (CRI-2) level was higher in T2DM with CV risk factors (5.12±1.63) as compared to without CV risk (3.376±0.62) with a p-value < 0.001, as shown in Table 3.

Table 3. The mean difference in lipid profile for patients with type 2 diabetes mellitus with and without cardiovascular risk factors.

Parameters	DM without CVR Factors Mean±SD. N= 40	DM with CVR Factors Mean±SD. N=40	P - value
Total cholesterol (mg\dL)	241.3±77.32	284.5±34.44	< 0.001 (S)
TG (mg\dL)	202.2±57.02	250.0±26.91	< 0.001 (S)
LDL (mg\dL)	121.4±14.13	131.7±20.65	< 0.05 (S)
VLDL (mg\dL)	40.42±11.42	50.11±5.69	< 0.001 (S)
HDL (mg\dL)	36.62±4.89	27.19±5.686	< 0.001 (S)
AIP Log [TG / HDL-C]	0.733±0.12	0.97±0.1	< 0.001(S)
CRI-1 (TC/HDL-C)	6.856±3.07	10.91±2.71	<0.001 (S)
CRI-2 (LDL-C / HDL-C)	3.376±0.62	5.12±1.63	< 0.001 (S)

T-test significant at p < 0.05, SD: Standard Deviation; S: Significant.

NS non-significant DM: Diabetes Mellitus, CVR: Cardiovascular Risk.

AIP= Atherogenic Index of Plasma, CRI-1= Cardiac Risk Index 1, CRI-2= Cardiac Risk Index 2.

Receiver operating characteristic curve (ROC) of MGO, sRAGE, and MDA biomarkers in the patients groups: As shown in Table 4, methylglyoxal (MGO) demonstrated a cutoff value > 0.98 with a 95% confidence interval (CI) of 1.000 to 1.000, indicating a strong diagnostic ability. The sRAGE biomarker exhibited excellent diagnostic performance, with

a sensitivity of 100%, specificity of 83.9%, and an area under the curve (AUC) of 0.938 (95% CI: 0.873 to 1.000). The optimal cutoff value for sRAGE was > 597.03. Furthermore, Malondialdehyde (MDA) showed high sensitivity (100%) and specificity (93.5%), with an AUC of 0.982 (95% CI: 0.947 to 1.000) and a cutoff value > 4.1.

Table 4. ROC curve of MGO, sRAGE, and MDA biomarkers between type 2 diabetes mellitus patients without and with cardiovascular risk factors.

Variable	AUC	95 % CI	Cutoffs	Sensitivity	Specificity
MGO(μg/mL)	1.000	1.000 to 1.000	> 0.98	100	100
sRAGE (pg/mL)	0.938	0.873 to 1.000	> 597.03	100	83.9
MDA (μmol/L)	0.982	0.947 to 1.000	> 4.1	100	93.5

Discussion

Type 2 diabetes mellitus (T2DM) is a chronic metabolic illness strongly associated with increased risk of macrovascular complications Multiple pathways contribute (3).macrovascular complications, such as oxidative inflammation. mitochondrial stress. and dysfunction (4).Inflammation is commonly indicated by C-reactive protein (CRP). In the present study, CRP levels were significantly elevated in T2DM patients with cardiovascular (CV) risk compared to those without. These results agree with Upreti et al., who reported that CRP is highly correlated with CV risk level in T2DM (24). In the current study, methylglyoxal (MGO) levels were significantly elevated in T2DM with cardiovascular risk compared to those without CV risk. This elevation may be attributed to impaired glyoxalase system activity and increased oxidative stress, which contribute to the accumulation of MGO, leading to the formation of advanced glycation end-products (AGEs) (25). These findings agree with a study by Hanssen et al., (26), who reported elevated levels of MGO in type 2 diabetes mellitus with cardiovascular disease, indicating that MGO contributes to both endothelial dysfunction and inflammation, thereby promoting cardiovascular complications in type 2 diabetes mellitus (26). Moreover, MGO readily reacts with proteins, DNA, and other macromolecules, leading to the formation of AGEs, which play a crucial role in diabetes-related complications. which supports the role of MGO as a potential biomarker for cardiovascular risk (9). Elevated MGO levels affect metabolic pathways, leading to increased lipid peroxidation, as indicated by elevated levels of MDA in patients with cardiovascular risk factors (27). This relationship shows the role of MGO, oxidative stress, and inflammation in the pathophysiology of diabetic cardiovascular disease. Furthermore, in the present study, the MDA level was higher in T2DM patients with

cardiovascular risk factors compared to those without CV risk. This finding agrees with Khan et al., who showed that lipid peroxidation increased in hyperglycemic diabetic patients, leading to diabetic complications (28). Oxidative stress is potentially associated with the development of diabetic complications. The negative correlation between lipid peroxidation and antioxidant cellular activity establishes a pathogenic link between hyperglycemia and complications in type 2 diabetes mellitus patients (29). In the current study, sRAGE levels were significantly elevated in type 2 diabetes mellitus with cardiovascular risk factors than without cardiovascular risk factors. sRAGE levels may reflect a compensatory response to the increased formation of AGEs. This result agrees with Sabbatinelli et al., who suggest that sRAGE plays a crucial protective role in vascular endothelial function. AGE-RAGE endothelial interactions impair integrity, triggering endothelial cell activation and vascular inflammation. However, sRAGE mitigates these effects by neutralizing circulating AGEs, thereby preserving vascular reducing homeostasis and the risk atherosclerosis (30). This mechanism may explain why the sRAGE levels in type 2 diabetes mellitus patients with cardiovascular risk are higher than those without cardiovascular risk, reflecting an adaptive response to increased vascular stress. Moreover, the current study indicates a significant increase in lipid profile parameters, including total cholesterol, LDL-C, triglycerides, and VLDL, accompanied by a decrease in HDL levels in patients with T2DM who have CV risk factors. These findings are consistent with the study by Mulla et al. (31). The atherogenic index of plasma (AIP) and Cardiac Risk Index 1 and 2 were significantly elevated in T2DM with CV risk compared to those without CV risk. Dyslipidemia and elevated levels of atherogenic lipoproteins are

markers for cardiovascular risk factors and key contributors to endothelial dysfunction, inhibiting its anti-thrombotic and pro-fibrinolytic functions, thereby impairing endothelial function (32). AIP is recognized as a valuable marker for assessing the risk of atherosclerosis and coronary heart disease. Given the strong association between dyslipidemia and T2DM, these indices serve as essential tools for evaluating cardiovascular risk in diabetic patients (33).

Moreover, the receiver operating characteristic (ROC) analysis (Table 4) supports the diagnostic potential of MGO, sRAGE, and MDA in distinguishing between diabetic patients with and without cardiovascular risk. The ROC analysis curve shows MGO level near perfect diagnostic performance, which is indicated by sensitivity and specificity. Additionally, sRAGEs and MDA demonstrated a good sensitivity and specificity, which is considered a good finding supporting their role as biomarkers of oxidative stress and inflammation in diabetic cardiovascular disease. Overall, MGO, MDA, and sRAGE may serve as a valuable indicator of cardiovascular risk in T2DM patients.

Conclusion

This study shows that T2DM patients with cardiovascular risk have higher levels of Methylglyoxal (MGO), Malondialdehyde (MDA), and sRAGE, indicating increased oxidative stress linked to both diabetes and cardiovascular complications. The elevated MGO and MDA reflect enhanced lipid peroxidation and glycation, while increased sRAGE may represent a protective response as a decoy receptor. These findings highlight the significant role of cardiovascular risk factors in amplifying oxidative stress in T2DM patients and emphasize the importance of monitoring these biomarkers to guide strategies for reducing oxidative stress and preventing complications. It is recommended to increase the sample size in future studies to enhance the accuracy and

statistical power of the findings. Additionally, conducting a case-control study is advised to elucidate the relationship between cardiovascular risk factors and biochemical markers in patients with type 2 diabetes mellitus. Furthermore, evaluating the impact of various medications on these biomarkers would provide valuable insights into their potential role in reducing cardiovascular complications.

Source of funding: No source of funding.

Ethical clearance: Official approval has been obtained to use data, and data were analyzed without the names to protect privacy. This study was conducted according to the approval of the College of Medicine/ University of AL-Nahrain and under the ethical guidelines of the Declaration of the ethical committee of the College (No.20230901).

Conflict of interest: None.

Use of Artificial Intelligence (AI): The authors state they did not use any generative AI tools for creating or editing the manuscript's language.

Acknowledgement: Special thanks to the College of Medicine at Al-Nahrain University.

References

- 1. DeFronzo RA, Ferrannini E, Groop L, Henry RR, Herman WH, Holst JJ, Hu FB, Kahn CR, Raz I, Shulman GI, Simonson DC. Type 2 diabetes mellitus. Nature reviews Disease primers. 2015 Jul 23;1(1):1-22. http://dx.doi.org/10.1038/nrdp.2015.19
- 2. Lu X, Xie Q, Pan X, Zhang R, Zhang X, Peng G, Zhang Y, Shen S, Tong N. Type 2 diabetes mellitus in adults: pathogenesis, prevention and therapy. Signal transduction and targeted therapy. 2024 Oct 2;9(1):262. http://dx.doi.org/10.1038/s41392-024-01951-9
- 3. Lu Y, Wang W, Liu J, Xie M, Liu Q, Li S. Vascular complications of diabetes: A narrative review. Medicine. 2023 Oct 6;102(40):e35285. http://dx.doi.org/10.1097/MD.00000000000035285

- Caturano A, Rocco M, Tagliaferri G, Piacevole A, Nilo D, Di Lorenzo G, Iadicicco I, Donnarumma M, Galiero R, Acierno C, Sardu C. Oxidative stress and cardiovascular 2 complications in type diabetes: from pathophysiology to lifestyle modifications. Antioxidants. 2025 Jan 9;14(1):72. http://dx.doi.org/10.3390/antiox14010072
- 5. Ellulu MS, Samouda H. Clinical and biological risk factors associated with inflammation in patients with type 2 diabetes mellitus. BMC Endocrine Disorders. 2022 Jan 6;22(1):16. https://doi.org/10.1186/s12902-021-00925-0
- 6. Chakraborty S, Verma A, Garg R, Singh J, Verma H. Cardiometabolic risk factors associated with type 2 diabetes mellitus: a mechanistic insight. Clinical Medicine Insights: Endocrinology and Diabetes. 2023 Dec:16:11795514231220780.

$\underline{http://dx.doi.org/10.1177/11795514231220780}$

- 7. Hinnen D, Kruger D, Magwire M. Type 2 diabetes and cardiovascular disease: risk reduction and early intervention. Postgraduate medicine. 2023 Jan 2;135(1):2-12. https://doi.org/10.1080/00325481.2022.2126235
- 8. Chen Y, Meng Z, Li Y, Liu S, Hu P, Luo E. Advanced glycation end products and reactive oxygen species: uncovering the potential role of ferroptosis in diabetic complications. Molecular Medicine. 2024 Sep 9;30(1):141. https://dx.doi.org/10.1186/s10020-024-00905-9
- 9. Berdowska I, Matusiewicz M, Fecka I. Methylglyoxal in Cardiometabolic disorders: Routes leading to pathology counterbalanced by treatment strategies. Molecules. 2023 Nov 24;28(23):7742.

http://dx.doi.org/10.3390/molecules28237742

10. Oliveira AL, de Oliveira MG, Mónica FZ, Antunes E. Methylglyoxal and advanced glycation end products (AGEs): Targets for the prevention and treatment of diabetes-associated bladder dysfunction?. Biomedicines. 2024 Apr

23;12(5):939.

http://dx.doi.org/10.3390/biomedicines1205093

11. Sutkowska E, Fecka I, Marciniak D, Bednarska K, Sutkowska M, Hap K. Analysis of methylglyoxal concentration in a group of patients with newly diagnosed prediabetes. Biomedicines. 2023 Nov 3;11(11):2968. https://doi.org/10.3390/biomedicines11112968
12. Erusalimsky JD. The use of the soluble receptor for advanced glycation-end products (sRAGE) as a potential biomarker of disease risk and adverse outcomes. Redox Biology. 2021 Jun 1;42:101958.

https://doi.org/10.1016/j.redox.2021.101958

- 13. Yue Q, Song Y, Liu Z, Zhang L, Yang L, Li J. Receptor for advanced glycation end products (RAGE): a pivotal hub in immune diseases. Molecules. 2022 Aug 2;27(15):4922. https://www.mdpi.com/1420-3049/27/15/4922
- 14. Liu J, Pan S, Wang X, Liu Z, Zhang Y. Role of advanced glycation end products in diabetic vascular injury: molecular mechanisms and therapeutic perspectives. European journal of medical research. 2023 Dec 2;28(1):553. https://doi.org/10.1186/s40001-023-01431-w
- 15. Mengstie MA, Chekol Abebe E, Behaile Teklemariam A, Tilahun Mulu A, Agidew MM, Teshome Azezew M, Zewde EA, Agegnehu Teshome A. Endogenous advanced glycation end products in the pathogenesis of chronic diabetic complications. Frontiers in molecular biosciences. 2022 Sep 15;9:1002710. http://dx.doi.org/10.3389/fmolb.2022.1002710
- 16. Dong H, Zhang Y, Huang Y, Deng H. Pathophysiology of RAGE in inflammatory diseases. Frontiers in Immunology. 2022 Jul 29;13:931473.

http://dx.doi.org/10.3389/fimmu.2022.931473

17. Yamagishi SI, Matsui T. Soluble form of a receptor for advanced glycation end products (sRAGE) as a biomarker. Frontiers in bioscience (Elite edition). 2010 Jun 1;2(4):1184-95.

https://imrpress.com/journal/FBE/2/4/10.2741/E 178

18. Bansal S, Burman A, Tripathi AK. Advanced glycation end products: Key mediator therapeutic target of cardiovascular complications in diabetes. World Journal of 2023 Diabetes. Aug 15;14(8):1146. http://dx.doi.org/10.4239/wjd.v14.i8.1146

19. Cordiano R, Di Gioacchino M, Mangifesta R, Panzera C, Gangemi S, Minciullo PL. Malondialdehyde as a potential oxidative stress marker for allergy-oriented diseases: an update. Molecules. 2023 Aug 9;28(16):5979. https://www.mdpi.com/1420-3049/28/16/5979

20. Jamil D, Al-Aubaidy H, Al-Wasiti E, Al Bayati M. Evaluating markers of oxidative stress in managing gestational diabetes mellitus: a cross-sectional study in Iraq. British Journal Of Medical and Health Research. 2014;4(21):3870-7. http://dx.doi.org/10.9734/bjmmr/2014/10139

21. "2. Diagnosis and classification of diabetes: standards of care in diabetes—2024." Diabetes care 47, no. Supplement 1 (2024): S20-S42. https://doi.org/10.2337/dc24-S002

22. Ogasawara Y, Tanaka R, Koike S, Horiuchi Y, Miyashita M, Arai M. Determination of methylglyoxal in human blood plasma using fluorescence high performance liquid chromatography after derivatization with 1, 2diamino-4, 5-methylenedioxybenzene. Journal of Chromatography B. 2016 Sep 1;1029:102-5. https://doi.org/10.1016/j.jchromb.2016.07.019

23. De Leon JA, Borges CR. Evaluation of oxidative stress in biological samples using the thiobarbituric acid reactive substances assay. Journal of visualized experiments: JoVE. 2020 12(159):10-3791. May

https://dx.doi.org/10.3791/61122

24. Upreti B, Sherpa ML, Bhutia KL. Effect of highly sensitive C-reactive protein cardiovascular risk of Type 2 diabetes mellitus adults: A systematic review. Asian Journal of

Medical Sciences. 2024 Jun 1;15(6):159-65. http://dx.doi.org/10.3126/ajms.v15i6.63068

CG. 25. Schalkwijk Stehouwer CD. Methylglyoxal, a highly reactive dicarbonyl diabetes, compound, in its vascular complications, and other age-related diseases. Physiological reviews. 2020 Jan 1;100(1):407-61.

http://dx.doi.org/10.1152/physrev.00001.2019

26. Hanssen NM, Westerink J, Scheijen JL, van der Graaf Y, Stehouwer CD, Schalkwijk CG; SMART Study Group. Higher methylglyoxal levels are associated with incident cardiovascular disease and mortality in individuals with type 2 diabetes. Diabetes Care. 2018 Aug 1;41(8):1689-1695. http://dx.doi.org/10.2337/dc18-0159

27. Wang Y, Chen J, Zheng Y, Jiang J, Wang L, Wu J, Zhang C, Luo M. Glucose metabolite methylglyoxal induces vascular endothelial cell pyroptosis via NLRP3 inflammasome activation and oxidative stress in vitro and in vivo. Cellular and Molecular Life Sciences. 2024 Dec;81(1):401. https://doi.org/10.1007/s00018-024-05432-8

28. Premkumar G, Bhagyalakshmi V, Sandhya S. A correlation biomarker between BMI and lipid peroxidation in type 2 diabetes mellitus with and without other complications. Indian Journal of Medical Sciences. 2023 Jan 2;74(3):122-5.

http://dx.doi.org/10.54112/bcsrj.v2023i1.253

29. Najafi A, Pourfarzam M, Zadhoush F. Oxidant/antioxidant status in Type-2 diabetes mellitus patients with metabolic syndrome. Journal of Research in Medical Sciences. 2021 1:26(1):6.

http://dx.doi.org/10.4103/jrms.JRMS 249 20

30. Sabbatinelli J, Castiglione S, Macrì F, Giuliani A, Ramini D, Vinci MC, Tortato E, Bonfigli AR, Olivieri F, Raucci A. Circulating levels of AGEs and soluble RAGE isoforms are associated with allcause mortality and development of cardiovascular complications in type 2 diabetes: a retrospective cohort study. Cardiovascular diabetology. 2022 Jun 6;21(1):95. https://doi.org/10.1186/s12933-022-01535-3

- https://doi.org/10.1186/s12933-022-01535-3
 31. Mulla IG, Anjankar A, Shinde A, Pratinidhi S, Agrawal SV, Gundpatil DB, Lambe SD. Comparison of Lipid Profiles Between Prediabetic and Non-prediabetic Young Adults. Cureus. 2024 Jul 24;16(7). https://doi.org/10.7759/cureus.65251
- 32. McGrowder DA. Biochemical parameters as cardiovascular risk factors in obese children and adults. Journal of Endocrinology, Diabetes and Obesity. 2018;6(1):1115.
- 33. Ahmed HS, Mohammed MS. Atherogenic indices in type 2 diabetic Iraqi patients and its association with cardiovascular disease risk. Journal of the Faculty of Medicine Baghdad. 2023 Oct 1;65(3):179-86. https://doi.org/10.32007/jfacmedbagdad.2075

تقييم ميثيل جليوكسال، RAGEs، ومالوند ديالديهايد في داء السكري من النوع γ مع وبدون عوامل خطر القلب والأوعية الدموية

ا وئام فاضل حسين، ٢ استبرق عبد الرسول الواسطى، ٣ محمود شاكر خضير، ٤ حيدر على العبيدي

الملخص

الخلفية: داء السكري من النوع ٢ هو اضطراب استقلابي مزمن يزيد من خطر الإصابة بأمراض القلب والأوعية الدموية. يُعد الإجهاد التأكسدي حلقة وصل فيزيولوجية مرضية رئيسية بين T2DM ومضاعفات القلب والأوعية الدموية. يسهم ارتفاع السكر في الدم في داء السكري من النوع ٢ إلى زيادة الإجهاد التأكسدي من خلال مسارات متعددة ، بما في ذلك تكوين المنتجات النهائية المتقدمة للجليكاسيون وميثيل جليوكسال. تعزز هذه العمليات توليد أنواع الأكسجين التفاعلية ، مما يؤدي إلى بيروكسيد الدهون مع عمل MDA كمؤشر حيوي.

الأهداف: تهدف هذه الدراسة إلى التحقيق في مستويات ميثيل جليوكسال ، MDA، sRAGEs لدى مرضى السكري من النوع ٢ مع أو بدون عوامل خطر القلب والأوعية الدموية.

المرضى والطرق: أجريت دراسة مقطعية شملت ٨٠ مريضا بمرض السكري من النوع ٢ مع وبدون عوامل خطر القلب والأوعية الدموية تم تشخيصها في مستشفى مدينة الإمامين الكاظمين، بغداد، العراق. تم جمع البيانات السريرية والمخبرية الأساسية لجميع المشاركين. تم قياس ميثيل جليوكسال المصل بواسطة كروماتو غرافيا سوائلة عالية الأداء (HPLC)، وتم قياس المنتجات النهائية للجليكاسيون المتقدمة للمستقبلات القابلة للذوبان باستخدام مجموعة ELISA، وتم تقييم مستويات MDA عن طريق القياس الطيفي. كما تم قياس، نسبة الجلوكوز في الدم الصائم، HbA1c البروتين التفاعلي C، الملف الدهني.

النتائج: كانت ميثيل جليوكسال، sRAGEs، و MDA أعلى بشكل ملحوظ من مرضى السكري الذين يعانون من عوامل خطر الأمراض القلبية الوعائية، فإن جلوكوز الدم الصائم، HbA1c ، الأنسولين ، HOMA-IR ، ملف الدهون والبروتين التفاعلي C أعلى في مرض السكري مع عوامل خطر الإصابة بأمراض القلب والأوعية الدموية .

الاستنتاج: بناء على نتائج هذا البحث، قد تكون ميثيل جليوكسال وsRAGEs و MDA بمثابة مؤشرات حيوية سريرية محتملة لتحديد مخاطر القلب والأوعية الدموية لدى مرضى T2DM.

الكلمات المفتاحية: ميثيل جليوكسال ، sRAGEs ، مخاطر الأمراض القلبية الوعائية.

المؤلف المراسل: وئام فاضل حسين

dr.weaamfadhil@gmail.com الايميل:

تاريخ الاستلام: ٣١ أيار ٢٠٢٥

تاریخ القبول: ۱۹ أیلول ۲۰۲۰

تاريخ النشر: ٢٠ تشرين الأول ٢٠٢٥

ا كلية الصيدلة ، جامعة النهرين، بغداد ، العراق.

٢ فرع الكيمياء والكيمياء الحياتية، كلية الطب، جامعة النهرين ، بغداد، العراق.

" فرع الطب الباطني، كلية الطب، جامعة النهرين ، بغداد، العراق.

أ التعليم الطبي الجديد في أستراليا ، بريسبان كوينزلاند ، ، ، ٤ ، استراليا.

Changes in the Levels of Methionine Adenosyltransferase, Methionine Sulfoxide Reductase A, and Thioredoxin are Associated with Oxidative Stress in Patients with Hyperthyroidism

Marwa A. Al-Badrany (6), Luay A. Al-Helaly (6)

OPEN ACCESS

Correspondence: Marwa A. Al-Badrany Email: marwa.24scp70@student.uomosul.edu.iq Copyright: ©Authors, 2025, College of Medicine, University of Diyala. This is an open access article under the CC BY 4.0 license (http://creativecommons.org/licenses/by/4.0/) Website:

https://djm.uodiyala.edu.iq/index.php/djm

 Received:
 22 May
 2025

 Accepted:
 01 August
 2025

 Published:
 25 October
 2025

Abstract

Background: Hyperthyroidism is associated with increased oxidative stress and alterations in enzymatic and non-enzymatic antioxidant systems. Methionine adenosyltransferase (MAT) plays a key role in cellular metabolism and may be involved in redox homeostasis in thyroid disorders.

Objectives: This study aimed to evaluate the levels of MAT and investigate its association with selected enzymatic and non-enzymatic oxidative stress markers in patients with hyperthyroidism.

Patients and Methods: A total of 90 blood serum samples were collected from patients with hyperthyroidism and compared with 50 healthy controls. Enzymatic markers measured included methionine sulfoxide reductase A (MsrA), thioredoxin (Trx), catalase (Cat), myeloperoxidase (MPO), lactoperoxidase (LP), xanthine oxidase (XO), glutathione S-transferase (GST), and senescence marker protein-30 (SMP-30). Non-enzymatic markers included glutathione (GSH), uric acid (UA), albumin (Alb), malondialdehyde (MDA), and peroxynitrite (ONOO⁻).

Results: Compared to healthy controls, patients with hyperthyroidism showed a significant increase in MAT, Cat, XO, GST, Trx, and LP levels, while SMP-30 was significantly decreased. Among non-enzymatic parameters, MDA and ONOO⁻ were significantly elevated, and albumin levels were decreased. No significant changes were found in the remaining markers. MAT showed a direct correlation with SMP-30, MPO, MsrA, UA, ONOO⁻, and Alb, and an inverse relationship with Cat, XO, and GSH. No correlation was observed between MAT and GST, LP, or Trx.

Conclusion: The findings suggest a strong association between MAT activity and oxidative stress in patients with hyperthyroidism. The observed changes point to metabolic imbalances and compromised antioxidant defense mechanisms in these patients.

Keywords: Hyperthyroidism, Enzyme, Methionine adenosyltransferase, Methionine sulfoxide reductase A, Thioredoxin.

Introduction

Hyperthyroidism is a condition that occurs when the thyroid gland secretes excess hormones (1). leading to accelerated metabolism pathways (2). Signs of this disorder may include heartbeats, struggles with heat sensitivity, feelings of unease, and unintended loss of weight (3). Hyperthyroidism

¹ Department of Chemistry, College of Science, University of Mosul, Mosul, Iraq.

manifest in subtle forms. Clear can hyperthyroidism is distinguished by levels of stimulation thyroid hormone (often abbreviated as TSH) paired with heightened levels of triiodothyronine (known as T3) or increased levels of thyroxine (referred to as T4). If T3 and T4 levels are elevated while TSH is diminished and T4 levels remain normal, the condition is termed "T3". Subclinical hyperthyroidism is when the TSH levels are low. Both T3 and T4 levels are within the normal range, which can lead to significant long-term complications in both overt and subclinical cases of hyperthyroidism **(4)**.

Hyperthyroidism impacts around 2.5% adults, affecting more women than men at a rate of 2% for women and 0.5% globally. If left untreated. It can lead to heart irregularities. Bone fragility and metabolism issues that result in weight loss Graves' disease, the cause of hyperthyroidism, is an autoimmune condition that appears more frequently in women (5). Research indicates that genetic factors play a role in determining the likelihood of developing Graves' disease accounting for approximately 60 to 80 percent of the risk involved (6). Toxic nodular goiter, the second most common cause, affects 1.5-18 cases per 100,000 people worldwide annually. This disease is characterized by thyroid nodules releasing excess thyroid hormone and is more common in areas with iodine deficiency (5). Excessive exposure to iodine can also lead to hyperthyroidism due to failure of normal homeostasis mechanisms. Iodineinduced hyperthyroidism occurs commonly in areas that have historically suffered from iodine deficiency Hashimoto's thyroiditis also cause can hyperthyroidism, although Hashimoto's thyroiditis is the most common cause of hypothyroidism (8).

Methionine adenosyltransferases (MATs; EC 2.5.1.6) are very important enzymes for living cells. There are three isomers of the enzyme:

MAT I, II, and III (9). MAT is the only enzyme that S-adenosylmethionine (SAM) adenosine triphosphate (ATP) and methionine (10). SAM is synthesized in the liver and plays a crucial role as an essential donor of the methyl group required for many biological functions (11). It methylates DNA, RNA, and proteins, which is necessary for maintaining genomic stability, regulating gene expression, and maintaining cellular homeostasis (12). Additionally, it regulates cellular processes whose dysregulation may contribute to pathological conditions (13). Low levels of SAM affect lipid metabolism, contributing to the development of fatty liver disease, injury, and even cancer. SAM deficiency may lead to increased fat accumulation in the liver, contributing to the development of fatty liver disease (12). SAM is used to treat liver dysfunction (14), and also in the treatment of depression (11) as it is necessary for the production of neurotransmitters that affect mental health (15, 16).

Furthermore, SAM plays a role in reducing increased homocysteine levels. After demethylation of SAM, it is converted to S-adenosylhomocysteine (SAH), which is then hydrolyzed to homocysteine (Hcy)(17). Homocysteine can enter the transsulfate pathway to promote glutathione synthesis, or it can be converted back to methionine and then to SAM (17, 18). Elevated homocysteine levels are primarily related to their association with endothelial dysfunction and atherosclerosis(19). In addition to elevated SAM levels, homocysteine levels can also be elevated for several other reasons, including genetic factors, deficiencies of B vitamins and folic acid, aging, certain medications, and pathological conditions (19, 20).

A 2020 study showed that changes in the activity of the MAT1A and MAT2A enzymes affect methionine metabolism in chronic liver disease, contributing to the development of cirrhosis and liver cancer (17).

A 2023 study on mice also found that MAT2A increases with age. Increased MAT2A activity in the skeletal muscles of elderly mice led to impaired metabolism, contributing to muscle weakness. However, inhibiting MAT2A has been shown to improve muscle strength (21). Previous studies have primarily focused on general oxidative markers in thyroid disorders, with limited evaluation of specific enzymatic systems such as MAT, MsrA, and Trx. However, none have systematically analyzed the interaction between these enzymatic antioxidants and non-enzymatic parameters in the context of hyperthyroidism. Given the lack of studies on the MAT and its relationship with enzymatic and enzymatic variables in patients with hyperthyroidism, as well as to understand the biological changes associated with these conditions and their relationship to oxidative balance and metabolism, this study was conducted to evaluate this enzyme and important measured variables, especially methionine sulfoxide reductase A thioredoxin.

Patients and Methods

Study design and blood sample collection:

Blood samples were collected from individuals with hyperthyroidism and healthy individuals at Al-Salam Teaching Hospital in Mosul, under the supervision of specialist physicians, between November 2024 and the end of February 2025(There was enough time due to the increasing number of patients in Mosul). After completing a questionnaire, blood was drawn from a vein, and serum was separated. The serum was not hemolyzed to ensure clarity. The sample was then divided into three parts and stored frozen at -20°C to measure the variables selected in the study: The study protocol was approved by the Institutional

Ethics Committee of the University of Mosul, Iraq (Approval No. DMED-2024-015). All participants gave informed consent before enrollment.

The age range of the hyperthyroid patients was 25–60 years, and samples were collected between 8:00 and 11:00 am to minimize diurnal variations in hormonal and oxidative stress markers.

Among the 90 hyperthyroid patients, 68 were female and 22 were male, reflecting the higher prevalence in women.

Biochemical assays:

Methods used to measure enzymatic and non-enzymatic variables:

Standard kits from the French company BioLabo were used to measure albumin and uric acid concentrations. Manual methods were also used to measure the levels of enzymatic and non-enzymatic parameters, as follows:

MAT activity: The activity of the MAT was assessed by catalyzing the conversion of methionine to SAM in the presence of ATP, which releases the resulting phosphate group, which can be detected by the Malachite green reaction (22).

Methionine sulfoxide reductase A activity: The activity of the methionine sulfoxide reductase A (MsrA) was assessed by catalyzing the reduction of methionine sulfoxide to methionine in the presence of dimethyl sulfoxide as a substrate and dithiothreitol (23).

Glutathione S-transferase activity: The activity of glutathione S-transferase (GST) was estimated according to the method used by researchers Habig et al. (1974) (24). GST enzyme catalyzes the binding of compounds containing electrophilic groups, especially aromatic rings such as 1-chloro-2,4-dinitrobenzene, with the thiol group (-SH) of glutathione. Then, the absorbance intensity of the resulting solution is measured using a spectrophotometer.

Trx activity: The researcher Holmgren (1979) (25) used the method to measure the activity of Trx in the sample. The measurement process involves using

Trx in the sample to reduce the disulfide bonds of the insulin hormone with dithiothreitol, resulting in a cloudy white color, the absorption intensity of which is measured spectroscopically.

Lactoperoxidase activity: The activity of lactoperoxidase (LP) was determined according to the method used by Tayefi-Nasrabadi *et al.* (2011) (26), as LP oxidizes the substrate pyrogallo to purpurogallin in the presence of hydrogen peroxide.

Gluconolactonase as SMP-30 Activity: SMP-30 activity was determined by measuring its gluconolactonase activity using the colorimetric method (27). It hydrolyzes the substrate D-gluconolactone, resulting in ring opening and the formation of acidity, which reduces the absorption of the added p-nitrophenol.

Catalase activity: The activity of the catalase (Cat) was estimated according to the method of Boriskin *et al.* (2019) (28), which is based on the oxidation of 4-ammonium molybdenum by hydrogen peroxide remaining from the enzymatic reaction of the Cat, producing a colored substance whose absorption intensity can be measured spectrophotometrically.

Myeloperoxidase activity:

Myeloperoxidase's (MPO) function was determined using the technique outlined in the study by Kumar *et al.* (2002) (29), which involves the enzyme oxidizing orthodiensidine with hydrogen peroxide to generate a colored compound that can be analyzed using a spectrophotometer.

Xanthine oxidase activity: The activity of xanthine oxidase was assessed following the technique outlined by Ackermann and Brill in 1974 (30), to measure the production of acid.

Albumin concentration: The concentration of albumin was determined using the

Bromocresol method with a kit from BioLabo, a company based in France.

Glutathione concentration: To determine serum glutathione concentration, a modified version of the method developed by Sedlak and Lindsay in 1968 (31), which utilizes Ellman's reagent, was employed. Uric acid concentration: The level of acid was measured using a BioLab kit that relies on an enzymatic approach. The enzyme uricase converts uric acid into allantoin and hydrogen peroxide.

Malondialdehyde concentration:

Malondialdehyde concentration was determined using a modified method from Guidet and Shah (1989) (32), which is based on the reaction of malondialdehyde with thiobarbituric acid (TBA).

Peroxynitrite concentration: Peroxynitrite was determined using a modified method from Vanuffelen *et al.* (1998) (33), which oxidizes phenol to nitrophenol.

Statistical Analysis

SPSS 21 was used to determine the mean, standard deviation (SD), and correlation. The t-test was chosen to compare each pair of variables and determine the significance of the difference indicated by the p-value. A significant difference occurs when the p-value is ≤ 0.05 , while a non-significant difference occurs when the p-value is ≥ 0.05 (34).

Results

Study of MAT enzyme and other enzyme variables in hyperthyroid patients: The enzymatic profile in hyperthyroid patients shows statistically significant alterations in several oxidative stressrelated enzymes when compared to the control group (Table 1). Specifically, levels of methionine adenosyltransferase (p=0.031),Thyroidoxin (p=0.031), Lactoperoxidase (p=0.017), Catalase (p=0.047), Xanthine oxidase (p=0.0001), and Glutathione S-transferase (p=0.002)significantly elevated in hyperthyroid patients, suggesting an upregulation of antioxidant and redoxmodulating enzymes in response to increased metabolic activity and oxidative stress associated with hyperthyroidism.

Interestingly, senescence marker protein-30 was significantly lower in hyperthyroid patients (p=0.0001), possibly indicating altered cellular aging processes or stress responses. No significant differences were observed in Methionine sulfoxide reductase A (p=0.382) and Myeloperoxidase (p=0.966),

suggesting these enzymes may not be directly influenced by the hyperthyroid state.

The findings highlight an enhanced oxidative stress environment in hyperthyroidism, triggering compensatory changes in enzymatic antioxidants (Table 1).

Table 1. Enzymatic results in hyperthyroidism patients compared with the control group.

Measured enzymes (U/L)	Control group		Hyperthyroid patients group		Probability
wieasureu enzymes (O/L)	Average	Standard deviation	Average	Standard deviation	Value
Methionine adenosyltransferase	50.04	3.17	60.99	5.58	0.031*
Methionine sulfoxide reductase A	353.12	12.2	378.85	12.55	0.382
Thyroidoxin	6.12	0.708	8.88	1.01	0.031*
Lactoperoxidase	40.81	1.82	50.06	2.76	0.017*
Catalase	69.15	4.32	81.99	5.38	0.047*
Xanthine oxidase	447.06	10.19	605.12	32.33	0.0001*
Glutathione S-transferase	94.66	8.65	189.1	21.15	0.002*
Myeloperoxidase	55.98	2.77	57.3	5.92	0.966
Aging marker protein-30	0.807	0.029	0.39	0.055	0.0001*
*Significant at (p≤0.05)					

Study of MAT and other non-enzymatic variables in hyperthyroid patients: Table 2 shows statistically significant differences in oxidative stress markers between hyperthyroid patients and the control group (P ≤ 0.05). Glutathione and albumin levels were significantly decreased in hyperthyroid

patients, indicating a compromised antioxidant defense system. In contrast, oxidative stress markers—peroxynitrite and malondialdehyde—were elevated considerably, reflecting increased lipid peroxidation and oxidative damage (Table 2).

Table 2. Levels of antioxidants and oxidants in hyperthyroid patients compared with the control group.

	Control group		Hyperthyroid patients group		Probabilit
Measured variables	Average	Standard deviation	Average	Standard deviation	y Values
Glutathione (μmol/L)	10.66	0.289	6.87	0.263	0.031*
Albumin (g/100ml)	51.25	0.54	38.18	0.893	0.0001*
Uric acid (µmol/L)	63.06	2.15	51.94	2.87	0.048*
Peroxynitrite (µmol/L)	33.44	2.34	46.52	2.95	0.032*
Malondialdehyde (μmol/L)	11.91	1.63	19.89	1.79	0.031*
*Significant at (p≤0.05)					

Correlation between MAT and measured variables in hyperthyroid patients: Table 3 presents the correlation coefficients (R values) and significance levels (p-values) between methionine adenosyltransferase (MAT)

and various biochemical variables. Several statistically significant correlations ($p \le 0.05$) were observed, indicating potential relationships between MAT activity and oxidative stress-related biomarkers in hyperthyroid patients.

A strong positive correlation was found between MAT and albumin ($R=0.888,\ p=0.0001$), suggesting a close association between MAT and plasma protein synthesis or antioxidant capacity. Similarly, MAT showed a significant positive correlation with methionine sulfoxide reductase A ($R=0.638,\ p=0.0001$) and myeloperoxidase ($R=0.705,\ p=0.001$), indicating potential co-regulation or shared pathways in redox balance.

Significant negative correlations were observed with catalase (R = -0.538, p = 0.005), xanthine oxidase (R = -0.673, p = 0.0001), and glutathione (R = -0.758, p = 0.0001), reflecting an inverse relationship between MAT and these oxidative stress markers. These findings suggest that increased MAT activity may be associated with

decreased levels or activity of certain antioxidant enzymes, potentially due to feedback mechanisms or shifts in redox homeostasis.

Additionally, uric acid exhibited a moderate positive correlation with MAT (R = 0.487, p = 0.010), which may reflect its role as a secondary antioxidant in compensating for oxidative stress.

In contrast, lactoperoxidase, glutathione S-transferase, peroxynitrite, malondialdehyde, and thioredoxin did not show statistically significant correlations with MAT (p > 0.05), suggesting limited or variable associations in the hyperthyroid context. Overall, the results indicate that MAT activity is significantly correlated with key oxidative stress and antioxidant parameters, highlighting its potential role in redox regulation during hyperthyroidism.

Table 3. Correlations of the measured biochemical variables with methionine adenosyl transferase.

Measured variables	R value	p value
Lactoperoxidase	-0.338	0.085
Catalase	-0.538	0.005*
Xanthine oxidase	-0.673	0.0001*
Glutathione S-transferase	0.135	0.501
Glutathione	-0.758	0.0001*
Albumin	0.888	0.0001*
Uric acid	0.487	0.010*
Methionine sulfoxide reductase A	0.638	0.0001*
Peroxynitrite	0.031	0.877
Malondialdehyde	-0.003	0.989
Myeloperoxidase	0.705	0.001*
Aging marker protein	0.765	0.0001*
Thioredoxin	-0.334	0.15

Discussion

The current findings demonstrate significant enzymatic alterations in hyperthyroid patients, reflecting increased oxidative stress and compensatory antioxidant responses. Methionine adenosyltransferase, thioredoxin, lactoperoxidase, catalase, xanthine oxidase, and glutathione S-transferase levels were significantly elevated in the hyperthyroid group compared to controls. These enzymes

have functions in maintaining redox balance

and defending against oxidative harm. This aligns with the heightened metabolic state linked with a thyroid (35, 36). An increase in xanthine oxidase activity could lead to the production of reactive oxygen species (ROS), intensifying oxidative stress (37). Likewise. In the same vein as well as similarly, the surge in thioredoxin and glutathiophoresis S transferase levels indicates a compensatory boost in cellular antioxidant mechanisms aimed at reducing

SEDJM

ORIGINAL RESEARCH Published: 25 October 2025 DOI: 10.26505/djm.v29i1.1494

oxidative harm (36). The notable rise in catalase and lactoperoxidase levels might also help counteract hydrogen peroxide production— a reactive oxygen species generated when metabolic activity is heightened (38).

It is quite intriguing that the noticeable reduction in SMP-30 among individuals with hyperthyroidism could point towards a cellular aging process or hampered stress response. This is because SMP- 30 typically diminishes in conditions. On the other hand, there were no significant variances noted in the levels of methionine sulfoxide reductase A and myeloperoxidase in hyperthyroid patients This might indicate regulation of enzymes in the hyperthyroid state due to tissue-specific expression potential differing regulatory pathways (40). These results back up the theory that an overactive thyroid leads to stress and prompts specific enzyme reactions to maintain the redox balance.

In individuals with a thyroid gland (hyperthyroidism), the rise in MAT activity is a typical reaction to the body's increased metabolic rate and the greater demand for methylation reactions essential for biosynthesis that rely upon SAM. Α compound derived from MAT itself. This phenomenon is directly influenced by the activation of genes prompted by thyroid hormones. Thyroid hormones, recognized for their metabolic effects, are heightened. The hormones trigger thyroid hormone receptors (TRs), which attach to gene promoters, like the MAT enzyme promoter, to produce the MAT enzyme. The activation of these genes results in MAT gene activity. As a result of the metabolic functions heightened during hyperthyroidism, there is a demand for Sadenosylmethionine (SAM), crucial compound in cell methylation processes. This

increased need for SAM is essential for DNA adjustments (DNA methylation), controlling gene expression patterns, and creating phospholipids and polyamines vital for cell expansion and development (41).

The notable rise in catalase (CAT) action among individuals with hyperthyroidism when compared to those who are in good health is linked to a rise, in oxidative stress. This increase is believed to stem from the overproduction of thyroid hormones (T3 and T4) (42). These hormones are known to boost metabolism and oxygen intake levels. Consequently, this leads to the generation of levels of reactive oxygen species (ROS) (43). The body responds by triggering its defense mechanisms, which involve boosting the activity of the catalase enzyme. This enzyme helps break down hydrogen peroxide into oxygen and water, mitigating the impact of oxidative stress (OS), minimizing oxidative damage, and upholding the balance within cells (44).

Supporting this interpretation, a recent study in mice with hyperthyroidism demonstrated increased activity of antioxidant enzymes, such as catalase, in pancreatic tissue (45, 46).

Elevated XO is a biomarker of exacerbated OS associated with hyperthyroidism significant increase in the activity of this enzyme in patients may be attributed to increased OS resulting from hypermetabolic syndrome associated with increased secretion of thyroid hormones, which leads to increased production of various ROS such as hydrogen peroxide and anion superoxide radical formed by XO (2, 48) through the conversion of xanthine to uric acid, with hydrogen peroxide being produced as a by-product (49). In cases of hyperthyroidism, an increase in the activity of XO is observed, which exacerbates OS, leading to cell and tissue damage (50). A study by Kihara et al. (51) on the effect of some compounds on the XO showed that inhibiting XO using allopurinol reduces ROS levels in animal models of hyperthyroidism. Studies have shown that the effectiveness of XO increases in cases of hyperthyroidism, which enhances OS.

The significant increase in thioredoxin (Trx) in hyperthyroid patients is attributed to the increased OS resulting from the increased production of thyroid hormones (52). This condition leads to the stimulation of gene and protein expression of thioredoxin as a defines mechanism against oxidative damage resulting from hyperthyroidism, which improves the ability of cells to resist free radicals and protects tissues from damage resulting from OS by reducing hydrogen peroxide to water and oxygen by Trx, improving the redox balance and maintaining the redox balance (53). A study by Kihara et al. (2005) (54) showed that serum Trx levels were significantly elevated in Graves' disease patients compared to healthy controls, thyroid regardless of function status. suggesting a role for thioredoxin in responding to OS and regulating thyroid hormone production. A recent study conducted on animal models showed that hyperthyroidism led to increased gene expression thioredoxins (TXN1 and TXN2) thioredoxin reductase 1 (TXNRD1) in the liver, suggesting a compensatory response to OS. Furthermore, treating these models with an antioxidant decreased this expression, demonstrating the role of antioxidant therapies in reducing oxidative damage (55).

The significant increase in lactoperoxidase (LP) levels in hyperthyroid patients may be attributed to elevated levels of T3 and T4 hormones, which stimulate the body's metabolism. This acceleration of metabolism leads to increased production of oxidizing compounds such as hydrogen peroxide, causing OS in cells (2, 56, 57). To reduce harmful hydrogen peroxide, the body stimulates the production of lactoperoxidase (LP). LPO contributes to the consumption of hydrogen peroxide, forming thiocyanate (OSCN⁻), a compound with antibacterial

properties that reduce oxidative damage to cells (58). GST is significantly elevated in hyperthyroid patients as a result of increased OS resulting from accelerated metabolic processes (2). GST acts as an antioxidant enzyme that contributes to detoxification and neutralization of free radicals by binding to the glutathione molecule, which explains its high level as a cellular defines response (59).

A study by Baek *et al.* (2021) (51) showed that SMP-30 is one of the proteins directly linked to aging indicators and OS. Due to severe OS resulting from metabolic hyperactivity in hyperthyroid patients (2, 37), SMP-30 becomes deficient due to cell damage and increased enzyme consumption in attempts to combat oxidative damage. Consequently, the efficiency of SMP-30 expression decreases, leading to lower levels in the blood. This accelerates cellular aging, which impairs the cells' ability to regenerate and perform their functions properly (60).

Recent studies indicate that hyperthyroid patients have significantly higher levels of malondialdehyde (MDA), a biomarker of lipid peroxidation and OS (61), compared to healthy individuals. This increase is attributed to the heightened production of ROS due to increased metabolic activity and high oxygen consumption associated with hyperthyroidism (2). Especially superoxide anion radical and nitric oxide, which rapidly react to form peroxynitrite (ONOO-) (62), a potent oxidizing molecule that can damage proteins, lipids, and DNA (54). Oxidants interact with lipids in cell membranes, leading to their decomposition and the formation of MDA upon lipid damage. Studies indicate that this elevation in MDA is associated with a decreased ability of the body to resist OS, leading to tissue damage and worsening clinical symptoms in hyperthyroid patients (61).

Low glutathione levels in hyperthyroid patients are an essential indicator of increased OS in the body. Evidence suggests that hyperthyroidism leads to an increase in the production of ROS, which depletes glutathione stores and leads to decreased levels. This decrease in glutathione may contribute to the worsening of oxidative damage associated with

that increased GFR plays a significant role in

hyperthyroid patients with each other, a direct

correlation was observed between MAT and

methionine sulfoxide reductase A, senescence

aging marker-30, myeloperoxidase, uric acid,

and albumin (Table 3), and an inverse

correlation with catalase, xanthine oxidase,

and glutathione: The correlation analysis

reveals that methionine adenosyltransferase

(MAT) is significantly associated with several

(64). When

comparing

this

decrease

ORIGINAL RESEARCH Published: 25 October 2025 DOI: 10.26505/djm.v29i1.1494

hyperthyroidism (63). A study published in 2022 analyzed the relationship between hyperthyroidism and OS. The results showed a positive correlation between thyroid hormone levels and OS markers such as malondialdehyde (MDA) and glutathione (GSH). This suggests that hyperthyroidism may lead to increased OS, reflected in decreased GSH levels (64). Low albumin Conclusion levels in hyperthyroid patients are caused by excessive secretion of thyroid hormones, which accelerates metabolism (2) increases the breakdown (consumption) of proteins in the body, including albumin (58). Albumin acts as an essential antioxidant in plasma, and continuous exposure to OS leads to the degradation and oxidative modification of albumin, reducing its functional levels and consequently causing a deficiency in active albumin in the body (59). In hyperthyroidism, metabolism accelerates, increasing uric acid production due to the accelerated purine metabolism. However, these hormones also improve kidney function by increasing glomerular filtration rate (GFR) and renal plasma flow, enhancing the kidneys' ability to excrete uric acid. Thus, despite increased uric acid production, increased renal excretion leads to lower blood levels. Supporting this interpretation, a recent study showed that patients with hyperthyroidism had significantly lower uric acid levels, suggesting

oxidative stress markers in hyperthyroid

patients. The strong positive correlations with albumin, methionine sulfoxide reductase A, and myeloperoxidase suggest a possible link between MAT activity and antioxidant defense mechanisms. Conversely, the negative correlations with catalase, xanthine oxidase, and glutathione indicate a potential compensatory or regulatory relationship in.

Our findings demonstrate that AI can effectively automate blood cell classification, reducing the subjectivity of manual microscopy. All three models-wavelet scattering with SVM, a custom CNN, and ResNet-achieved high accuracy (>95%), with the wavelet-SVM combination performing best (~98.9%). However, a limitation of this study is the genetic properties of our dataset, which differs from others and may impact model generalizability. Future research should expand datasets and incorporate genetic variability to strengthen clinical applicability. Despite this, our work confirms that AI-driven frameworks are promising tools for enhancing hematological diagnostics

Source of funding: No source of funding. Ethical clearance: The Research Ethics Committee of Department of Chemistry, College of Sciences, Mosul University approved this study, and in accordance with the ethical guidelines of the Declaration of Ethical Committee of the College (2024-015). Written consent was obtained from all patients before inclusion.

Conflict of interest: None.

Use of Generative Artificial Intelligence (AI): The authors state that they did not use any generative AI tools for creating or editing the language of the manuscript.

Acknowledgments: We sincerely thank physicians and laboratory staff of Al-Salam Teaching Hospital in Mosul and the staff and management of the Chemistry Department at the College of Science, University of Mosul, for their invaluable support and contributions, which were instrumental in the successful completion of this

study.

References

- 1. Chaker L, Cooper DS, 1. Chaker L, Cooper DS, Walsh JP, Peeters RP. The Hyperthyroidism. Lancet. 2024 Feb 24;403(10428):768-80.
- https://doi.org/10.5772/intechopen.1007146
- 2. Sultana R, Shahin AD, Jawadul HM. Measurement of oxidative stress and total antioxidant capacity in hyperthyroid patients following treatment with carbimazole and antioxidant. Heliyon. 2022 Jan 1;8(1). https://doi.org/10.1016/j.heliyon.2021.e0865
- 3. Battikh E, Mostafa S, Alfar H, Obaid K, Ahmed AI, Sawaf B, Al-Mohanadi D. Hyperthyroidism-Induced Nondiabetic Ketoacidosis: A Rare Case Report. Clinical Case Reports. 2025 Feb;13(2):e9698. https://doi.org/10.1002/ccr3.9698
- 4. Mathew P, Kaur J, Rawla P, Fortes K. Hyperthyroidism (Nursing). DOI: https://doi.org/10.1001/jama.2023.190.
- 5. Lee SY, Pearce EN. Hyperthyroidism: a review. Jama. 2023 Oct 17;330(15):1472-83. https://doi.org/10.1001/jama.2023.19052
- 6. Grixti L, Lane LC, Pearce SH. The genetics of Graves' disease. Reviews in endocrine and metabolic disorders. 2024 Feb;25(1):203-14. https://doi.org/10.1007/s11154-023-09848-8
- 7. Braverman KD, Pearce EN. Iodine and Hyperthyroidism: A Double-Edged Sword. Endocrine Practice. 2025 Mar 1;31(3):390-5. https://doi.org/10.1016/j.eprac.2024.10.014
- 8. Fariduddin MM, Singh G. Thyroiditis. InStatPearls 2023 Aug 8. https://www.ncbi.nlm.nih.gov/books/NBK55
- 9. Gou L, Liu D, Fan TP, Deng H, Cai Y. Efficient spermidine production using a multi-enzyme cascade system utilizing methionine adenosyltransferase from Lactobacillus fermentum with Reduced Product Inhibition and Acidic pH Preference. Journal of Biotechnology. 2025 Mar 1;399:141-52. https://doi.org/10.1016/j.jbiotec.2025.01.016 10. Zhu X, Zhang T, Tang C, Wang Z, Guo L, Wang P, Zhang S, Wu J. Methionine

- adenosyltransferase MAT3 positively regulates pear pollen tube growth, possibly through interaction with pectin lyase-like protein PLL1. Physiologia Plantarum. 2025

 Jan;177(1):e70122. https://doi.org/10.1111/ppl.7012
- 11. Limveeraprajak N, Nakhawatchana S, Visukamol A, Siripakkaphant C, Suttajit Srisurapanont M. Efficacy and acceptability of Sadenosyl-L-methionine (SAMe) for depressed patients: A systematic review and meta-analysis. Neuro-Psychopharmacology Progress in Biological Psychiatry. 2024 Jun 8;132:110985. https://doi.org/10.1016/j.pnpbp.2024 .110985
- 12. Fernández-Ramos D, Lopitz-Otsoa F, Lu SC, Mato JM. S-adenosylmethionine: a multifaceted regulator in cancer pathogenesis and therapy. Cancers. 2025 Feb 5;17(3):535. https://doi.org/10.3390/cancers17030535
- 13. Xing Z, Tu BP. Mechanisms and rationales of SAM homeostasis. Trends in biochemical sciences. 2025 Mar 1;50(3):242-54. https://doi.org/10.1016/j.tibs.2024.12.009
- 14. Baden KER, McClain H, Craig E, Gibson N, Draime JA, Chen AMH. S-Adenosylmethionine (SAMe) for liver health: A systematic review. Nutrients. 2024;16(21):3668. https://doi.org/10.3390/nu16213668
- 15. Abdulhameed O, Al-Helaly L. Methionine Sulfoxide Reductase A And Neurotransmission Enzymes In Autism Spectrum Disorder And Dystocia Related Autistics. Georgian medical news. 2024 May(350):36-41.
- 16. Al-Taee KM, Al-Helaly LA. Hydrogen Sulfide and Cystathionine γ–Lyase with Oxidants and Antioxidants Levels for Patients with Epilepsy Diseases. Pharmacognosy Journal. 2024;16(2). https://doi.org/10.5530/pj.2024.16.48
- 17. Bravo AC, Aguilera MN, Marziali NR, Moritz L, Wingert V, Klotz K, Schumann A, Grünert SC, Spiekerkoetter U, Berger U, Lederer AK. Analysis of S-adenosylmethionine and S-adenosylhomocysteine: method optimisation and profiling in healthy adults upon short-term dietary intervention. Metabolites. 2022 Apr 20;12(5):373. https://doi.org/10.3390/metabo12050373
- 18. Li Z, Wang F, Liang B, Su Y, Sun S, Xia S, Shao J, Zhang Z, Hong M, Zhang F, Zheng S. Methionine metabolism in chronic liver diseases: an update on

molecular mechanism and therapeutic implication. Signal transduction and targeted 2020 4;5(1):280.https://doi.org/10.1038/s41392-

020-00349-7

- 19. Yuan D, Chu J, Lin H, Zhu G, Qian J, Yu Y, Yao T, Ping F, Chen F, Liu X. Mechanism of homocysteine-mediated endothelial injury and its consequences for atherosclerosis. Frontiers in cardiovascular medicine. 2023 Jan16;9:1109445. https://doi.org/10.3389/fcv m.2022.1109445
- 20. Hameed OM, Al-Helaly LA. Evaluation the level of total fucose and some enzymes in the blood of patients with neurological diseases. Egyptian Journal of Chemistry. 2021 Oct1;64(10):5613-8.

https://doi.org/10.21608/ejchem.2021.76538. 3745

- 21. Yin C, Zheng T, Chang X. Biosynthesis of S-Adenosylmethionine by magnetically immobilized Escherichia coli cells highly expressing a methionine adenosyltransferase variant. Molecules. 2017 18;22(8):1365. https://doi.org/10.3390/molec ules22081365
- 22. Rajabian N, Ikhapoh I, Shahini S, Choudhury D, Thiyagarajan R, Shahini A, Kulczyk J, Breed K, Saha S, Mohamed MA, Udin SB. Methionine adenosyltransferase2A inhibition restores metabolism to improve regenerative capacity and strength of aged skeletal muscle. Nature Communications. 2023 Feb 16;14(1):886. https://doi.org/10.1038/s41467-023-36483-3
- 23. Wu PF, Zhang Z, Guan XL, Li YL, Zeng JH, Zhang JJ, Long LH, Hu ZL, Wang F, Chen JG. A specific and rapid colorimetric method to monitor the activity of methionine sulfoxide Enzvme and reductase Α. Microbial Technology. 2013 Dec 10;53(6-7):391-7. https://doi.org/10.1016/j.enzmictec.2013.08.0 05
- 24. Habig WH, Pabst MJ, Jakoby WB. Glutathione S-transferases: the first enzymatic step in mercapturic acid formation. Journal of biological Chemistry. 1974 Nov 25;249(22):7130-9.

https://doi.org/10.1016/S0021-9258(19)42083-8

25. Holmgren A. Thioredoxin catalyzes reduction of insulin disulfides by dithiothreitol and dihydrolipoamide. Journal of Biological Chemistry. 1979 10;254(19):9627-32. https://doi.org/10.1016/S0021-9258(19)83562-7

ORIGINAL RESEARCH Published: 25 October 2025

DOI: 10.26505/djm.v29i1.1494

- 26. Tayefi-Nasrabadi H, Hoseinpour-fayzi MA, Mohasseli M. Effect of heat treatment on lactoperoxidase activity in camel milk: comparison with bovine lactoperoxidase. Small Ruminant Research. 2011 Aug 1;99(2-3):187-90. https://doi.org/10.1016/j.smallrumres.2011.04.007
- 27. Hucho F, Wallenfels K. Glucono-δ-lactonase from Escherichia coli. Biochimica et Biophysica Acta (BBA)-Enzymology. 1972 Jul 13;276(1):176-9. https://doi.org/10.1016/00052744(72)90018-6
- 28. Boriskin P, Deviatkin A, Nikitin A, Pavlova O, Toropovskiy A. Relationship of catalase activity distribution in serum and tissues of small experimental animals. InIOP Conference Series: Earth and Environmental Science 2019 Dec 1 (Vol. 403, No. 1, p. 012113). IOP Publishing. https://doi.org/10.1088/17551315/403/1/012113
- 29. Kumar P, Pai K, Pandey HP, Sundar S. NADHoxidase, NADPH-oxidase and myeloperoxidase activity of visceral leishmaniasis patients. Journal of medical microbiology. 2002 Oct;51(10):832-6. https://doi.org/10.1099/0022-1317-51-10-832
- 30. Bergmeyer HU, editor. Methods of enzymatic analysis. Elsevier; 2012 Dec 2.
- 31. Sedlak J, Lindsay RH. Estimation of total, protein-bound, and nonprotein sulfhydryl groups in tissue with Ellman's reagent. Analytical biochemistry. 1968 Jan 1;25:192-205.
- 32. Guidet BE, Shah SV. Enhanced in vivo H2O2 generation by rat kidney in glycerol-induced renal failure. American Journal of Physiology-Renal Physiology. 1989 Sep 1;257(3):F440-5. https://doi.org/10.1152/ajprenal.1989.257.3.F440
- 33. VanUFFELEN EB, Van der ZEE J, de KOSTER VanSTEVENINCK J, ELFERINK Intracellular but not extracellular conversion of nitroxyl anion into nitric oxide leads to stimulation of human neutrophil migration. Biochemical Journal. 1998 1;330(2):719-22. https://doi.org/10.1042/bj3300719
- 34. Morgan GA, Barrett KC, Leech NL, Gloeckner GW. IBM SPSS for introductory statistics: Use and Jul 15. interpretation. Routledge; 2019 https://doi.org/10.4324/9780429287657

35. Chattopadhyay S, Sahoo DK, Subudhi U, Chainy GB. Differential expression profiles of antioxidant enzymes and glutathione redox status in hyperthyroid rats: a temporal analysis. Comparative Biochemistry and Physiology Part C: Toxicology & Pharmacology. 2007 Sep 1;146(3):383-91. https://doi.org/10.1016/j.cbpc.2007.04.010

36. Kochman J, Jakubczyk K, Bargiel P, Janda-Milczarek K. The influence of oxidative stress on thyroid diseases. Antioxidants. 2021 Sep10;10(9):1442. https://doi.org/10.3390/antiox10091442

37. Bortolotti M, Polito L, Battelli MG, Bolognesi A. Xanthine oxidoreductase: One enzyme for multiple physiological tasks. Redox biology. 2021 May 1;41:101882. https://doi.org/10.1016/j.redox.2021.101882

38. Carmo de Carvalho e Martins MD, da Silva Santos Oliveira AS, da Silva LA, Primo MG, de Carvalho Lira VB. Biological indicators of oxidative stress [malondialdehyde, catalase, glutathione peroxidase, and superoxide dismutase] and their application in nutrition. In Biomarkers in nutrition 2022 Oct 15 (pp. 833-856). Cham: Springer International Publishing. https://doi.org/10.1007/978-3-031-07389-2

39. Pereira FC. Bioactive Effects of Selected Marine-derived Compounds on Breast Cancer Cell Lines (Master's thesis, Universidade do Porto (Portugal)).

40. Younes SH, Al-Helaly LA. Glutaredoxin-1 and other antioxidant enzymes in two subtypes (B-cell and T-cell) of acute lymphoblastic leukemia patients. South Eastern European Journal of Public Health.2024;11:10–7.

https://doi.org/10.70135/seejph.vi.1105

41. Wu SM, Huang YH, Lu YH, Chien LF, Yeh CT, Tsai MM, Liao CH, Chen WJ, Liao CJ, Cheng WL, Lin KH. Thyroid hormone receptor-mediated regulation of the methionine adenosyltransferase 1 gene is associated with cell invasion in hepatoma cell lines. Cellular and molecular life sciences. 2010Jun;67(11):1831-43.

https://doi.org/10.1007/s00018-010-0281-2

42. Festus O, Dic-Ijiewere E, Ailemen F, Imafidon N, Ebo J, Nwankwo C, Iweka F. Oxidative stress pattern of patients with abnormal thyroid function in Southern Nigeria. Journal of Research in

Applied and Basic Medical Sciences. 2025 Jan 10;11(1):85-97.

http://dx.doi.org/10.61186/rabms.11.1.85

43. Bushra SK, Mahmood T. Study of oxidative stress and inflammatory status in thyroid dysfunction: A systematic Review. International Journal of Drug Delivery Technology.2024;14(1):516-22.

https://doi.org/10.25258/ijddt.14.1.71

44. Wang Y, Ding L, Feng J, Lin Z, Yao H, You X, Zhang X, Sun W, Liu Y, Wang P. Mesoporous cerium oxide nanoenzyme for Efficacious impeding tumor and metastasis via Conferring resistance to anoikis. Biomaterials. 2025 Mar 1;314:122876. 2025;314:122876.

https://doi.org/10.1016/j.biomaterials.2024.122876

45. AL-Hamdani IH, Al-Helaly PEROXIREDOXIN 3 AND OXIDATIVE STRESS **ABORTION** IN RECURRENT PATIENTS. Military Medical Science Letters/Vojenské zdravotnické Listy. 2023 1;92(1). Jan https://doi.org/10.31482/mmsl.2022.034

46. Mahmood ES, Al-Helaly LA. Biochemical and Histological Study of Aminoacylase-1 Purified from Amniotic Fluid in Rats with Oxidative Stress Induced by Lead Acetate. Baghdad Science Journal. 2021 Jul 1;18(3). http://dx.doi.org/10.21123/bsj.2021.18.3.0583

47. Alfathi M, Alabdaly Y, Al-Hayyali F. Ameliorative Effect of Spirulina against gentamicin toxicity in liver and kidney tissues of male rat. Egyptian Journal of Histology. 2023 Dec 1:46(4):1666-75.

https://doi.org/10.21608/ejh.2022.155247.1750

48. Badawi LF. Isolation and characterization of xanthine oxidase from tissues of benign and malignant colon tumors patients. Raf J Sci. 2012;23(4):70–82.

https://search.emarefa.net/detail/BIM-322203

49. Pannala VR, Dash RK. Mechanistic characterization of the thioredoxin system in the removal of hydrogen peroxide. Biophysical Journal. 2015 Jan 27;108(2):610a-1a. . https://doi.org/10.1016/j.bpj.2014.11.3323.

50. Kihara M, Kontani K, Yamauchi A, Miyauchi A, Nakamura H, Yodoi J, Yokomise H. Expression of thioredoxin in patients with Graves' disease. International journal of molecular medicine. 2005 May1;15(5):7959.

https://doi.org/10.3892/ijmm.15.5.795

51. Najafi Z, Chamani E, Zarban A, Rezaei Z, Sharifzadeh G. The molecular evaluation of thioredoxin (TXN1 & TXN2), thioredoxin reductase 1 (TXNRd1), and oxidative stress markers in a binary rat model of hypo-and hyperthyroidism after treatment with gallic acid. Drug and Chemical Toxicology. 2023 Nov2;46(6):1108-15.

https://doi.org/10.1080/01480545.2022.2131 812

52. Alabdaly YZ. Effect of diclofenac on the pharmacokinetics of ciprofloxacin in quail. Iraqi Journal of Veterinary Sciences. 2021;35(4):777–81.

https://doi.org/10.33899/ijvs.2021.128440.15

- 53. Lu P, Huang H, Liu J, Cao Y, Hua Liu S, Yin J. Small Molecule Fluorescent Probes for Glutathione S-Transferase. ChemBioChem. 2025 May 5;26(9):e202400994. https://doi.org/10.1002/cbic.202400994
- 54. Hamdon AA, Al-Helaly LA. Biochemical and histopathological study of thioredoxin reductase isolation from blood serum in normal and oxidative stress-exposed rats. Iraqi Journal of Veterinary Sciences. 2019 Sep 1;33(2):115-24.

https://doi.org/10.33899/ijvs.2019.163243

- 55. Abdulhameed OQ, Al-Helaly LA. Enzymatic Study of Methionine Sulfoxide Reductase A, some other Enzymes Associated with Neural Pathways and Oxidative Stress in Down Syndrome Patients in Mosul City. https://doi.org/10.33899/rjs.2024.185386
- 56. Cordiano R, Di Gioacchino M, Mangifesta R, Panzera C, Gangemi S, Minciullo PL. Malondialdehyde as a potential oxidative stress marker for allergy-oriented diseases: an update. Molecules. 2023 Aug 9;28(16):5979. https://doi.org/10.3390/molecules28165979
- 57. Jomova K, Alomar SY, Nepovimova E, Kuca K, Valko M. Heavy metals: toxicity and human health effects. Archives of toxicology. 2025 Jan;99(1):153-209.

https://doi.org/10.1007/s00204-024-03903-2

58. Chandimali N, Bak SG, Park EH, Lim HJ, Won YS, Kim EK, Park SI, Lee SJ. Free radicals and their impact on health and antioxidant defenses: A review. Cell death

discovery. 2025 Jan 24;11(1):19. https://doi.org/10.1038/s41420-024-02278-8

- 59. Olia BH, Khadem Ansari MH, Rasmi Y, Hasanzadeh-Moghadam M. Evaluation of malondialdehyde levels and total antioxidant capacity in patients with hyperthyroidism. Journal of Research in Applied and Basic Medical Sciences. 2019 May 10;5(2):121-7. http://ijrabms.umsu.ac.ir/article-1-86-en.html
- 60. Macvanin MT, Gluvic Z, Zafirovic S, Gao X, Essack M, Isenovic ER. The protective role of nutritional antioxidants against oxidative stress in thyroid disorders. Frontiers in endocrinology. 2023 Jan 4;13:1092837. https://doi.org/10.3389/fendo.2022.1092837
- 61. Gurina TS, Mohiuddin SS. Biochemistry, Protein Catabolism. In: StatPearls. Treasure Island (FL): StatPearls Publishing; 2025 Jan—.
- 62. Roche M, Rondeau P, Singh NR, Tarnus E, Bourdon E. The antioxidant properties of serum albumin. FEBS letters. 2008 Jun 11;582(13):1783-7. https://doi.org/10.1016/j.febslet.2008.04.057
- 63. Xing Y, Yang L, Liu J, Ma H. The association with subclinical thyroid dysfunction and uric acid. International journal of endocrinology. 2021;2021(1):9720618.

https://doi.org/10.1155/2021/9720618

64. Xing Y, Yang L, Liu J, Ma H. The association with subclinical thyroid dysfunction and uric acid. Int J Endocrinol. 2021;2021:9720618. DOI: https://doi.org/10.1155/2021/9720618.

التغيرات في مستويات ميثيونين أدينوسيل ترانسفيريز، وميثيونين سولفوكسايد ريدوكتيز A، وثايوريدوكسين وعلاقتها بالإجهاد التأكسدي لدى مرضى فرط نشاط الغدة الدرقية

ا مروة البدراني، الوي الهلالي

الملخص

الخلفية: يرتبط فرط نشاط الغدة الدرقية بزيادة الإجهاد التأكسدي وحدوث اضطرابات في أنظمة مضادات الأكسدة الإنزيمية وغير الإنزيمية. يُعد إنزيم ميثيونين أدينوسيل ترانسفيريز (MAT) يلعب دورا حيويًا في عمليات الأيض الخلوي، وفي الحفاظ على التوازن الاكسدة والاختزال في اضطرابات الدرقية.

الأهداف: هدفت هذه الدراسة إلى تقييم مستويات MAT واستقصاء علاقته مع مجموعة من المؤشرات الإنزيمية وغير الإنزيمية للإجهاد التأكسدي لدى مرضى فرط نشاط الغدة الدرقية.

المرضى والطرق: تم جمع ٩٠ عينة مصل دم من مرضى مصابين بفرط نشاط الغدة الدرقية، ومقار نتها بـ ٥٠ عينة من أصحاء كمجموعة ضابطة. شملت المؤشرات الإنزيمية المقاسة: الميثيونين سلفوكسايد ردكتيز (MsrA)، الثايوريدوكسين (Trx)، الكتاليز (Cat)، الماليوبيروكسيديز (MPO)، الكلوتاثايون إس-ترانسفيريز (GST)، وبروتين علامة الشيخوخة-٣٠ (MPO)، الكلوتاثايون إس-ترانسفيريز (GST)، وبروتين علامة الشيخوخة-٣٠ (SMP-30). أما المؤشرات غير الإنزيمية فقد تضمنت: الكلوتاثايون (GST)، الحامض اليوريك (UA)، الألبومين (Alb)، المالوندايالديهايد (MDA)، وبيروكسينيترايت (ONOO).

النتائج: أظهرت نتائج المرضى ارتفاعًا معنويًا في مستويات MAT، وCat، وCat، وTrx، وLP، مقارنةً بالأصحاء، بينما سُجّل انخفاض معنوي في SMP-30، وSMP-30، وانخفاضًا في مستوى الألبومين. لم الطهرت المؤشرات غير الإنزيمية ارتفاعًا في MDA و-ONOO، وانخفاضًا في مستوى الألبومين. لم أنسجّل تغيّرات معنوية في باقي المؤشرات. وقد أظهر MAT علاقة ارتباط مباشرة مع SMP-30، وMSrA، وMPO، وWsrA، و UA، و GST، وGST، بينما لم تُلاحظ علاقة ارتباطية بين MAT و GST، وCat، وGST، وGST، بينما لم تُلاحظ علاقة ارتباطية بين MAT و GST، وCat، وGST، وGST، بينما لم تُلاحظ علاقة ارتباطية بين MAT و GST، وكارتباطية بين Trx

الاستنتاج: تشير النتائج إلى وجود ارتباط قوي بين فعالية MAT والإجهاد التأكسدي لدى مرضى فرط نشاط الغدة الدرقية. وتشير التغيرات الملحوظة إلى اختلالات أيضية وضعف آليات الدفاع المضادة للأكسدة لدى المرضى.

الكلمات المفتاحية: فرط نشاط الغدة الدرقية، إنزيم، ميثيونين أدينوسيل ترانسفيريز، ميثيونين سلفوكسايد ريدكتيز A، ثايوريدوكسين.

المؤلف المراسل: مروة البدراني

marwa.24scp70@student.uomosul.edu.iq الايميل:

تاريخ الاستلام: ٢٢ أيار ٢٠٢٥

تاریخ القبول: ۱ أب ۲۰۲۵

تاريخ النشر: ٢٥ تشرين الاول ٢٠٢٥

ا قسم الكيمياء، كلية العلوم، جامعة الموصل، الموصل، العراق.

DJM

مجلة ديالى الطبية تصدر عن كلية الطب - جامعة ديالى – ديالى - العراق

رئيس التحرير أ.م.د. انفال شاكر متعب دكتوراه بايولوجي جزيئي- كلية الطب - جامعة ديالى anfal_shaker@yahoo.com

مدير التحرير م.د. سعد احمد علي جدوع العزي دكتوراه طب مجتمع-كلية الطب - جامعة ديالى saadalezzi@uodiyala.edu.iq

هيئلة التحريس

```
أ.د. أسماعيل ابراهيم لطيف
                  دكتوراه مناعة سريرية - كلية الطب - جامعة ديالي
                               ismail 6725@yahoo.com
                                     أ.د.غانم مصطفى الشيخ
        دكتوراه علوم عصبية - كلية امبريال الطبية - المملكة المتحدة
                                  alsheikhg@gmail.com
                                        أ.د.كريم علوان محمد
دكتوراه في علم الأمراض وطب العدلي - رئيس وحدة الأمراض والطب
                               العدلي في جامعة SEGi الماليزية
                                   jashamy@yahoo.com
                                        أ.د. طالب جواد كاظم
                        دكتوراه تشريح - كلية الطب - جامعة ديالي
                                   talibjwd@yahoo.com
                                أ.د. سعد محمود حسين الاركى
    بورد جراحة عامة - كلية الطبّ - جامعة نيوكستل الطبية- ماليزيا
                                  Drsaad1961@gmail.com
                                      أ.د.جليل ابراهيم العزي
                  دكتوراه طب الاطفال - كلية الطب - جامعة ديالي
                               jaleel@uodiyala.edu.iq
                                         أ.د.عامر داود مجيد
                    دكتوراه فيزياء طبية - كلية الطب - جامعة ديالي
                                amer_dmk@yahoo.com
                                     أ.د.زهير معروف حسين
                  دكتوراه كيمياء حياتية - كلية الطب - جامعة ديالي
                     zuhair@medicine.uodiyala.edu.iq
                                       اً.د.مهدي شمخي جبر
                      بورد طب الاطفال - كلية الطب- جامعة ديالي
                              meh_sh2000@yahoo.com
                                        أ.د.احمد محمد باذيب
دكتوراه طب باطني و اورام الدم – رئيس قسم الاورام في مستشفى الملك
                                      خالد - نجران - السعودية
                                 abadheeb@moh.gov.sa
                                  أ.د سلوى شلش عبد الواحد
                       دكتوراه طب مجتمع - كلية الطب - جامعة ديالي
                           s_sh_abdulwahid@yahoo.co.uk
```

أ.د. صالح مهدى سلمان دكتوراة كيمياء عضوية - كلية الطب - جامعة ديالي salih@medicine.uodiyala.edu.iq ا.د. كاملة مراك اوغلو دكتوراه في طب الأسرة - كلية الطب - جامعة سلجوق - قونية - تركيا ا.د. ایدن بیادلی دكتوراه في طب العيون - جامعة أنقرة - تركيا aydinbeyatli@hotmail.com أ.د.مروان صالح النمر دكتوراه في الصيدلة والمداواة - كلية الطب - جامعة ديالي marwanalnimer@yahoo.com أ.د.على محمد باطرفي جراحة عامة - جامعة العرب- كلية الطب والعلوم الصحية المكلا - حضر موت - اليمن ambatarfi@yahoo.com أ.م.د.مقداد فؤاد عبد الكريم بورد جراحة - كلية الطب - جامعة ديالي muqdadfuad@yahoo.com ا.م.د.فايز بن عبد الله الغفيلي دكتوراه الأحياء الدقيقة الطبية - كلية العلوم التطبيقية - جامعة المجمعة - المملكة العربية السعودية F.alghofaily@mu.edu.sa ا.م.د.مليكة أمير اوغلو دكتوراه في صحة الطفل وأمراضه - كلية الطب بجامعة سلجوق - قونية - تركيا mkeser17@gmail.com د.عمر ليث قاصد FRCPath (المملكة المتحدة) FFCAP (الولايات المتحدة الأمريكية) - استشاري أمراض الأنسجة بجامعة ليستر - المستشفيات الجامعية في ليستر - المملكة المتحدة Omer.qassid@uhl-tr.nhs.uk ا.م.د.مصطفى غني طاهر دكتوراة في أمراض الفم والوجه والفكين - كلية الطب - جامعة ديالي gheny@uodiyala.edu.iq ا.د ناظم غزال نعمان رئيس قسم طب المجتمع - كلية الطب - جامعة ديالي drnadhimg@yahoo.com

> تصميم المجلة احمد جبار محمد ماجستير علوم الفيزياء – فرع الفسلجة و الفيزياء الطبية – كلية الطب – جامعة ديالى ahmed.jabbar@uodiyala.edu.iq

المراسلة: مكتب مجلة ديالى الطبية /كلية الطب/جامعة ديالى/ ص.ب(٢) مكتب بريد بعقوبة /بعقوبة /ديالى/ العراق. djm.diyala@yahoo.com editor@djm.uodiyala.edu.iq, البريد الالكتروني:

